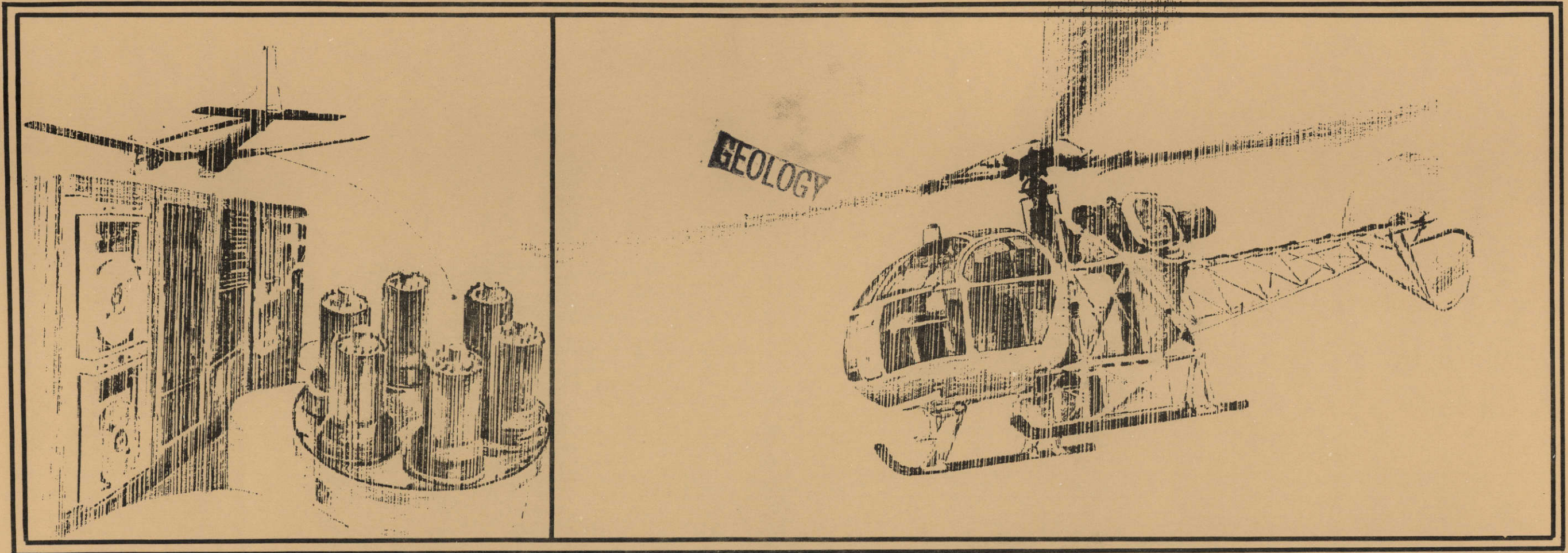


Geology
GJBX-68-80-68

GJBX- 68 '80



**AERIAL RADIOMETRIC AND MAGNETIC SURVEY
NATIONAL TOPOGRAPHIC MAP**

**WILMINGTON
DELAWARE, MARYLAND, NEW JERSEY, PENNSYLVANIA**

PREPARED FOR THE U. S. DEPARTMENT OF ENERGY
GRAND JUNCTION OFFICE
GRAND JUNCTION, COLORADO
UNDER BENDIX FIELD ENGINEERING CORPORATION SUBCONTRACT #79-337-S

GEOLOGICAL SURVEY OF WYOMING

CAUTION
This is a time release report.
Do not release any part of this
publication before



Geodata International, inc.

7035 JOHN W. CARPENTER FREEWAY • DALLAS, TEXAS 75247
(214) 630-1600 • TWX: 910-861-4359

metadc958507

LEGAL NOTICE

This report was prepared as an account of work sponsored by the United States Government. Neither the United States nor the United States Department of Energy, nor any of their employees, nor any of their contractors, subcontractors, or their employees, makes any warranty, express or implied, or assumes any legal liability or responsibility for the accuracy, completeness or usefulness of any information, apparatus, product or process disclosed, or represents that its use would not infringe privately owned rights.

"WILMINGTON TOPOGRAPHIC MAP SURVEY"

TABLE OF CONTENTS

AERIAL RADIOMETRIC AND MAGNETIC SURVEY
WILMINGTON NATIONAL TOPOGRAPHIC MAP
DELAWARE/MARYLAND/NEW JERSEY/PENNSYLVANIA
SOUTHEAST U.S. PROJECT

ABSTRACT

The results of analyses of the airborne gamma radiation and total magnetic field survey flown for the region identified as the Wilmington National Topographic Map NJ18-2 is presented in this report. The airborne data gathered is reduced by ground computer facilities to yield profile plots of the basic uranium, thorium and potassium equivalent gamma radiation intensities, ratios of these intensities, aircraft altitude above the earth's surface, total gamma ray and earth's magnetic field intensity, correlated as a function of geologic units. The distribution of data within each geologic unit, for all surveyed map lines and tie lines, has been calculated and is included. Two sets of profiled data for each line are included, with one set displaying the above-cited data. The second set includes only flight line magnetic field, temperature, pressure, altitude data plus magnetic field data as measured at a base station. A general description of the area, including descriptions of the various geologic units and the corresponding airborne data, is included also.

ABSTRACT

<u>SECTION</u>	<u>PAGE</u>
I. INTRODUCTION	I-1
A. Survey Area	I-1
B. Summary of Map Location, Geology and Physiography	I-1
II. FLIGHT OPERATIONS	II-1
A. Survey Time Summary	II-1
B. Line Coordinate Location	II-1
C. Test Line Results	II-1
D. Magnetic Diurnal Correction - Base Station	II-1
E. Altitude and Ground Speed Summary	II-1
III. GEOLOGY OF THE SURVEYED AREA	III-1
A. Location and General Physiography	III-1
B. Geology	III-2
C. Description of Geologic Map Units	III-11
D. Radioactive Mineral Prospects in the Surveyed Area	III-14
IV. RESULTS OF DATA ANALYSIS	IV-1
A. Description of Stacked Data Profiles	IV-1
1. Multivariable Radiometric Profiles	IV-1
2. Residual Magnetic Field Profiles	IV-1
B. Single and Average Record Listings	IV-2
C. Statistical Presentation of Data by Geologic Type	IV-2
D. Frequency Distribution of Data of each Geologic Type	IV-2
E. Data Interpretation	IV-2
1. Analysis of Geologic Histograms	IV-2
2. Discussion of Anomalies	IV-2
3. Summary and Recommendations	IV-17
F. National Gamma Ray Map Series	IV-16
G. Line Printer Contours	IV-18
H. Stacked Data Profiles and Geologic Histograms	IV-20

PREPARED FOR THE U.S. DEPARTMENT OF ENERGY
GRAND JUNCTION OFFICE
GRAND JUNCTION, COLORADO

UNDER BENDIX FIELD ENGINEERING SUBCONTRACT NO. 79-337-S
BY
GEODATA INTERNATIONAL, INC.
DALLAS, TEXAS

Geodata International, Inc.
7035 John W. Carpenter Freeway
Dallas, Texas 75247

(Table of Contents Cont'd.)

<u>SECTION</u>	<u>PAGE</u>
V. GEODATA DATA ACQUISITION AND PROCESSING	V-1
A. Data Acquisition System	V-1
B. Data Processing	V-6
1. Data Reduction	V-6
2. Description of Data Processing	V-10
3. Data Presentation	V-14
4. Statistical Analysis Procedures	V-15
 <u>APPENDICES</u>	
I. PRODUCTION SUMMARY	AI-1
A. Production Summary Table	AI-1
B. Test Line Results Table	AI-2
C. Diurnal Corrections Table	AI-3
D. Explanatory Notes	AI-4
E. Speed and Altitude Tables and Histograms	AI-5
II. TAPE FORMAT STATEMENTS	
III. COMPUTER LISTINGS	
IV. LINE PRINTER CONTOURS	
 <u>BIBLIOGRAPHY</u>	

LIST OF FIGURES

<u>FIGURE</u>	<u>PAGE</u>
I.1 Survey Index Map	I-2
I.2 Geologic Base Map	I-3
II.1 NTMS Showing Flight Line Location	II-2
IV.(1-6) National Gamma Ray Map Series	IV-19
V.1 Survey Aircraft	V-2
V.2 System Block Diagram	V-3
V.3 Typical End-of-Flight-Line Spectral Plot	V-5
V.4 Data Reduction Flow Chart	V-12

LIST OF TABLES

<u>TABLE</u>	<u>PAGE</u>
IV.(1-6) Geologic Unit Average Value as a Function of Map Line	IV-(3-8)
IV.7 Mean (\bar{X}) and Standard Deviation (σ) for Each Geologic Type	IV-9
IV.8 Geologic Units with Significant Variations from Unimodal Distributions, Based on the Analysis of the eTh Histograms	IV-10
IV.9 Summary of Anomalies	IV-11
IV.10 Radioactivity Anomalies per Geologic Map Unit	IV-12
IV.11 Statistical Summary of Radioactivity Anomalies by Geologic Unit	IV-13
V.1 Data Reduction Parameters and Constants for N540S	V-11

SECTION I

INTRODUCTION

SECTION I.

INTRODUCTION

A. SURVEY AREA

Geodata International, Inc., Dallas, Texas, conducted an airborne gamma ray and total magnetic field survey for the Wilmington National Topographic Map Sheet as outlined in Figure I.1. This survey was performed from a fixed-wing aircraft, using a computer-controlled, large-volume radiation detector system to detect the gamma radiation flux emanating from the surface materials. Each map line was flown in an east-west direction with an average line length of 78.2 miles; each tie line was flown in a north-south direction with line lengths of 69.0 miles. Map lines and tie lines are shown in Figure II.1.

Sections I through IV of this report present information and results associated with this specific survey. Section V gives the data acquisition and the processing procedures which are generally applicable to any survey flown with the equipment described.

B. SUMMARY OF MAP LOCATION, GEOLOGY AND PHYSIOGRAPHY

The Wilmington map area (N.T.B.M.S., 1972) is delimited by the latitudes 39°00' to 40°00' north and longitudes 74°00' to 76°00' west. The surveyed area occupies parts of Delaware, Maryland, New Jersey and Pennsylvania (Figure I.2).

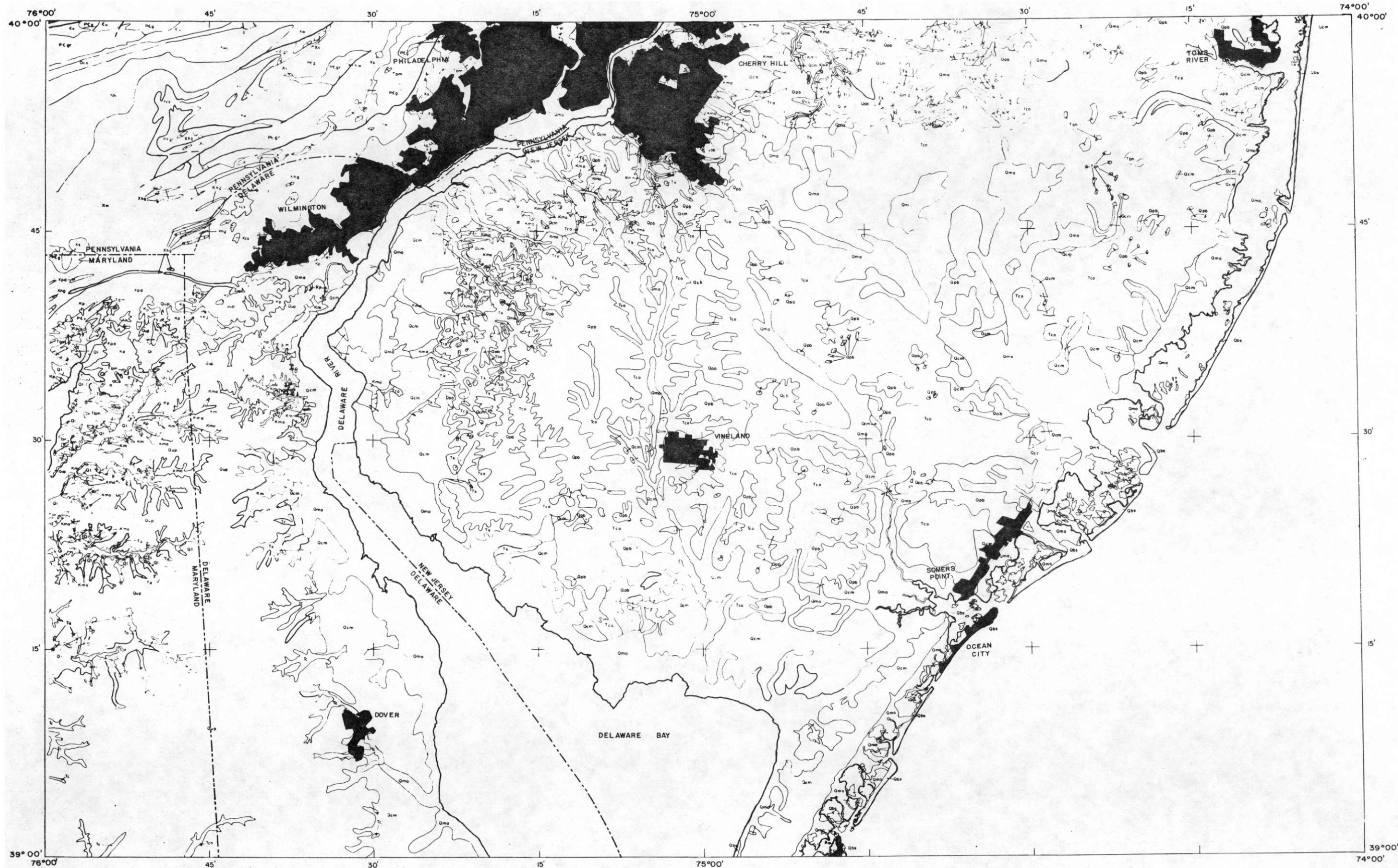
Two geologic and physiographic divisions occur within the area. Most of the land is within the confines of the Atlantic Coastal Plain. In the west and northwest, the Fall Line Zone and Piedmont units are very different.

The Coastal Plain is a sedimentary-structural feature with strata ranging in age from Cretaceous to Holocene. Much of the surface area has outcrops of either Tertiary or Quaternary age. The Piedmont is crystalline rock, mainly metasedimentaries of Paleozoic or Precambrian ages, and metaigneous rocks of both intrusive and volcanic variety.

Economically significant deposits of radioactive minerals have not been found within the surveyed area. However, rocks of both the Coastal Plain and Piedmont could be potential hosts for both thorium and uranium concentrations.



Figure I.1 Survey Index Map

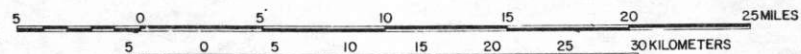


GEODATA INTERNATIONAL, INC.
 7035 JOHN W. CARPENTER FRWY. DALLAS, TEXAS 75247
 NATIONAL GAMMA RAY MAP SERIES



Figure I.2 Geologic Base Map

I-3



By
 MINERAL RESOURCES DEVELOPMENT, INC.

WILMINGTON, DELAWARE

GEOLOGY

SECTION II

FLIGHT OPERATIONS

SECTION II.

FLIGHT OPERATIONS

A. SURVEY TIME SUMMARY

The Wilmington map sheet was flown between July 22 and July 30, 1979. A detailed list of dates flown and lines flown on those dates, as well as average altitude and speed for those dates, appears in Appendix I.A.

B. LINE COORDINATE LOCATION

Doppler navigation system data have been used to locate the positions of the flight lines. These lines are positioned and verified by point locations, determined by visual sighting by the navigator or photographic recovery, and corresponding record numbers displayed by the on-board computer. The data are then plotted as solid lines with ticks every ten records, circles every fifty records, and record numbers every one hundred records. Record numbers and circles also appear at the end of each line. The points used for location reference (at least every 10 miles) are marked with an "X". The flight base is then photographed with the geologic base map to produce the composite map in Figure II.1.

C. TEST LINES

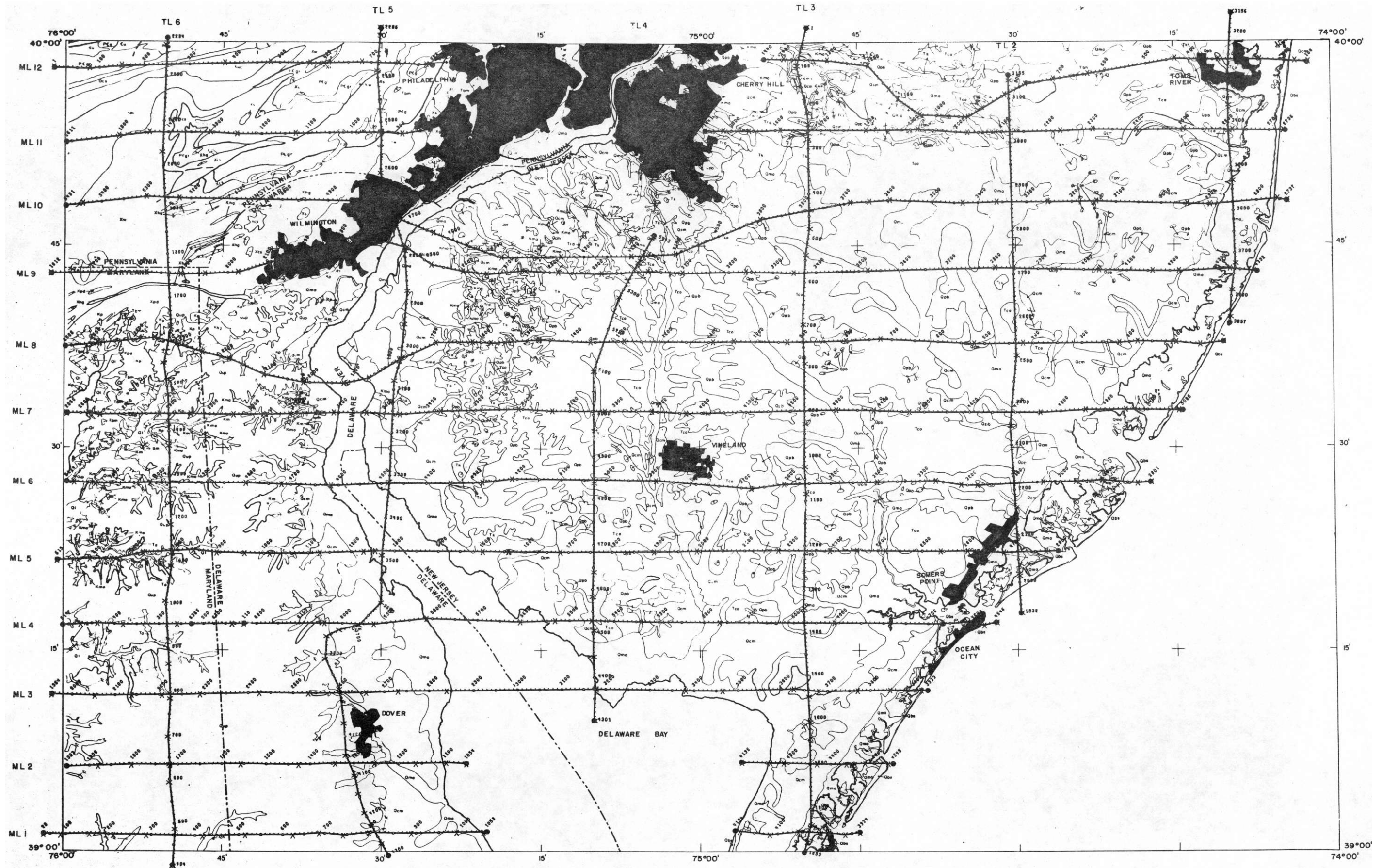
When conditions allow, two five-mile test lines are flown, one at the beginning of the day and one at the end of the day, over the same base. The data are used to check the repeatability of the system's measurements, and are presented in Appendix I.B.

D. MAGNETIC DIURNAL CORRECTION - BASE STATION

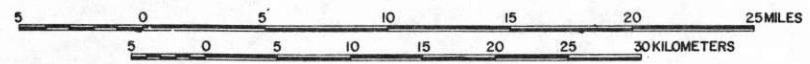
A base station magnetometer is set up in the area to acquire data pertaining to the diurnal changes in the magnetic field. These data are analyzed to evaluate a diurnal correction to the magnetic data obtained by the aircraft. A list of these corrections appears in Appendix I.C.

E. ALTITUDE AND GROUND SPEED SUMMARY

The average altitude and ground speed for each line is determined. A list by date appears in Appendix I.A, and is discussed in Section II.A. A list by flight line is given in Appendix I.E.



GEODATA INTERNATIONAL, INC.
 7035 JOHN W. CARPENTER FRWY. DALLAS, TEXAS 75247
 NATIONAL GAMMA RAY MAP SERIES



WILMINGTON, DELAWARE
 FLIGHT BASE

Figure II.1 NTMS Showing Flight Line Location
 II-2

SECTION III

GEOLOGY OF THE SURVEYED AREA

SECTION III.

GEOLOGY OF THE SURVEYED AREA

A. LOCATION AND GENERAL PHYSIOGRAPHY

The aerial radiometric and magnetic survey was conducted over the land area of the Wilmington National Topographic-Bathymetric Map Sheet (N.T.B.M.S., 1972). The surveyed area includes a part of northeastern Maryland, northern Delaware, southern New Jersey and southeastern Pennsylvania. It is delimited by the latitudes of 39°00' to 40°00' north and longitudes 74°00' to 76°00' west. It includes part or all of the following counties: Chester and Delaware counties in Pennsylvania; Caroline, Cecil, Kent and Queen Annes counties in Maryland; Kent and Newcastle counties in Delaware; Atlantic, Burlington, Camden, Cape May, Cumberland, Gloucester, Ocean, and Salem counties in New Jersey.

The surveyed area is located in two major Physiographic Provinces (Fenneman, 1938). These are the Atlantic Coastal Plain, and the Piedmont Plateau. The transitional zone between the physiographic provinces is known as the Fall Line (Fenneman, 1938).

The eastern margin of the United States is a lowland which passes under the Atlantic Ocean with little change of its gentle surface gradient (Fenneman, 1938). The shallow, submerged part of the lowland is termed the Continental Shelf. The emerged part is termed the Coastal Plain. The shoreline between emerged and submerged portions of the plain is temporary, and significant shifts of the coastal boundary have occurred during the Mesozoic and Cenozoic eras. Seaward of the emerged area, there are barrier beaches; these are broken or interrupted in places, but extend along most the coastal zone.

The Coastal Plain is comprised of many sedimentary strata, ranging from Cretaceous to Holocene in age. The strata dip downslope toward the Atlantic Ocean, and pass beneath the sea onto the Continental Shelf. The dip of the sediments increases with depth of burial and with age of origin. Many of the sediments were deposited under shallow water conditions.

The landward limit of the Coastal Plain is generally considered to be the inland margin of the Cretaceous units. The altitude of the boundary increases from sea level near New York City, to greater than 300 feet in Maryland.

From Cape Lookout, North Carolina northward, the Atlantic Coastal Plain is deeply indented by bays and estuaries. It is little more

than a fringe of peninsulas (Fenneman, 1938). Two "peninsulas" make up the Coastal Plain within the surveyed area. Between Chesapeake and Delaware bays, there is the Delmarva Peninsula; north of Delaware Bay and south New York Bay is the New Jersey coastal area.

From the Hudson River to the Potomac River, there is a lowland, 5 to 20 miles wide, at the inland margin of the Coastal Plain. The lowland is formed in the less resistant beds of an Upper Cretaceous clay. More resistant sediments of younger age overlie the easily eroded strata. These more resistant strata are marl formations and indurated limestones; the more resistant beds form a cuesta seaward of the lowland, and constitute some of the highest topographic points of the Coastal Plain.

A variety of Pleistocene terraces have been delimited for the Atlantic Coastal Plain. In places, low scarps separate one terrace from another. The terraces were first described in Maryland. Cooke (1931) lists the terraces by name and elevation. They are, in descending order and decreasing age, the Brandywine, the Coharie, the Sunderland, the Wicomico, the Penholoway, the Talbot, and the Pamlico. The origins of the terraces have variously been ascribed to both coastal and fluvial processes. In recent years, less emphasis has been placed on the significance of the terraces in interpreting the Pleistocene and Holocene geology of the area.

The Piedmont Plateau is one of six physiographic provinces of the Appalachian Highland. It is the non-mountainous portion. The surface is eroded into deformed crystalline rocks of Precambrian and Paleozoic ages. The Piedmont surface generally slopes away from the Appalachian Highlands toward the Coastal Plain. At its seaward edge, the resistant rocks of the Piedmont pass beneath the sediments of the Coastal Plain. The steeper margin of the Piedmont has been termed the Fall Line.

Typical landscape of the Piedmont is a gently undulating surface of minor local relief, cut by steep-sided valleys. Interfluvial areas are of limited areal extent; valleys are steepest in the Fall Line Zone.

B. GEOLOGY

Piedmont Plateau - Precambrian and Cambrian Rocks

The Piedmont is a gently undulating plateau bounded on the west by the Blue Ridge Hills and on the east by the Coastal Plain. It is an erosional surface cut into deformed and metamorphosed synclinal rocks of Late Precambrian to Early Paleozoic age (Fisher, 1970). Intrusive rocks are common. The older Precambrian rocks appear in

New Jersey in a series of anticlinoria and recumbent folds. Southward, they reappear in Maryland. These basement rocks are mainly quartzofeldspathic gneisses and migmatites, but include anorthosite and hypersthene granodiorite (Fisher, 1970).

The oldest of the Precambrian formations has been termed the Franklin (Buckwalter, 1955). In Pennsylvania, the bulk of the formation is a group of graphitic gneisses and graphite quartz schists. The Franklin Formation has been correlated with the Pickering Gneiss of the Piedmont.

Gabbro gneiss, hornblende gneiss, and several other types of basic gneisses occur in the Piedmont. The gabbro gneiss is a dark-grey to black, medium-grained rock, with little gneissic structure. It contains some 50 percent labradorite and 50 percent ferromagnesian minerals, including hornblende, augite, hypersthene and minor biotite. The hornblende gneiss is composed primarily of labradorite and hornblende with local minor garnet (Buckwalter, 1955).

The granite gneiss is light-buff to light-pink, and fine- to medium-grained. The gneissic structure tends to be ill-defined or almost absent. Essential minerals are quartz, microcline, with some five to ten percent of biotite and hornblende gneiss combined. In some localities, the ferromagnesian minerals are few, and the rock is leucogranitic. Orthoclase and albite may occur in minor quantities. Accessories include magnetite and zircon (Buckwalter, 1955).

The Port Deposit Gneiss is a moderately to strongly deformed gneissic quartz diorite, hornblende-biotite quartz diorite, and includes biotite granodiorite. It crops-out in southeastern Pennsylvania.

The Wissahickon Formation is a thick sequence of metamorphosed greywackes, shales and submarine slump deposits. It overlies thin deposits of metamorphosed quartz sandstone, potassic shale, and the Cockeysville Marble. These three units comprise the Glenarm Series in the Potomac area (Fisher, 1970b).

Southwick and Fisher (1967) in Maryland divided the Wissahickon into five informal lithofacies. These lithofacies are: (i) a metagreywacke; (ii) a boulder gneiss; (iii) an upper pelitic schist; and (v) a metaconglomerate lithofacies. In Pennsylvania, the Wissahickon Formation is subdivided into: (i) an albite chlorite schist, which includes the octararophyllite and some granitized members; and (ii) an orthoclase mica schist, which includes hornblende gneiss members, augen gneiss, and some quartz and feldspar-rich members, which show varying degrees of metamorphism (Buscom and Stose, 1932).

The Settlers Formation is present on the flanks of the Woodville and London Grove-Avondale anticlines. It consists chiefly of quartzite and quartzitic schists. In places, it may be a mica schist. The formation is estimated to be about 1,000 feet thick.

The Cockeysville Marble is exposed on the flanks of the Woodville and London Grove-Avondale anticlines and, in small areas, scattered along the southern side of the Poorhouse Prong and the Bailey lineament. It is a medium- to coarse-grained, saccharoidal rock, which ranges in color from white to light blue-grey. It is often banded with flakes of phlogopite. Its thickness is between 100 and 500 feet (Bascom and Stose, 1932) to 1,700 feet (McKinstry, 1961).

The Peters Creek Schist is found in the central part of the Peach Bottom Synclinorium. It is distinguished from the weakly metamorphosed phases of the Wissahickon by its abundant quartzite beds. It is a fine-grained, finely laminated, non-fissile mica schist, with numerous thin beds of quartzite, interleaved with layers of muscovite.

The Glenarm Series were deposited in a shallow marine environment. The sea extended southeastward of the present Piedmont, and included much of the area now occupied by the Coastal Plain. The two uppermost formations were a limestone, some 200 feet thick - Cockeysville Marble, and some 5,000 feet of shale - Wissahickon Formation. No local record exists in Delaware of the Glenarm Series above the Wissahickon.

During the Paleozoic, one or more of the orogenic disturbances that formed the Appalachian Mountain System metamorphosed the Glenarm sediments. It is thought that this occurred during Middle and Late Paleozoic times (Ward and Groot, 1957).

During metamorphism, magma was intruded into the marble and schist. Much of the eastern and southern Delaware Piedmont is underlain by gabbro. The gabbro was also regionally metamorphosed.

Although Bascom and Stose (1932) consider the gabbro to be intrusive, McKinstry (1961) states that in the Wissahickon, he has seen no gabbro that is clearly intrusive. McKinstry (1961) suggests that the gabbro may be volcanic in origin and possibly of post-Glenarm age.

Within the Wissahickon Formation, and elsewhere, there are irregular masses and tabular bodies of amphibolite. They may represent small apophyses of gabbro pluton completely recrystallized during metamorphism.

No metagabbro is found in the zone of low grade metamorphism; however, a greenstone schist that is present may be its equivalent. The schist is composed of very fine-grained amphibole, plus epidote, plagioclase, biotite, chlorite and quartz, and would be represented in the high grade zone by a hornblende gneiss.

Small bodies of serpentine have been intruded into the Wissahickon and metamorphosed. Pegmatites occur in northern Delaware. They are largest and most abundant north and west of Newark. Generally, in the eastern Piedmont, they are small and uncommon.

In the very northwestern portion of the map area, there is a transition from flysch-like, locally volcanic, highly metamorphic rocks, of eugeosynclinal origin, to Early Paleozoic rocks of miogeosynclinal origin. This line of transition is termed the Martic Line, and is generally drawn along the junction of known Cambro-Ordovician rocks, mainly the Conestoga Limestone, with the pelitic schists of the Glenarm Series. Rapid facies changes are involved (Wise, 1970). The line marks the edge of a deeply subsiding paleo-basin to the northwest of the surveyed area. Along this basin edge, the effect of several stages of deformation are concentrated (Wise, 1970).

Coastal Plain - Mesozoic and Cenozoic

The Coastal Plain is underlain by a series of dipping layers of relatively unconsolidated sand and clay and lesser amounts of gravel. These are deposited upon an eastward continuation of the crystalline rocks of the Piedmont. The interface between the two types of rocks dips to the southeast (Vokes, 1957).

The nature of the crystalline rocks is not well known, except where they crop-out near the Fall Line. The Hammond Well, in Wicomico County, reached the basement at a depth of almost 5,500 feet. The drill hole penetrated a mica gneiss similar to the Baltimore gneiss of the Piedmont (Vokes, 1957).

The Bethards Well, in Worcester County, reached the crystalline basement at a depth of 7,154 feet. It penetrated a dark, greenish-black rock similar to the Baltimore Gabbro (Vokes, 1957).

The interface between the crystalline rocks and the overlying sedimentaries is irregular. The general level of the surface tends to slope steeply away from the Fall Line. Maximum slope is about 125 feet to the mile; however, it is only about 43 feet to the mile under Calvert County, and under the central and western counties of the Eastern Shore. It steepens as the Atlantic Coast is approached.

The sedimentary rocks of the Coastal Plain comprise a wedge of Late Mesozoic and Cenozoic deposits. These strata thicken southeastward

and eastward from a feather-edge at the Fall Line to as much as 8,000 feet near the Atlantic Coast Line (Pickett, 1976). They continue to thicken seaward to as much as 40,000 at the edge of the Continental Shelf. The strata dip to the southeast, and become less steep with decreasing age of the geologic unit (Pickett, 1976, p.2).

The depositional area lies astride the axis of the Salisbury Embayment, at least through Miocene times. The orientation of the axis is not precisely known, and almost certainly shifted through time.

The Coastal Plain strata display major up-dip/down-dip facies changes within the emerged segment of the wedge. Such facies changes are a source of confusion in nomenclature and correlation (Pickett, 1976).

At a depth of 5,300+ feet in the Hammond Well, and 6,700+ feet in the Bethards Well, a series of red and green conglomerates, sandstones, and shales were encountered. They are similar to those of the Upper Triassic Newark Series of the western Piedmont. They are thought to be an easterly extension of the Newark Series, and are the oldest known sediments in the Coastal Plain section (Vokes, 1957).

The sediments of the Potomac Group, the basal sediments of the Cretaceous in Maryland and Delaware, are of continental origin. They are fluvial, lacustrine, paludal and swamp sediments. They are some 600 feet thick along the edge of the Piedmont Plateau, but thicken to 5,380 feet thick near the coast line (Vokes, 1957).

The basal unit within the Potomac Group is the Patuxent Formation. It is comprised of unconsolidated sand and gravel.

Superimposed on the Patuxent is the Arundel Clay. This is composed of red and brown clay, and includes layers and concretionary masses of sandstone, cemented with iron oxide or iron carbonate, and geodes and nodules of iron carbonate and limonite (Vokes, 1957).

The uppermost unit of the Potomac Group is the Patapsco Formation. It is comprised of sand and clay, which are highly colored and variegated red and brown. The clays tend to predominate, and locally contain iron carbonate. Lignitic beds occur in the unit. The Potomac Group is considered to be Lower Cretaceous, perhaps, some 120 million years old. It is the thickest sedimentary formation in Delaware. The deposition of the Potomac Group was followed by a period of erosion or non-deposition. A non-conformity exists, which represents the encroachment of the sea over much of Delaware (Pickett, 1976).

Most of the Upper Cretaceous formations overlying the Potomac Group are named from sections in New Jersey. Fossil leaves in the two lower units suggest the strata were deposited under continental conditions. The upper units have marine fossils.

The basal unit is the Raritan Formation. It is difficult to distinguish from the Patapsco, in Maryland, and is comprised of white-to-buff sands and variegated clays.

The overlying Magothy Formation consists of light-colored sands with minor amounts of clay. Lignite beds occur. It reaches a maximum thickness of 130 feet in Maryland. In Delaware, Pickett (1976) suggests the unit is transitional from stream to marine environments.

The Matawan Formation is the first truly marine unit in the Maryland Coastal Plain section. It consists of dark micaceous sandy clays that contain an abundance of glauconite (Vokes, 1957). Concretions of clay and ironstone are common. It is thought that the marine seas were shallow during Matawan time.

In Delaware, Pickett (1976) elevates the Matawan to Group status, and includes within the group the Merchantville, Englishtown and Marshalltown formations. However, Pickett (1976) states that these formations are not distinguishable south of the C and D Canal, and the Matawan assumes formational status in the down-dip surface.

The Merchantville Formation in Delaware is a dark-grey to dark-blue, micaceous, glauconitic sandy silt and silty fine sand. It was deposited in a fairly shallow, perhaps marine environment (Pickett, 1976).

The Englishtown Formation is a well sorted, micaceous, glauconitic, fine sand with thin, interbedded layers of dark-grey silty sand. It is thought to have been deposited in a low energy sand flat near the intertidal zone (Pickett, 1976).

The Marshalltown Formation is a dark, greenish-grey, massive, highly glauconitic, very fine sand. The inferred environment of deposition is inner marine shelf (Pickett, 1976).

In Maryland, the uppermost Cretaceous Formation is the Monmouth Sandstone. It is comprised almost totally of glauconite. A rich, well preserved fauna of marine invertebrates has been collected from the unit. In Maryland, the Matawan and Monmouth Formations can be up to 130 feet thick.

The equivalent to the Monmouth, in Delaware, is the Mount Laurel Formation. The unit is glauconitic, fine-to-medium quartz sand, with some silt. The depositional environment may have been embayed marine (Pickett, 1976).

The Brightseat Formation, Paleocene age, is widely present in the subsurface of the Coastal Plain. It does not crop-out within the map area (Vokes, 1957). The dark-grey micaceous and sandy clays of the Brightseat are unconformable with the Monmouth Formation. They contain in their lower portion some reworked Upper Cretaceous fossils. The Brightseat is some 70 to 100 feet thick.

In Delaware, the Rancocas Group spans the Late Cretaceous to Early Tertiary time (Pickett, 1976). It is a heterogeneous array of mainly glauconitic, marine units. In the subcrop area, the group includes the Hornerstown and Vincentown formations. Down-dip, these become a thick clay-rich sequence that has not been formally named (Pickett, 1976).

The Hornerstown Formation is a fine-to-medium, greenish, highly glauconitic sand and sandy silt. It is the Delaware equivalent of the Brightseat Formation, and was deposited on an inner marine shelf environment.

In New Jersey, the Manasquan Marl rests unconformably upon the Vincentown. The lower part of the Manasquan is composed chiefly of glauconite, but the upper part is made up of very fine sand mixed with greenish-white clay. Total thickness is some 25 feet. It is generally succeeded unconformably by Tertiary or Quaternary deposits, but locally may be overlain by a bluish marl of later Eocene age (Kummel, 1940).

The Lower and Middle Eocene Aquia and Nanjerry Formations have long been among the best known of the Eocene formations of the Atlantic Coastal Plain. The Aquia is a clayey glauconitic sandstone. The unit is up to 100 feet thick in the subsurface of Maryland.

The Nanjerry Formation is also comprised of glauconitic sands. At the base, there is a pink clay, some 10 to 30 feet thick, which is known as the Marlboro Clay (Vokes, 1957). The Nanjerry unit is generally less than 100 feet thick. It was deposited in an inner shelf environment.

In Delaware, on the up-dip side, the Nanjerry passes into a sandy facies, the Vincentown Formation. The Vincentown is a green and grey, fine-to-coarse, highly quartzose glauconitic sand, with some silt. It is more quartzose than the Hornerstown, and was deposited in a shallower portion of the shelf (Pickett, 1976).

In Maryland, the Aquia and Nanjerry formations are unlike other Coastal Plain deposits. They are not blankets of sediments. They were deposited in a channel or trough that crossed the northern part of the Eastern Shore (Vokes, 1957).

Oligocene age deposits are not known in the Maryland, New Jersey or Delaware portion of the Atlantic Coastal Plain.

The Miocene deposits of Maryland are referred to as the Chesapeake Group. The lowest formation within the group is named the Calvert Formation. The lowest member of the Calvert is the Fairhaven, a diatomaceous earth member. It is comprised of microscopically small tests of diatoms. The lower 20 feet is almost wholly diatomaceous, and is grey-to-white in color. The upper beds contain a mixture of clay and diatoms. The Fairhaven Member may be as much as 60 feet thick. Overlying the Fairhaven is a series of dark sandy clays; foraminifera and mollusca are abundant. The uppermost member is known as the Plum Point Marl, and has a thickness of some 135 feet in the Calvert Cliffs (Vokes, 1957).

The Choptank Formation is the middle formation of the Chesapeake Group. It is easily distinguished by its yellow sands. Generally, the formation is buried beneath younger deposits; it dips to the southeast at about ten feet to the mile. The thickness ranges from 50 to nearly 100 feet (Vokes, 1957).

The St. Mary's Formation crosses Maryland from northeast to southwest in a belt immediately to the southeast of the Choptank Formation. On the Eastern Shore, it is buried beneath a mantle of Late Cenozoic deposits, and does not crop-out within the Wilmington map area. It is comprised of bluish sandy clays and fine sandstones that are extremely fossiliferous, and is especially rich in gastropods (Vokes, 1957). The St. Mary's is some 150 feet thick, and dips seaward at 10 feet per mile.

The Chesapeake Group was probably deposited under inner shelf conditions, with shelly, fossiliferous zones that represent shallow marine conditions. The Chesapeake sediments are generally very similar to the overlying Late Cenozoic sediments, and, in part, may be younger than their assigned Miocene age (Pickett, 1976).

In New Jersey, during Miocene time, the sea invaded the southern portion of the state. During this submergence, sediments now grouped under the term Kirkwood were deposited (Kummel, 1940). These beds are predominantly fine, micaceous quartz sand, and, in places, they are banded in pink and yellow hues. Black lignitic clays occur, locally, near the base. In Salem County, the Kirkwood consists of thick beds, 80 to 90 feet, of brown and drab-colored clays. Above these beds, there is a fine clayey sand with abundant shells. The unit is termed the Shiloh Marl.

In southern New Jersey, the Kirkwood is overlain disconformably by the Cohansey Sand. The Cohansey is composed chiefly of quartz sand, with local clay laminae, and occasional lenses of gravel. It forms the surface of the Coastal Plain in New Jersey over a wider area than any other single formation (Kummel, 1940).

The cycles of deposition of the Miocene Epoch were terminated in Early Pliocene time by the arching of the Appalachian Region (Kummel, 1940). The erosional surface of the Appalachian Region had been deeply mantled with weathered residuum. This residuum was transported by the rejuvenated streams over a wide area. The Beacon Hill Formation of New Jersey and the Bryn Mawr Formation in Pennsylvania, Maryland and Delaware were formed at this time (Kummel, 1940). They are units of gravel, sand, silt and clay with coarser sand, cobbles and boulders near the base. These "gravels" cap some of the higher hills of the area. The Beacon Hill Gravel is chiefly quartz, but contains chert and pebbles of sandstone and quartzite (Kummel, 1940).

Overlying the older Cenozoic deposits, there is a series of gravels with sand and silt. In the past, these gravels have been considered to lie on terrace surfaces cut into the Coastal Plain. The mineralogical composition of the gravel units are generally similar. Differences are essentially textural, and are enhanced by various sedimentary structures.

In general, the sands are subarkosic with minor chert and mica. Composition of the gravels vary with size. Generally, the gravels are quartz, sandstone-quartzite, chert, and a few are crystalline rocks from the Piedmont. The sand-size, heavy minerals are generally ilmenite, magnetite and leucocene. Non-opaque heavy minerals consist of zircon, epidote, staurolite, kyanite, garnet, amphiboles, sillimanite, chloritoid, pyroxene, andalusite, apatite, monazite, sphene and spinel.

The Columbia Formation of Kent County is a medium- and coarse-grained sand with abundant gravel; cobbles and boulders are common. The coarseness of the unit decreases from north to south. Bedding is distinct, and different textures tend to segregate into distinct beds. The beds exhibit some cross-cutting. Cut and fill and slump textures exist. The sediments are generally oxidized. Limonite is abundant, and black wad staining is common (Jordan, 1976).

Early in Pleistocene time, the streams in southern New Jersey ceased eroding, and began to aggrade. The Bridgetown Formation was deposited. The unit is essentially gravel and sand, with a maximum thickness of 30 feet. The materials are derived from various older formations. The unit occurs as outliers, capping hills and interfluves. After deposition of the Bridgetown, there was renewed down-cutting and general degradation.

The Pensauken was deposited in southern New Jersey during post-Bridgetown time (Kummel, 1940). The unit is comprised of sand, and smaller pebbles that are mainly quartz. Pebbles of shale, sandstone, quartzite and crystalline rock occur. In addition, pebbles of chert, water-worn ironstone and glauconite occur, and were probably derived from erosion of older Coastal Plain sediments. The average thickness of the Pensauken is 10 to 20 feet (Kummel, 1940).

A subsequent period of prolonged erosion partially removed the Pensauken Gravel. In southern New Jersey, terraces were formed along the coast. Deposits of sand and gravel occur at low elevations. These deposits extend up-valley to elevations of 140 or 150 feet (Kummel, 1940), and are known as the Cape May Formation.

Along the coast and lower Delaware River, terraces of Cape May age are not more than 40 feet above sea level, and are lower than the Pensauken terraces (Kummel, 1940). Along tributary streams, they rise to greater elevations than 40 feet.

In latest Pleistocene and Holocene times, alluviation along larger streams and silting of shallow lakes and ponds occurred. Beds of peat formed. Along the coast, barrier beaches have been built from Manasquan southward. Broad and shallow lagoons have been formed behind the barrier beaches (Kummel, 1940).

C. DESCRIPTION OF GEOLOGIC MAP UNITS

(Modified from legend of "Geology of the Wilmington Quadrangle" - Mineral Resources Development, Inc., 1979).

Cenozoic - Quaternary

Qma: Marsh and Alluvial Deposits

Qbs: Beach Deposits

Ql: Lowland Deposits

Gravel, sand, silt and clay; medium- to coarse-grained sand and gravel. Cobble and boulders near base.

Qcm: Cape May Formation

Sands and gravels, with clay and silt, locally, at the base.

Qpb: Pensauken and Bridgeton Formation

Deeply weathered gravels and sandy gravels.

Qup: Upland Gravels

Gravel, sand, silt and clay. Mostly cross-bedded, poorly sorted, medium- to coarse-grained sand and gravel.

Cenozoic - Tertiary

Tbm: Bryn Mawr Formation (Type not encountered during survey.)

High level terrace sands and gravels; some silt.

Tbh: Beacon Hill Formation

Tch: Choptank Formation

Interbedded, brown-to-yellow, very fine-grained sand, and dark-grey argillaceous silt.

Tco: Cohansey Formation

Tc: Calvert Formation

Dark clays and fine-grained sands, with prominent local shell beds.

Tk: Kirkwood Formation

Ta: Aquia Formation

Green, argillaceous, glauconitic, well sorted, fine- to medium-grained sand.

Tra: Rancocas Group

Includes Hornerstown, Vincentown, and Manasquan formations.

Mesozoic - Cretaceous

Kmo: Monmouth Formation

Dark-grey to reddish-brown, micaceous, glauconitic, argillaceous, fine- to coarse-grained sand.

Kma: Matawan Formation

Dark-grey, micaceous, glauconitic, argillaceous, fine-grained sand and silt.

Km: Magothy Formation

Loose, white, cross-bedded, "sugary", lignitic sands, and dark-grey, laminated silty clays.

Kp: Potomac Group

Interbedded, quartzose gravels, argillaceous sands, and multi-colored silts and clays.

Paleozoic

Ocs: Conestoga Formation

Bluish-grey, thin-bedded, impure, contorted limestone with shale partings; conglomerate at the base.

Gu: Cambrian Sedimentary Rocks, Undivided

Xgr: Granite Gneiss and Granite

Unit includes the Springfield granodiorite, granitized Wissahickon and related rocks.

Xs: Serpentine

Serpentine, steatite and associated products of alterations of peridotites and pyroxenites.

Xhg: Hornblende Gneiss

Unit includes rocks of probable sedimentary origin; may be equivalent to the P6g unit.

Xcs: Cockeysville Marble and Settlers Formation

Marble, feldspathic quartzite, mica schist and mica gneiss.

Xpc: Peters Creek Schist

Chlorite sericite schist with quartzite.

Xw; Xwc: Wissahickon Formation

Xwc: albite chlorite schist; includes octararophyllite, and some hornblende gneiss and granitized members.

Xw: Orthoclase mica schist; includes some hornblende gneiss members, some augen gneiss, quartz and feldspar-rich members showing various degrees of granitization.

Xpd: Port Deposit Gneiss

Moderately-to-strongly deformed gneissic biotite quartz diorite, hornblende-biotite quartz diorite, and biotite granodiorite.

Precambrian

P6gr: Granite Gneiss

P6g: Gabbro Gneiss

Includes rocks of probable sedimentary origin. It may be equivalent to Xhg.

P6v: Volcanics

Metamorphosed andesitic and dacitic volcanic rocks.

Miscellaneous

unk: Unknown Geologic Type

D. RADIOACTIVE MINERAL PROSPECTS IN THE SURVEYED AREA

Delaware

"There is no production of uranium in Delaware and no known uranium deposits..." (Southern Interstate Nuclear Board, 1969). However, radiometric anomalies have been noted in the clays of the Potomac Formation, the Rancocas greensands, and in the Miocene brown clays (Southern Interstate Nuclear Board, 1969).

Maryland

There are no known uranium deposits in Maryland (Southern Interstate Nuclear Board, 1969).

New Jersey

Thorium-rich minerals have been noted in certain of the beach sands in Atlantic, Cape May and Ocean counties. They are not of economic significance (Cooper, 1958). In Burlington County, radioactivity has been traced to the black and blue-black glauconitic sands of the Hornerstown Formation. The deposits are not of economic significance.

Pennsylvania

Radioactivity occurrences occur in both Chester and Delaware counties, but none of economic significance appear to occur within the confines of the map area (Cooper, 1958).

SECTION IV

RESULTS OF DATA ANALYSIS

SECTION IV.

RESULTS OF DATA ANALYSIS

A. DESCRIPTION OF STACKED DATA PROFILES

1. Multivariable Radiometric Stacked Data Profiles

These profiles are presented at a horizontal scale of 1:500,000. The vertical scales are:

Altitude: 100 feet/div.; aircraft altitude above the surface

TL(^{208}Tl)* .75 ppm/div; 7.24 c/s = 1 ppm/eTh

BI(^{214}Bi)* 0.25 ppm/div; 13.85 c/s = 1 ppm/eU

K (^{40}K)* 0.15 %/div; 105.0 c/s = 1%K

BiAir 2.5 c/s/div. 50 seconds averaged

Residual Magnetic Field 100 gammas/div. (See Sec.V.B.1)

GC (Count from 400 keV to 3.0 MeV) 250 c/s/div.

Bi/TL 0.07 /div.

Bi/K 0.5 /div.

TL/K 1.0 /div.

Geology Strip: An approximate six-mile width of the geology map, containing each line, is displayed above the profiles.

* 7-second average weighted 1:2:3:4:3:2:1 is used and plotted at center.

2. Residual Magnetic Field Profiles

Altitude: 100 feet/div.

Temperature: 1.0 $^{\circ}\text{C}$ /div.

Pressure: 3 mm of Hg/div.

Base Magnetic Field: 10 gammas/div.

Residual Magnetic Field: 10 gammas/div.

Geology Strip: An approximate six-mile width of the geology map, containing each line, is displayed above the profiles.

All profiles appear in Section IV.H.

B. SINGLE AND AVERAGE RECORD LISTINGS

Single and average record listings are provided on microfiche. Samples of each type are presented in Appendix III.

C. STATISTICAL PRESENTATION OF DATA BY GEOLOGIC TYPE

Tables IV.(1-6) contain the average value of each variable as a function of line number and geologic type. The tables are in order eTh, eU, K, eU/eTh, eU/K, eTh/K.

D. FREQUENCY DISTRIBUTION OF DATA FOR EACH GEOLOGIC TYPE

Table IV.7 contains the mean, standard deviation, and number of events for each geologic type encountered over the entire map sheet. Histograms for these data appear in Section IV.H.2.

E. DATA INTERPRETATION

1. Analysis of Geologic Histograms

The radioactivity data is shown in histogram form with parts per million or percent plotted against number of events (Appendix I). The histograms for ^{208}Tl and ^{40}K were examined for conformity to a Gaussian curve. It is generally assumed that a geologic map unit, which encompasses a fairly homogeneous lithology, would have a unimodal distribution. Where map units vary significantly from a unimodal distribution, a further subdivision into more homogeneous lithologic types may be recommended. Table IV.8 shows the map units, which vary from a unimodal model, and for which separation of two or more distributions is feasible. Only units with excess of 200 events are considered.

2. Discussion of Anomalies

Introduction

The ^{208}Tl , ^{214}Bi , and $^{214}\text{Bi}/^{208}\text{Tl}$ (ratio) data were examined for anomalous values. An anomaly is defined by a minimum of two adjacent, two-standard deviation values, or a single, three-standard deviation value. The anomalies were listed by flight line in Table IV.9; by geologic map unit in Table IV.10; Table IV.10 is statistically summarized in Table IV.11. Only positive anomalies were examined for ^{208}Tl and ^{214}Bi , but both positive and negative values were studied for the ratio anomaly.

	QMA	QBS	QL	QCM	OPB	QUP	TBH	TCH	TCO	TC	TK	TA	TRA	KMO	KMA	KM	KP	OCS
ML 1	19	5		23		38		26		38								
ML 2	14	12		39		41				30								
ML 3	18	10		33		42				34								
ML 4	12	16		28		56			20	52		80						
ML 5	32	18	36	33	29	54			22	45	29	58						
ML 6	16	13	34	18	38	60			27					49	52	35	8	
ML 7	9	10	43	42	40	65			22		41		68		55	47	47	
ML 8	13	10		42	39	71			23		69		77			72	63	
ML 9	10	8		27	40	77			23		37		38	34	23			
ML10	15	9		25	38		14		23		36		37	29	33			
ML11	13	5		36	35		28		19		29		40		49			
ML12	18			46	29				15		27			30	17			64
TL 1	15	12		20	31				31									
TL 2	11	25		17	18				17									
TL 3	13			23	29				23		25		44	41	25			
TL 4	12			25	34				26		26							
TL 5	19			43	68	42				43				53	24			
TL 6			42			51				33		33		56	76		68	81

	CU	XGR	XS	XHG	XCS	XPC	XWC	XW	XPD	PCGR	PCG	PCV	UNK
ML 1													
ML 2													
ML 3													
ML 4													
ML 5													
ML 6													
ML 7													
ML 8			94					62				44	66
ML 9			83	69			97				77		
ML10				71		86	92						
ML11		99		66	107	96	94			86	60		
ML12	107		50			89	92	72		104	60		
TL 1													
TL 2													
TL 3													
TL 4													
TL 5				70			69	74		74	71		
TL 6	67			71		91	88	87	74		63		

Table IV.1 Geologic Unit Average Value as a Function of Map Line for eTh (PPM Times 10)

	QMA	QRS	QL	QCM	QPB	QUP	TBH	TCH	TCO	TC	TK	TA	TRA	KMO	KMA	KM	KP	OCS
ML 1	8	3		11		12		7		13								
ML 2	6	6		14		12				13								
ML 3	5	5		11		12				11								
ML 4	5	7		10		16				15		21						
ML 5	10	14	12	12	9	15		6	8	9	9	16						
ML 6	7	12	12	6	12	17			9					15	19	12	5	
ML 7	3	3	14	13	12	16			9		10		17		15	15	13	
ML 8	5	5		12	12	19			8		20		27			17	16	
ML 9	5	4		10	13	17			9		15		16	16	11			
ML10	7	8		10	13		5		9		16		16	16	13			
ML11	8	3		16	17		10		9		16		20	16	24			
ML12	9			19	15				8		15			12	11			18
TL 1	6	4		7	10				10									
TL 2	4	6		5	6				5									
TL 3	5			6	9				7		10		12	11	7			
TL 4	4			7	10				8		12							
TL 5	6			12	18	11				11				11	8			
TL 6			11			13				8		10		14	20		16	18

	CU	XGR	XS	XHG	XCS	XPC	XWC	XW	XPD	PCGR	PCG	PCV	UNK
ML 1													
ML 2													
ML 3													
ML 4													
ML 5													
ML 6													
ML 7													
ML 8			23					15				11	16
ML 9			21	16			21				18		
ML10				19		19	20						
ML11		29		17	21	20	19			14	10		
ML12	29		14			19	19	17		29	14		
TL 1													
TL 2													
TL 3													
TL 4													
TL 5				17			17		14	14			
TL 6	18			14		20	16	21	17		23		

Table IV.2 Geologic Unit Average Value as a Function of Map Line for eU (PPM Times 10)

	QMA	QBS	QL	QCM	QPR	QUP	TBH	TCH	TCO	TC	TK	TA	TRA	KMO	KMA	KM	KP	OCS
ML 1	53	24		74		91		67		91								
ML 2	34	40		77		109				102								
ML 3	38	36		51		104				97								
ML 4	25	39		39		106		20		118		110						
ML 5	45	42	63	49	28	111		23		115	41	83						
ML 6	32	31	71	25	43	106		28						91	70	76	12	
ML 7	24	17	51	55	42	100		22			49		93		54	96	48	
ML 8	24	8		61	44	111		24			92		111			116	73	
ML 9	12	14		38	47	93		18			63		67	63	50			
ML10	23	16		39	48		11	20			54		73	64	61			
ML11	11	13		42	55		19	13			15		124		80			
ML12	15			74	46			15			19			81	64			128
TL 1	20	17		16	22			21										
TL 2	16	49		25	14			11										
TL 3	20			33	52			16			31		87	82	34			
TL 4	28			33	40			33			30							
TL 5	38			76	107	132				127				89	32			
TL 6			60			95				84		62		87	100		68	155

	CU	XGR	XS	XHG	XCS	XPC	XWC	XW	XPD	PCGR	PCG	PCV	UNK
ML 1													
ML 2													
ML 3													
ML 4													
ML 5													
ML 6													
ML 7													
ML 8			103						62			45	59
ML 9			98	94				145			83		
ML10				106		158		130					
ML11		110		101	188	182		150		135	96		
ML12	109		85			190	156	140		118	124		
TL 1													
TL 2													
TL 3													
TL 4													
TL 5				87				94		105	90		
TL 6	134			75		161	134	129	85		108		

Table IV.3 Geologic Unit Average Value as a Function of Map Line for K (PC Times 100)

	QMA	QBS	QL	QCM	QPB	QUP	TBH	TCH	TCD	TC	TK	TA	TRA	KMO	KMA	KM	KP	OCS
ML 1	57	73		56		34		31		38								
ML 2	51	57		39		33				48								
ML 3	38	44		40		30				33								
ML 4	55	53		40		30			35	31		27						
ML 5	34	113	36	46	31	28			39	21	32	30						
ML 6	51	132	36	39	32	30			40					31	39	38	101	
ML 7	47	51	29	35	32	25			45		28		25		27	33	30	
ML 8	54	70		34	30	27			42		29		35			24	26	
ML 9	63	53		43	34	23			42		42		43	49	52			
ML10	57	93		44	36		41		42		46		43	57	42			
ML11	71	58		48	52		35		52		54		51		50			
ML12	53			43	52				65		59			45	64			28
TL 1	35	27		35	32				37									
TL 2	46	29		27	45				39									
TL 3	48			27	32				37		44		27	32	31			
TL 4	37			27	32				33		49							
TL 5	33			29	26	26				25				21	35			
TL 6			29			27				27		46		25	28		24	22

	CU	XGR	XS	XHG	XCS	XPC	XWC	XW	XPD	PCGR	PCG	PCV	IMK
ML 1													
ML 2													
ML 3													
ML 4													
ML 5													
ML 6													
ML 7													
ML 8			24					24				27	24
ML 9			25	24				22			24		
ML10				28		22		21					
ML11		30		25	19	21		21		17	17		
ML12	26		30			22	21	24		28	23		
TL 1													
TL 2													
TL 3													
TL 4													
TL 5				25			25		19		21		
TL 6	27			21		22	19	24	24		36		

Table IV.4 Geologic Unit Average Value as a Function of Map Line for eU/eTh (Times 100)

	QMA	QBS	QL	QCM	OPB	QUP	TBH	TCH	TCO	TC	TK	TA	TRA	KMO	KMA	KM	KP	DCS
ML 1	1861	1982		2498		1466		1162		1515								
ML 2	2014	1718		2506		1227				1433								
ML 3	1758	1297		2973		1258				1208								
ML 4	2717	2176		3199		1588			3397	1353		1985						
ML 5	2251	3901	2128	3419	3786	1453			4401	854	2544	1993						
ML 6	2612	4470	1730	3276	3299	1792			4074					1694	2765	1852	6240	
ML 7	2650	2815	2667	2883	3497	1831			4982		2577		1863		2803	1633	3097	
ML 8	3787	7098		3493	3064	1799			4897		2202		2455			1488	2408	
ML 9	6506	2855		3826	3427	1923			6169		2842		2500	2591	2290			
ML10	6187	6020		3667	3105		5409		5904		3172		2237	2655	2275			
ML11	8732	2341		5070	5731		5461		7712		11394		1837		3224			
ML12	7354			2867	4553				6455		9560			1670	1747			1414
TL 1	3535	2721		5084	5057				5372									
TL 2	4535	1393		2510	5714				6336									
TL 3	4713			2226	2551				5549		4502		1385	1606	2356			
TL 4	1456			2162	2895				2713		4282							
TL 5	1620			1720	1702	873				875				1316	2678			
TL 6			1984			1489				992		1830		1644	2065		2429	1162

	CU	XGR	XS	XHG	XCS	XPC	XWC	XW	XPD	PCGR	PCG	PCV	UNK
ML 1													
ML 2													
ML 3													
ML 4													
ML 5													
ML 6													
ML 7													
ML 8			2296						2464			2684	2755
ML 9			2164	1806				1520			2754		
ML10				1917		1240		1558					
ML11		2672		1755	1202	1152		1350		1103	1104		
ML12	2695		1670			1061	1298	1242		2540	1155		
TL 1													
TL 2													
TL 3													
TL 4													
TL 5				2078				1829		1409	1658		
TL 6	1376			1990		1262	1262	1671	2131		2224		

Table IV.5 Geologic Unit Average Value as a Function of Map Line for eU/K (Times 1000)

	QMA	QBS	QL	QCM	QPB	QUP	TBH	TCH	TCO	TC	TK	TA	TRA	KMO	KMA	KM	KP	OCS
ML 1	3617	1525		4214		4322		3847		4222								
ML 2	4297	3012		6431		3896				2998								
ML 3	4408	2960		7149		4197				3564								
ML 4	5412	4460		8168		5370			10138	4500		7296						
ML 5	6711	4151	6214	8131	11667	5152			11355	3916	7649	6901						
ML 6	5389	3954	4801	7974	10307	5707			10521					5443	7293	5029	5533	
ML 7	4636	5111	8445	8317	10715	6962			11744		9125		7281		10263	5049	10320	
ML 8	6927	12570		10193	10174	6630			12391		7584		6936			6248	9206	
ML 9	11317	5635		9627	9668	8295			15252		6967		6037	5567	4873			
ML10	12928	6422		8487	8882		12753		14834		7016		5198	4835	5565			
ML11	13153	5260		10699	11016		15376		15684		20560		3775		6328			
ML12	13851			6598	9319				12027		16337			3692	2727			5166
TL 1	8470	7275		13191	14668				14875									
TL 2	10275	4761		8634	14911				17331									
TL 3	9200			8129	7991				15051		10394		5113	5034	7379			
TL 4	4003			7671	8868				8119		8929							
TL 5	4949			5963	6409	3303				3424				6075	7430			
TL 6			7076			5505				3723		4743		6384	7508		9890	5308

	CU	XGR	XS	XHG	XCS	XPC	XWC	XW	XPD	PCGR	PCG	PCV	UNK
ML 1													
ML 2													
ML 3													
ML 4													
ML 5													
ML 6													
ML 7													
ML 8			9178					10091				9918	11162
ML 9			8542	7468			6809			9241			
ML10				6824		5470	7180						
ML11		9385		6740	6000	5290	6399		6404	6310			
ML12	9911		6292			4692	5995	5194	8888	4984			
TL 1													
TL 2													
TL 3													
TL 4													
TL 5				8159			7363		7279	8045			
TL 6	5090			9487		5667	6606	6958	8956	6018			

Table IV.6 Geologic Unit Average Value as a Function of Map Line for eTh/K (Times 1000)

eTh		eU		K		eU/eTh		eU/K		eTh/K		MAX. NO. EVENTS	GEOL. UNIT
σ	\bar{x}	σ	\bar{x}	σ	\bar{x}	σ	\bar{x}	σ	\bar{x}	σ	\bar{x}		
1.2117	1.6	0.4041	0.6	0.2175	0.3	0.3072	0.5014	3.5930	3.7712	5.6884	7.5952	4730	QFA
0.9250	1.5	0.4675	0.8	0.1785	0.3	0.5713	0.7217	1.9854	3.0107	2.3588	4.7896	248	QHS
1.7532	4.1	0.4896	1.2	0.2542	0.6	0.1343	0.3190	0.7735	2.0972	2.1967	6.8859	269	QL
1.9630	3.2	0.6122	1.1	0.3661	0.5	0.1946	0.3884	1.9684	2.9339	4.1253	7.7788	4097	QCM
1.5061	3.5	0.7189	1.2	0.2788	0.4	0.1789	0.3673	2.5299	3.6801	4.8825	10.2545	3206	QPR
1.7348	5.0	0.4629	1.4	0.2773	1.0	0.0839	0.3005	0.5331	1.4348	1.7571	4.9186	4958	QUP
0.7886	2.2	0.2883	0.8	0.0589	0.2	0.1255	0.3821	2.2491	5.4379	4.0591	14.2007	29	TRH
0.7538	2.6	0.3033	0.8	0.1772	0.7	0.1585	0.3139	0.4145	1.1622	0.5804	3.8478	23	TCH
1.0834	2.3	0.3858	0.9	0.1442	0.2	0.2299	0.4268	3.3018	5.2260	6.5454	12.9753	6455	TCD
1.1551	4.1	0.3778	1.2	0.2350	1.1	0.1049	0.3159	0.3846	1.1878	0.9355	3.8563	288	TC
1.5473	3.6	0.5381	1.5	0.2864	0.4	0.1702	0.4520	5.0202	5.6220	7.2447	11.6560	847	TK
2.5239	5.4	0.5763	1.5	0.2710	0.8	0.1854	0.3457	0.3467	1.9416	1.7703	6.2862	80	TA
1.7046	4.7	0.5579	1.9	0.3594	1.0	0.1394	0.4308	0.7516	2.1414	2.0386	5.3574	194	TRA
1.1612	3.8	0.4805	1.5	0.1996	0.7	0.2150	0.4386	0.8821	2.1851	1.0940	5.2348	310	KMO
2.0346	4.4	0.6960	1.7	0.2336	0.7	0.1570	0.4174	0.7996	2.5893	1.8125	6.5714	255	KMA
2.1581	4.6	0.6152	1.5	0.3439	0.9	0.1167	0.3400	0.6671	1.6808	1.7255	5.1323	204	KM
1.6841	5.7	0.4960	1.5	0.2620	0.6	0.1238	0.2892	1.0043	2.7336	2.3701	9.6282	263	KP
1.1708	6.9	0.3336	1.8	0.2039	1.3	0.0704	0.2704	0.2523	1.3588	1.0753	5.1978	72	OCS
2.3654	9.3	0.7245	2.5	0.1625	1.2	0.0286	0.2704	0.8242	2.2264	2.7767	8.1973	45	CU
3.6361	9.9	0.4597	3.0	0.2124	1.1	0.1303	0.3067	0.6013	2.6724	1.8437	9.3855	73	XGR
1.5837	8.1	0.4115	2.1	0.1401	1.0	0.0510	0.2598	0.4389	2.1253	1.5009	8.3244	89	XS
1.4603	7.0	0.4688	1.8	0.1926	1.0	0.0726	0.2613	0.5603	1.9036	1.5586	7.4070	598	XHG
1.4814	10.7	0.4756	2.1	0.4390	1.9	0.0306	0.1970	0.4038	1.2026	1.6066	6.0009	43	XCS
1.0341	9.3	0.3409	2.0	0.1967	1.8	0.0423	0.2216	0.2365	1.1596	0.5644	5.2457	242	XPC
1.1335	9.2	0.3925	2.0	0.2621	1.5	0.0415	0.2153	0.2585	1.2950	0.7230	6.0492	215	XWC
1.5317	9.1	0.4370	2.1	0.2502	1.4	0.0480	0.2265	0.3799	1.5322	1.2819	6.8259	1798	XW
1.4420	7.1	0.3713	1.7	0.1970	0.8	0.0436	0.2423	0.5193	2.2202	1.8408	9.2577	196	XPD
2.8038	9.1	1.0138	2.1	0.2707	1.2	0.0756	0.2252	0.8614	1.7476	2.0857	7.6036	486	PCGR
1.6310	6.6	0.5102	1.5	0.2276	1.1	0.0692	0.2319	0.6114	1.4757	2.2510	6.4649	403	PCG
0.5606	4.4	0.1710	1.2	0.0714	0.4	0.0466	0.2704	0.6205	2.6844	1.2937	9.9183	52	PCV
0.7296	6.6	0.3351	1.6	0.0693	0.6	0.0460	0.2445	0.6838	2.7555	1.0931	11.1627	22	UNK

Table IV.7 Mean (\bar{x}) and Standard Deviation (σ) for Each Geologic Type.

TABLE IV.8 Geologic Units with Significant Variations from Unimodal Distributions, Based on the Analysis of the eTh Histograms

Geologic Unit	No. Events	²⁰⁰ T _{1/2} Recommended Split (c/s)
Qma	4709	none
Qbs	224	none
Ql	266	46;
Qcm	4097	none
Qpb	3206	none
Qup	4954	none
Tc	288	none
Tk	847	51;
Kmo	310	47;
Kna	255	51;
Km	204	52;
Kp	259	47;
Xpc	242	none
PGgr	486	103;
PGg	403	none

TABLE IV.9 Summary of Anomalies

	^{208}Tl	^{214}Bi	$^{214}\text{Bi}/^{208}\text{Tl}$
ML1W	Qma,920-930;		Qup,310,460,695-700;
ML1E			Qma,4045-4055;Qcm,4100-4115,4150
ML2W	Qcm,1150-1165;		Qup,1335-1340,1360,1585,1605-1610;
ML3	Qcm,2715-2735,2760-2775	Qma,2770-2775;	Qup,2065,2310-2315;Qcm,3780-3800;
ML4E	Qcm,5905-5965;	Qup,025-040,065-070;	Qcm,5155
ML4W	Qup,460-470;		
ML5	Qma,1530-1540,1470,1450-1455,1200-1250;Qcm,1170-1185;	Qma,1205-1240;Qcm,1175-1180;	Qcm,2385;Qma,2730-2740;
ML6	Qpb,4165-4185,4200-4210,4230-4250;Tco,4250-4265,4280-4285;Qma,4665-4670;Km,5120-5125;	Tco,4255-4260;Qma,4670;Km,5120-5125;	Qbs,2850;Qma,2990;3000;Qcm,3030;Tco,3725-3730,3870;
ML7	Kmo,3100-3105,3150;Qcm,3320;Qpb,3615-3690;	Kmo,3105-3110;Qcm,3305-3310;Tk,3620;Tco,3700-3705;	Qpb,4240-4245,4265,Tco,4550;
ML8	Qpb,1430-1450;Tco,1460-1500;Qma,1525-1535;Qpb,1580-1610;Tk,1640-1660;Qma,1790-1825;Qup,2040-2055,2345;	Tco,1450,1470-1500;Qcm,1640-1660,1790-1795,1810-1815;Qup,2035-2065,2260;	Qma,475,540,610;Tco,625,670;
ML9	Tco,3340,3390;	Qma,2460;Tco,3380-3390;	Xw,1980;Qcm,2475,2490,2500;Tco,3220;Qma,3550;Tco,3615-3620;Qpb,3720;
ML10	Tco,3635-3640,3655-3680,3875;Kma,4960-4965,4980;	Tco,3660-3675;Kma,4510,4660-4670;Xw,5335-5340;	Kmo,4465;Qma,2960,3280-3290,3315;
ML11E		Qpb,1430,1530,1545;Qcm,1750-1760;Tk,1850-1870;Qma,1840;Tk,1880-1885;Tco,1910-1920;	Qpb,1835-1840;Tco,1880-1895,2160-2170;
ML11W			P6g,930;
ML12E	Qpb,1160-1175;	Qma,1050;Qcm,1135-1175;	Tco,510,550,570,580,650,690,700,725;Qpb,840-845,1210;
ML12W	P6gr,160-180;	P6gr,170-180;	Xpc,485;

(TABLE IV.9 Cont'd.)

	^{208}Tl	^{214}Bi	$^{214}\text{Bi}/^{208}\text{Tl}$
TL1			
TL2			Tco,2990;Qpb,3065-3070,3090;
TL3	Kma,050;		Qma,440;
TL4	Tco,4795-4800;		
TL5	Qcm,3165-3170;Qma,3120;	Qcm,3680-3690;	Qma,2960;
TL6	Qup,1345-1360,1200-1220,1235-1245;		P6g,2265;

TABLE IV.10 Radioactivity Anomalies per Geologic Map Unit

Geologic Unit	^{208}Tl	^{214}Bi	$^{214}\text{Bi}/^{208}\text{Tl}$
Qma	9	5	15
Qbs	0	0	2
Qcm	8	8	10
Qpb	7	3	8
Qup	6	4	9
Tco	8	6	13
Tk	1	3	0
Kmo	2	1	1
Kma	3	2	0
Km	1	1	0
Xpc	0	0	1
Xw	0	1	1
P6gr	1	1	0
P6g	0	0	2

TABLE IV.11 Statistical Summary of Radioactivity Anomalies by Geologic Unit

Geologic Unit	²⁰⁸ Tl	²¹⁴ Bi	²¹⁴ Bi/ ²⁰⁸ Tl
<u>Quaternary</u>			
No. of Units w/Anomalies	4	4	5
No. of Anomalies	30	20	44
<u>Tertiary</u>			
No. of Units w/Anomalies	2	2	1
No. of Anomalies	9	9	13
<u>Mesozoic</u>			
No. of Units w/Anomalies	3	3	1
No. of Anomalies	6	4	1
<u>Paleozoic/Precambrian</u>			
No. of Units w/Anomalies	1	2	3
No. of Anomalies	1	2	4
<u>Total Sample</u>			
No. of Units w/Anomalies	10	11	10
No. of Anomalies	46	35	62

(...) denotes negative anomaly

Relationship between Radioactivity Anomalies and the Geologic Map Units

Quaternary Geologic Units: Qma,Qbs,Qcm,Qpb,Qup

²⁰⁸Tl Anomalies

Sixty-five percent of the ²⁰⁸Tl anomalies occur in four Quaternary units, these units occupy some fifty percent of the surveyed area. The radiometric anomalies are evenly distributed amongst the four units (Qma,9; Qcm,8; Qpb,7 and Qup,6). Great variety in type and lithology of the sediments occurs in all four units. This, coupled with considerable variation in near-surface drainage and water-table conditions, probably accounts for most of the anomalous readings. However, placer deposits with minerals derived from the Piedmont may occur. There are no incidences of ²⁰⁸Tl anomalies coinciding with ratio anomalies.

²¹⁴Bi and ²¹⁴Bi/²⁰⁸Tl Anomalies

Fifty-seven percent of the ²¹⁴Bi anomalies, and seventy percent of the ²¹⁴Bi/²⁰⁸Tl anomalies, occur in four and five, respectively, of the Quaternary units. These units occupy some fifty percent of the surveyed area. None of the ²¹⁴Bi anomalies coincide geographically with the ratio anomalies. Most of the anomalies are thought to be the result of either intra-unit changes in lithology or intra-unit changes in near-surface hydrology. In some cases, there may be placer deposits with material derived from the crystalline Piedmont rocks.

Tertiary Geologic Units: Tco,Tk

²⁰⁸Tl Anomalies

Almost twenty percent of the ²⁰⁸Tl anomalies occur in two Tertiary units, Tco and Tk. Most of the anomalies are in the Tco unit (8), which occupies over nineteen percent of the surveyed area. None of the anomalies coincide with ratio anomalies. Unless some of the deposits are placer, most of the anomalies are due to intra-unit changes in lithology and variations in lithofacies.

²¹⁴Bi and ²¹⁴Bi/²⁰⁸Tl Anomalies

Twenty-five percent of the ²¹⁴Bi anomalies, and almost twenty-one percent of the ²¹⁴Bi/²⁰⁸Tl anomalies, occur in two and one, respectively, of the geologic units. All of the ratio anomalies and two-thirds of the ²¹⁴Bi anomalies in the Tertiary units occur in unit Tco. Tco occupies some nineteen percent of the surveyed area. None of the the ²¹⁴Bi anomalies coin-

cide with ratio anomalies. Unless some of the anomalies are placer deposits, which are also rich in thorium minerals, it seems unlikely that any of the ²¹⁴Bi anomalies are associated with significant uranium ore concentrations.

Mesozoic Geologic Units: Kmo,Kna,Km

²⁰⁸Tl Anomalies

Some thirteen percent of the ²⁰⁸Tl anomalies occur in three Mesozoic units, which occupy two to three percent of the surveyed area. None of the ²⁰⁸Tl anomalies coincide with ratio anomalies. Placer deposits are the most likely source of thorium-rich minerals within the Mesozoic units.

²¹⁴Bi and ²¹⁴Bi/²⁰⁸Tl Anomalies

Greater than eleven percent of the ²¹⁴Bi, but less than two percent of the ²¹⁴Bi/²⁰⁸Tl anomalies, occur in Mesozoic units. The units occupy less than three percent of the surveyed area. None of the ²¹⁴Bi anomalies coincide geographically with the ratio anomalies. Most of the ²¹⁴Bi anomalies are thought to be associated with either intra-unit changes in lithology or with lithofacies changes. Some may be associated with uranium and thorium-rich minerals in placer deposits.

Paleozoic and Precambrian Geologic Units: Xpc,Xw,PGgr,PGg

²⁰⁸Tl Anomalies

One ²⁰⁸Tl anomaly occurs in the PGgr unit. It may be associated with a vein deposit, a pegmatite, or a change in lithology within the granite gneiss. It does not coincide geographically with a ratio anomaly.

²¹⁴Bi and ²¹⁴Bi/²⁰⁸Tl Anomalies

Greater than five percent of the ²¹⁴Bi anomalies, and six percent of the ratio anomalies, occur in two and three, respectively, of the Paleozoic/Precambrian geologic units. These units occupy greater than six and seven percent, respectively, of the surveyed area. None of the ²¹⁴Bi anomalies coincide with ratio anomalies. Most of the anomalies are thought to be associated with intra-unit changes in lithology; some, however, may be associated with either vein or pegmatite units.

Relationship between Radioactivity Anomalies and Known Occurrences of Radioactive Minerals

There does not appear to be any coincidence between the location of the radioactivity anomalies, and specific sites, where radioactive minerals or anomalous radioactivity have been previously recorded.

Relationship between the Occurrence of Radioactivity Anomalies and Cultural Features

^{208}Tl Anomalies

An anomaly on ML2, station 1150-1160, is near the Dover Air Force Base in Kent County, Delaware.

^{214}Bi Anomalies

Three ^{214}Bi anomalies on ML11, between stations 1450 and 1550, are near the Marlton urban area, on the eastern side of Philadelphia.

$^{214}\text{Bi}/^{208}\text{Tl}$ Anomalies

Two ratio anomalies on ML6, stations 3725-3730 and 3870, are southeast and south of the town of Vereland in New Jersey.

Trends

^{208}Tl Anomalies

The eastern half of the map sheet has very few ^{208}Tl anomalies. The westcentral portion of the map area, in southwestern New Jersey and northern Delaware, has the greatest concentration.

A large cluster of anomalies is noted between TL4 and TL6 and ML4 and ML8. The area involved has a variety of Cretaceous, Middle and Early Tertiary, and Quaternary outcrops. It lies on either side of the Delaware River, to the south of Philadelphia.

^{214}Bi Anomalies

The distribution of ^{214}Bi anomalies is extremely uneven throughout the surveyed area. Two major clusters are apparent.

East of Philadelphia, north of ML10 and west of TL2, ^{214}Bi anomalies occur over Quaternary, Tertiary and Cretaceous outcrops.

South of Philadelphia, between TL4 and TL6, and north of ML5, a larger cluster occurs on both the eastern and western sides of the Delaware River. The anomalies occur over a variety of Mesozoic and Cenozoic outcrops.

$^{214}\text{Bi}/^{208}\text{Tl}$ Anomalies

The ratio anomalies are unevenly distributed throughout the map area. Very few ratio anomalies occur in the central portion of the surveyed area or in the northwestern corner in Pennsylvania. Two areas of anomaly concentration occur.

In the northeastern quadrant, north of ML8 and east of TL3, a large number of anomalies are recorded over the Quaternary and Tertiary units of the New Jersey Coastal Plain. Most of these ratio anomalies have very limited areal extent.

In the southwestern corner, to the west of Delaware Bay, anomalies occur on ML1, ML2 and ML3. Most of these anomalies occur over the Quaternary units.

3. Summary and Recommendations

The area can be divided into two major physiographic and geologic units; the crystalline rocks of the Piedmont and the sedimentaries of the Coastal Plain. The Piedmont area is small, and confined to the northwestern corner of the map area. It has very few anomalies. Most of the anomalies are in the Coastal Plain. The ^{214}Bi and ^{208}Tl anomalies concentrate in the central part of the map area, in western New Jersey and northern Delaware. Mainly they are to the south of Philadelphia. The anomalies crop-out in a variety of sedimentary units, which range in age from Quaternary to Cretaceous. The ^{214}Bi anomalies are also concentrated in the area to the east of Philadelphia, in the Mesozoic and Cenozoic outcrops. The $^{214}\text{Bi}/^{208}\text{Tl}$ anomalies are mainly in the northeastern corner of the surveyed area over the New Jersey Coastal Plain.

Most of the anomalies are in Quaternary units, or in the extensive Cohansy Formation. The Quaternary units and the Cohansy occupy seventy percent of the surveyed area. None of the ^{214}Bi or ^{208}Tl anomalies coincide geographically with ratio anomalies. A number of ^{208}Tl anomalies do coincide with ^{214}Bi anomalies. The anomalies in the Quaternary units are thought to be associated mainly with intra-unit changes in lithology or near-surface hydrology. However, placer deposits may occur within the Quaternary units.

F. NATIONAL GAMMA RAY MAP SERIES (NGRMS)

The geologic base has been photographically screened to allow emphasis of the flight line locations and of the information regarding data analysis. These maps are used as the base for presenting statistical information on the six variables:

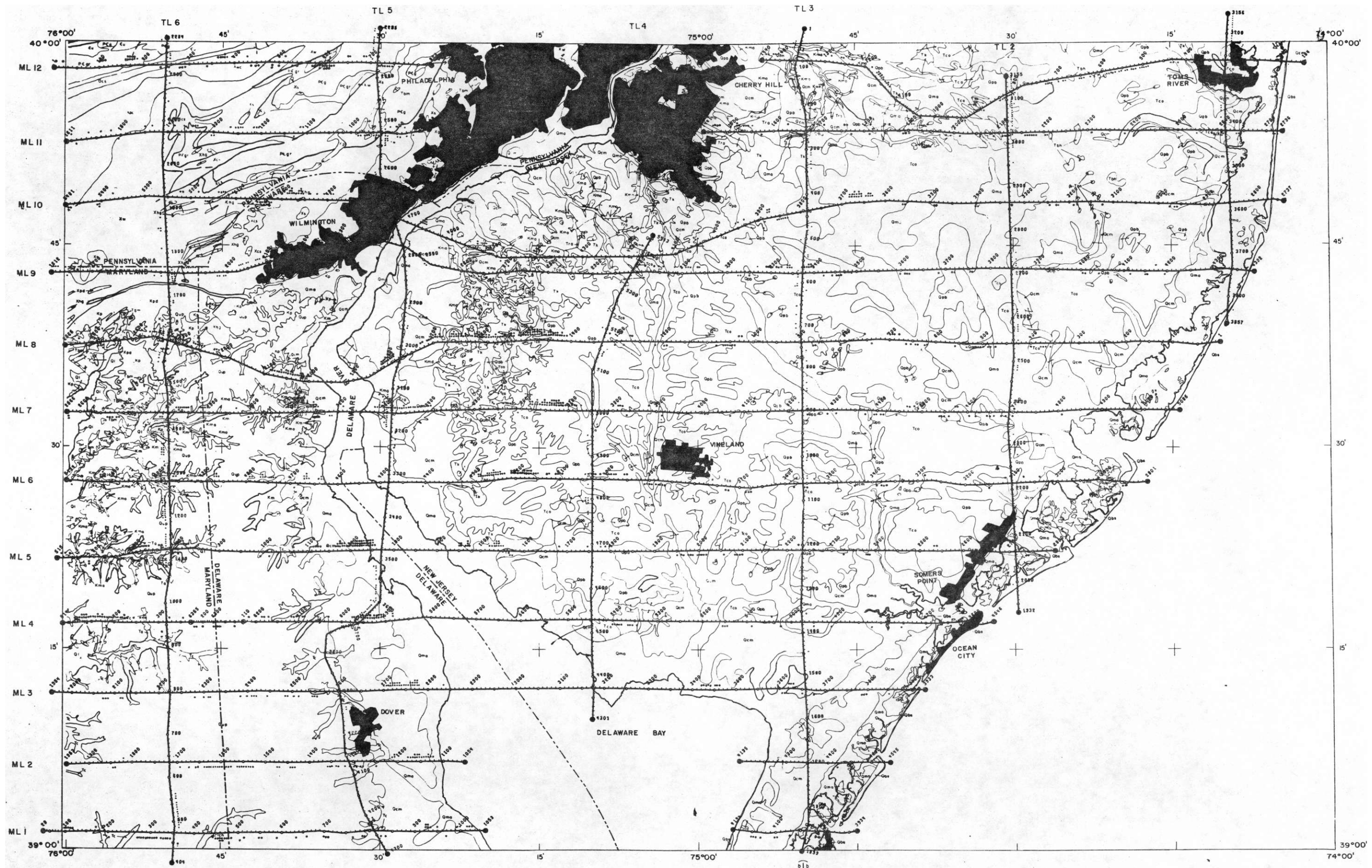
- * ^{208}Tl
- * ^{214}Bi
- * ^{40}K
- * $^{214}\text{Bi}/^{208}\text{Tl}$ Ratio
- * $^{214}\text{Bi}/^{40}\text{K}$ Ratio
- * $^{208}\text{Tl}/^{40}\text{K}$ Ratio

The six NGRMS sheets are presented in Figures IV.(1-6) of this report at a scale of 1:500,000 and as separate sheets at a scale of 1:250,000.

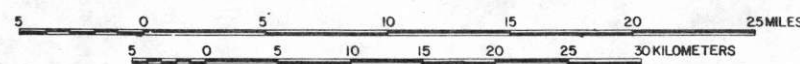
The statistical information is summarized on these maps through the utilization of one, two or three dots above or below the flight line at every fifth data point. One dot above the line indicates that the variable value at that point is between 1σ and 2σ greater than the mean value for that geologic type where σ values are determined for each geologic type based on all flight line data from the area, as is discussed further in Section V.B.4. Two dots indicate values between 2σ and 3σ , and three dots show values greater than 3σ . Dots below the line indicate the variable values which are less than the mean value by 1, 2 or 3σ in the same manner.

G. LINE PRINTER CONTOURS

Printer contours have been generated at a 1:500,000 scale for seven variables (eTh, eU, K, eU/eTh, eU/K, eTh/K, RMag, respectively). They appear in Appendix IV. Note that every alternate contour interval is composed of blanks to help delineate contour boundaries. Dots are used where the denominator value for a ratio is approaching zero, and to denote non-data areas.



GEODATA INTERNATIONAL, INC.
 7035 JOHN W. CARPENTER FRWY. DALLAS, TEXAS 75247
 NATIONAL GAMMA RAY MAP SERIES

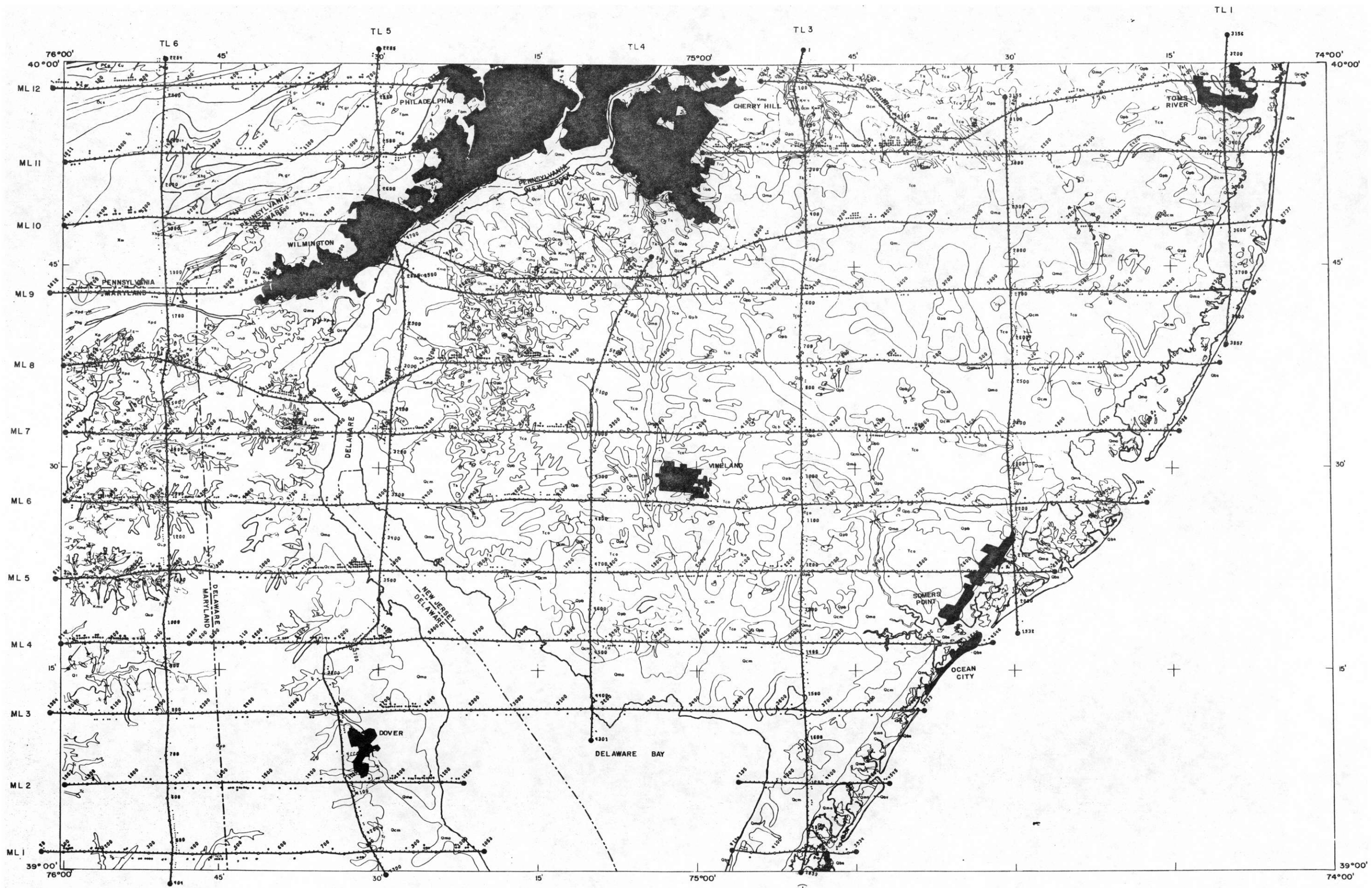


WILMINGTON, DELAWARE

208 T1 ± STANDARD DEVIATIONS



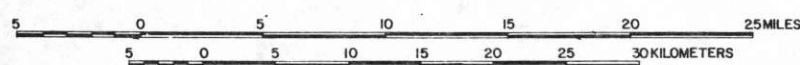
Figure IV.1 National Gamma Ray Map Series
 IV.19a



GEODATA INTERNATIONAL, INC.
 7035 JOHN W. CARPENTER FRWY. DALLAS, TEXAS 75247
 NATIONAL GAMMA RAY MAP SERIES

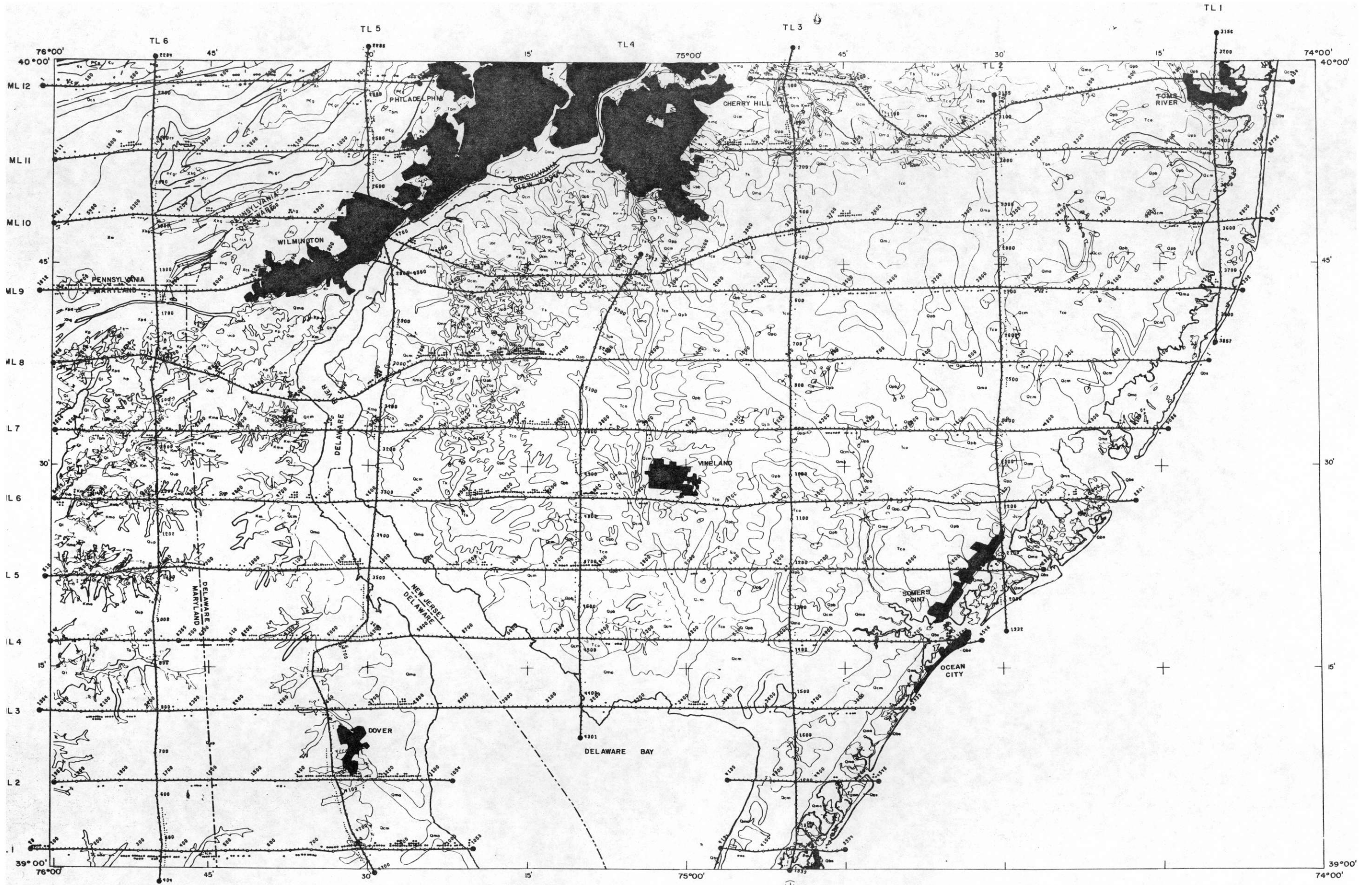


Figure IV.2 National Gamma Ray Map Series
 IV.19b



WILMINGTON, DELAWARE

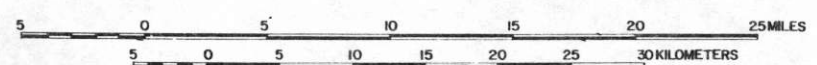
24 BI ± STANDARD DEVIATIONS



GEODATA INTERNATIONAL, INC.
 7035 JOHN W. CARPENTER FRWY. DALLAS, TEXAS 75247
 NATIONAL GAMMA RAY MAP SERIES

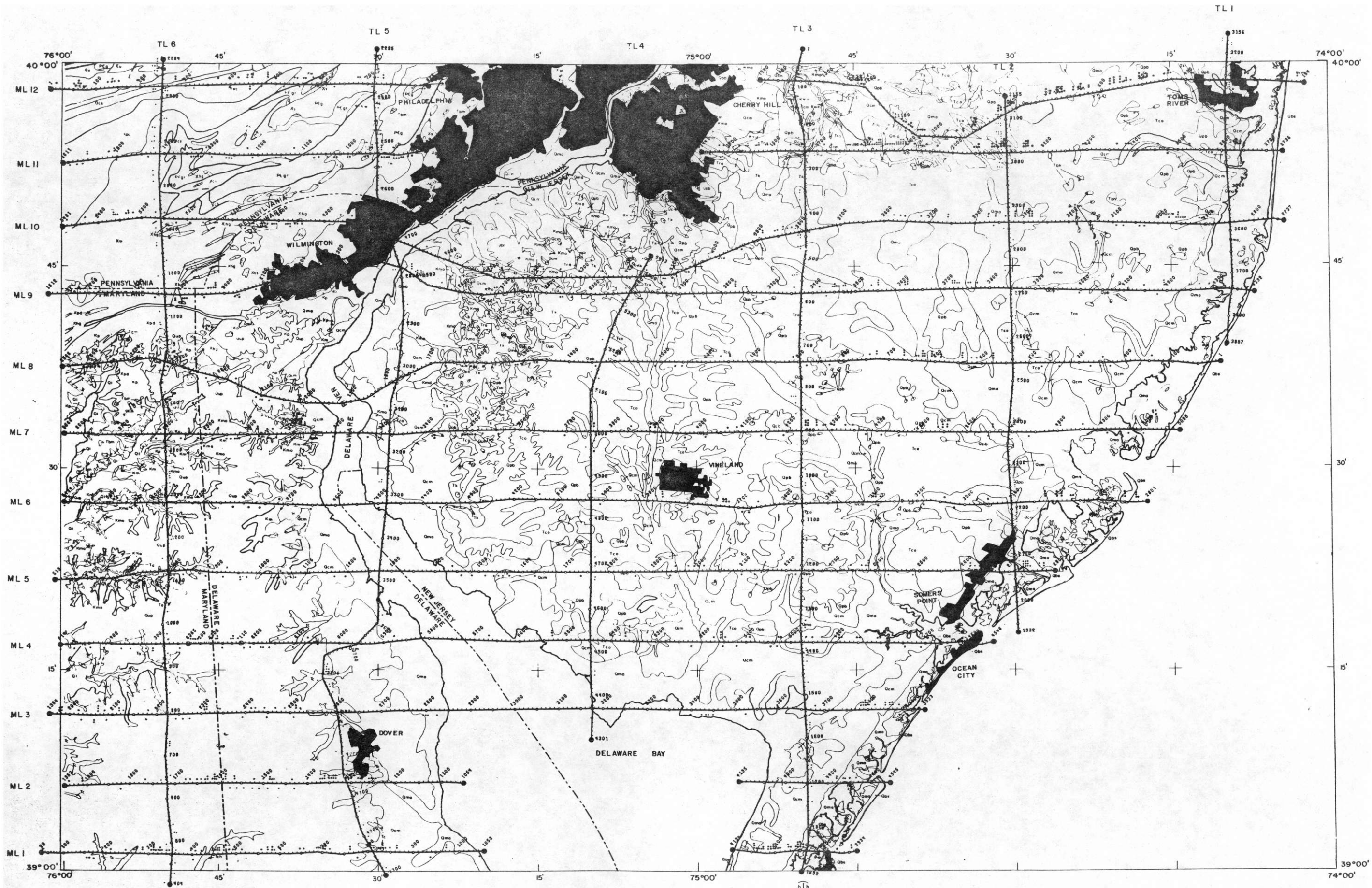


Figure IV.3 National Gamma Ray Map Series
 IV.19c



WILMINGTON, DELAWARE

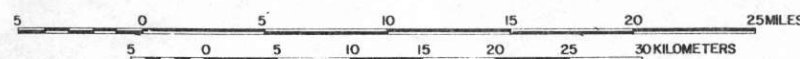
40K ± STANDARD DEVIATIONS



GEODATA INTERNATIONAL, INC.
 7035 JOHN W. CARPENTER FRWY. DALLAS, TEXAS 75247
 NATIONAL GAMMA RAY MAP SERIES

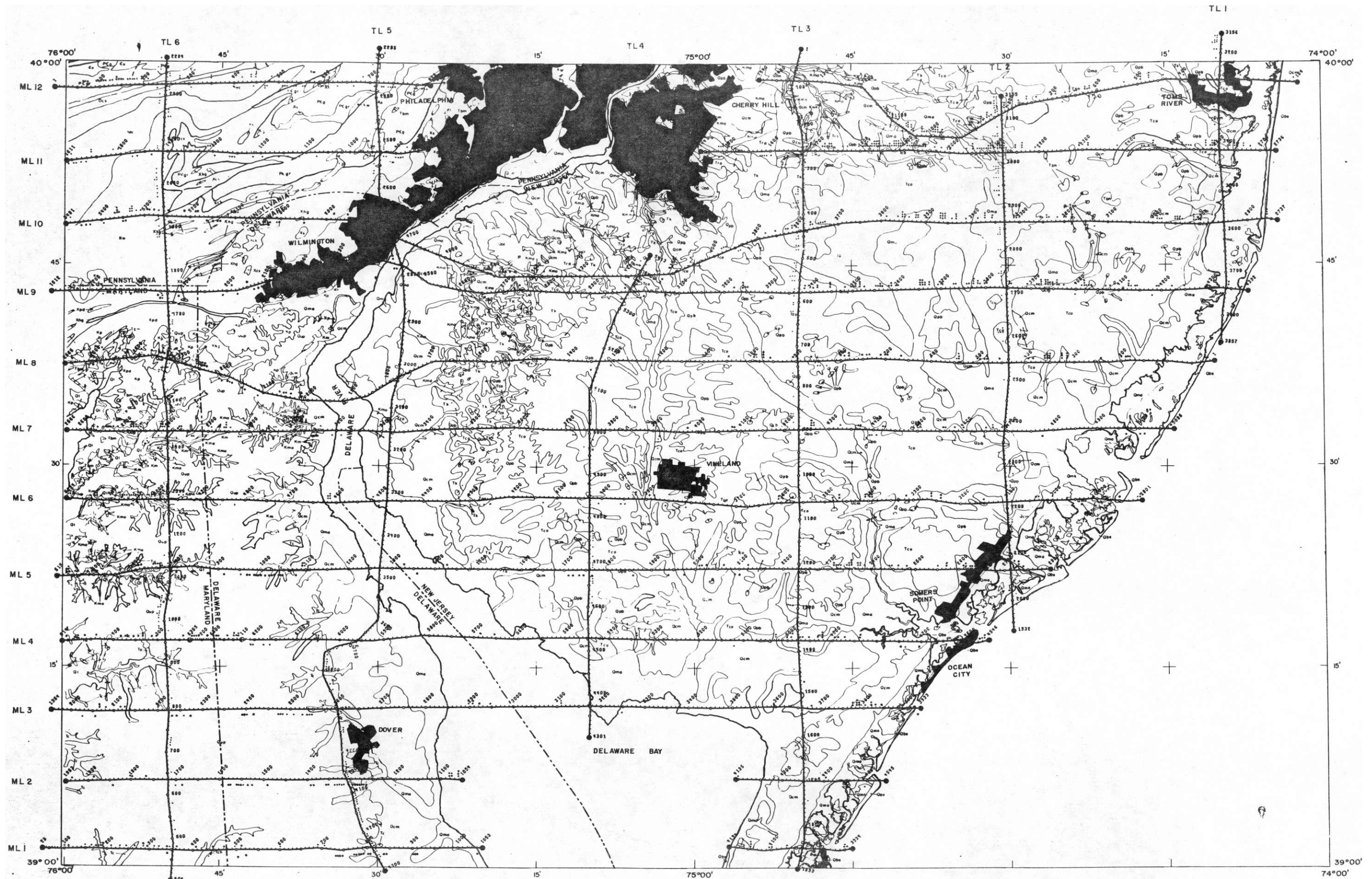


Figure IV.4 National Gamma Ray Map Series
 IV 19d



WILMINGTON, DELAWARE

214 B1 / 208 T 2 ± STANDARD DEVIATIONS

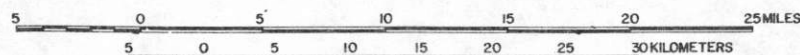


GEODATA INTERNATIONAL, INC.
 7035 JOHN W. CARPENTER FRWY. DALLAS, TEXAS 75247

NATIONAL GAMMA RAY MAP SERIES

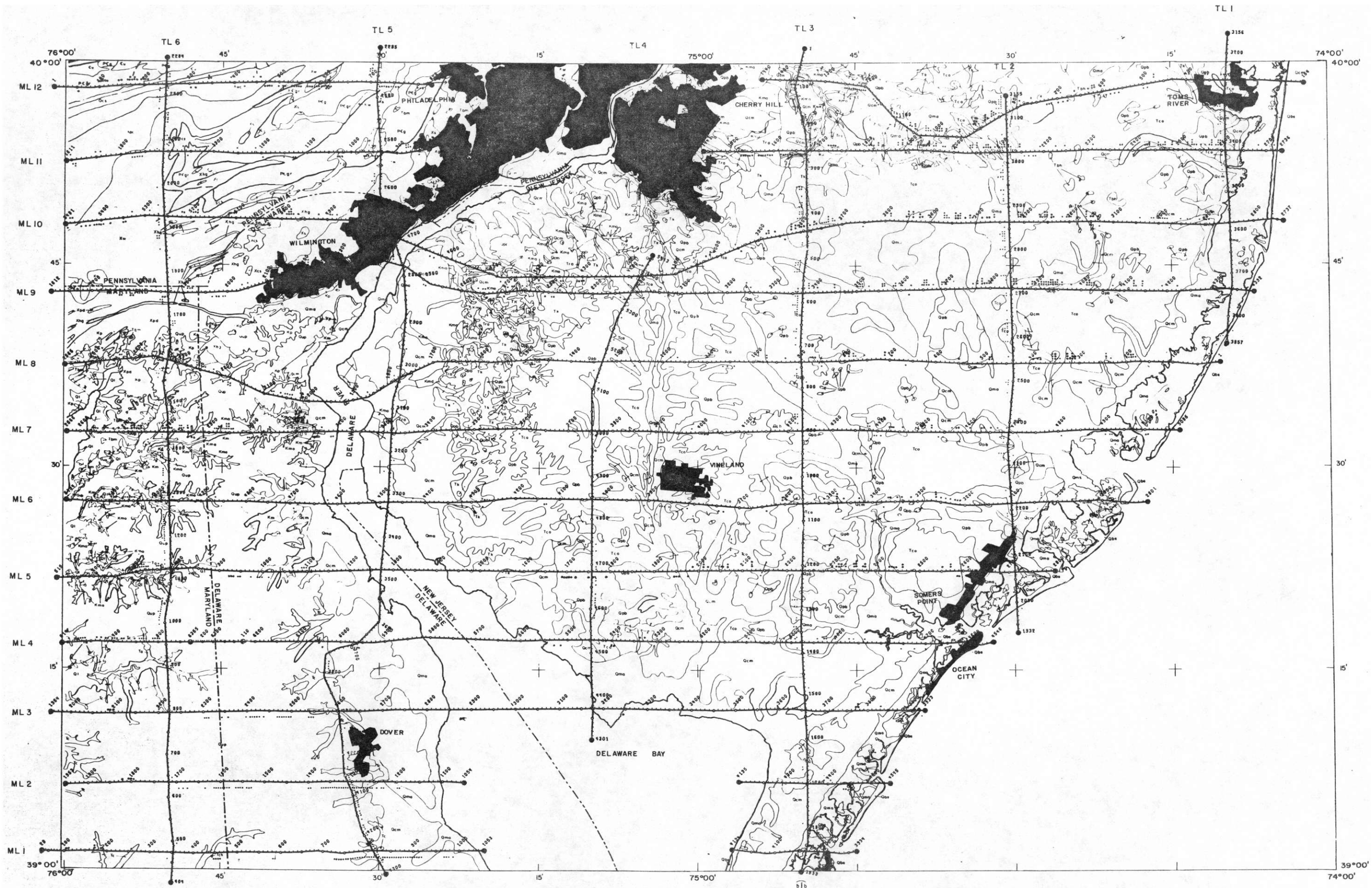


Figure IV.5 National Gamma Ray Map Series
 IV.19e



WILMINGTON, DELAWARE

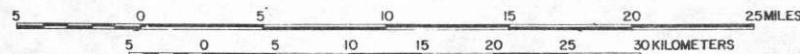
$214 \text{ Bi} / ^{40} \text{K} \pm \text{STANDARD DEVIATIONS}$



GEODATA INTERNATIONAL, INC.
 7035 JOHN W. CARPENTER FRWY DALLAS, TEXAS 75247
 NATIONAL GAMMA RAY MAP SERIES



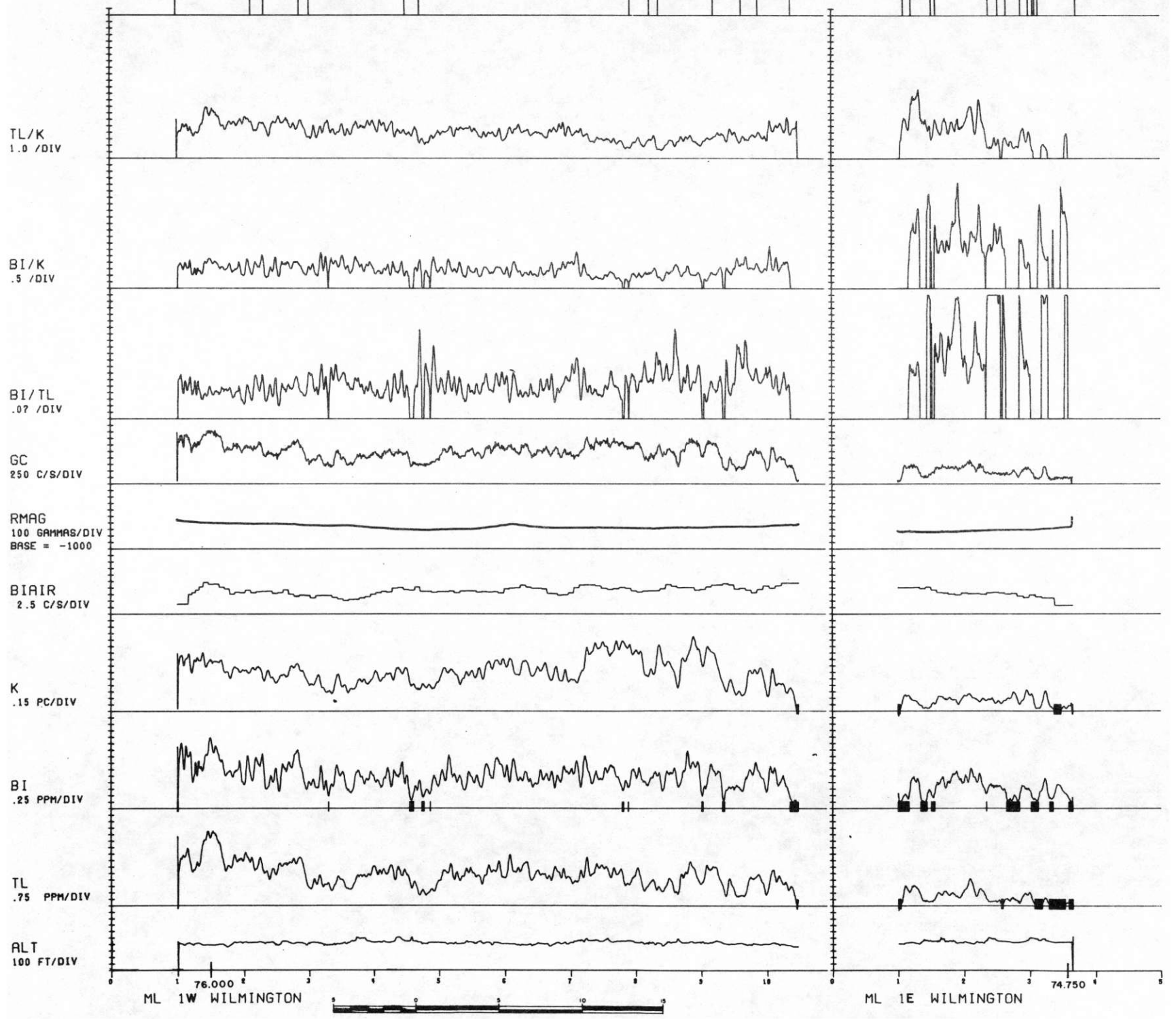
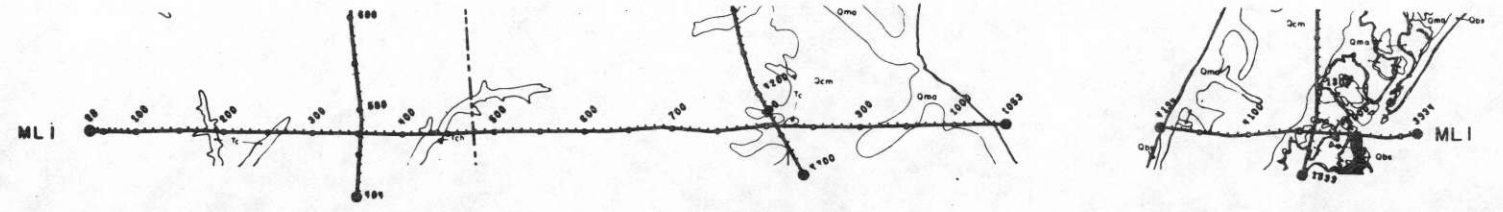
Figure IV.6 National Gamma Ray Map Series
 IV.19f

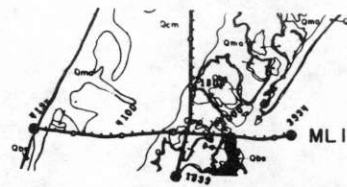
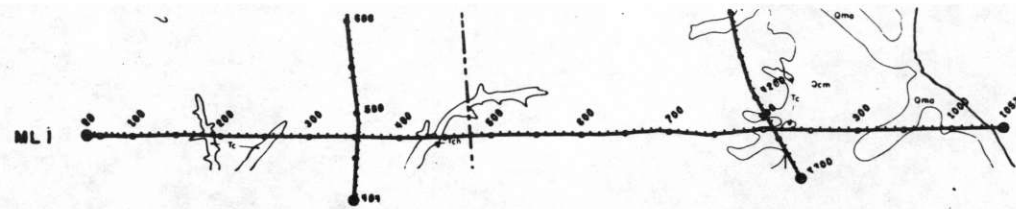


WILMINGTON, DELAWARE

208 T1/40K ± STANDARD DEVIATIONS

H. STACKED DATA PROFILES AND GEOLOGIC HISTOGRAMS





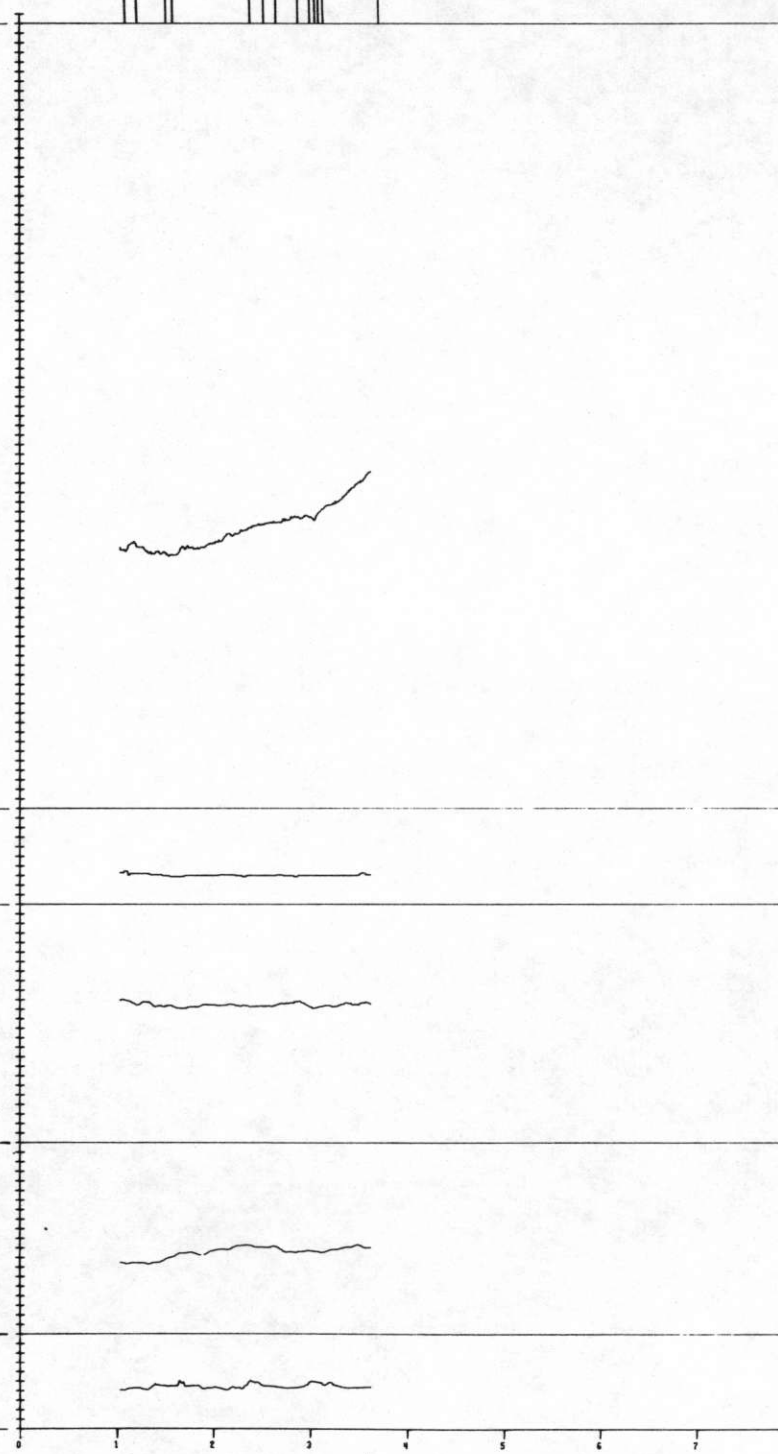
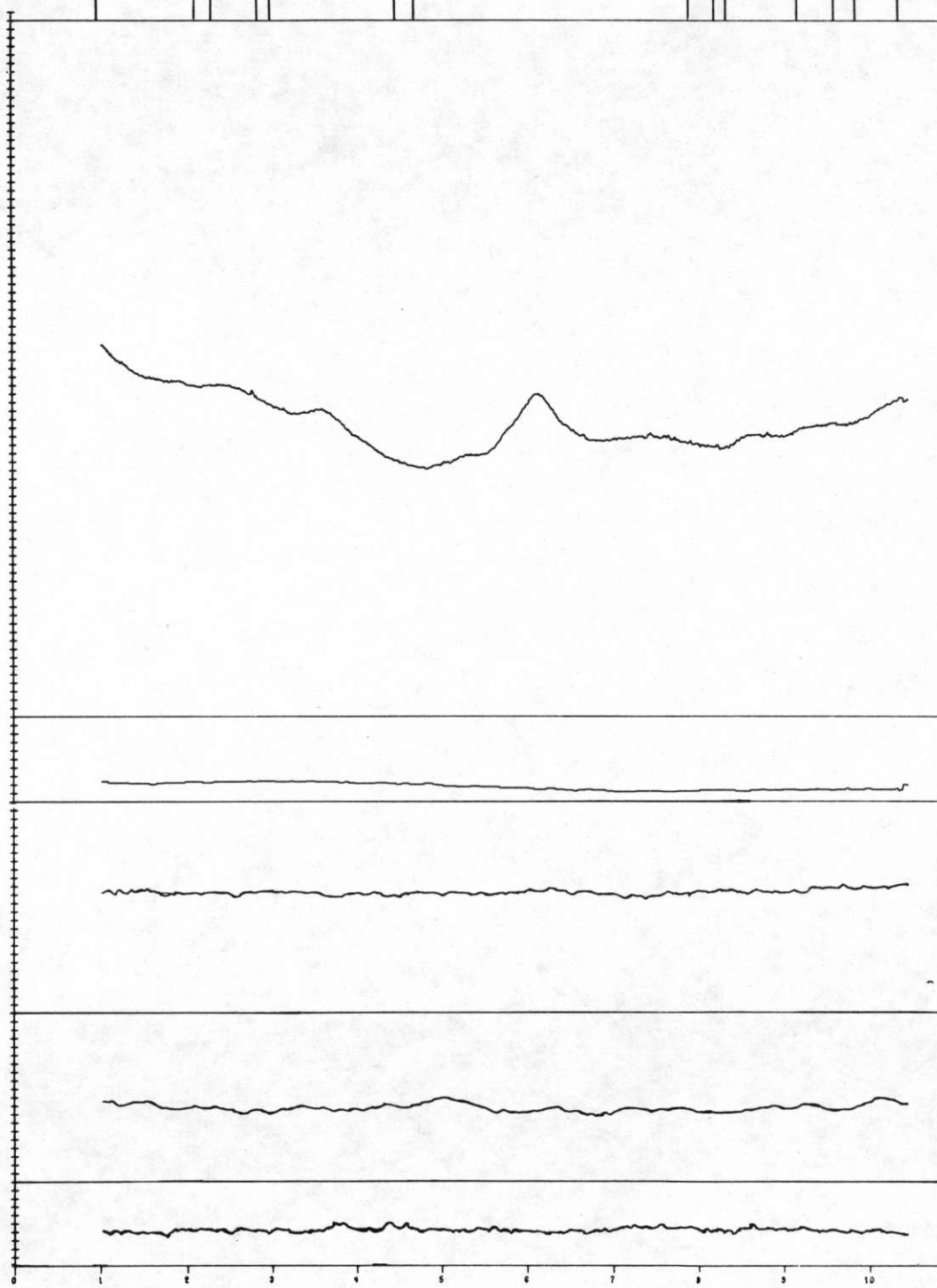
RMAG
10 GAMMA/DIV
BASE = -1000

BMAG
10 GAMMA/DIV
BASE = 54180

BP
3 MM HG/DIV
BASE = 700

TEMP
1 DEG C/DIV
BASE = 15

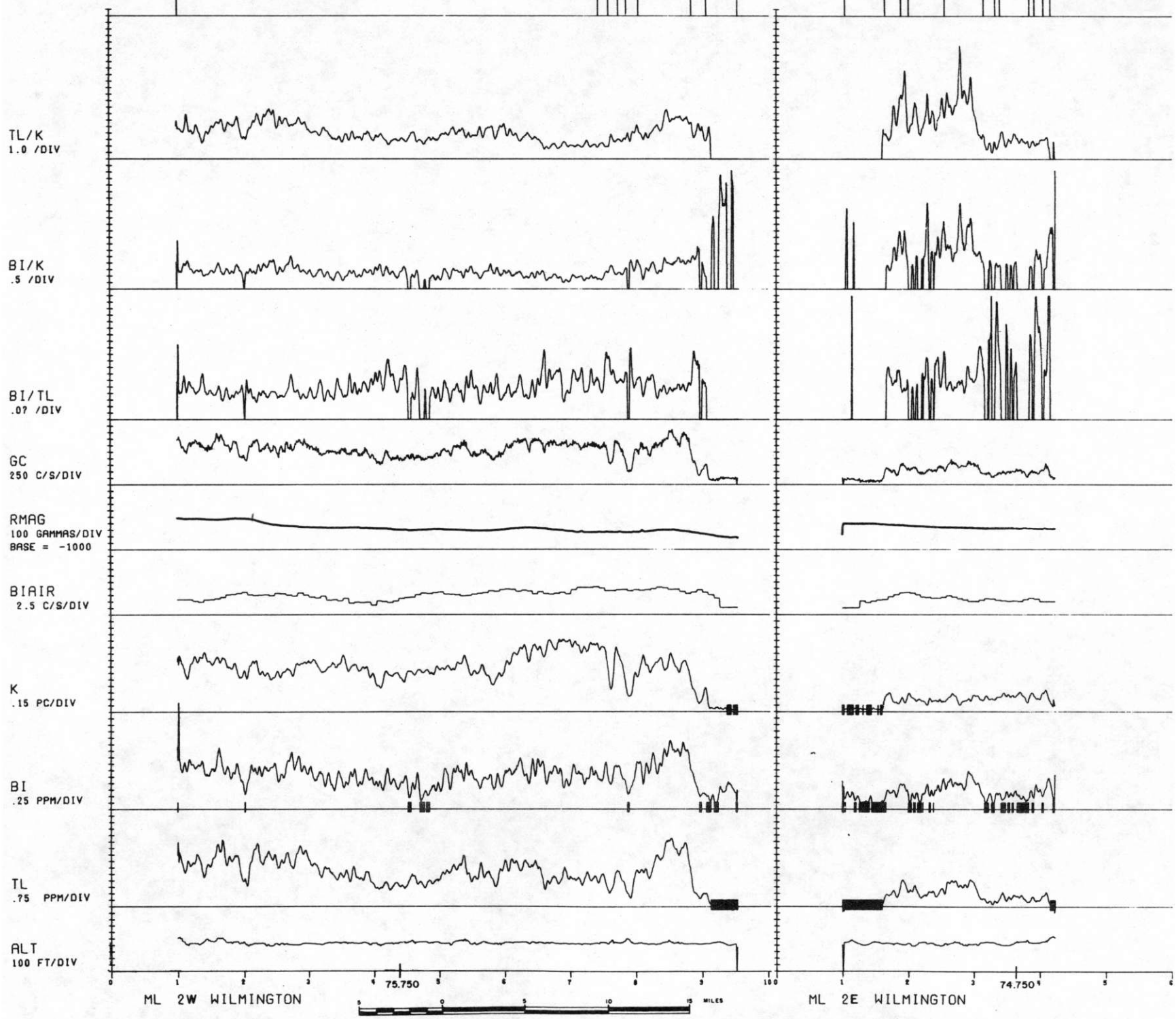
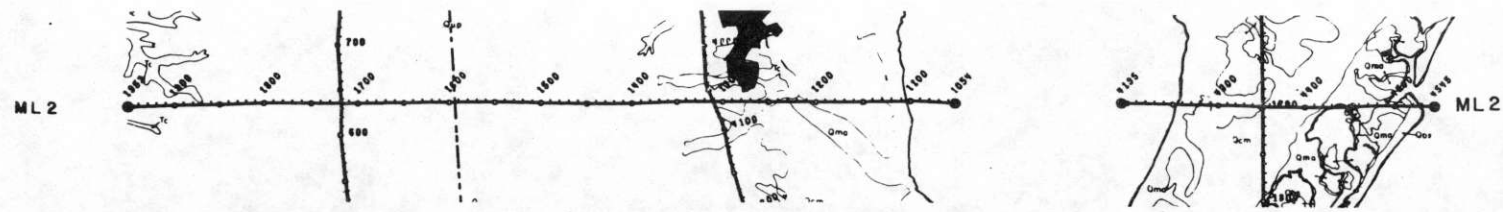
ALT
100 FT/DIV

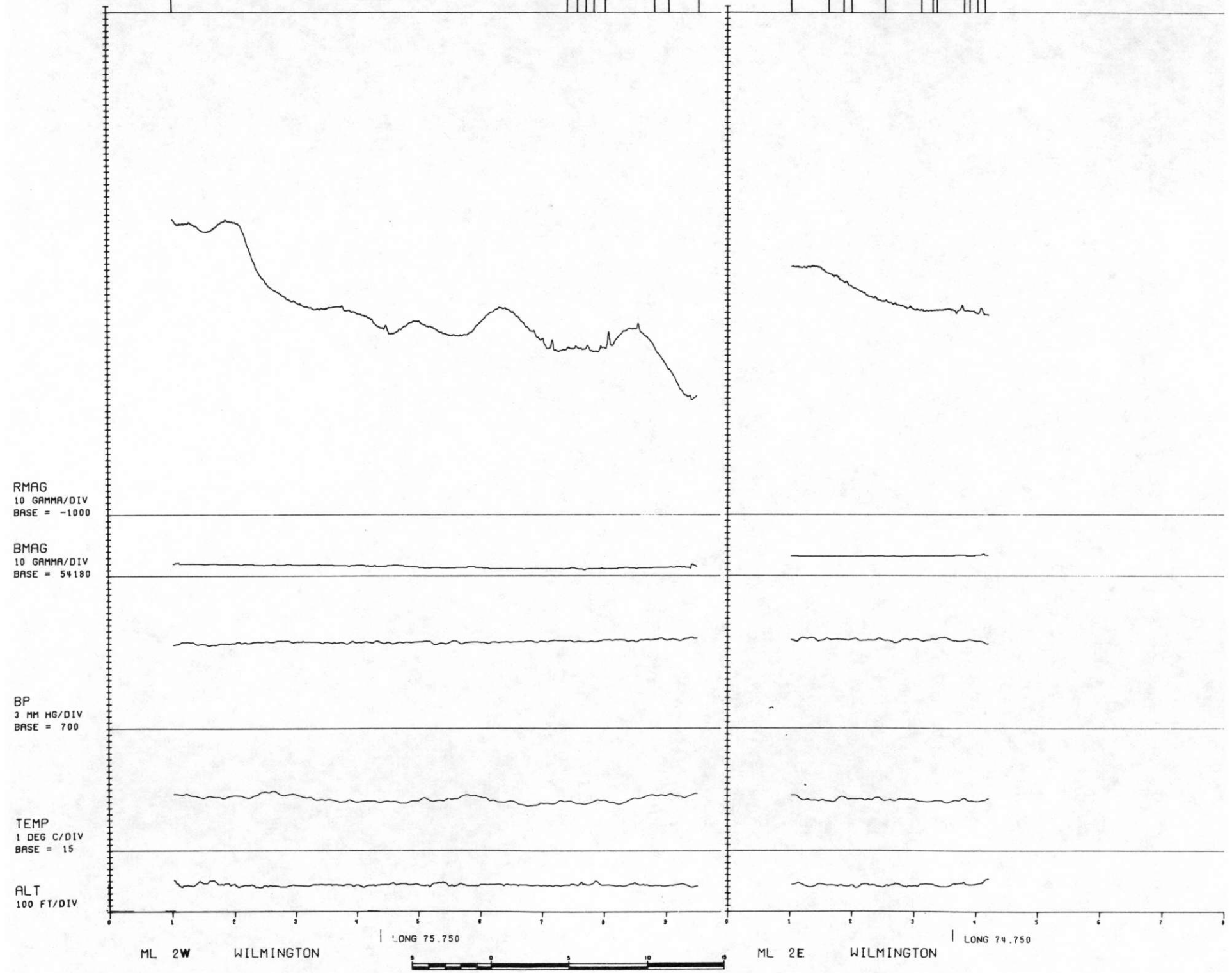
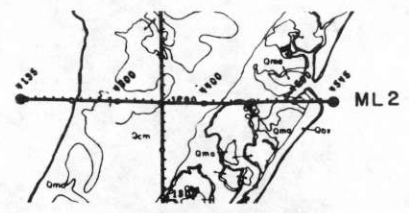
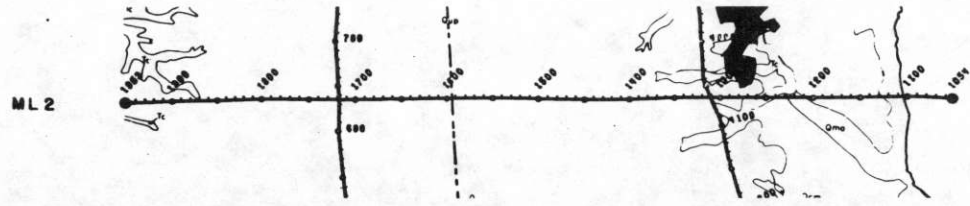


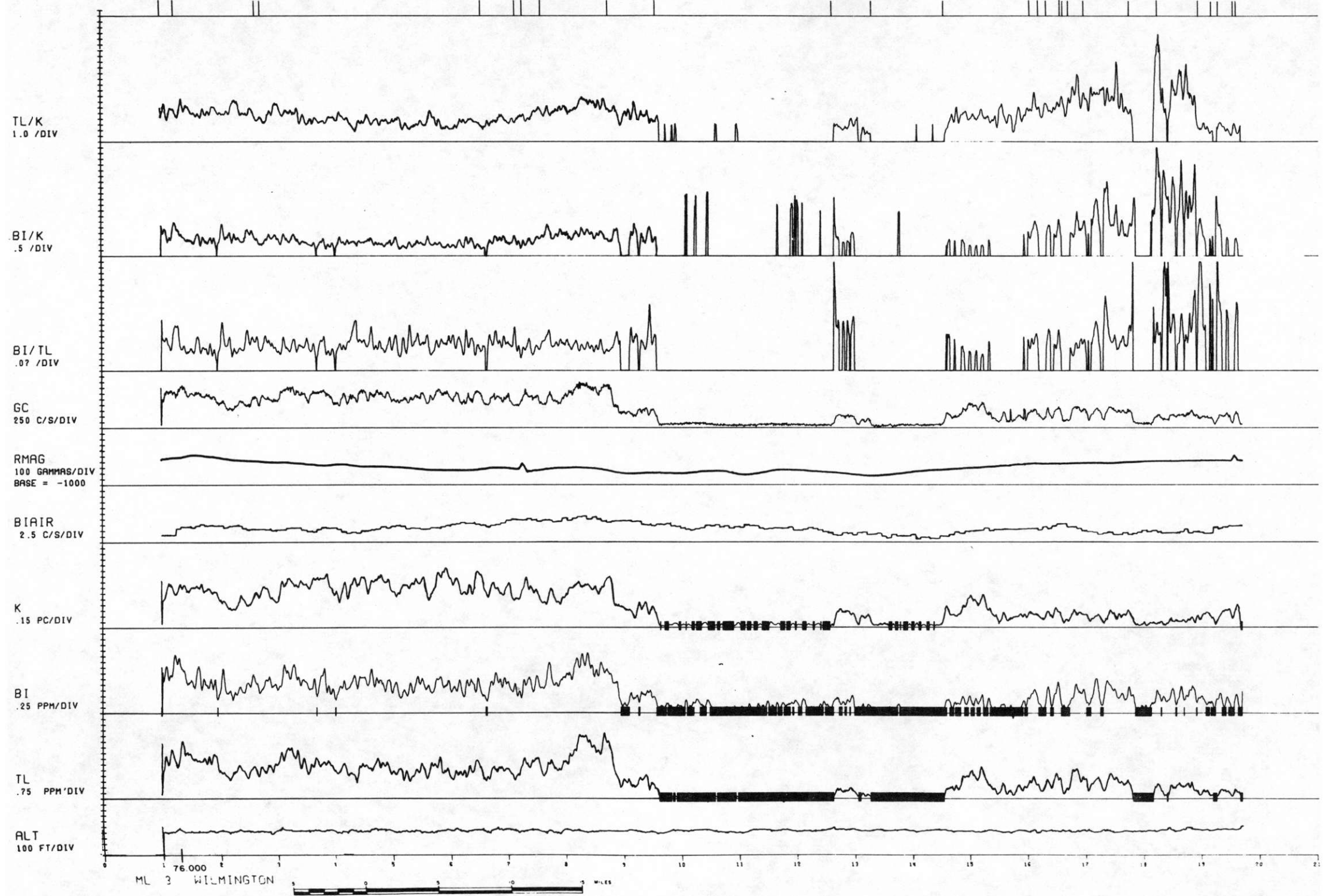
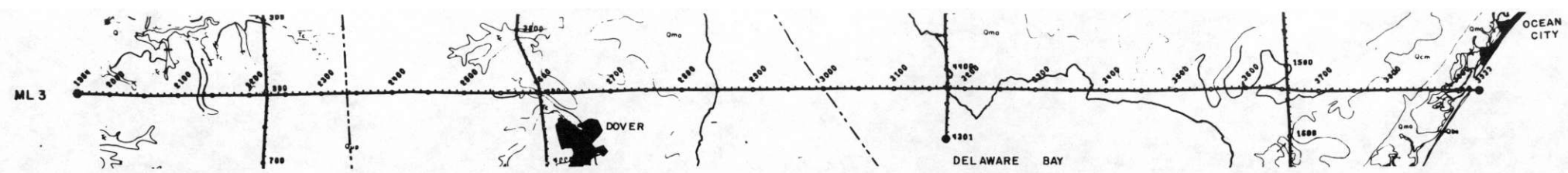
ML 1 | LONG 76.000
WILMINGTON

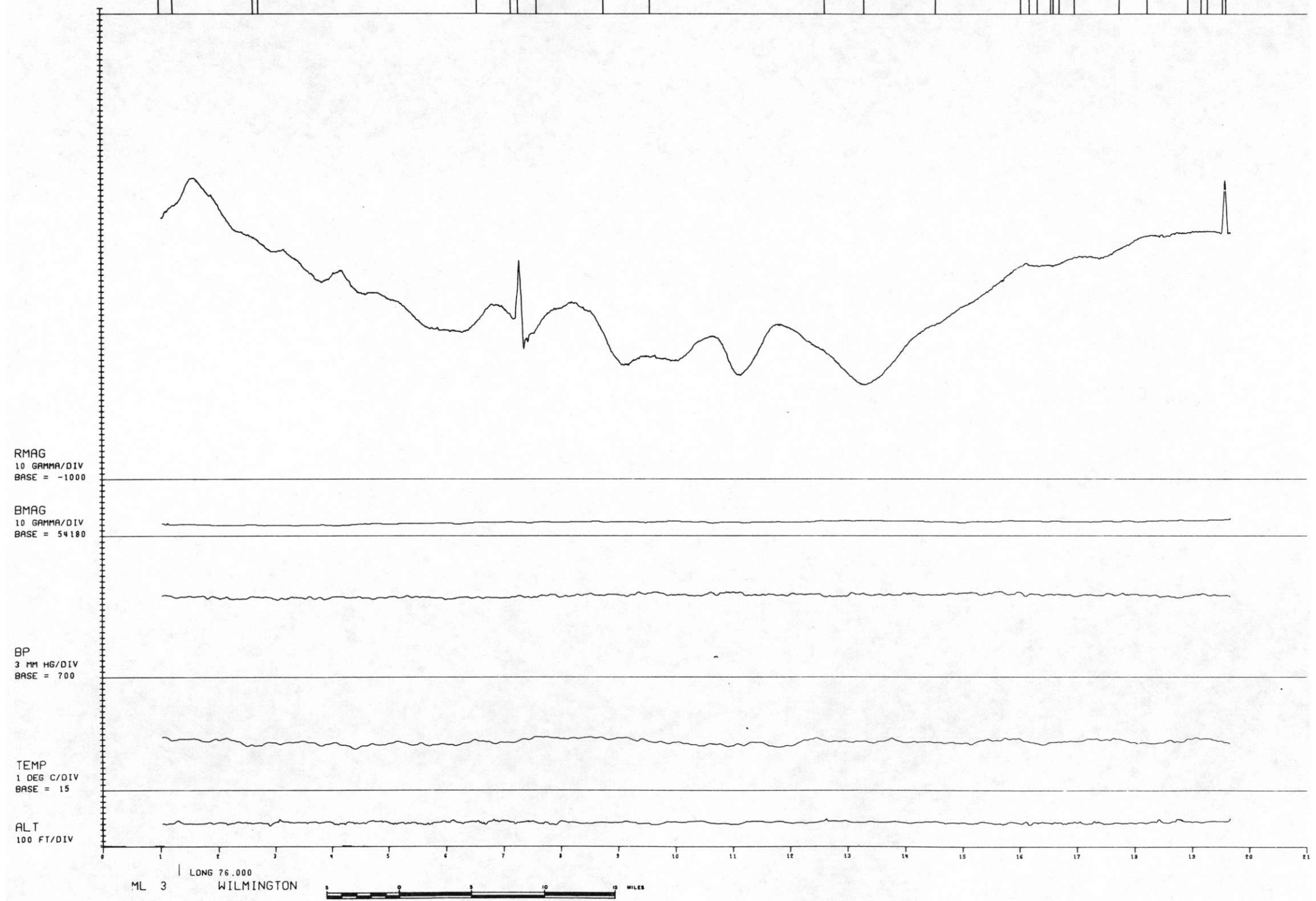
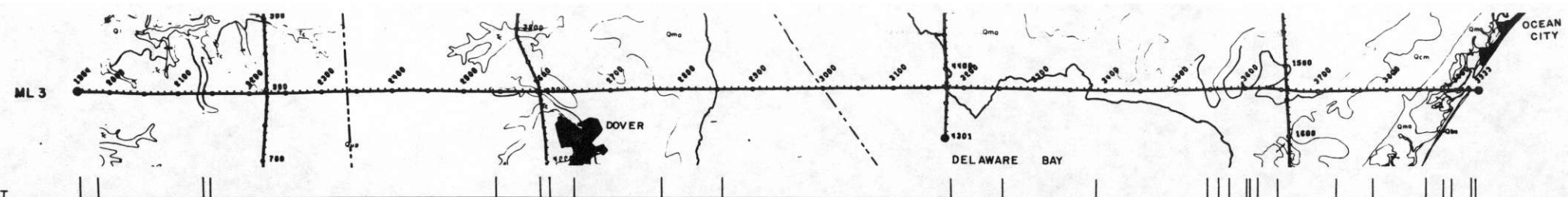
0 5 10 MILES

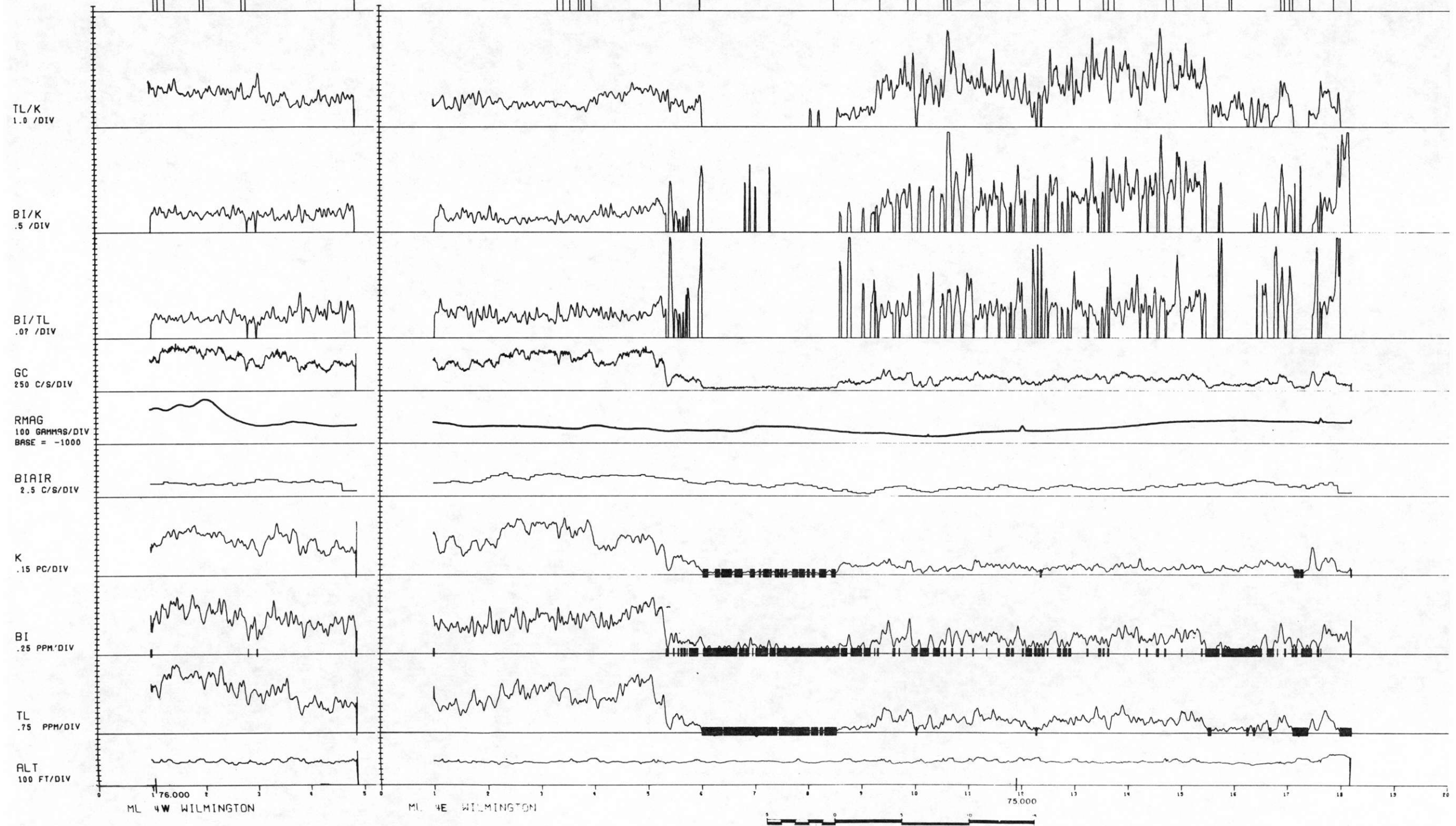
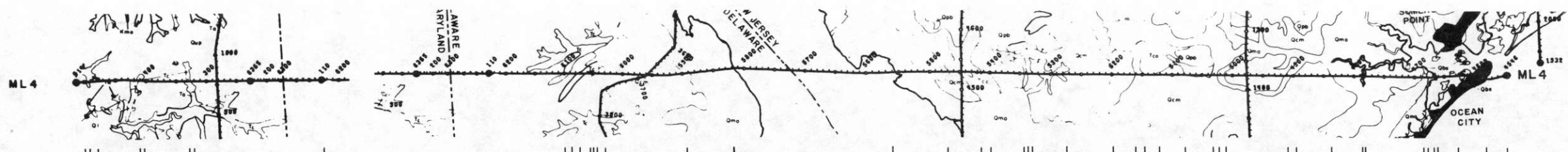
ML 1 | LONG 74.750
WILMINGTON

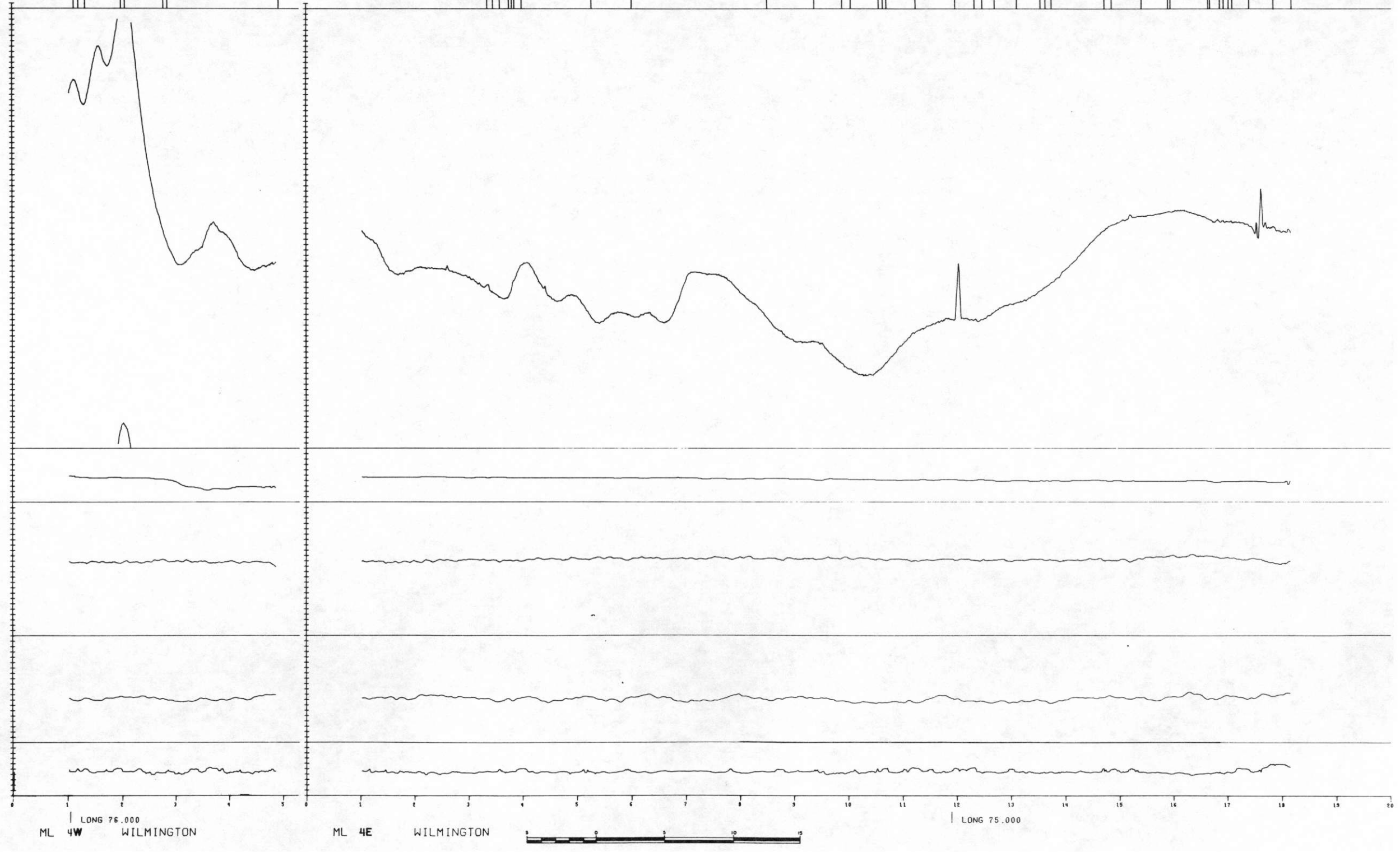
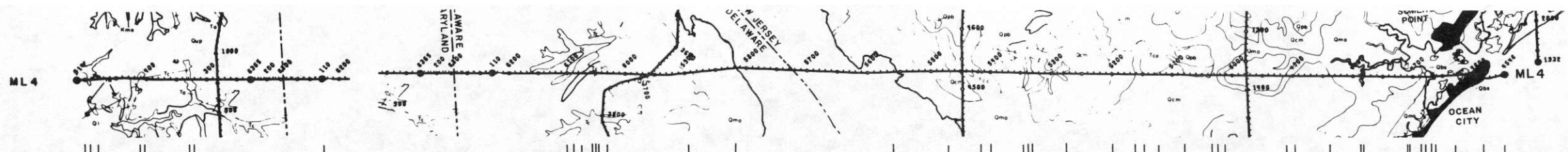












RMAG
10 GAMMA/DIV
BASE = -1000

BMAG
10 GAMMA/DIV
BASE = 54180

BP
3 MM HG/DIV
BASE = 700

TEMP
1 DEG C/DIV
BASE = 15

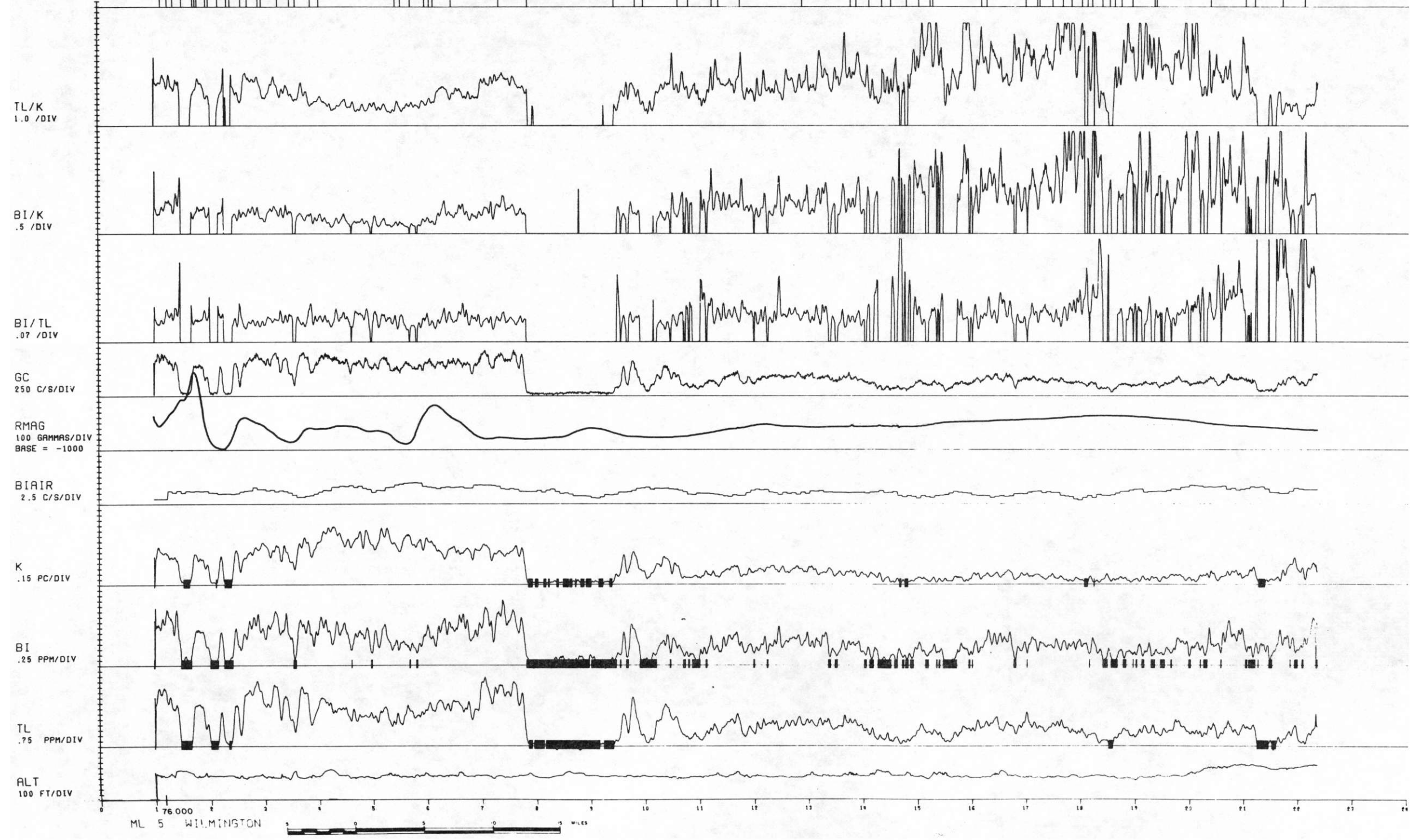
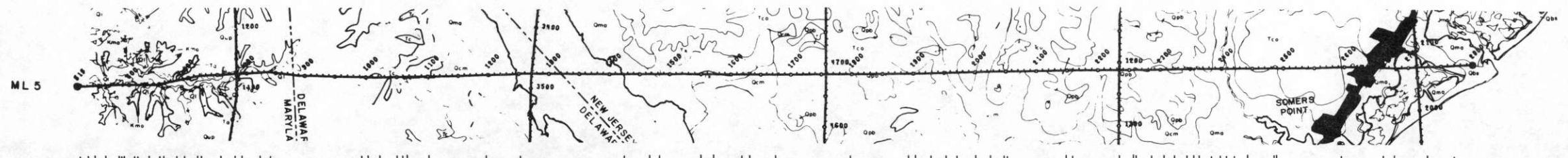
ALT
100 FT/DIV

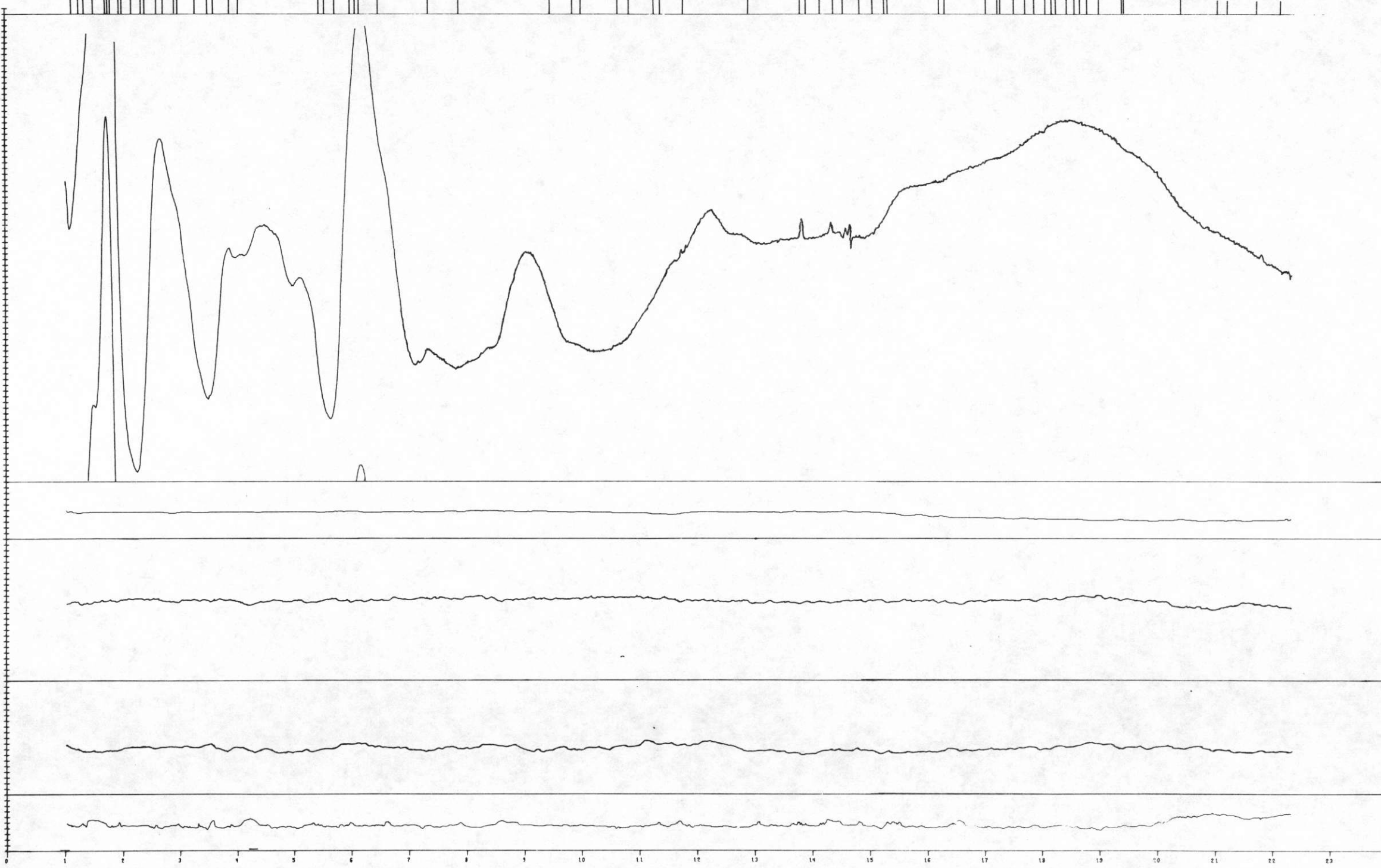
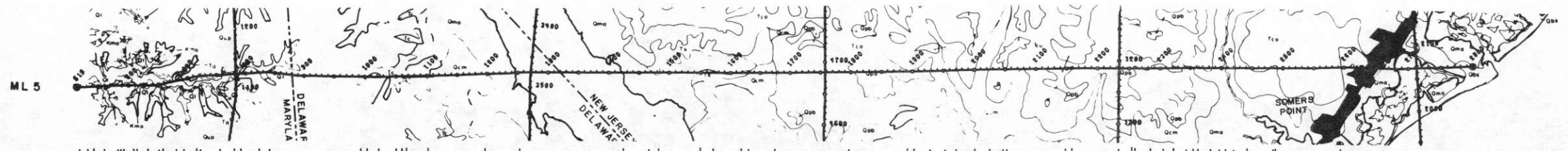
LONG 76.000
ML 4W WILMINGTON

ML 4E WILMINGTON

LONG 75.000







RMAG
10 GAMMA/DIV
BASE = -1000

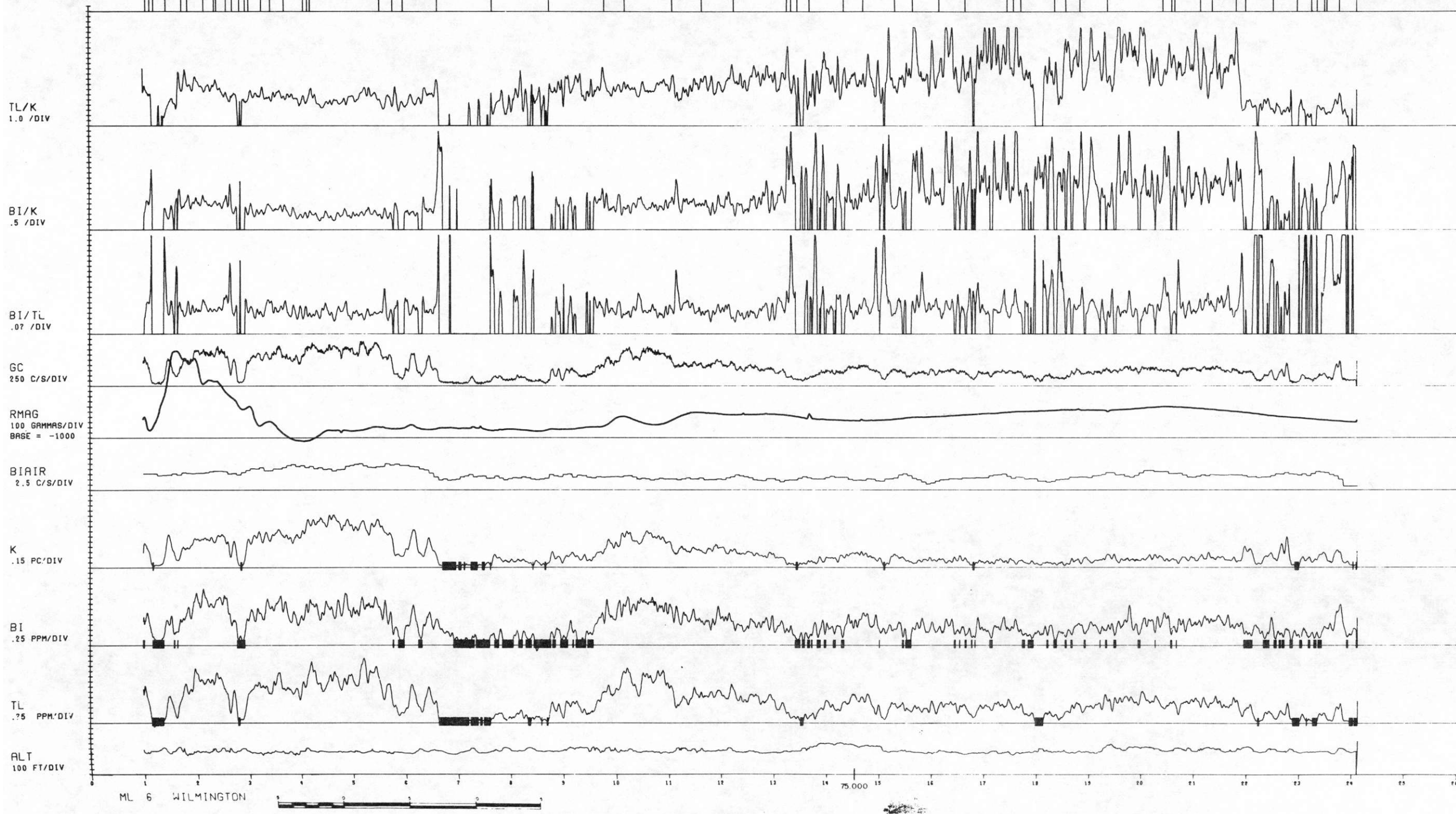
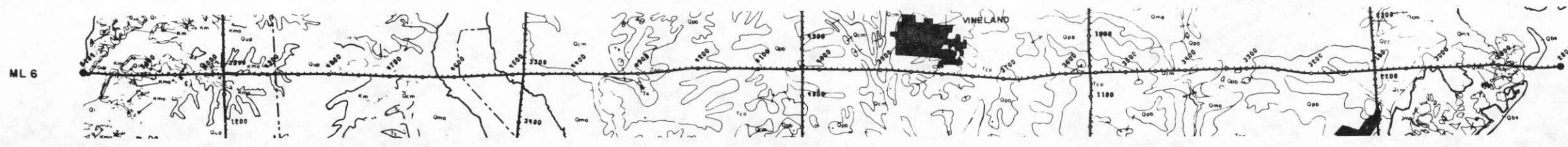
BMAG
10 GAMMA/DIV
BASE = 54190

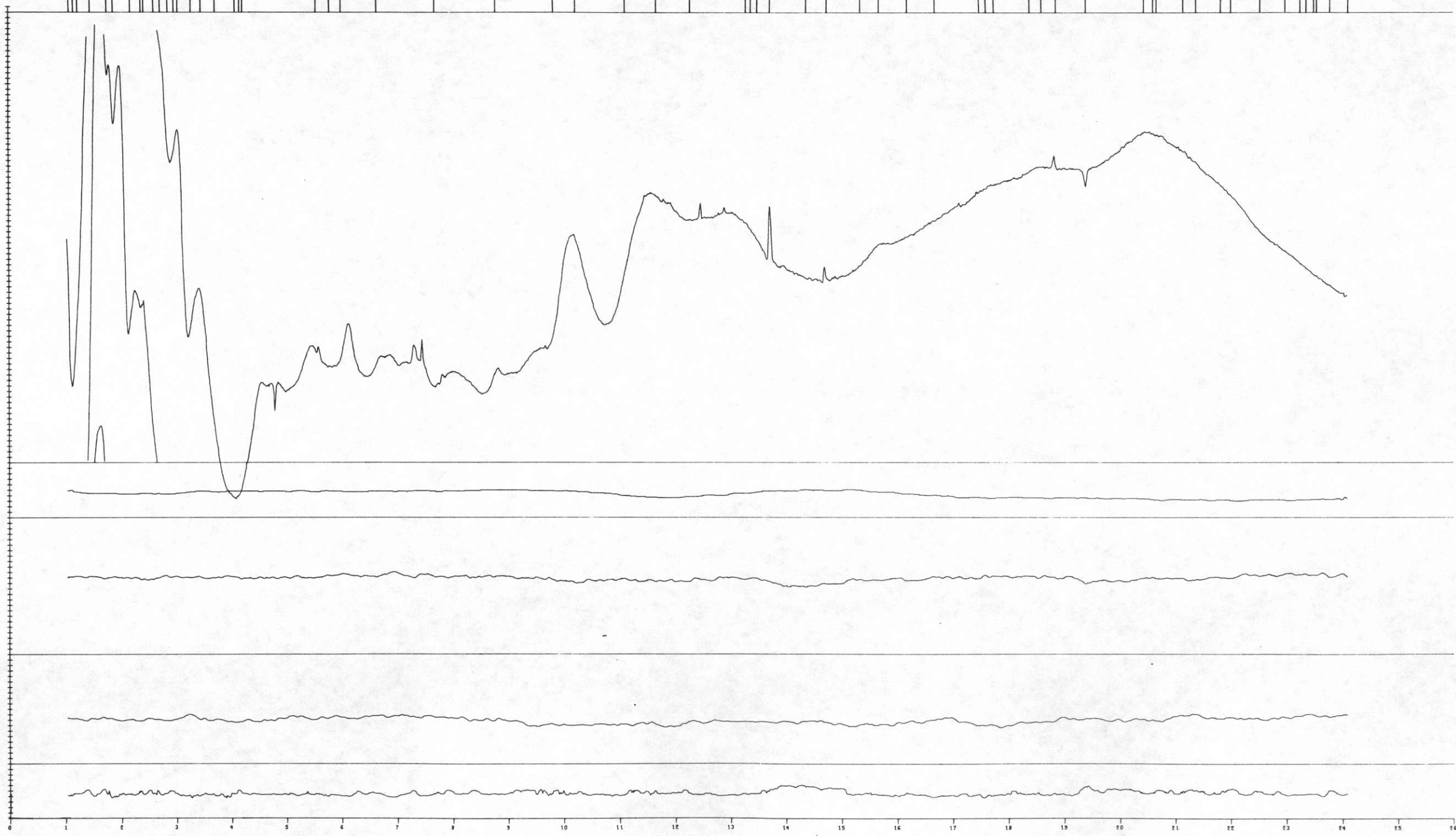
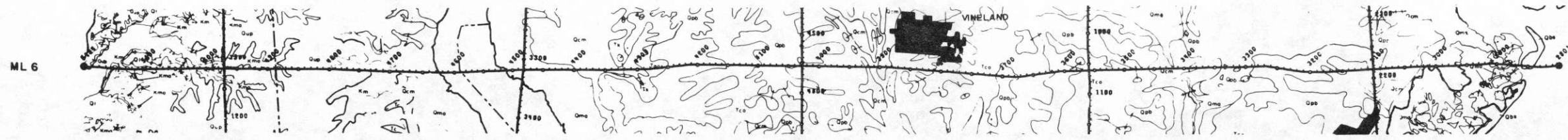
BP
3 MM HG/DIV
BASE = 700

TEMP
1 DEG C/DIV
BASE = 15

ALT
100 FT/DIV

LONG 76.000
ML 5 WILMINGTON





RMAG
10 GAMMA/DIV
BASE = -1000

BMAG
10 GAMMA/DIV
BASE = 54180

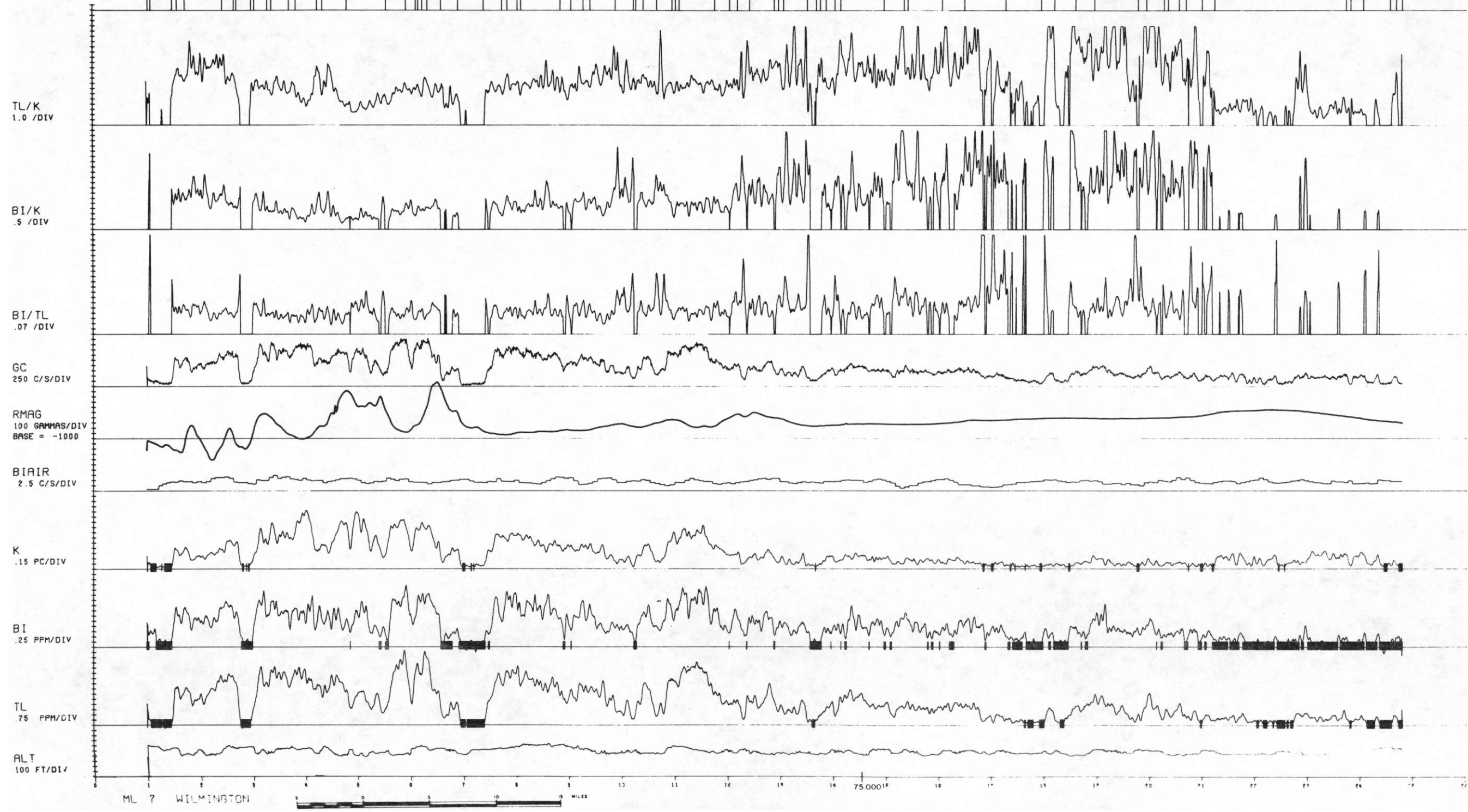
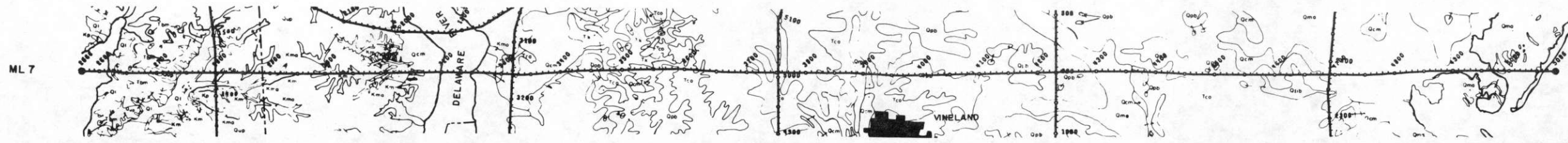
BP
3 MM HG/DIV
BASE = 700

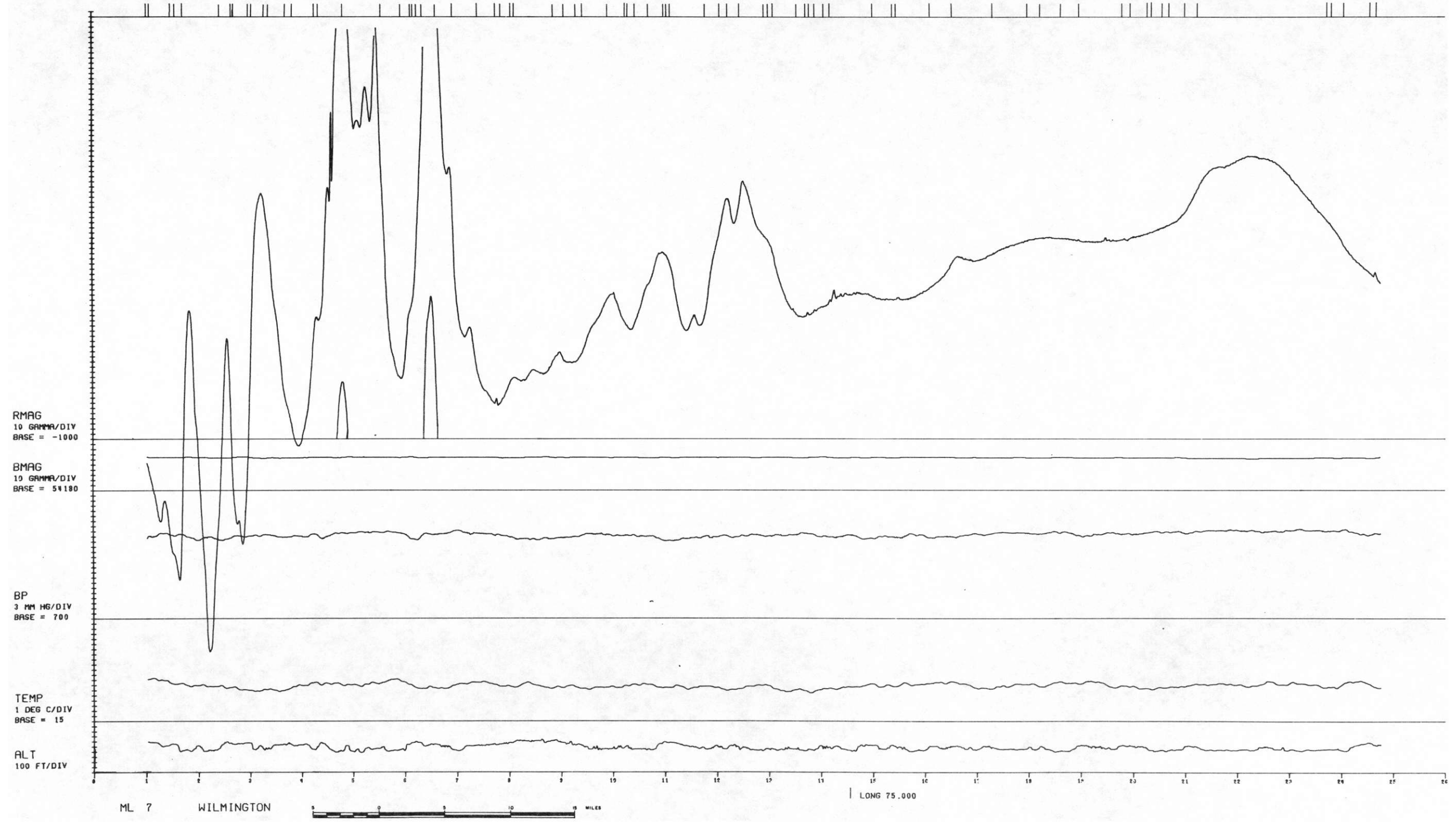
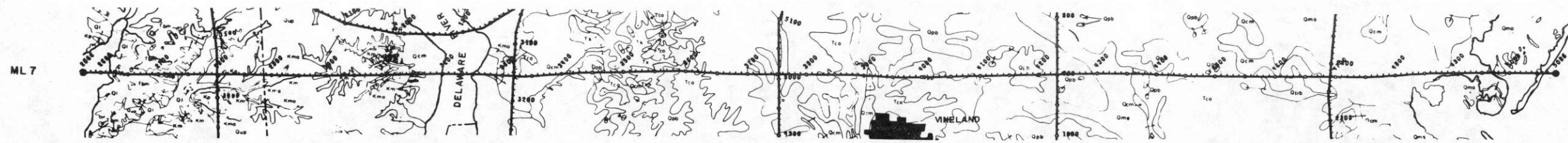
TEMP
1 DEG C/DIV
BASE = 15

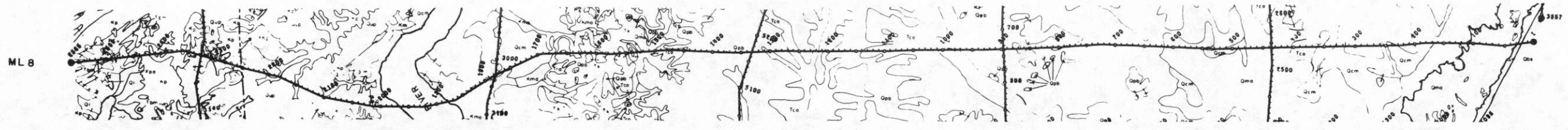
ALT
100 FT/DIV

ML 6 WILMINGTON

LONG 75,000







TL/K
1.0 /DIV

BI/K
.5 /DIV

BI/TL
.07 /DIV

GC
250 C/S/DIV

RMAG
1.0 GAMMAS/DIV
BASE = -1000

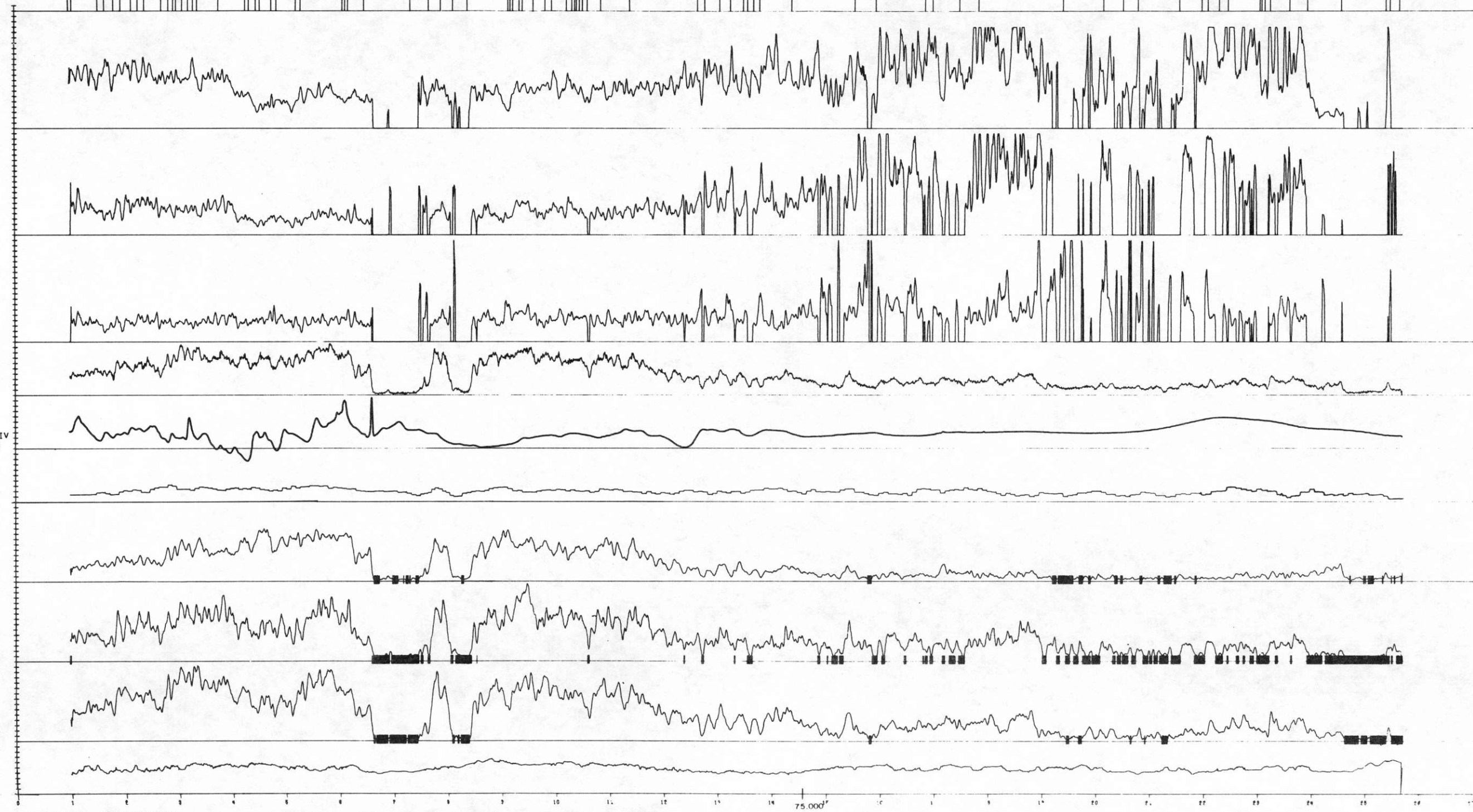
BIAIR
2.5 C/S/DIV

K
.15 PC/DIV

BI
.25 PPM/DIV

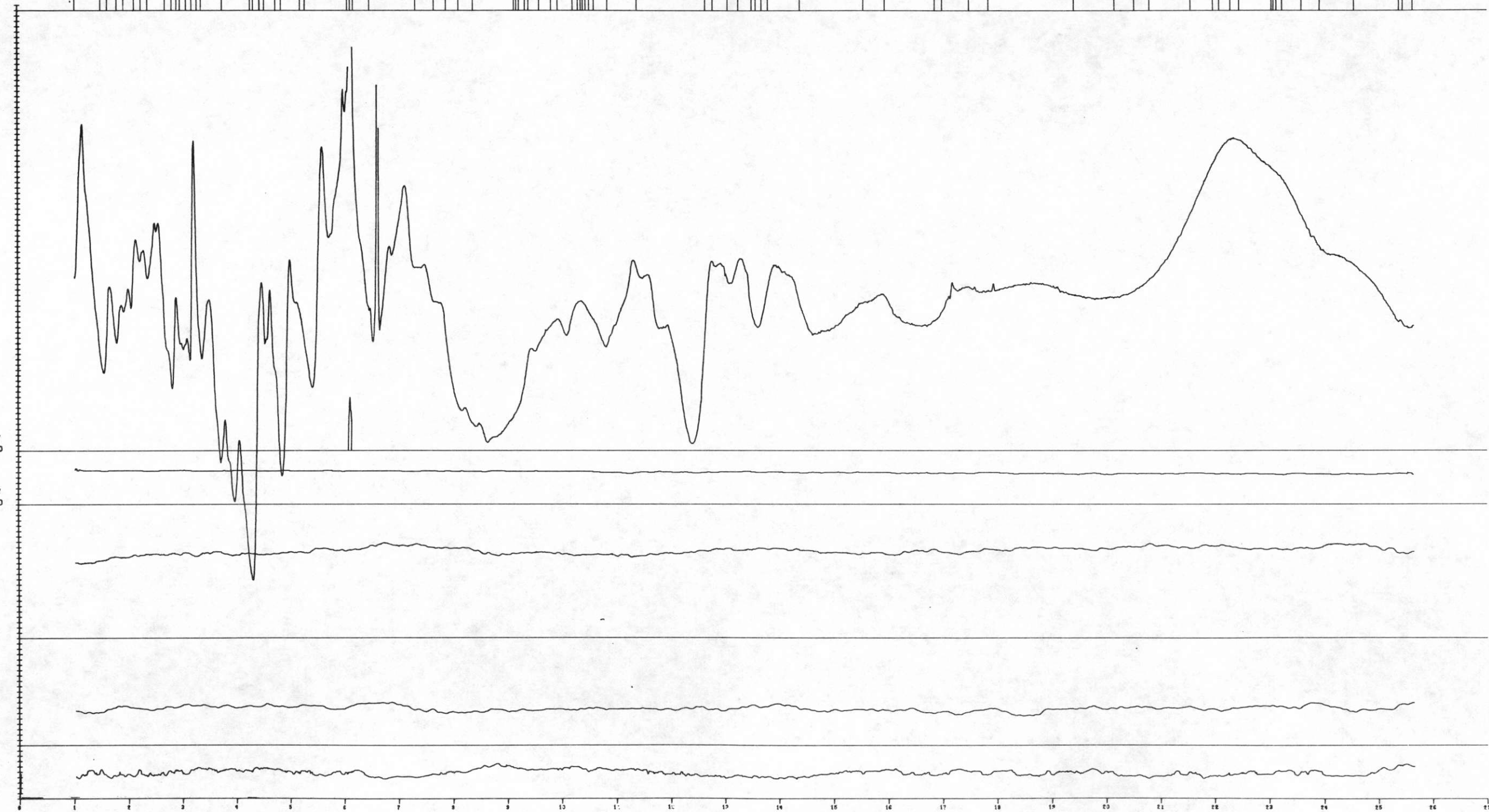
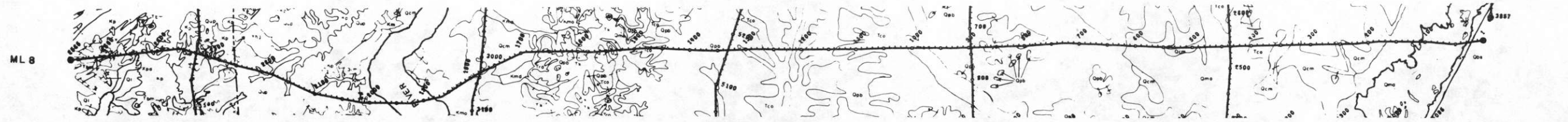
TL
.75 PPM/DIV

ALT
100 FT/DIV



ML 8 WILMINGTON





RMAG
10 GAMMA/DIV
BASE = -1000

BMAG
10 GAMMA/DIV
BASE = 51100

BP
3 MM HG/DIV
BASE = 700

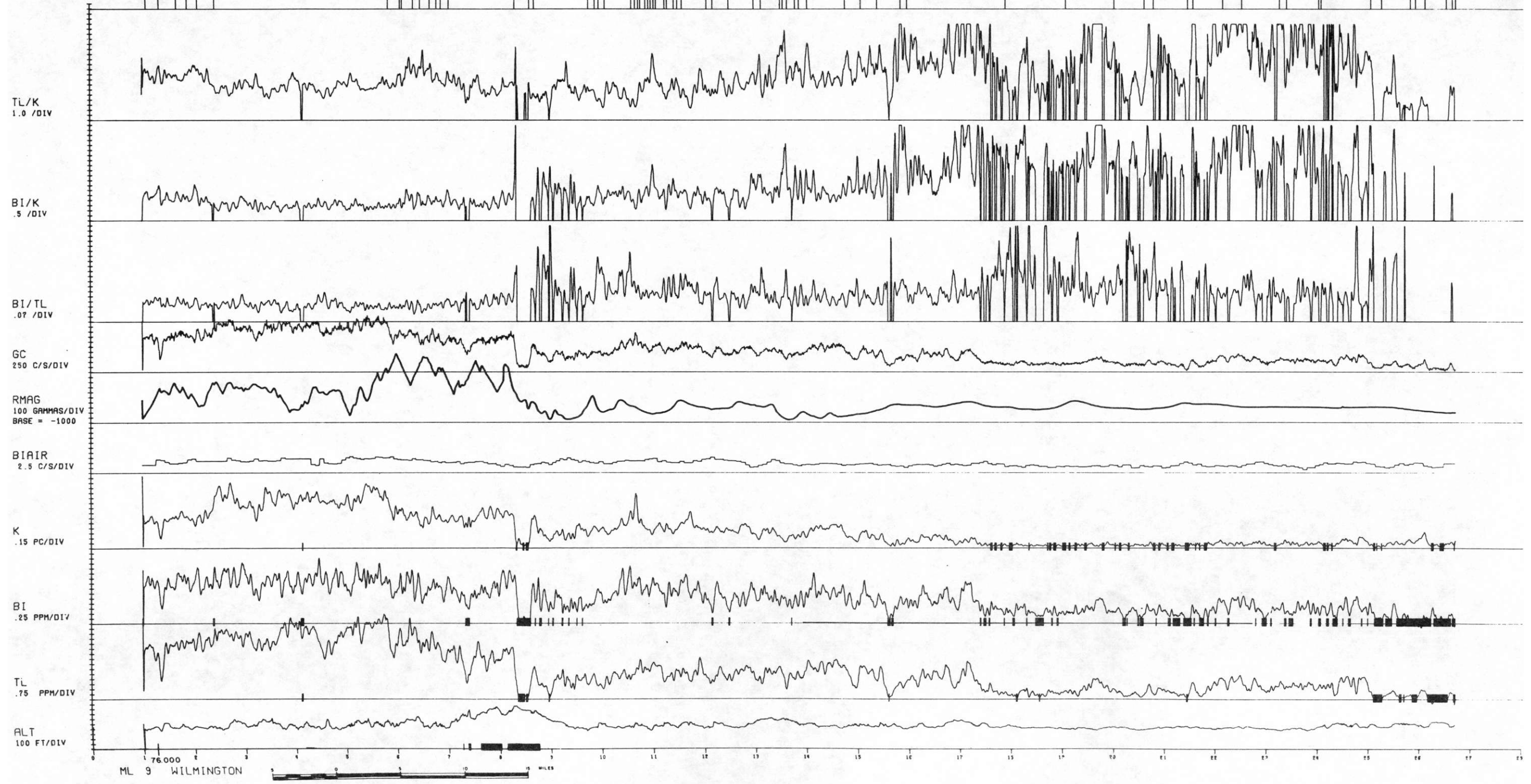
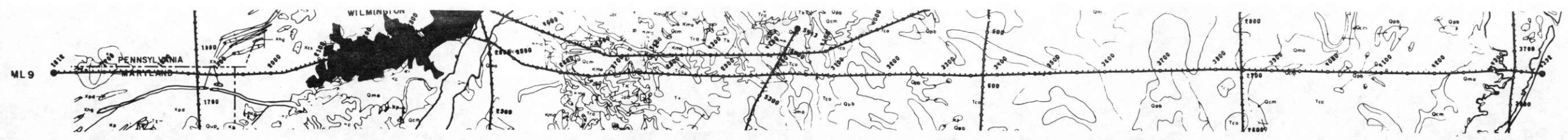
TEMP
1 DEG C/DIV
BASE = 15

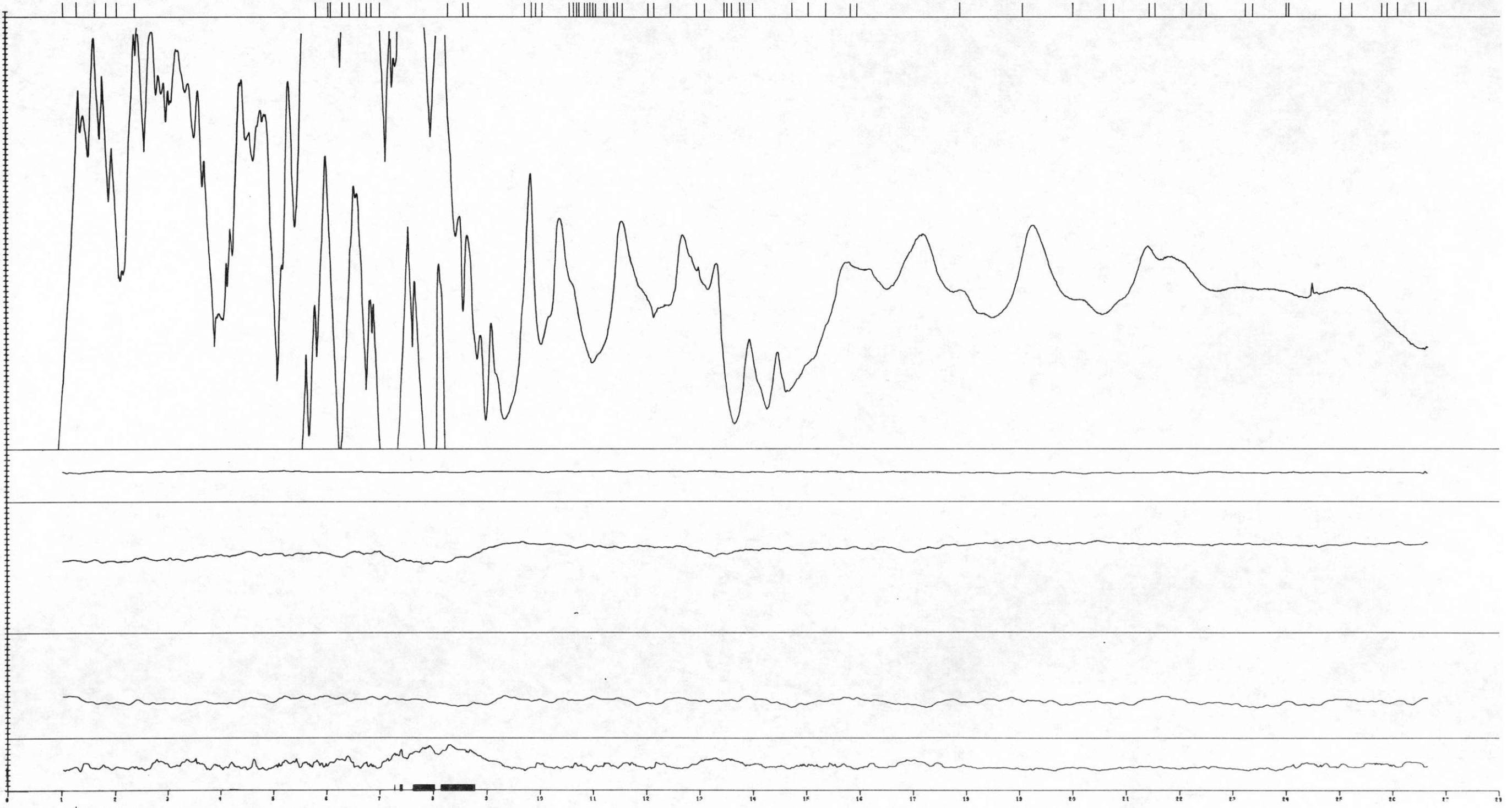
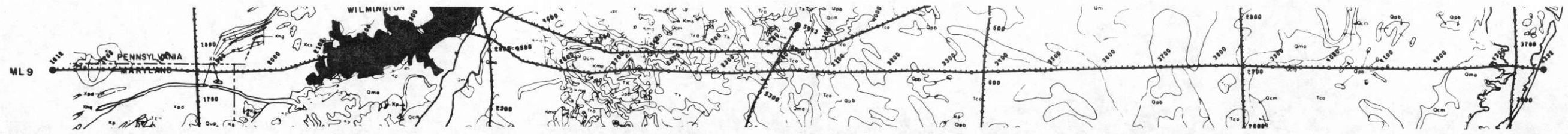
ALT
100 FT/DIV

ML 8 WILMINGTON



LONG 75.000





RMAG
10 GAMMA/DIV
BASE = -1000

BMAG
10 GAMMA/DIV
BASE = 54180

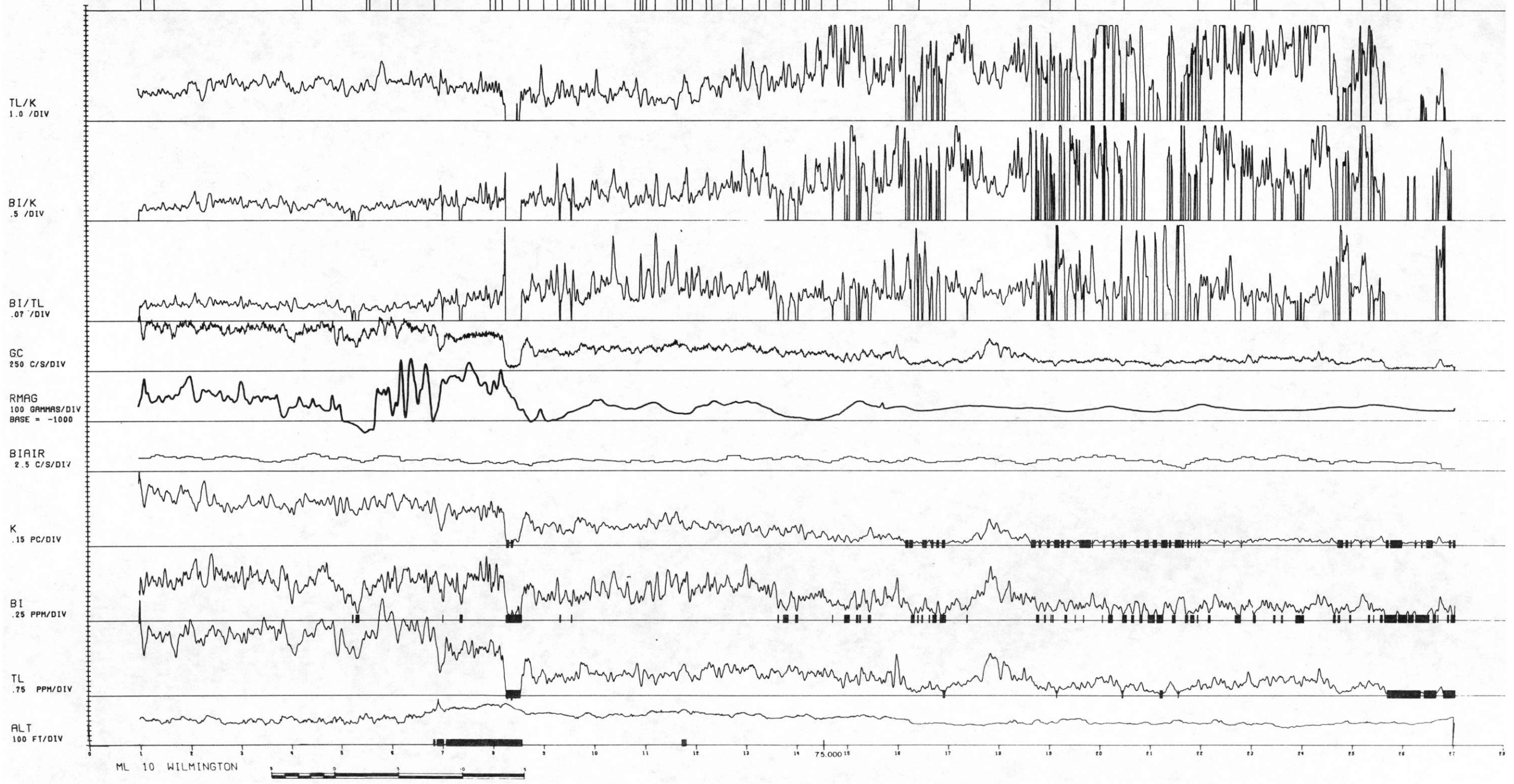
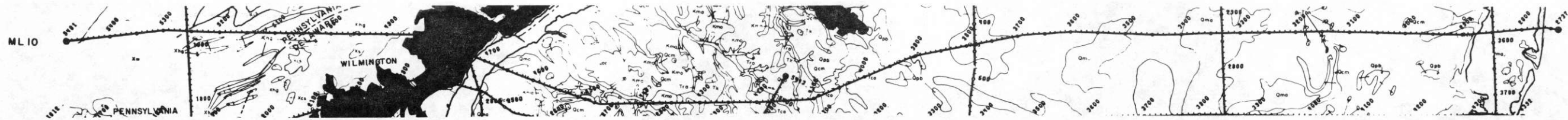
BP
3 MM HG/DIV
BASE = 700

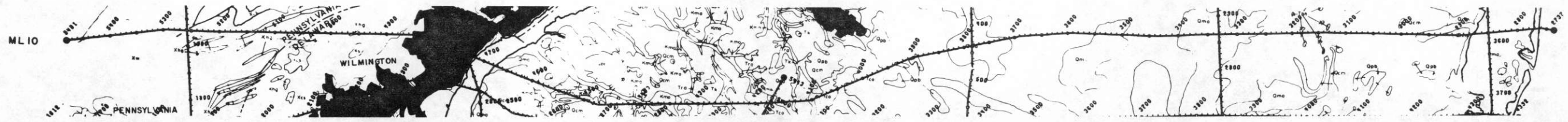
TEMP
1 DEG C/DIV
BASE = 15

ALT
100 FT/DIV

ML 9 | LONG 76.000
WILMINGTON







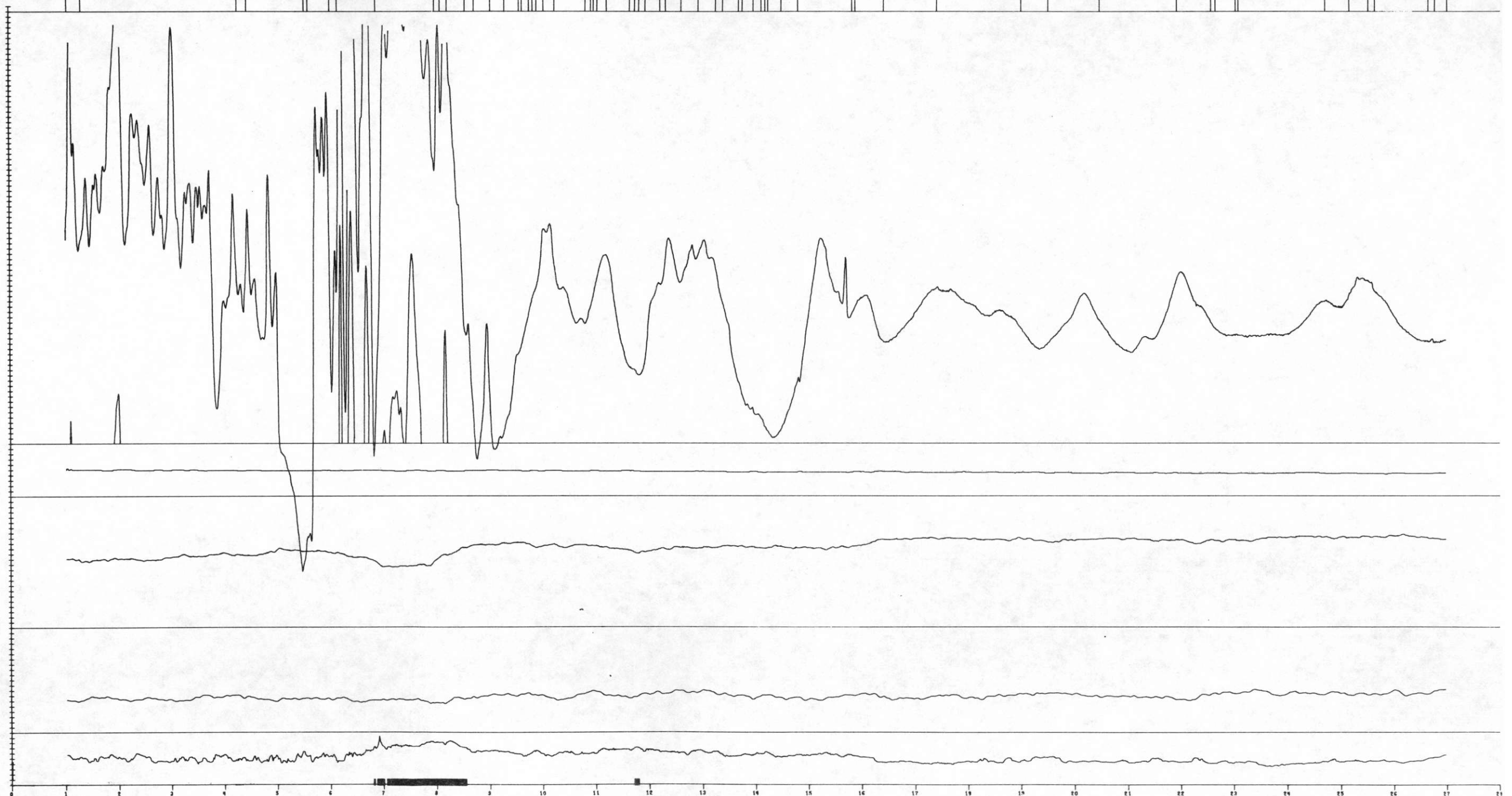
RMAG
10 GAMMA/DIV
BASE = -1000

BMAG
10 GAMMA/DIV
BASE = 54180

BP
3 IN HG/DIV
BASE = 700

TEMP
1 DEG C/DIV
BASE = 15

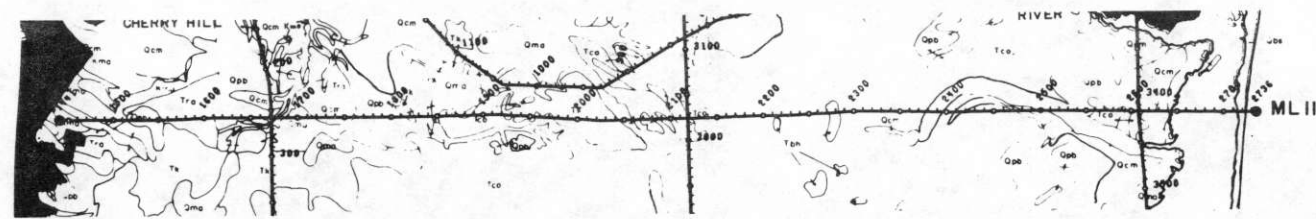
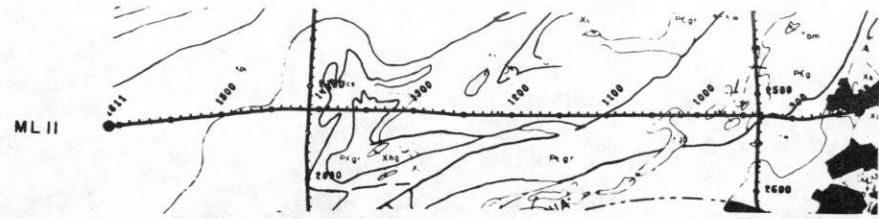
ALT
100 FT/DIV



ML 10 WILMINGTON



LONG 75,000



TL/K
1.0 /DIV

BI/K
.5 /DIV

BI/TL
.07 /DIV

GC
250 C/S/DIV

RMAG
100 GAMMAS/DIV
BASE = -1000

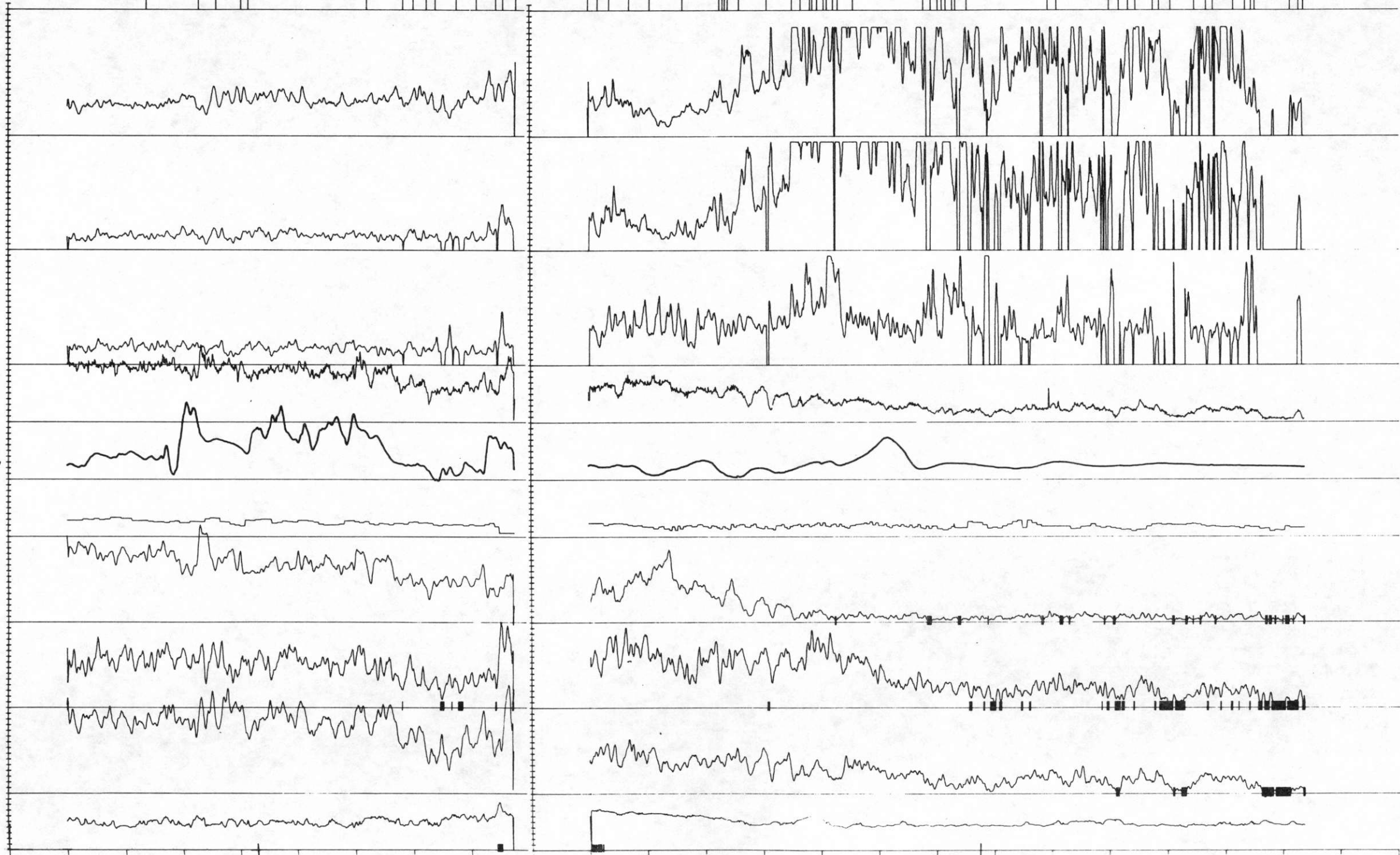
BIAIR
2.5 C/S/DIV

K
.15 PC/DIV

BI
.25 PPM/DIV

TL
.75 PPM/DIV

ALT
100 FT/DIV

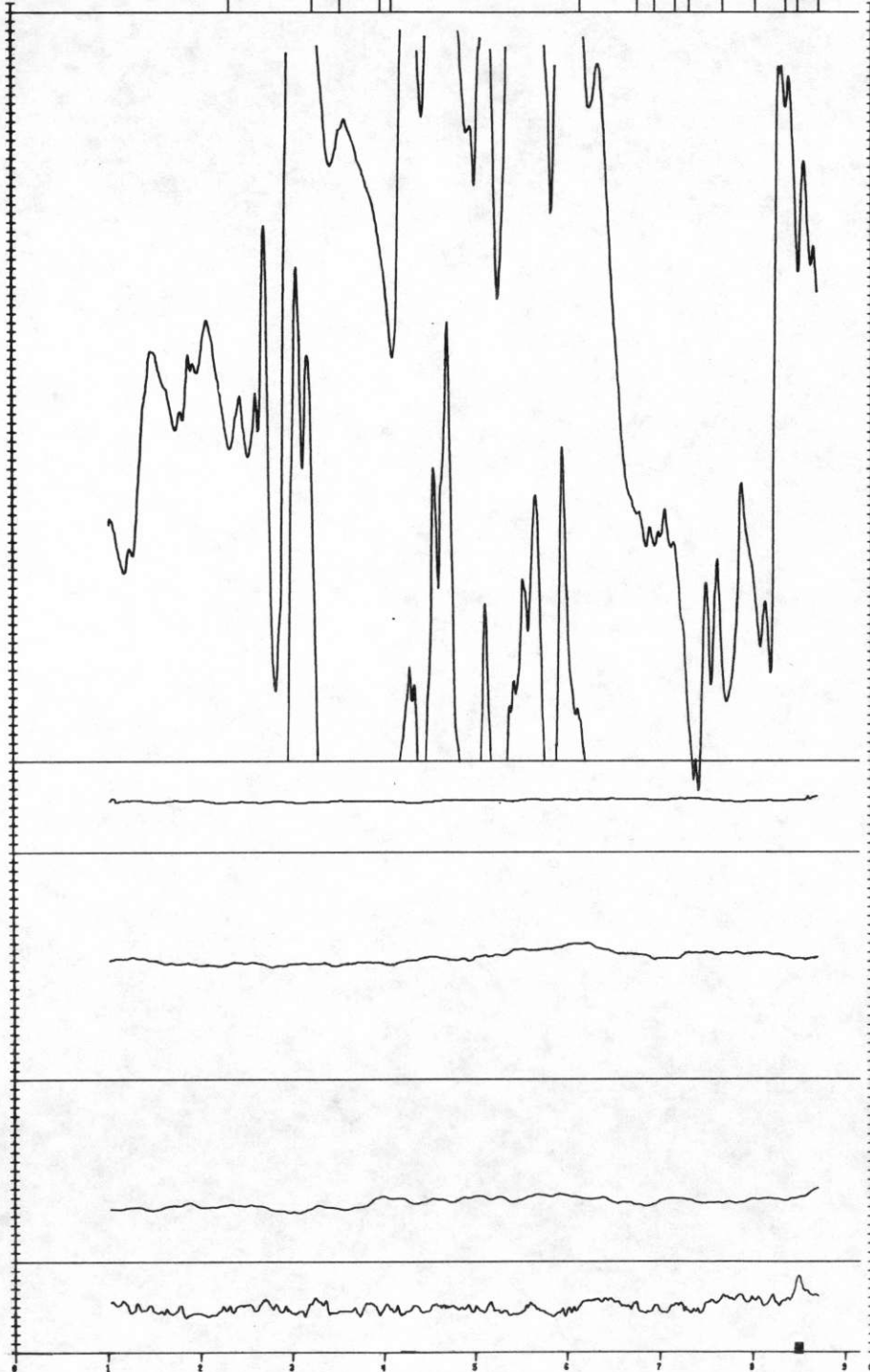
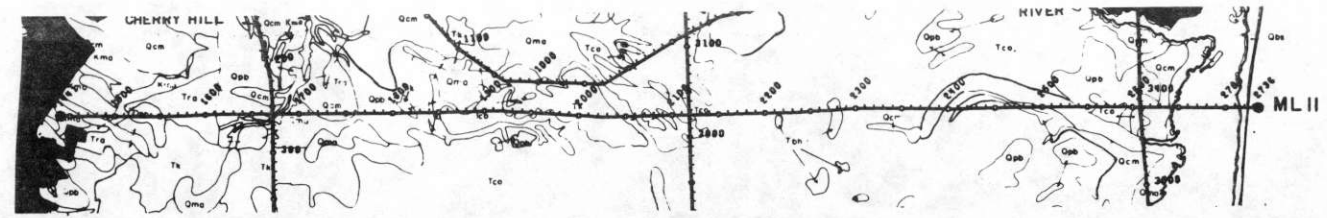
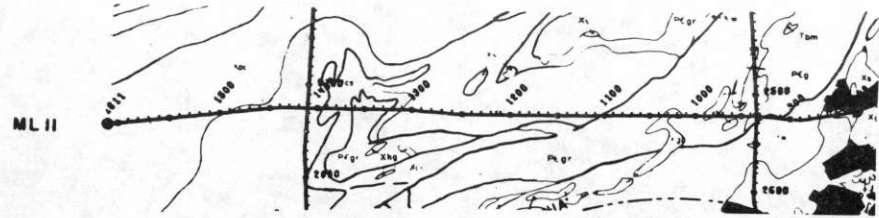


ML 11W WILMINGTON



E WILMINGTON





RMAG
10 GAMMA/DIV
BASE = -1000

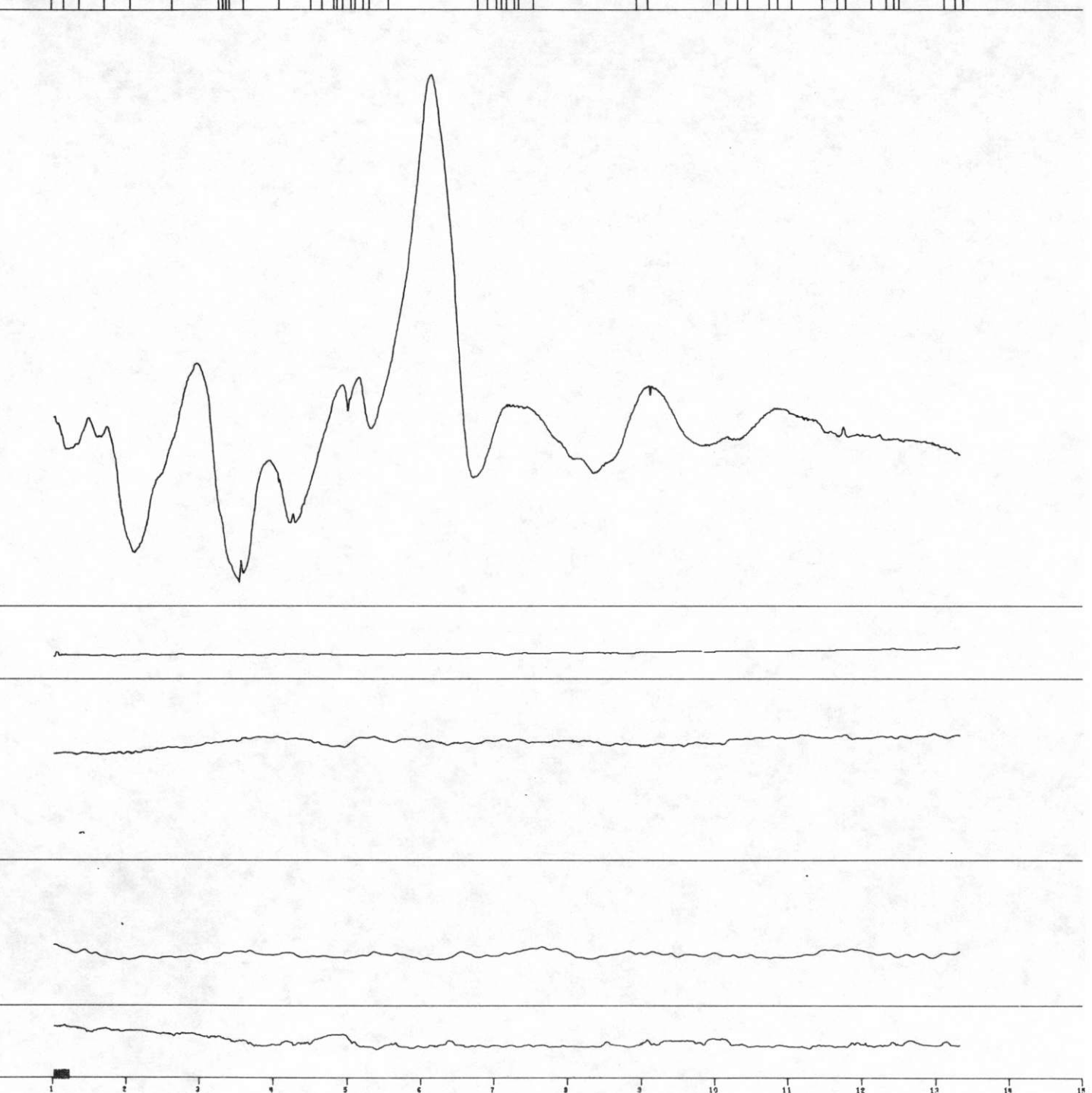
BMAG
10 GAMMA/DIV
BASE = 54100

BP
3 MM HG/DIV
BASE = 700

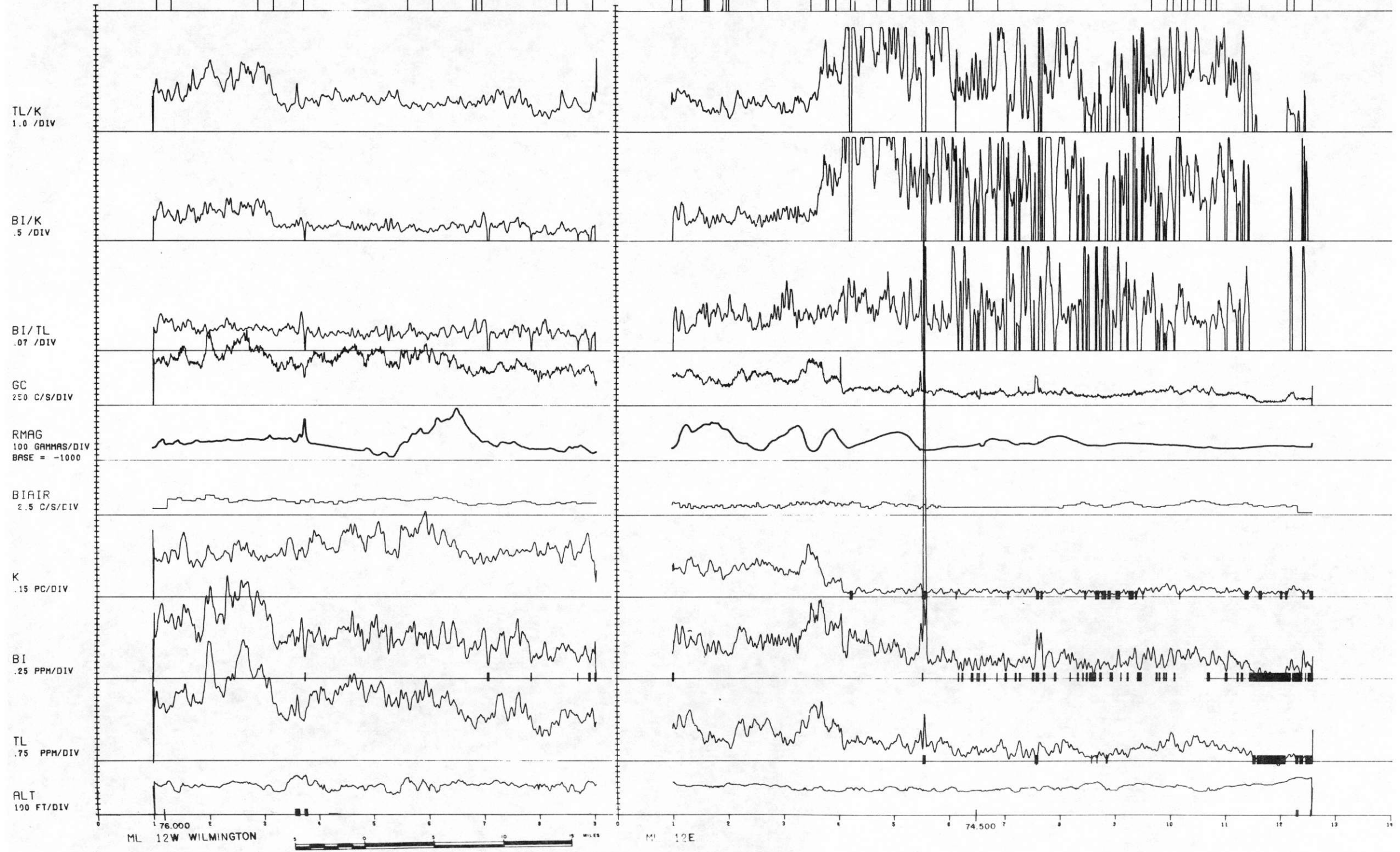
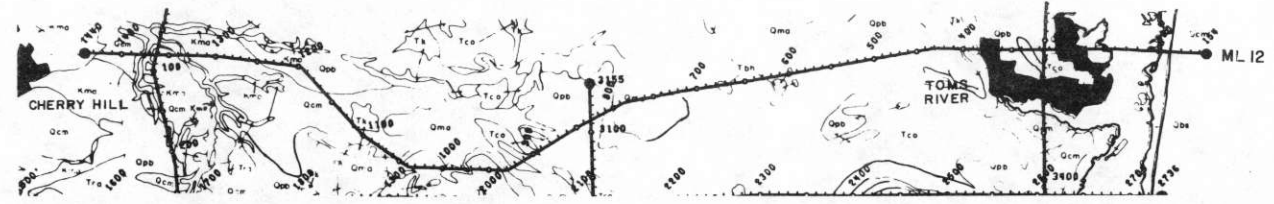
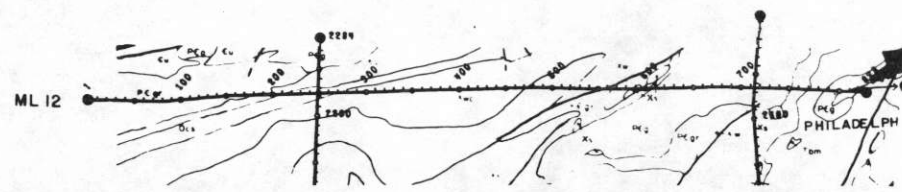
TEMP
1 DEG C/DIV
BASE = 15

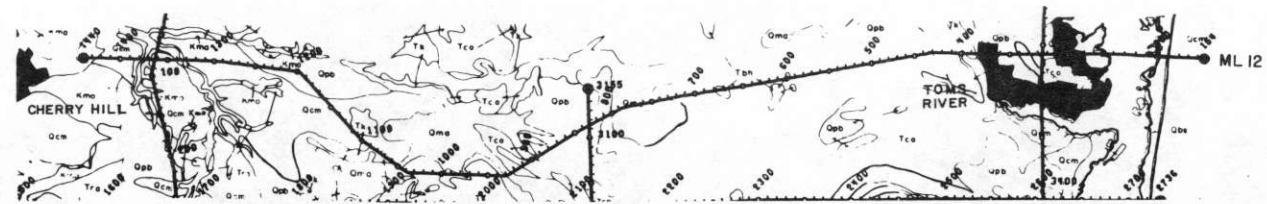
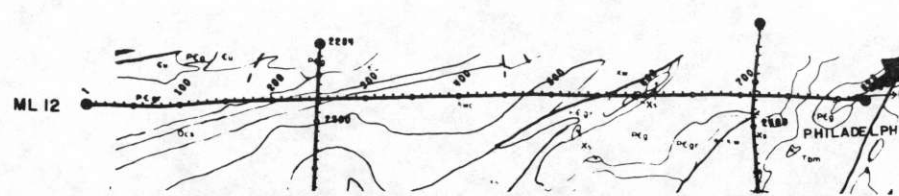
ALT
100 FT/DIV

ML 11W WILMINGTON LONG 75.750



ML 11E WILMINGTON LONG 74.500





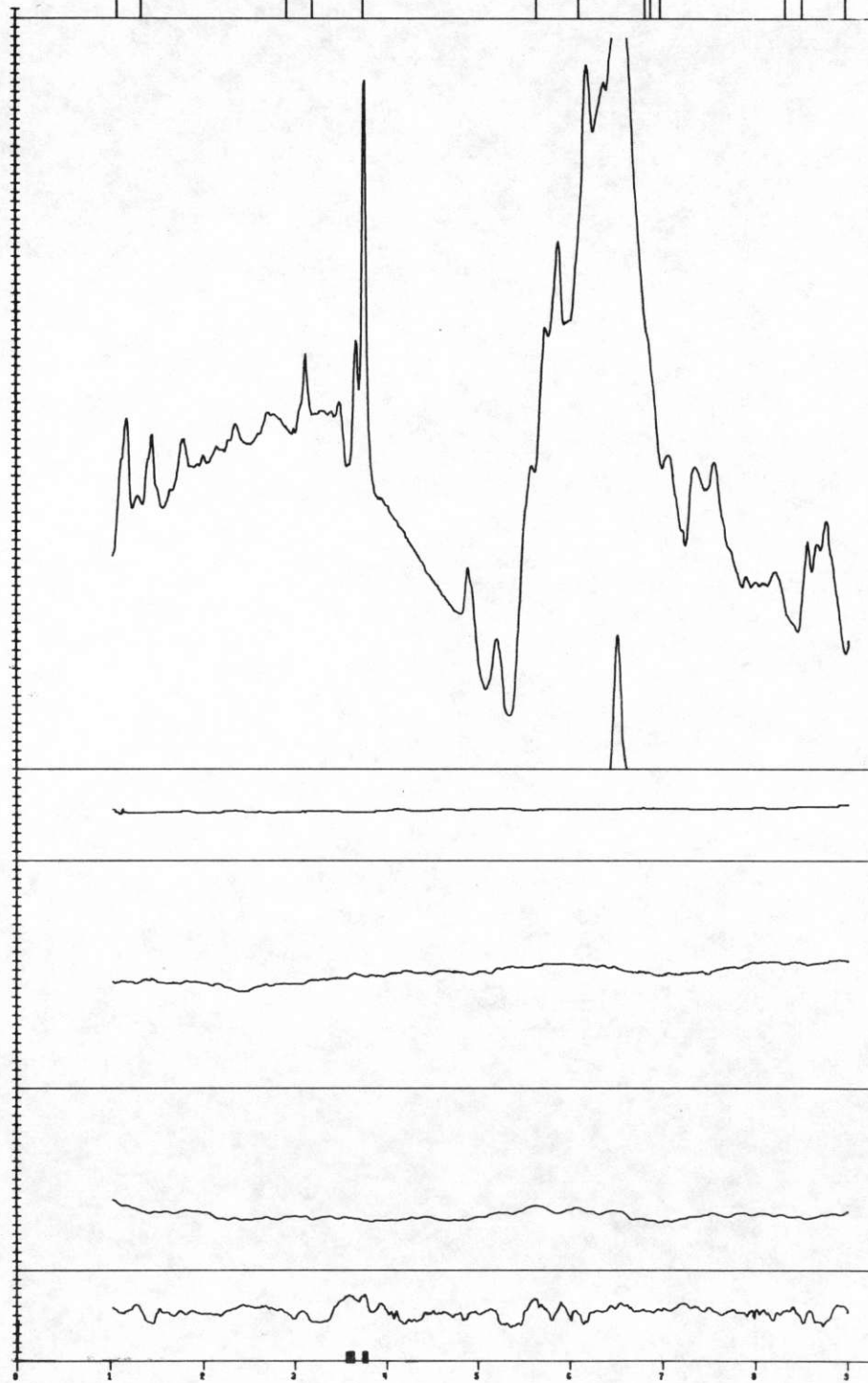
RMAG
10 GAMMA/DIV
BASE = -1000

BMAG
10 GAMMA/DIV
BASE = 54180

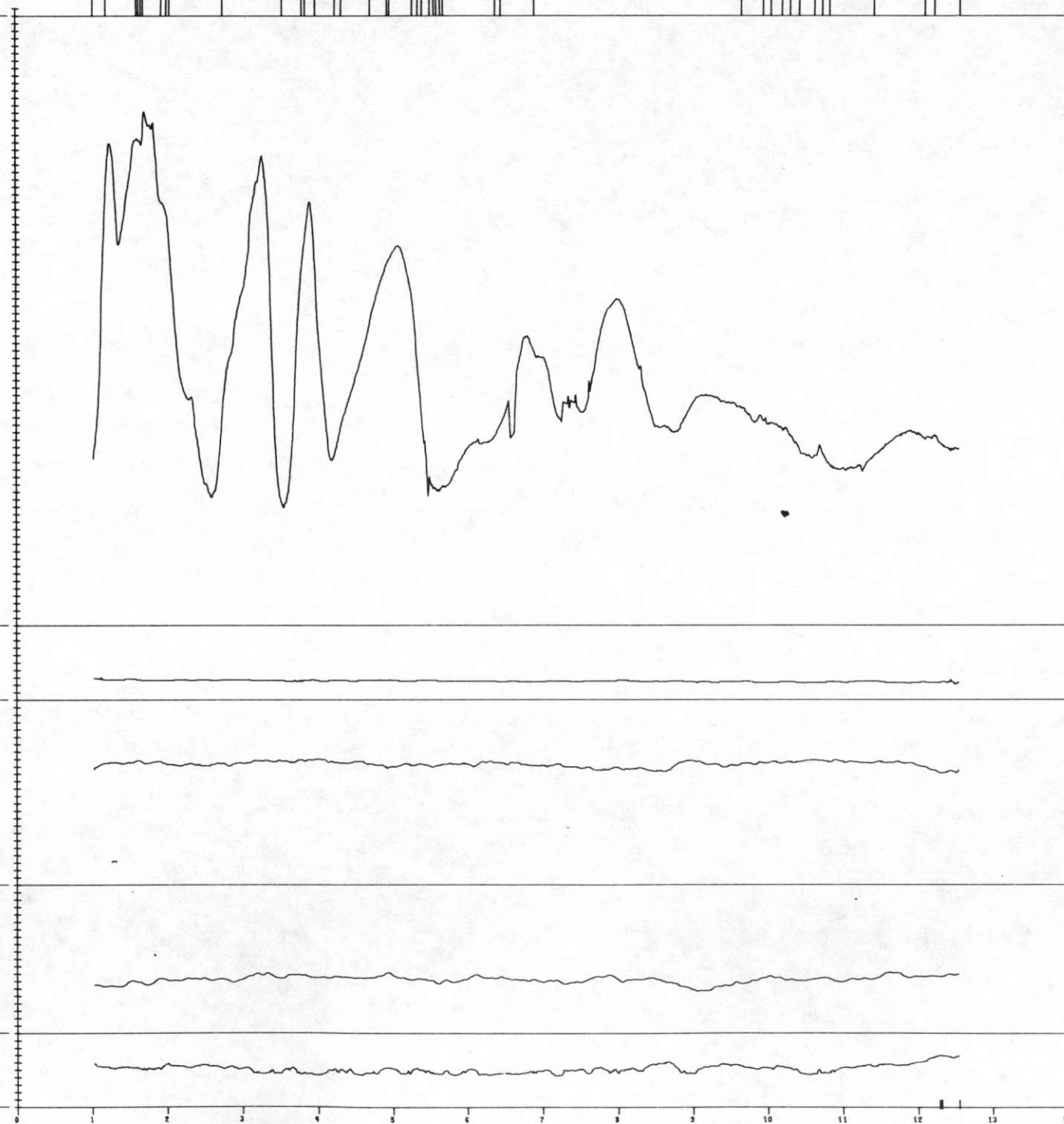
BP
3 MM HG/DIV
BASE = 700

TEMP
1 DEG C/DIV
BASE = 15

ALT
100 FT/DIV

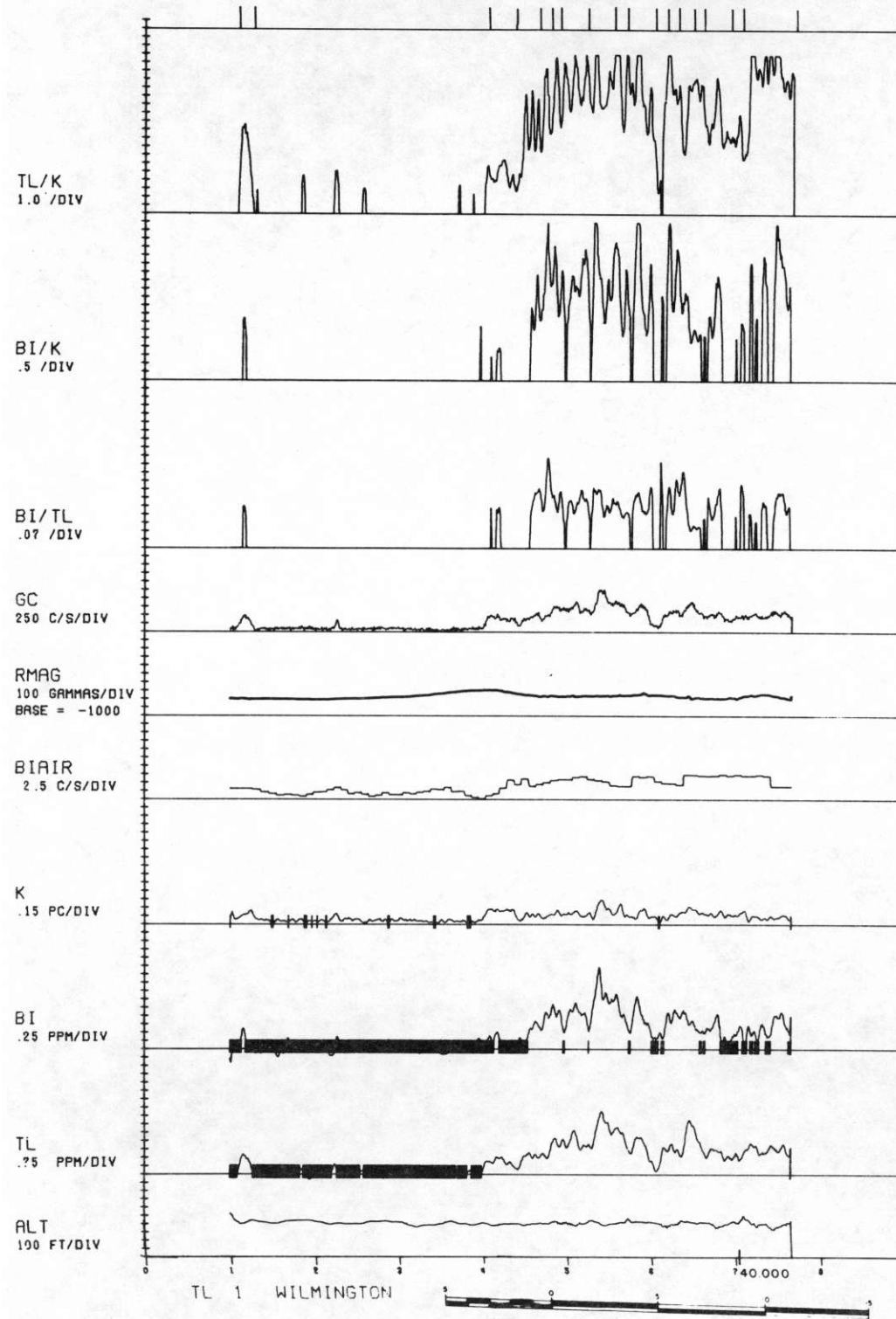
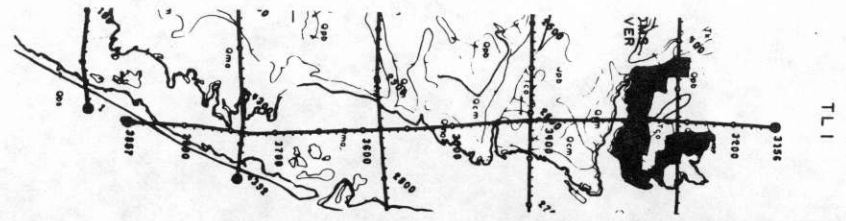


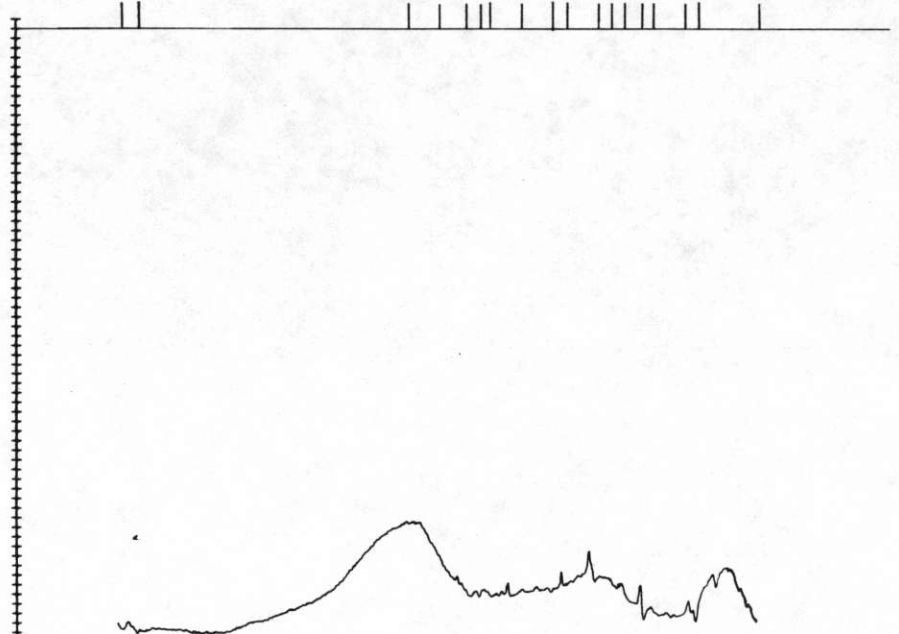
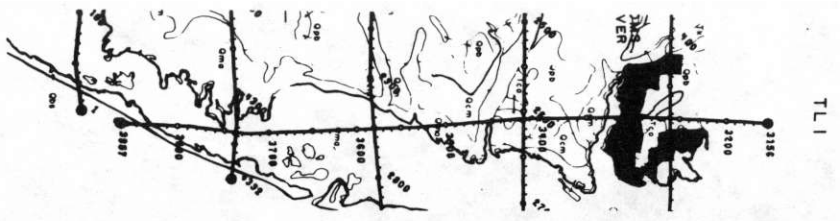
LONG 76.000
ML 12 W WILMINGTON



ML 12 E WILMINGTON

LONG 74.500

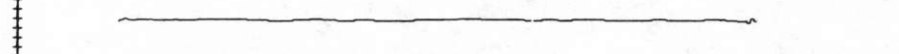




RMAG
10 GAMMA/DIV
BASE = -1000



BMAG
10 GAMMA/DIV
BASE = 54180



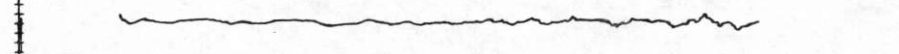
BP
3 MM HG/DIV
BASE = 700



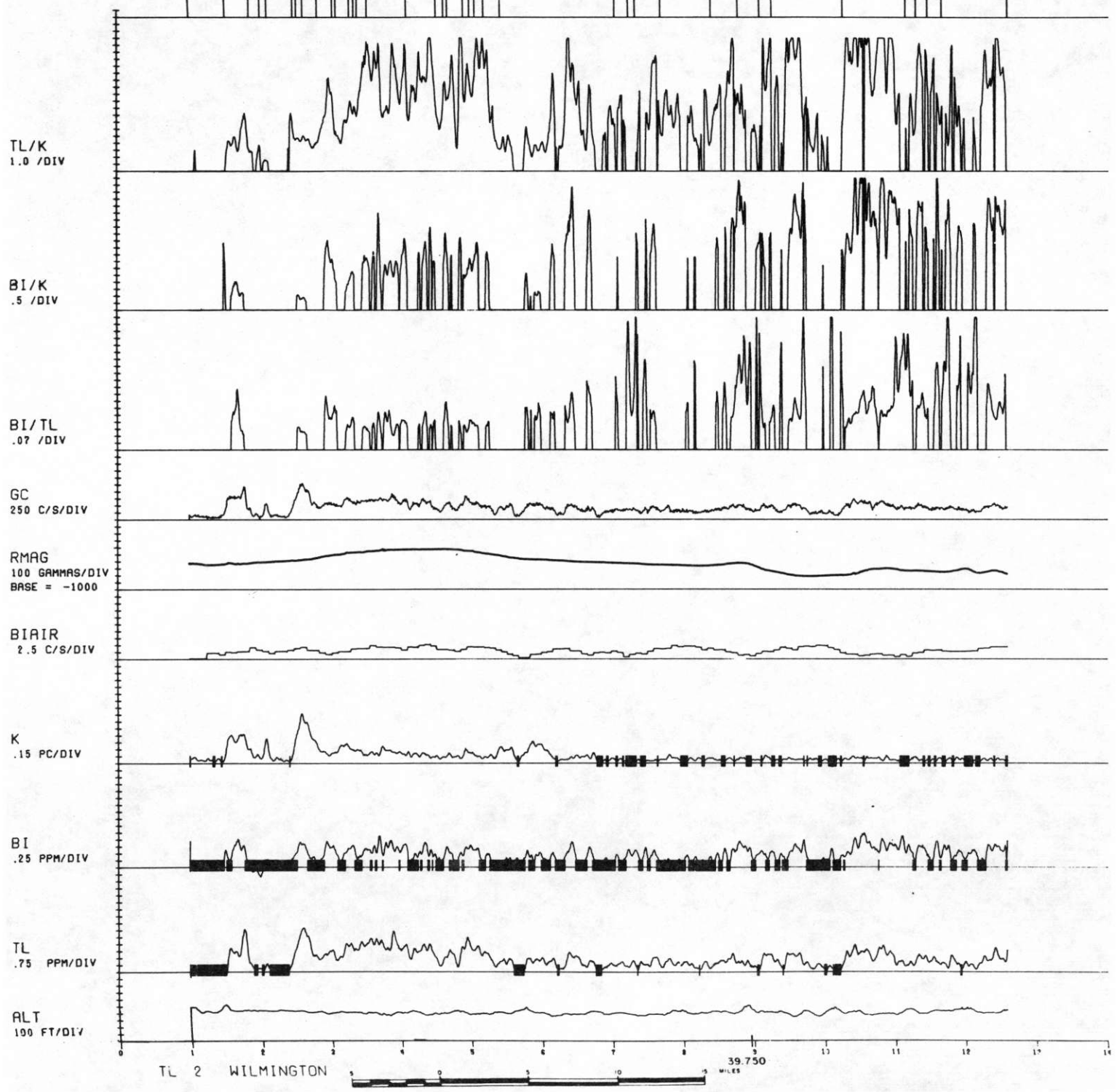
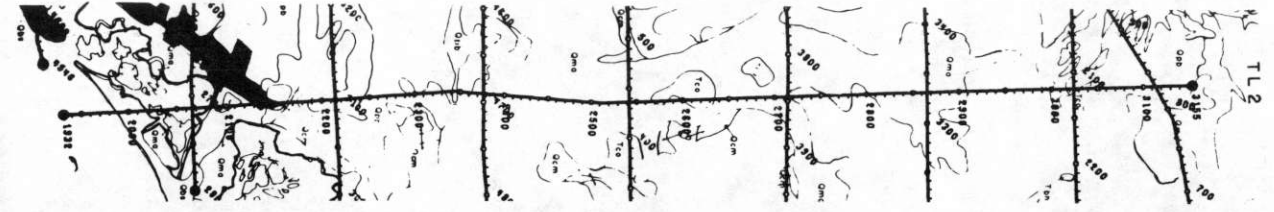
TEMP
1 DEG C/DIV
BASE = 15

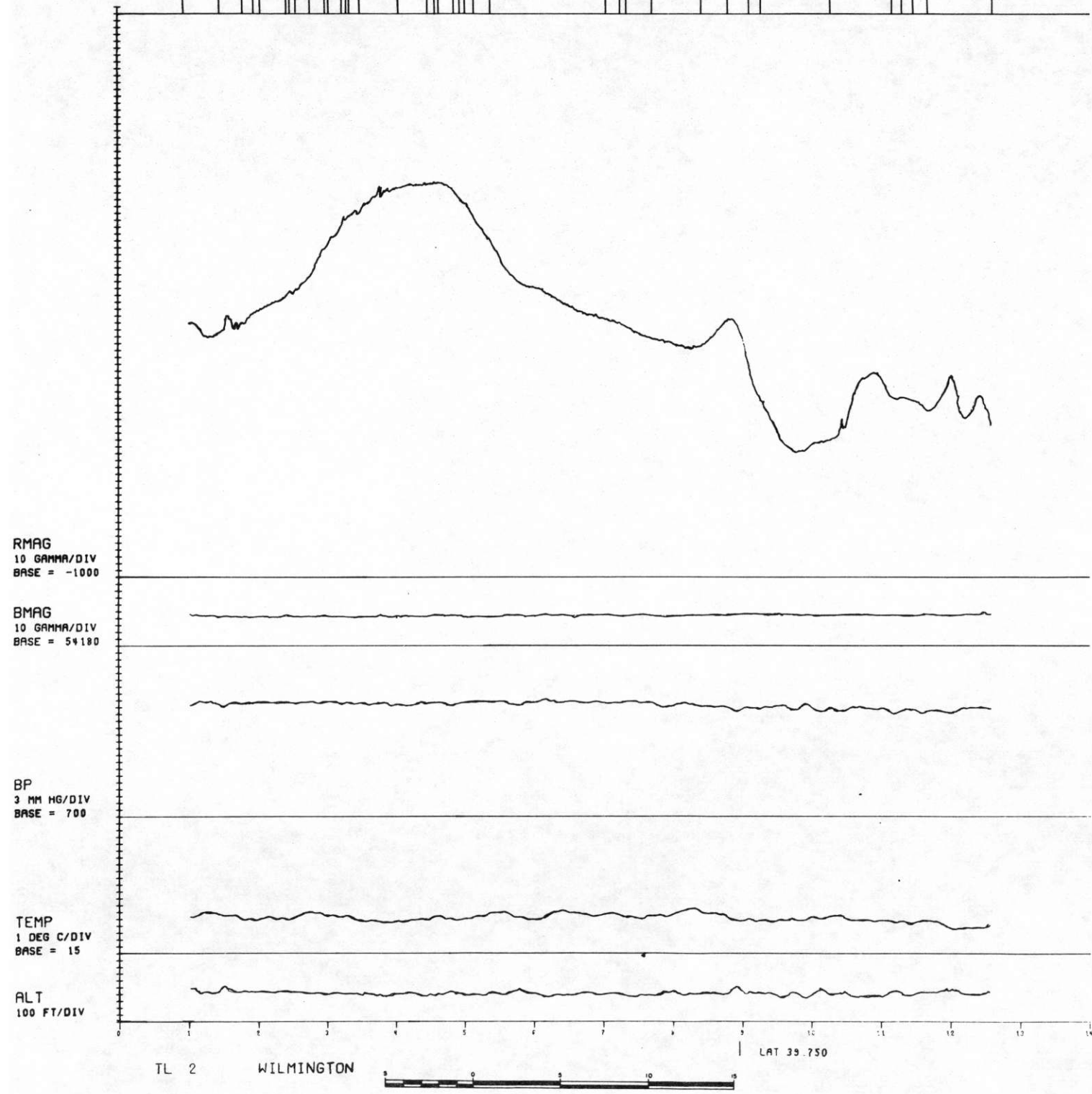
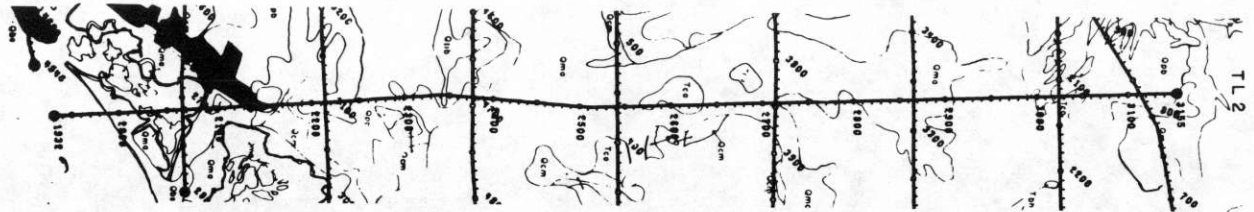


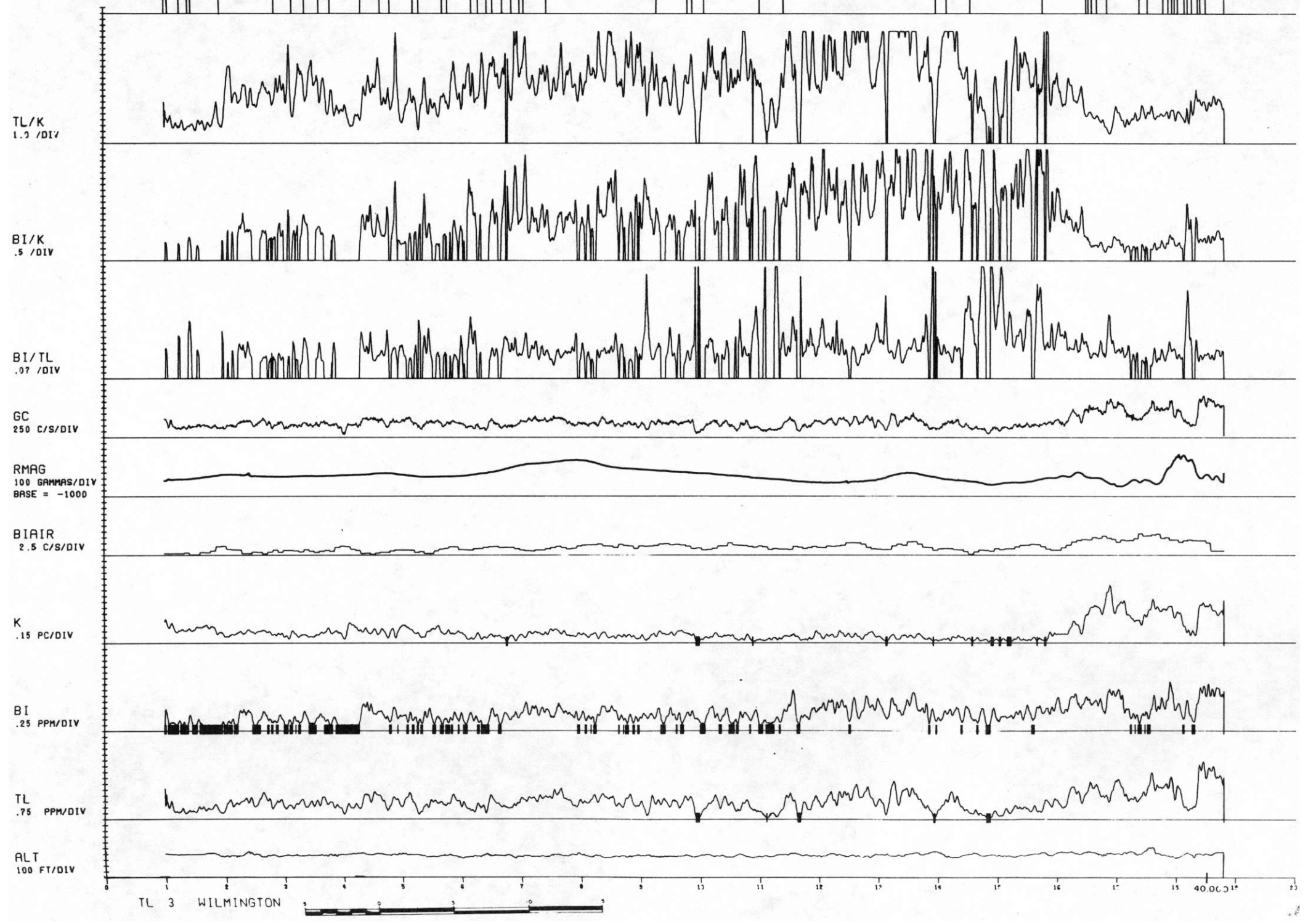
ALT
100 FT/DIV

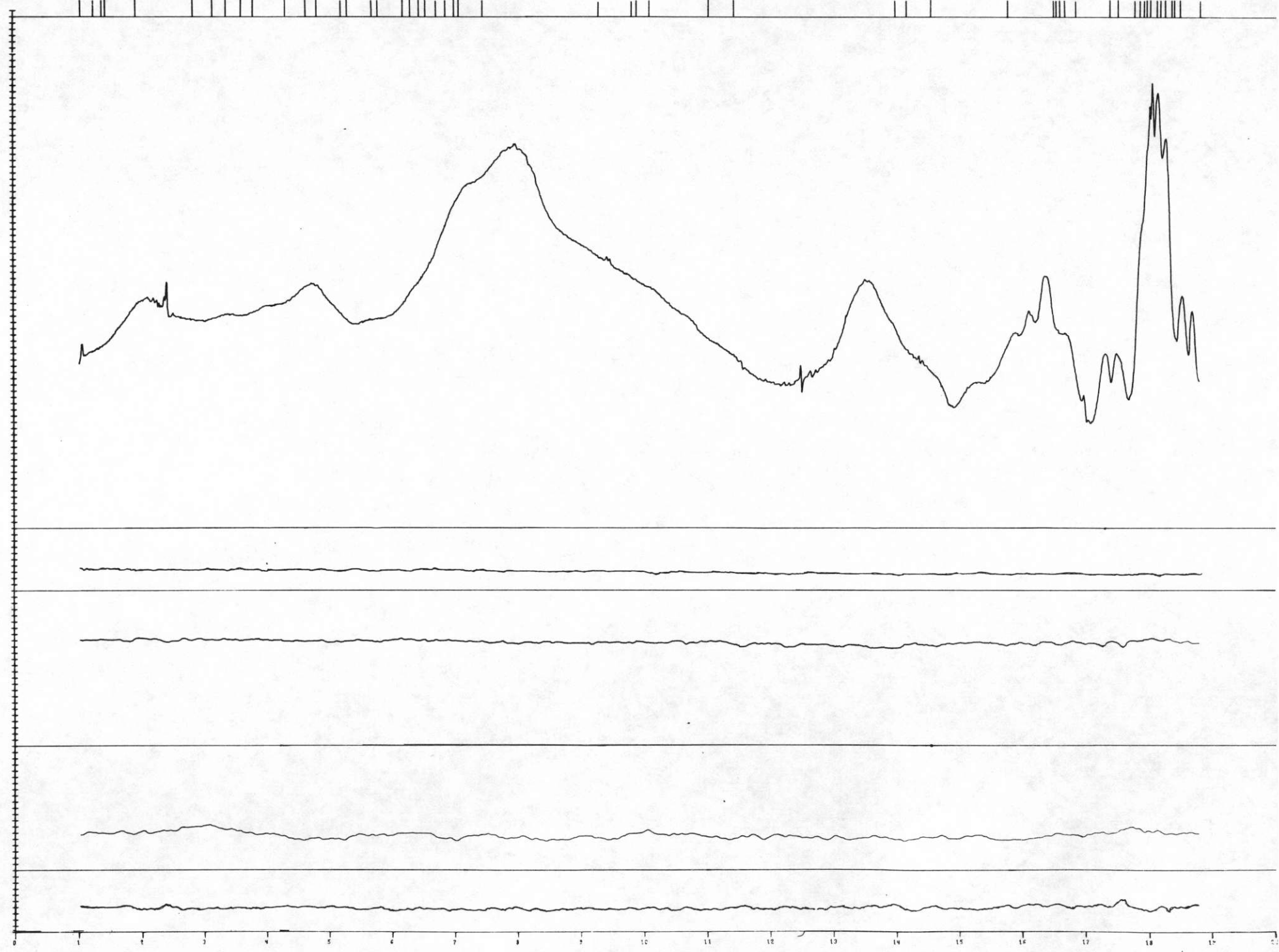
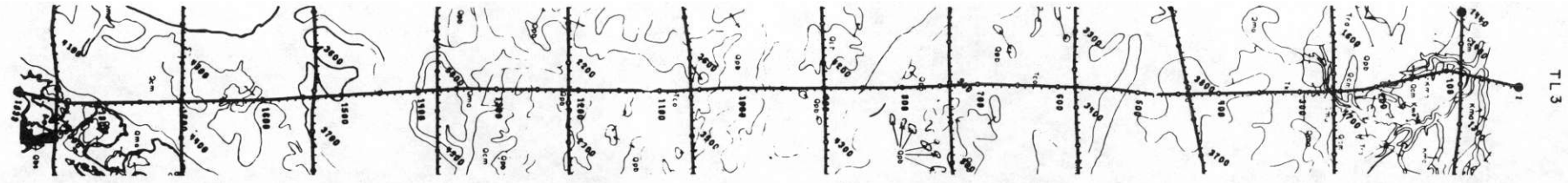


TL 1 WILMINGTON LAT 43.000 0 10 MILES









RMAG
10 GAMMA/DIV
BASE = -1000

BMAG
10 GAMMA/DIV
BASE = 54180

BP
3 MM HG/DIV
BASE = 700

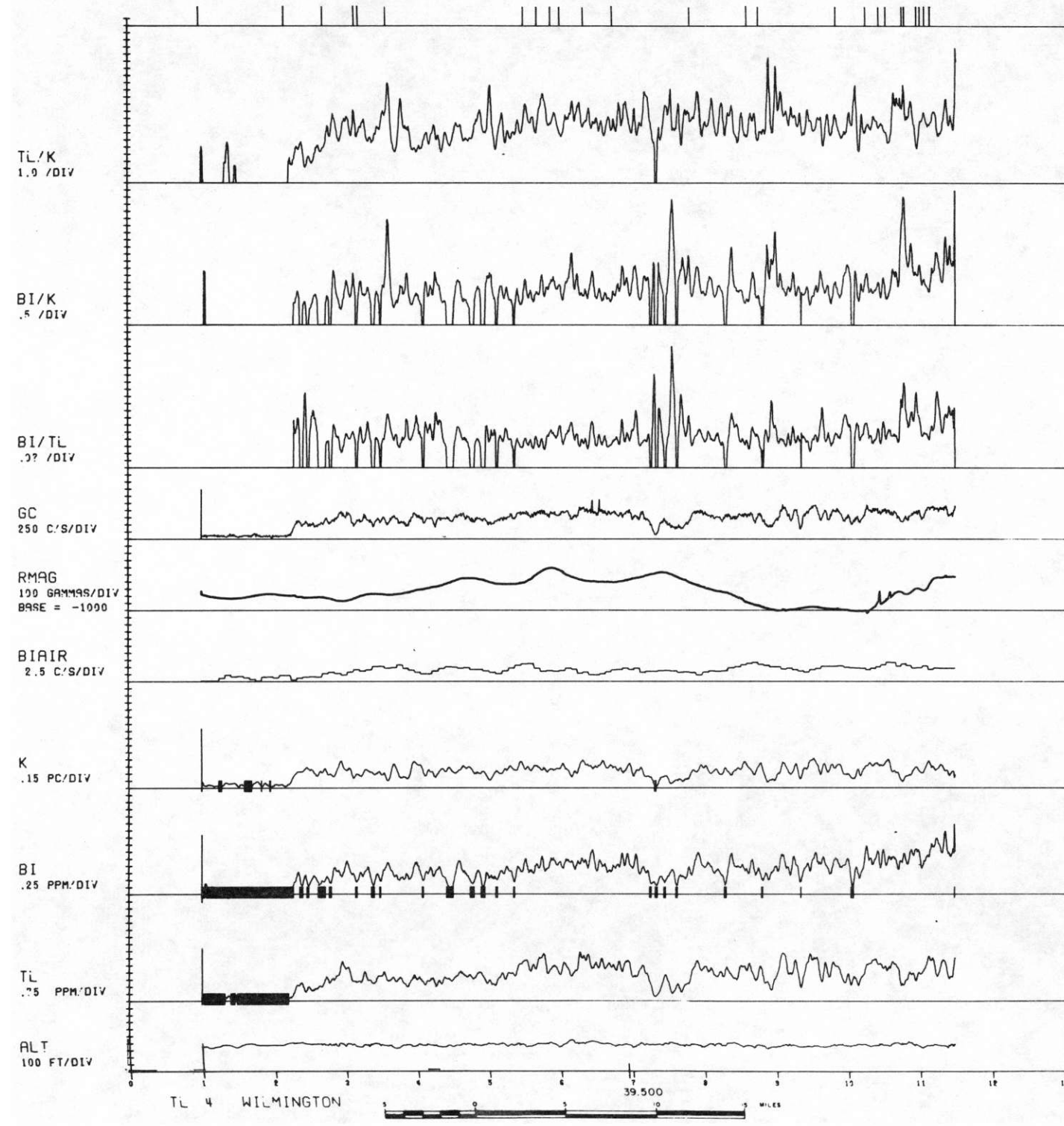
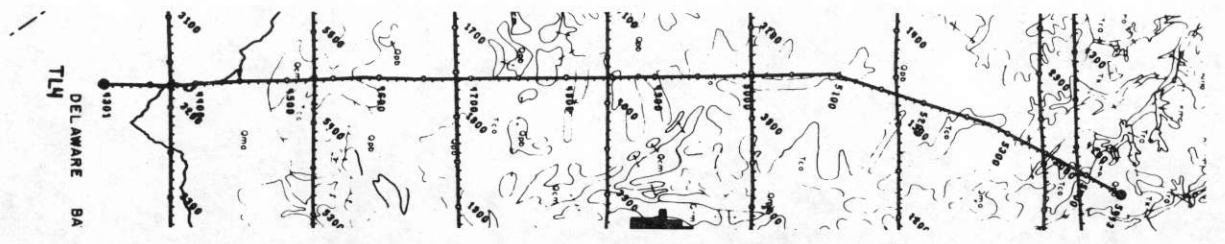
TEMP
1 DEG C/DIV
BASE = 15

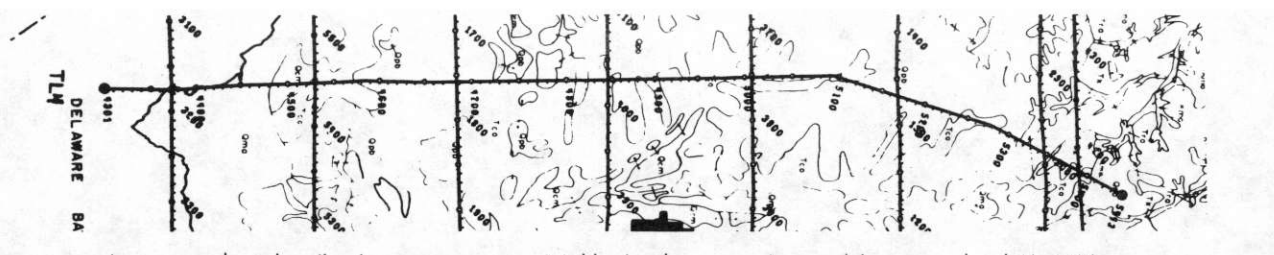
ALT
100 FT/DIV

TL 3 WILMINGTON



LAT 40.000





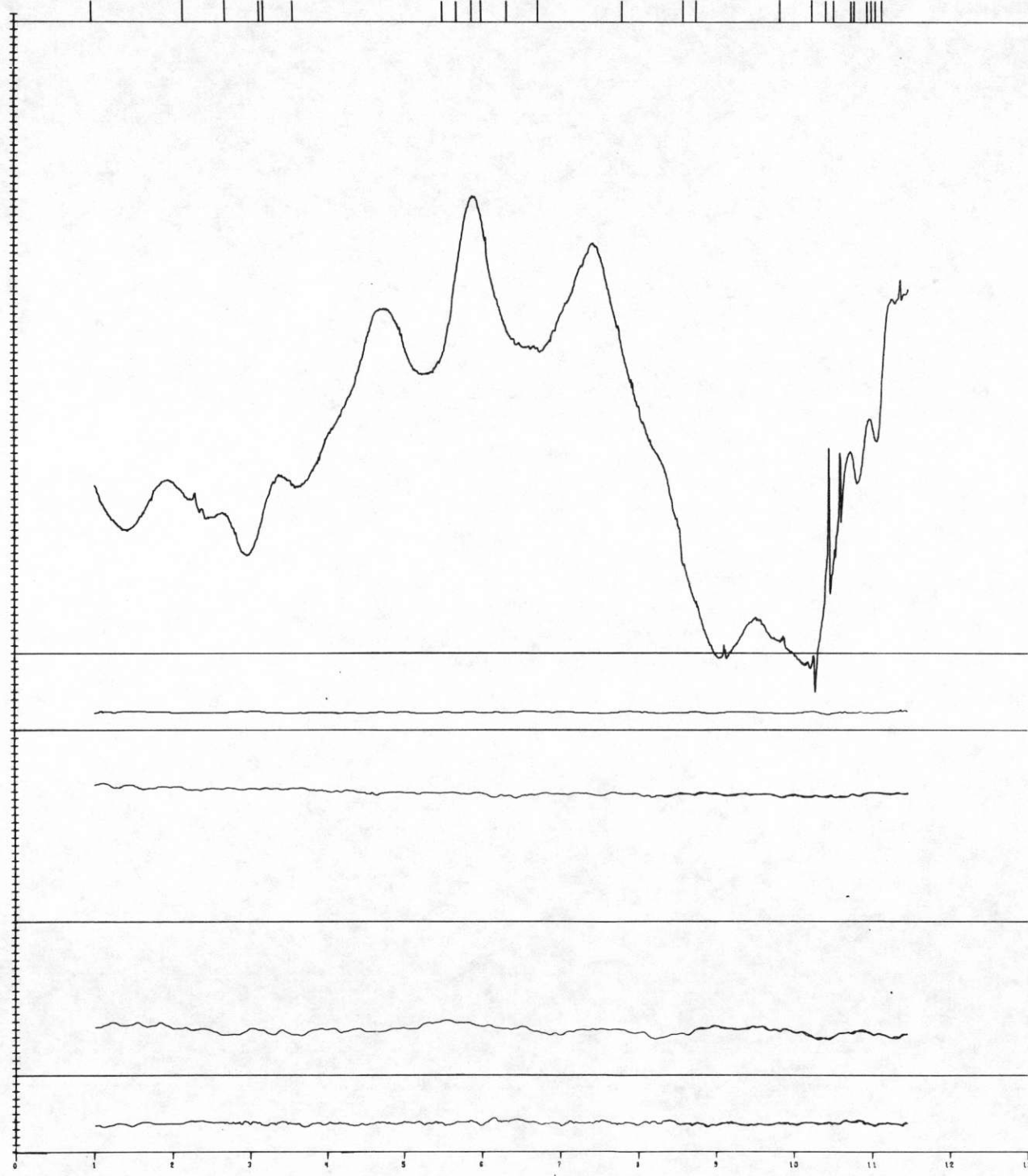
RMAG
10 GAMMA/DIV
BASE = -1000

BMAG
10 GAMMA/DIV
BASE = 54180

BP
3 MM HG/DIV
BASE = 700

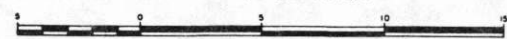
TEMP
1 DEG C/DIV
BASE = 15

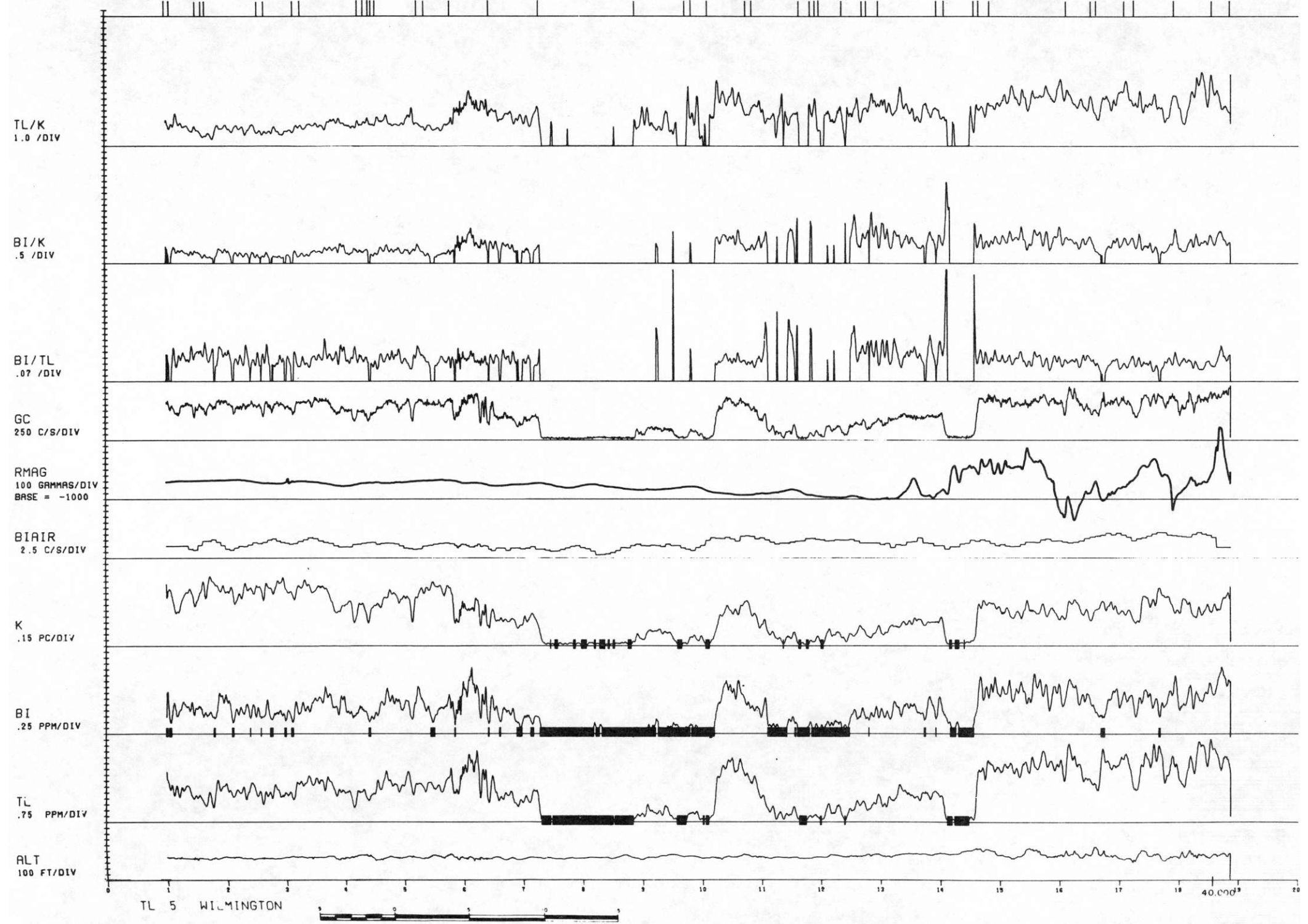
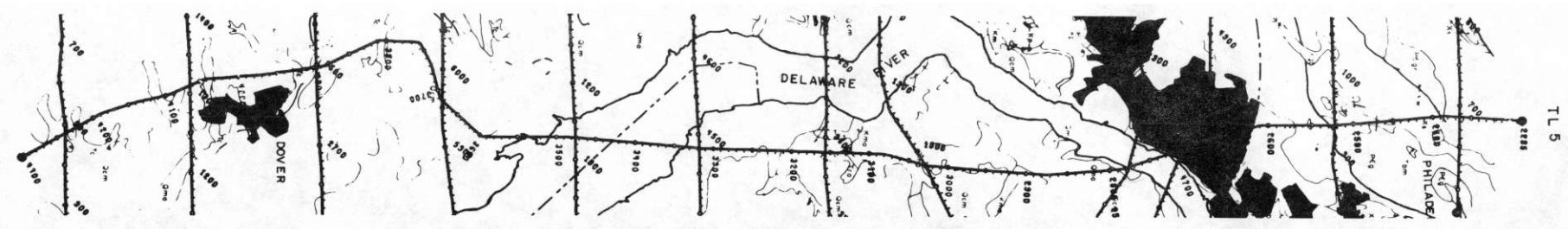
ALT
100 FT/DIV

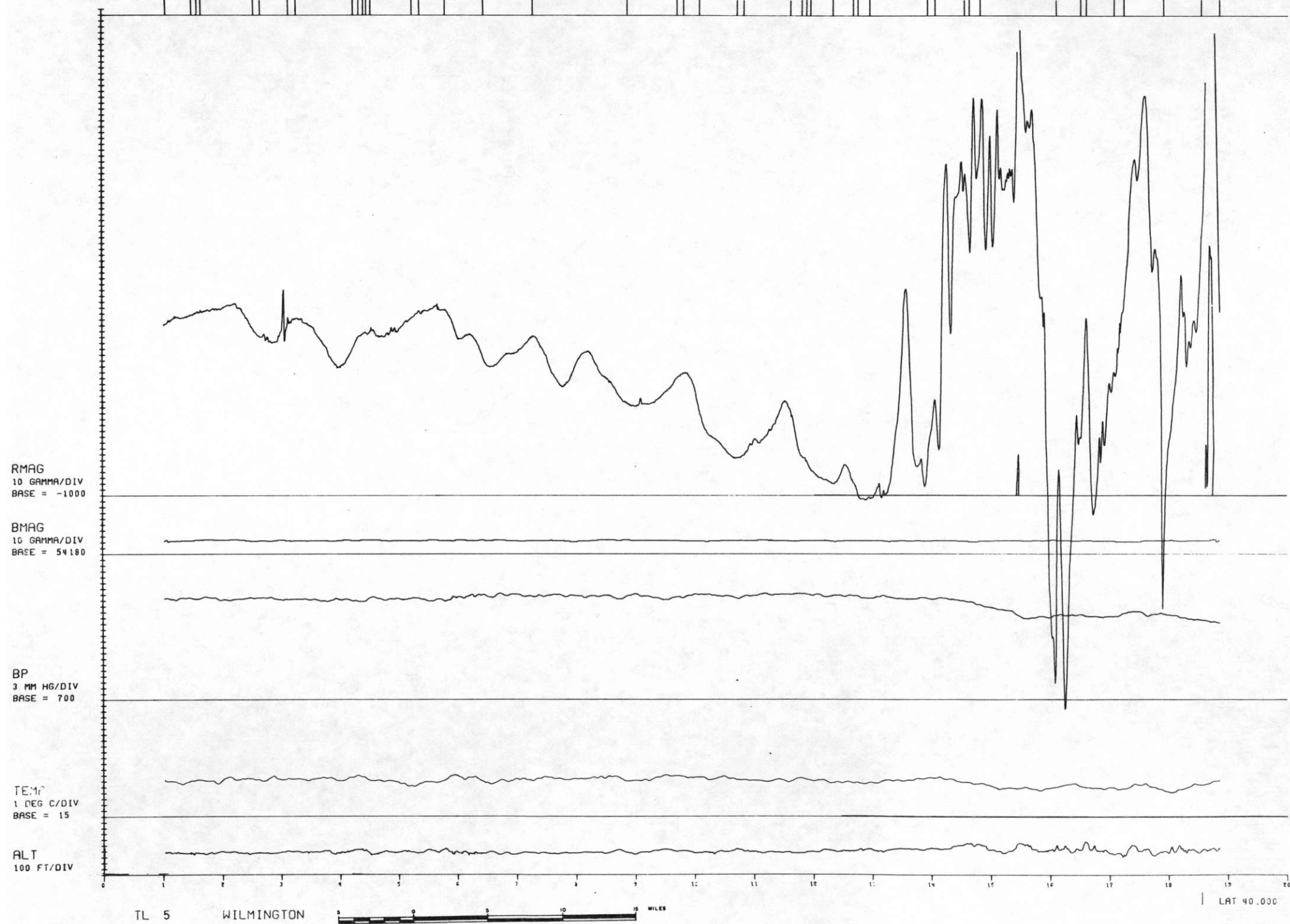


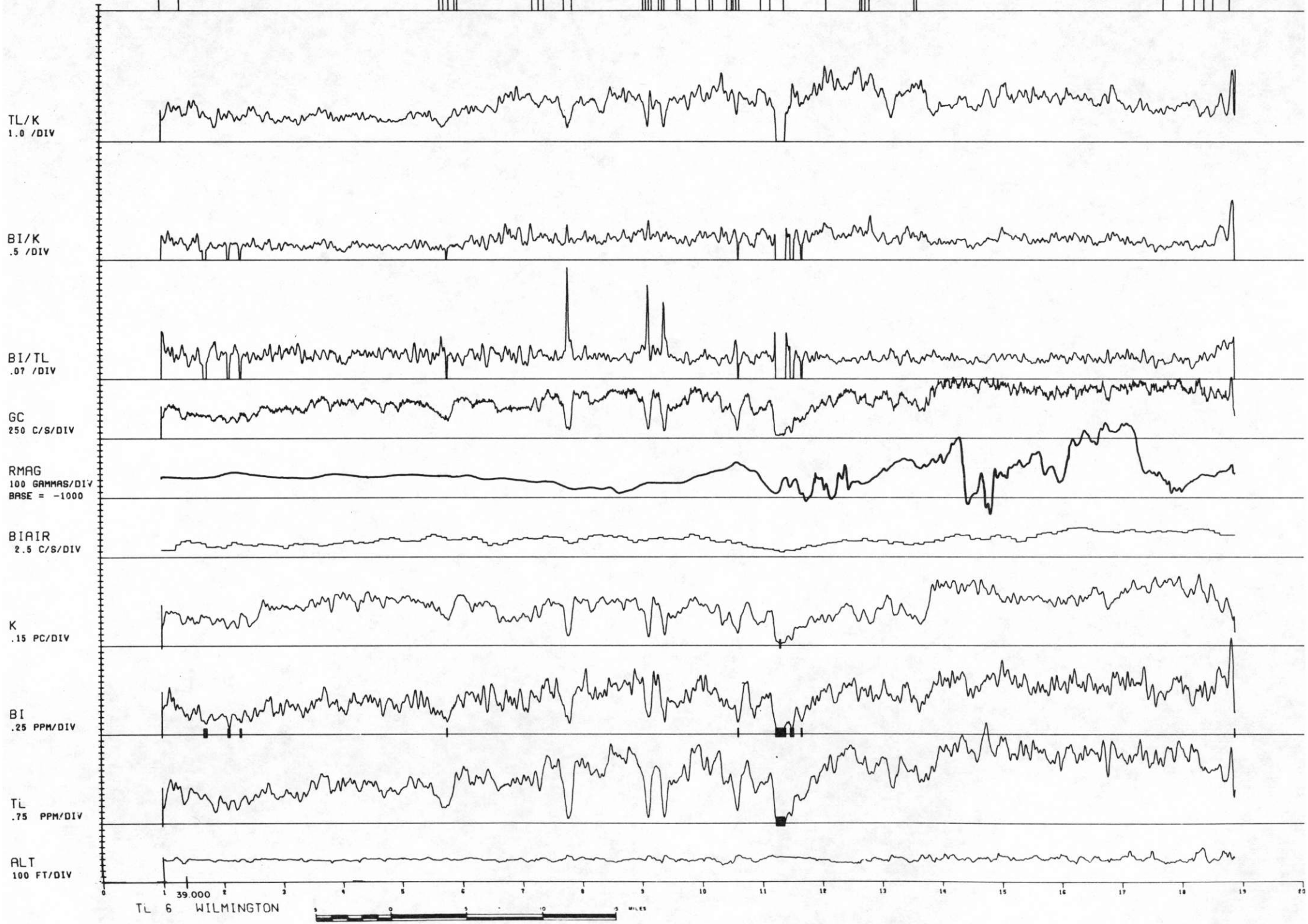
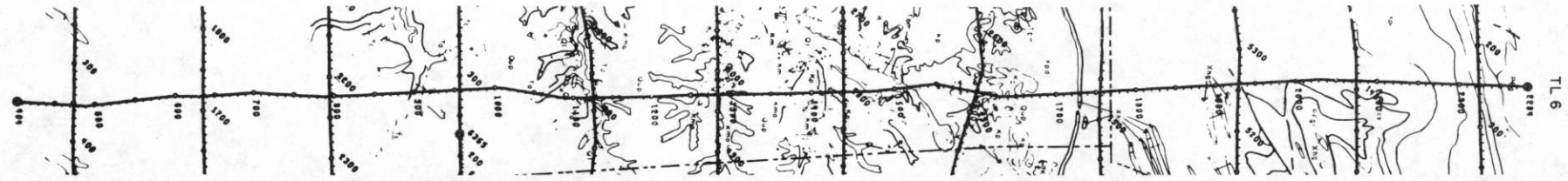
TL 4 WILMINGTON

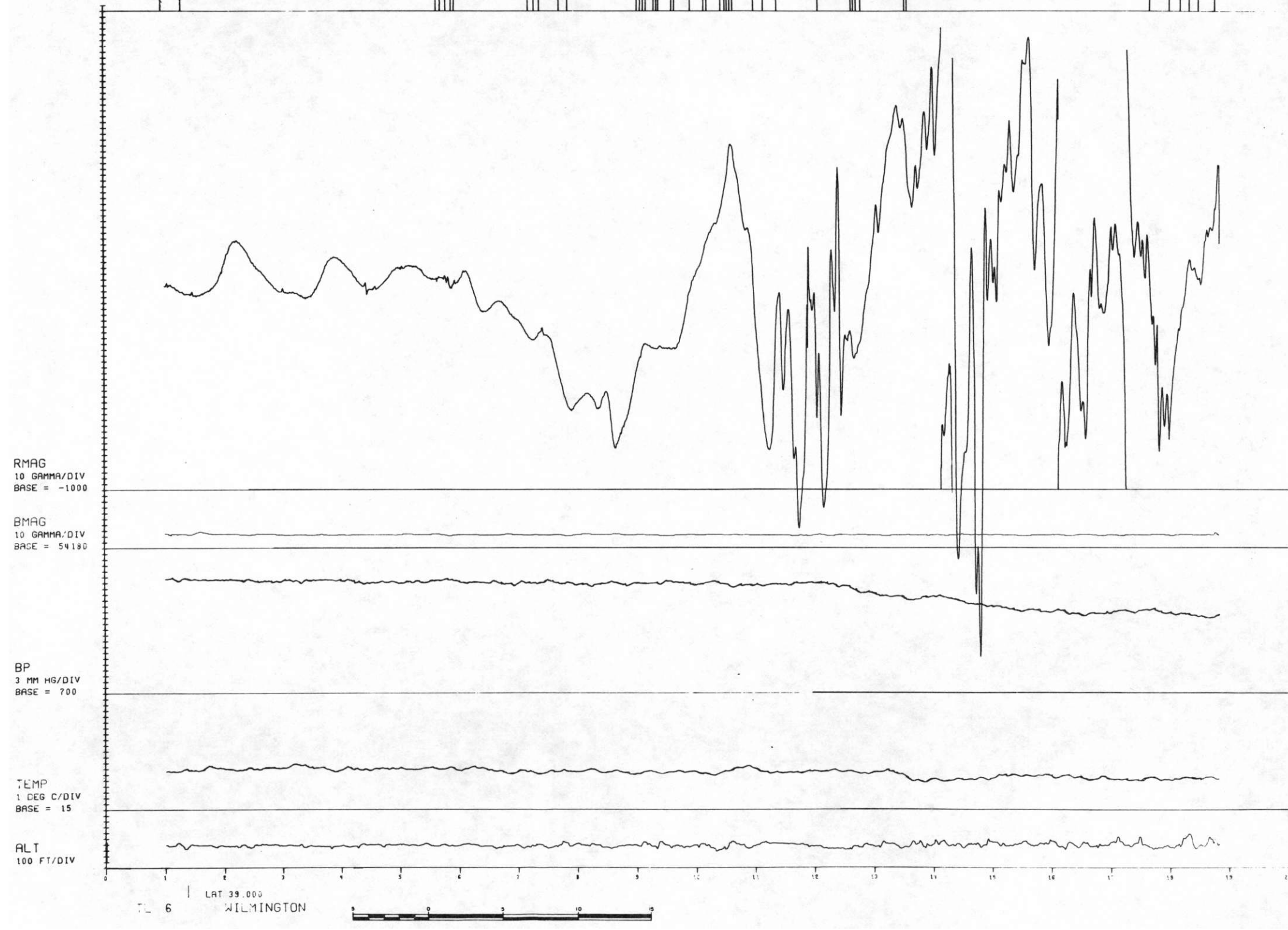
LAT 39.500

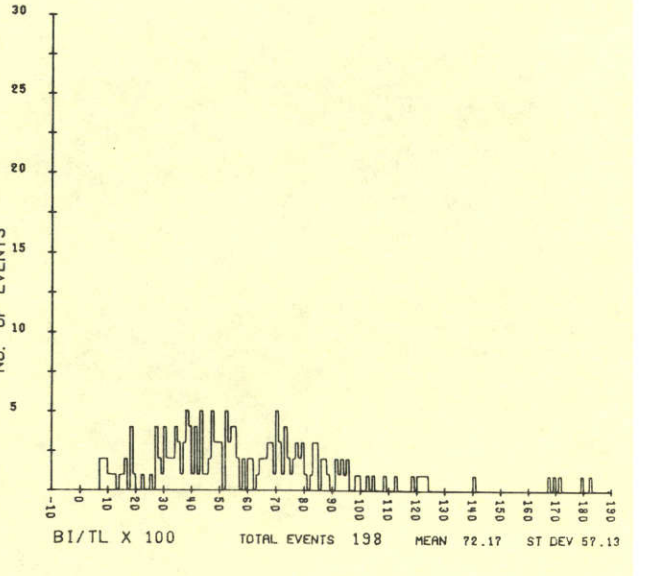
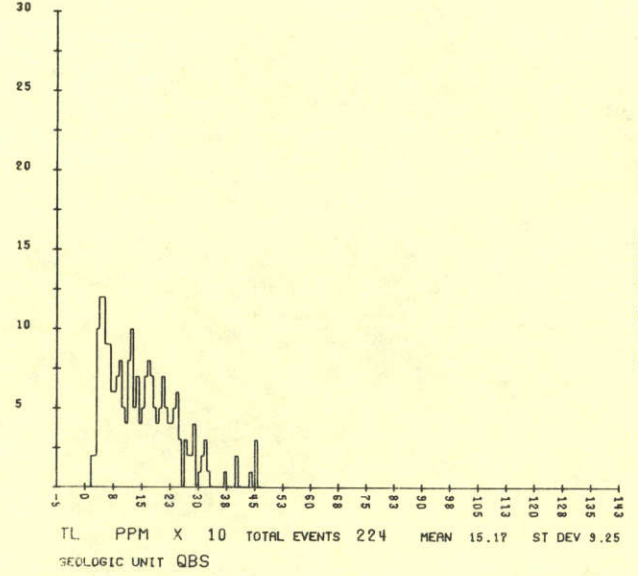
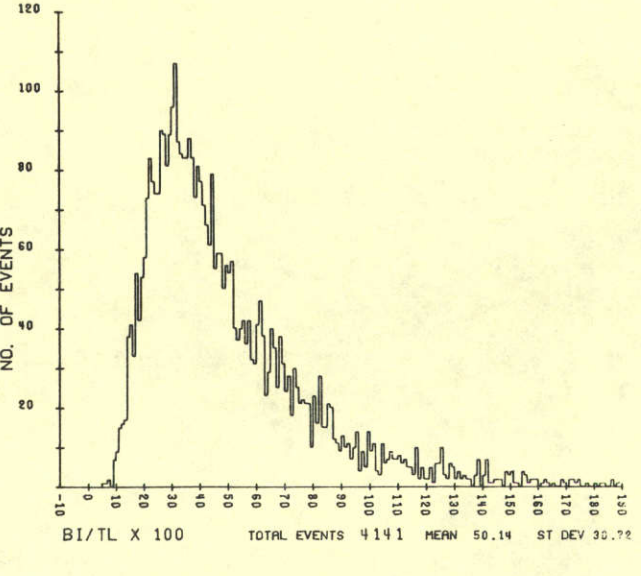
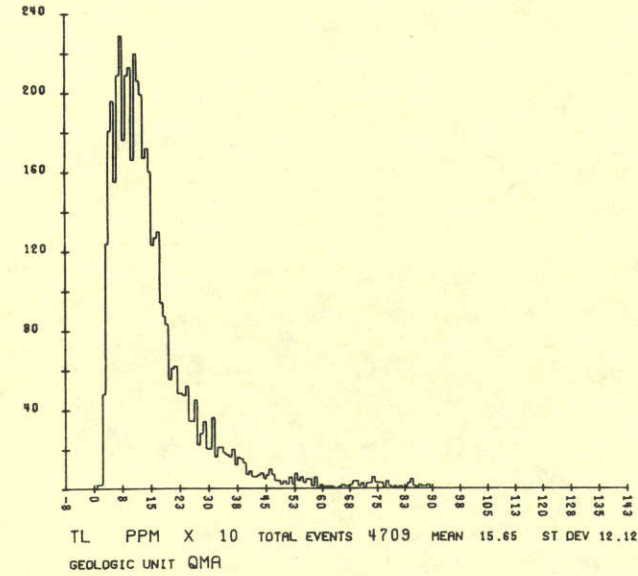
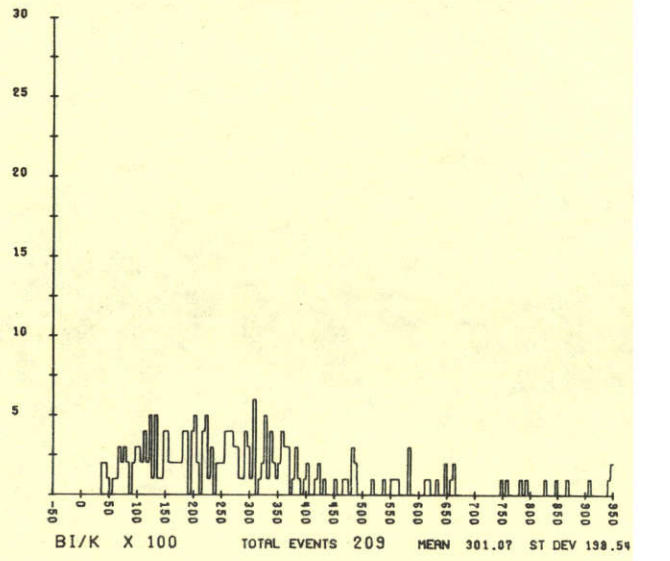
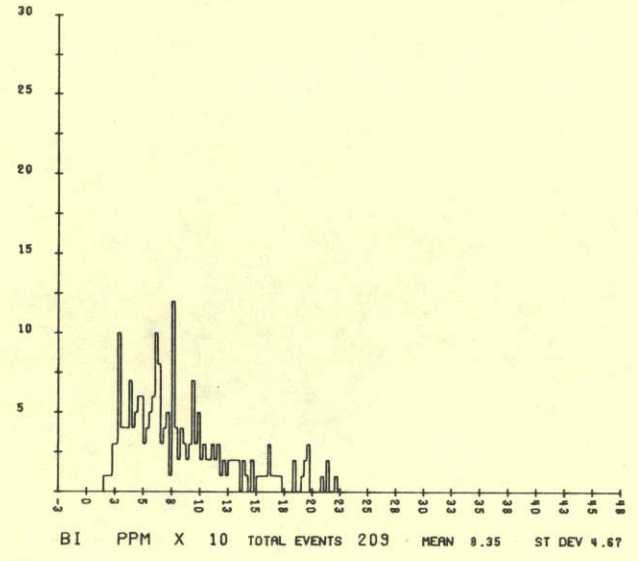
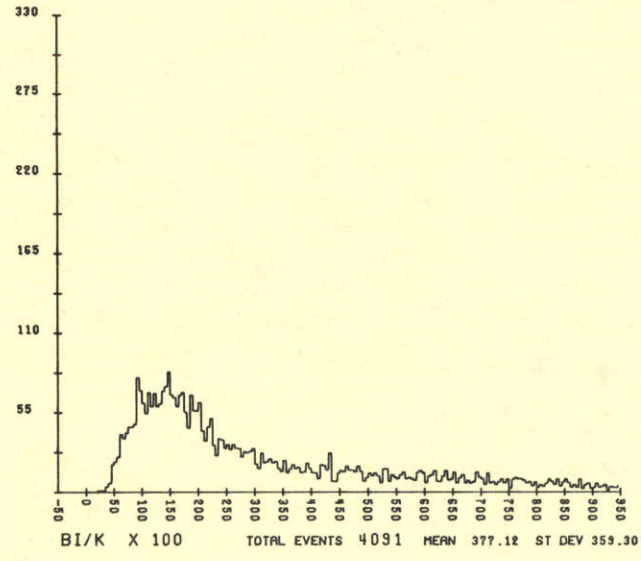
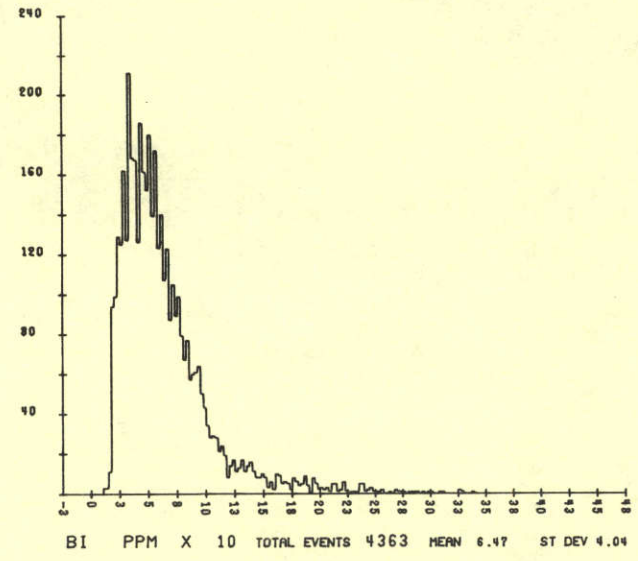
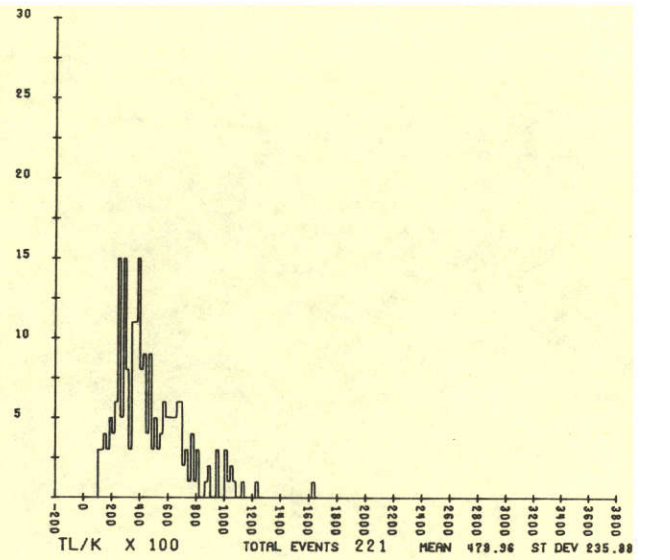
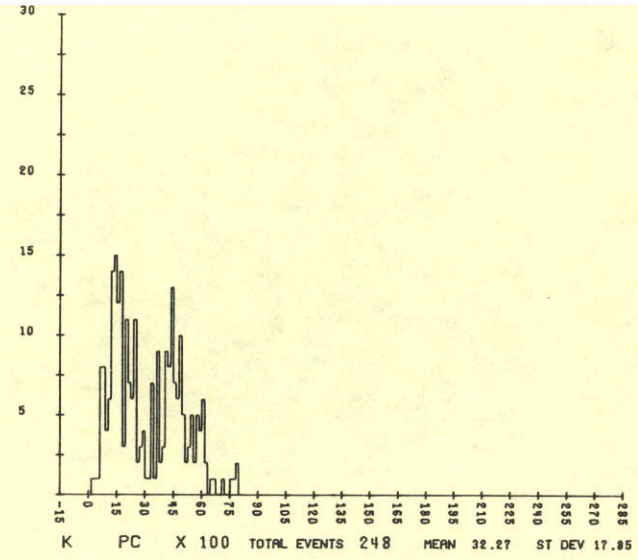
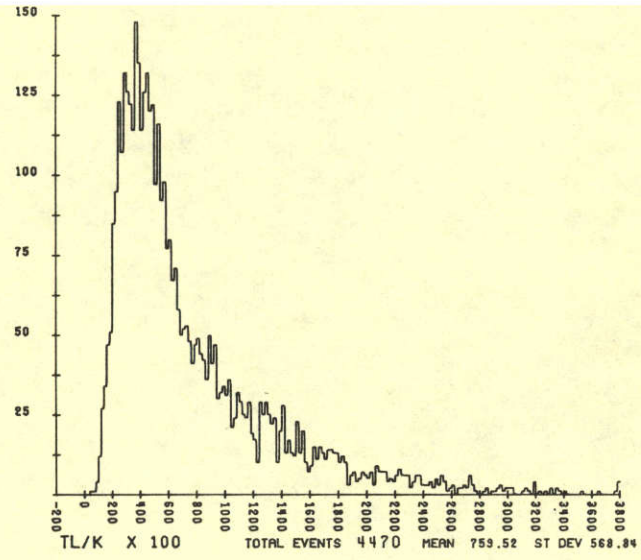
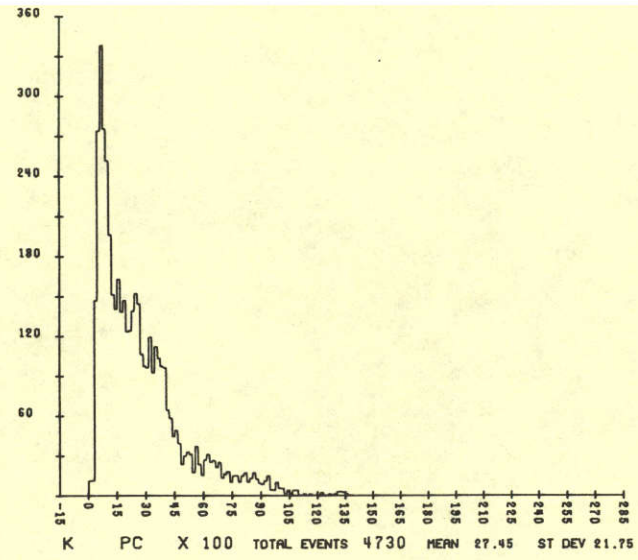






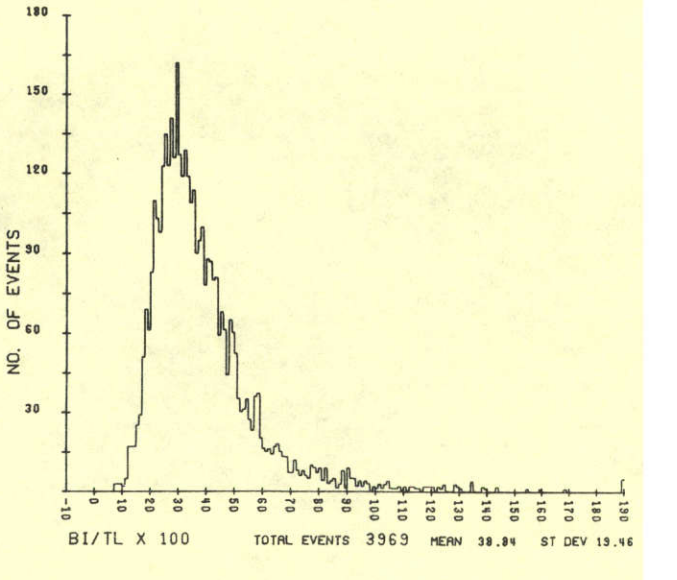
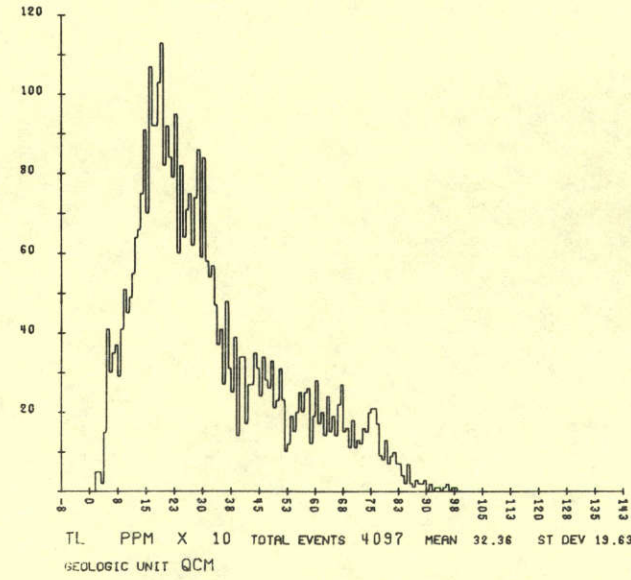
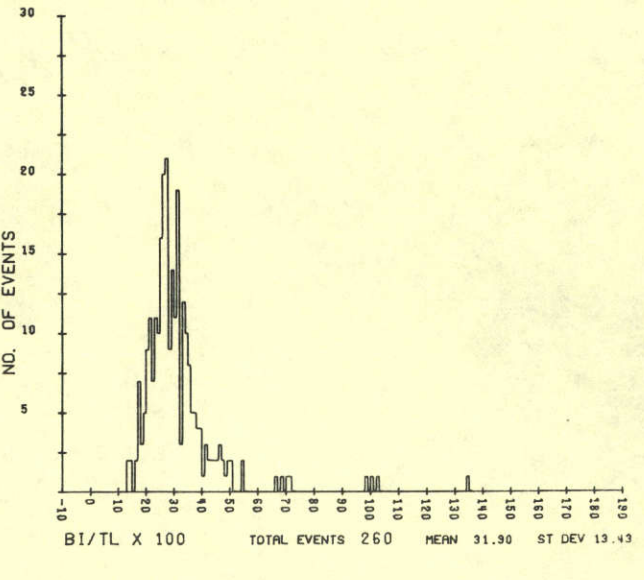
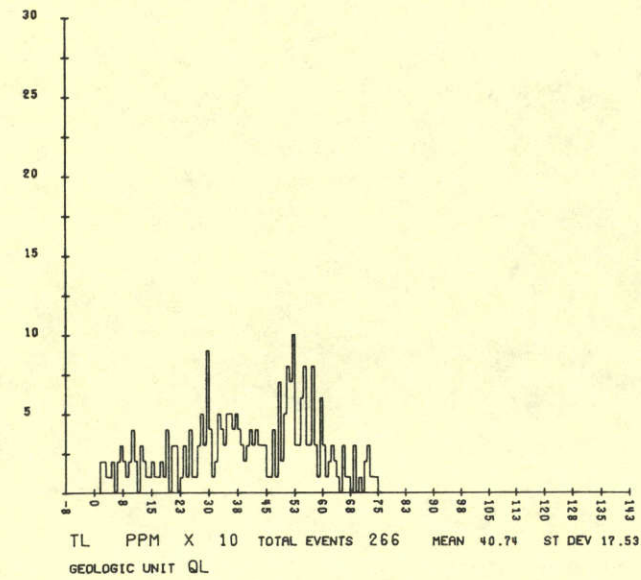
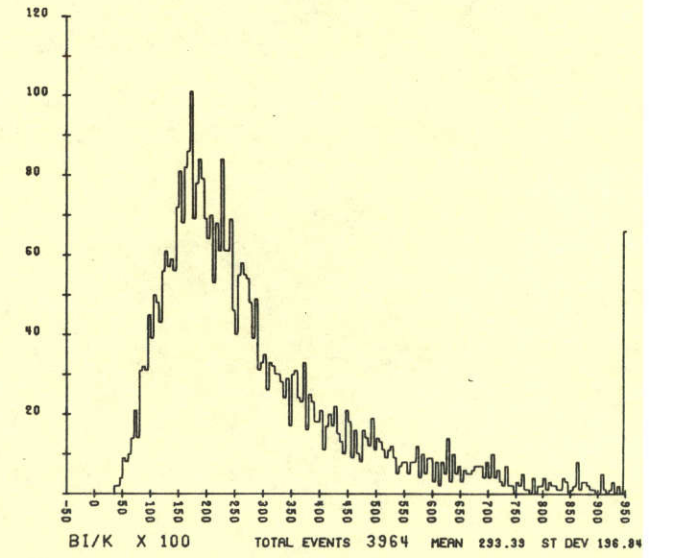
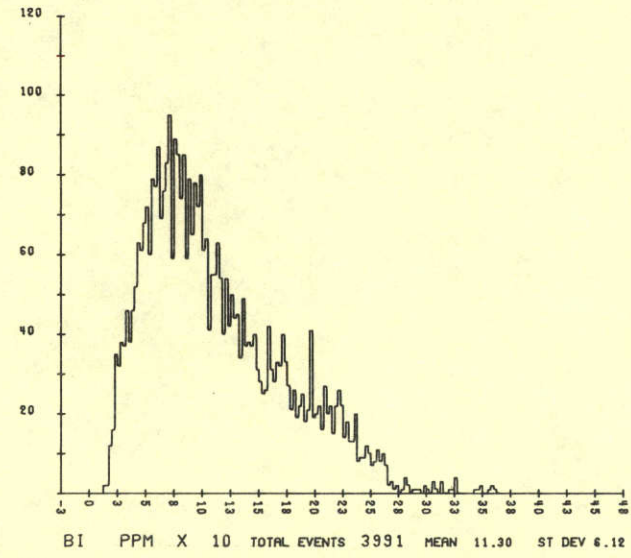
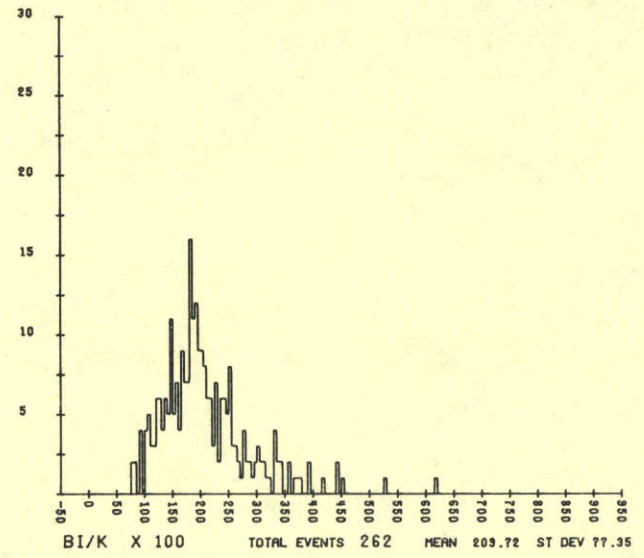
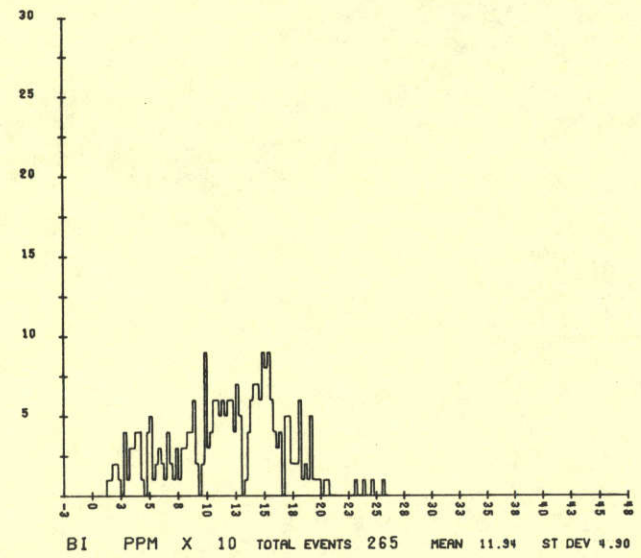
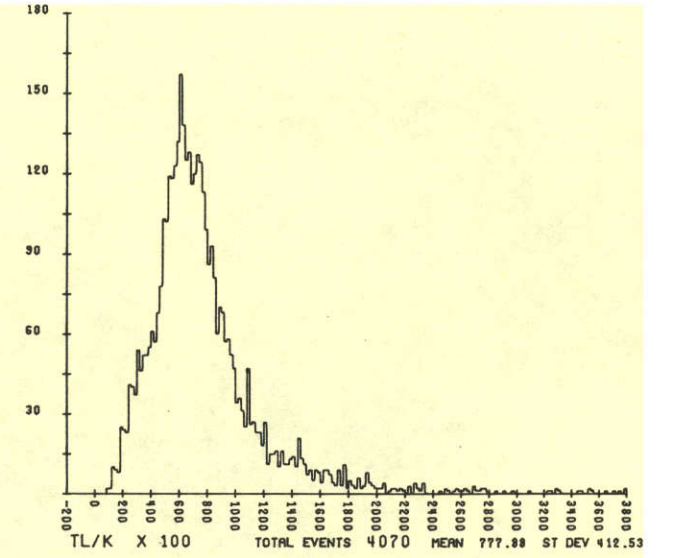
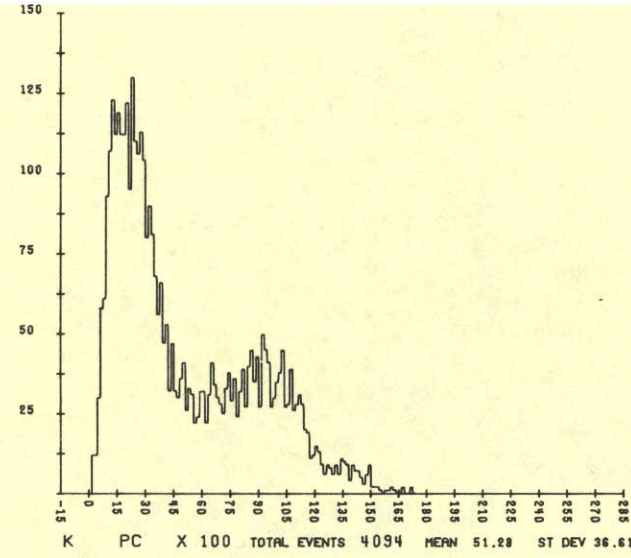
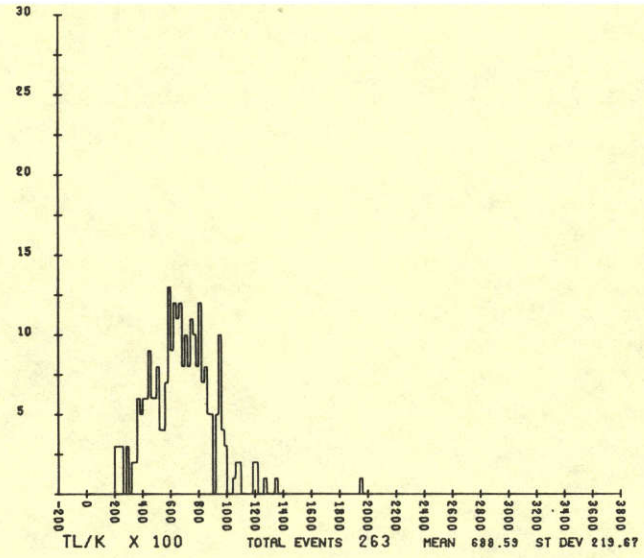
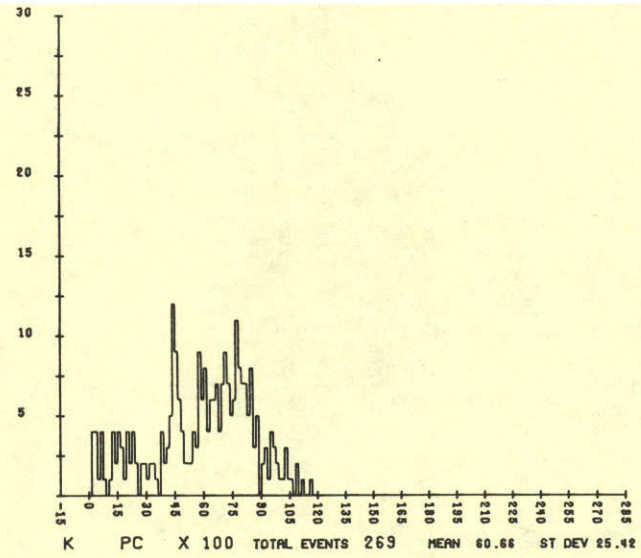






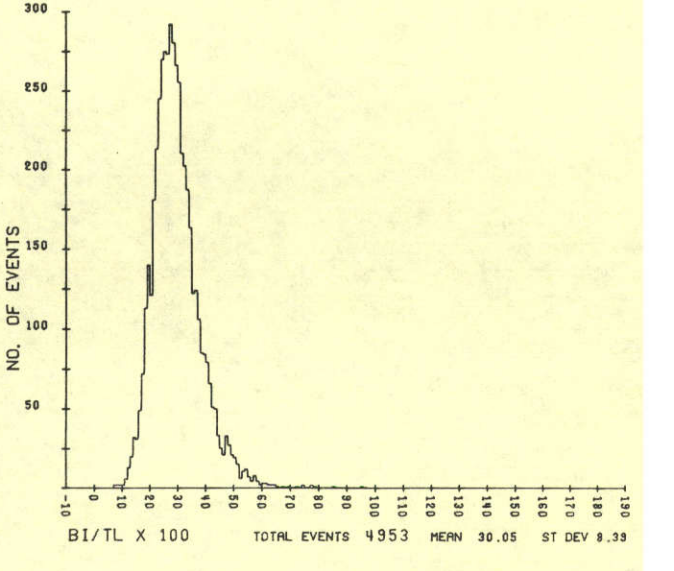
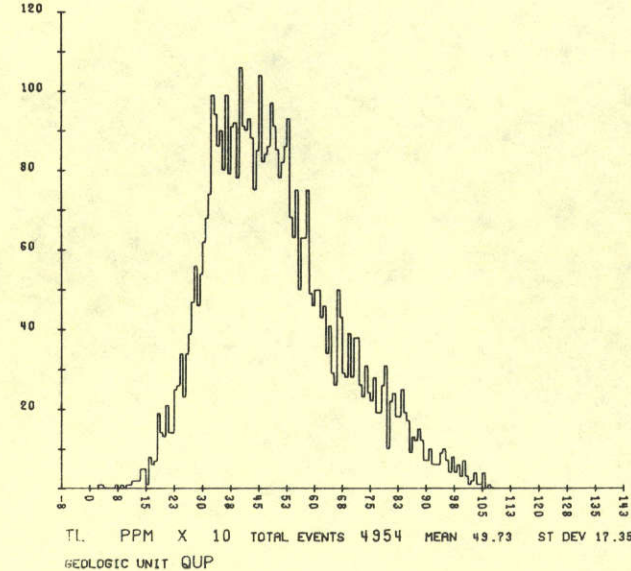
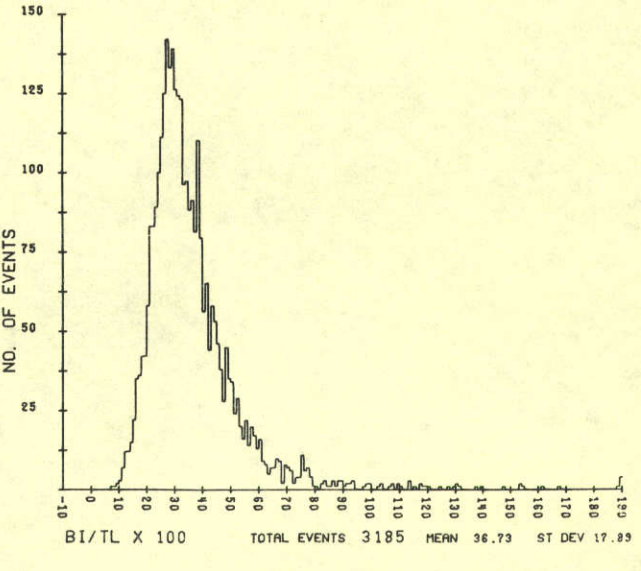
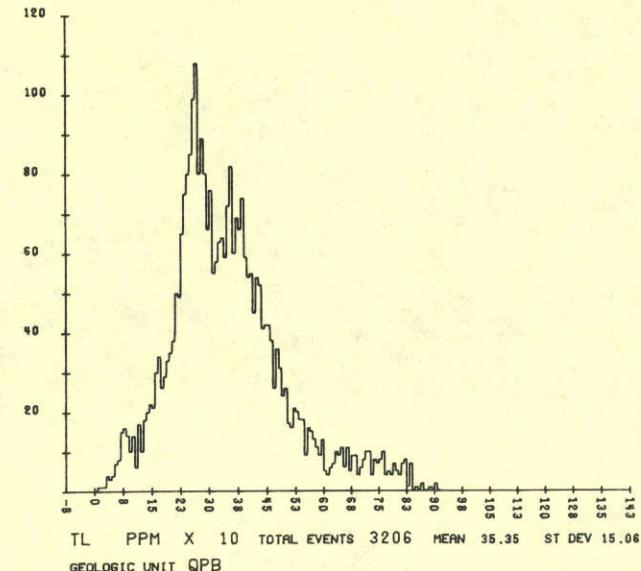
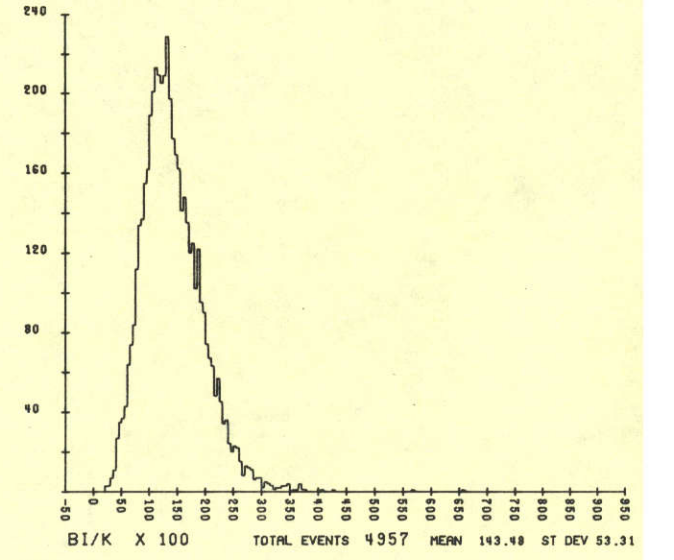
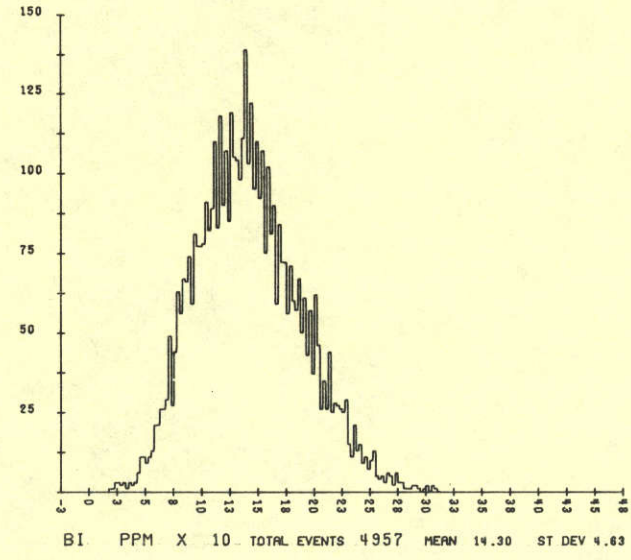
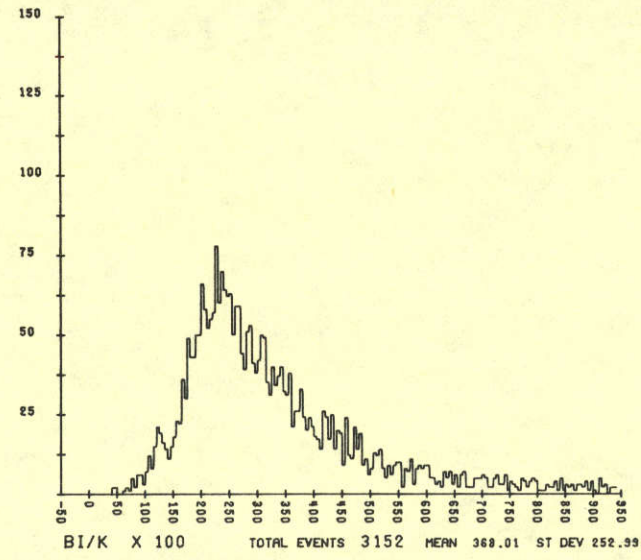
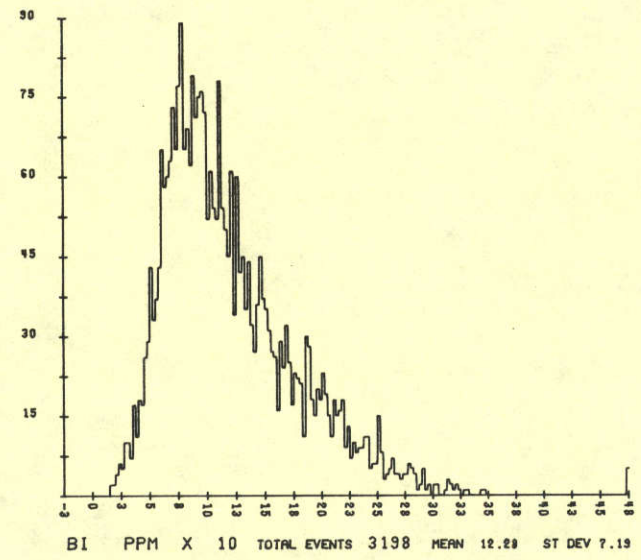
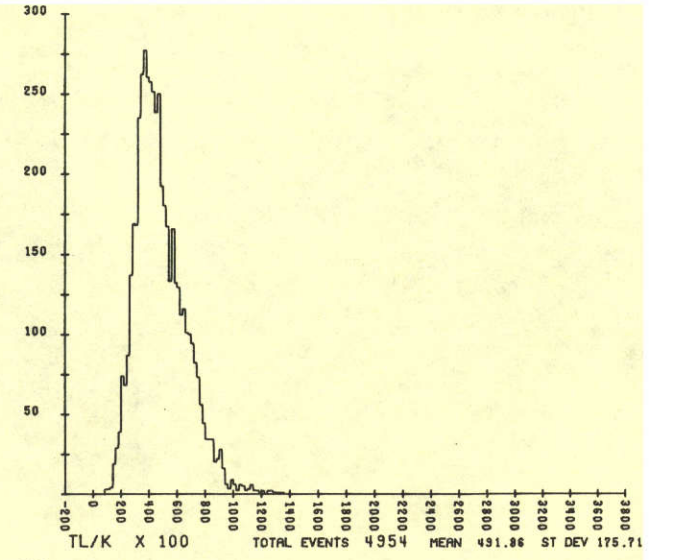
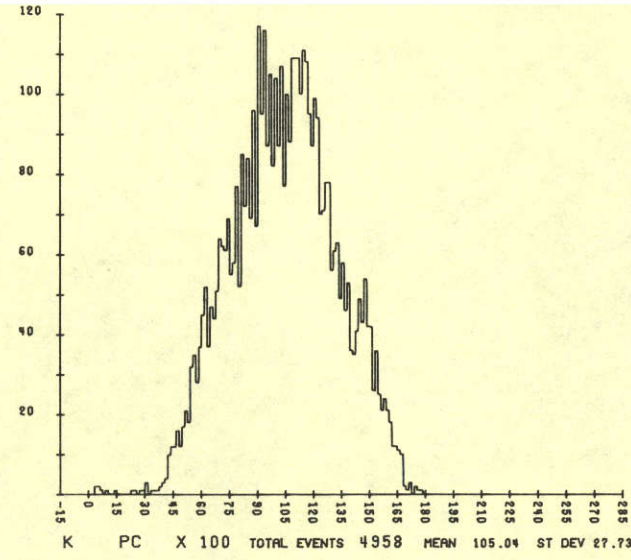
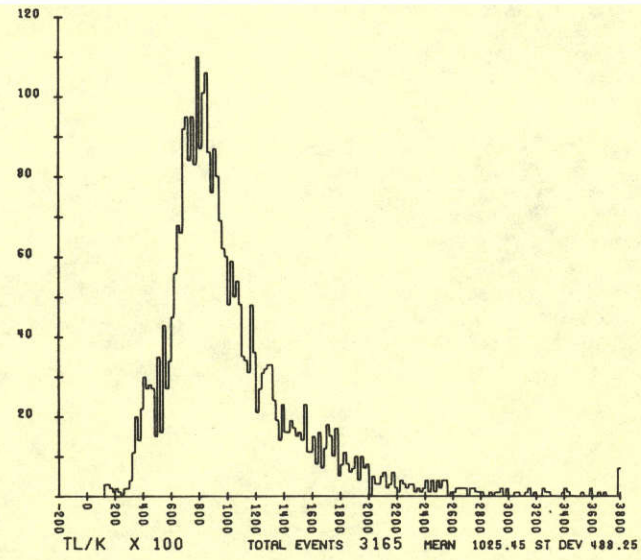
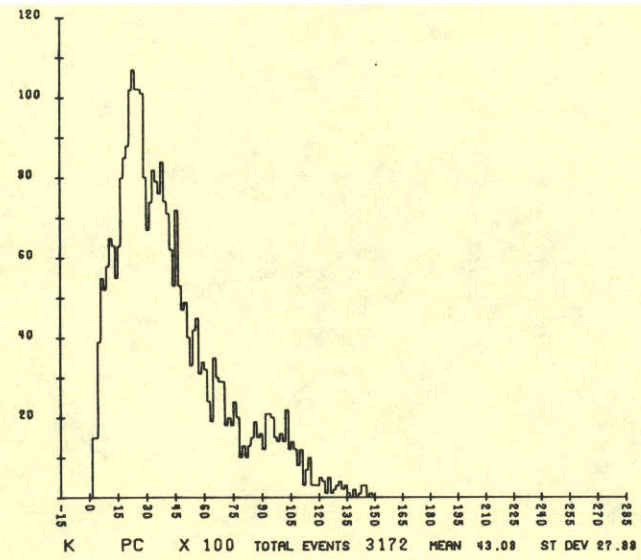
A1

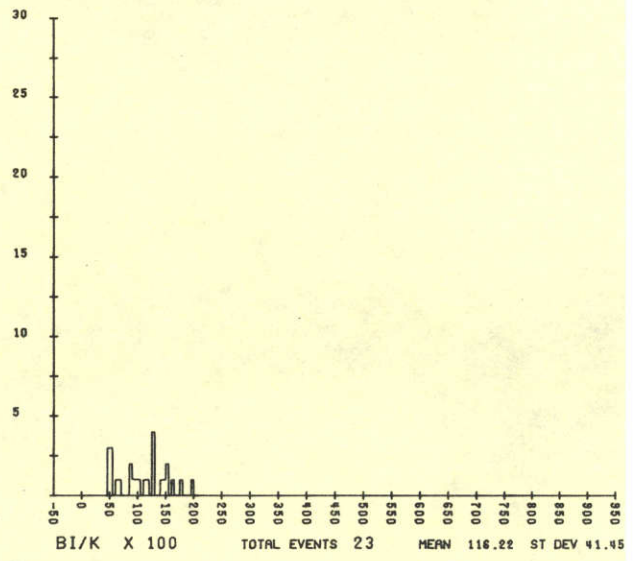
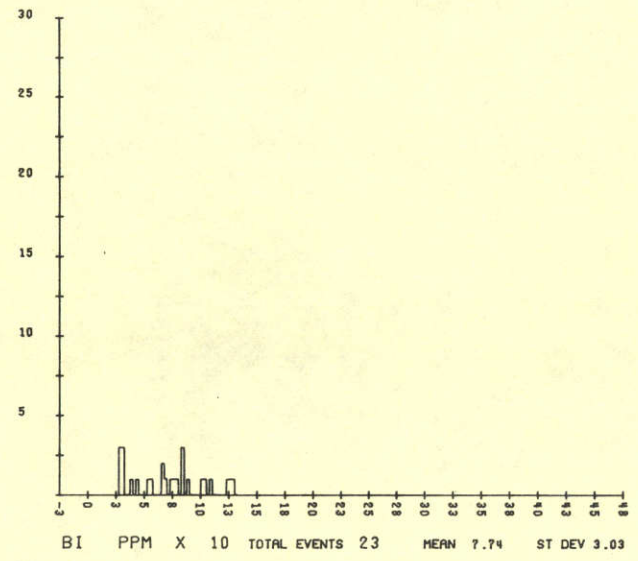
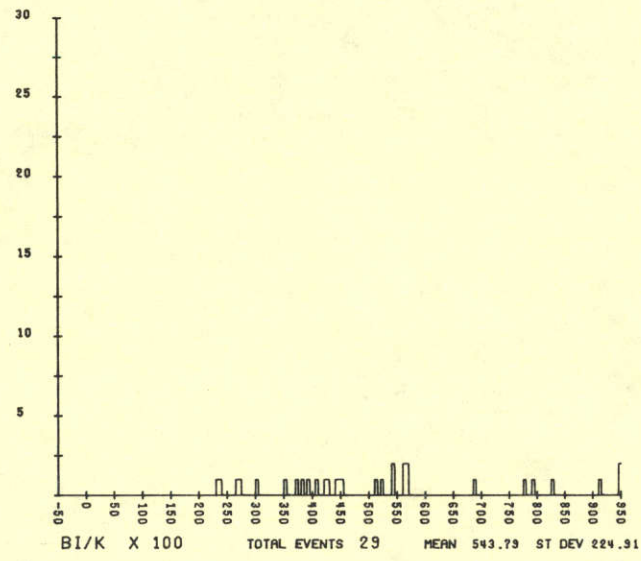
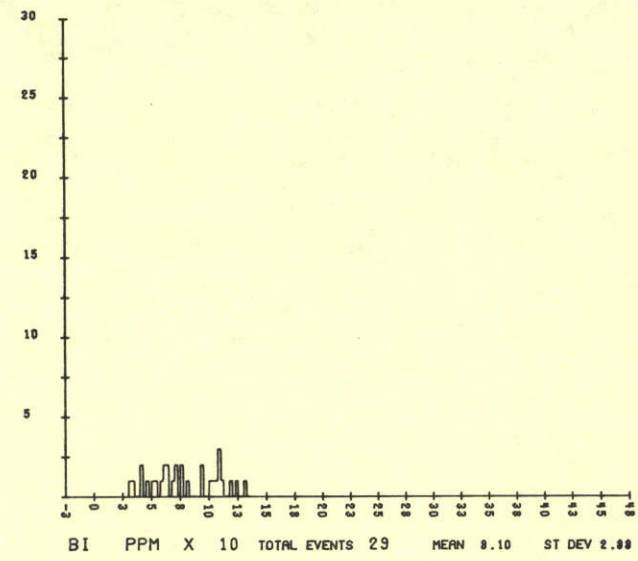
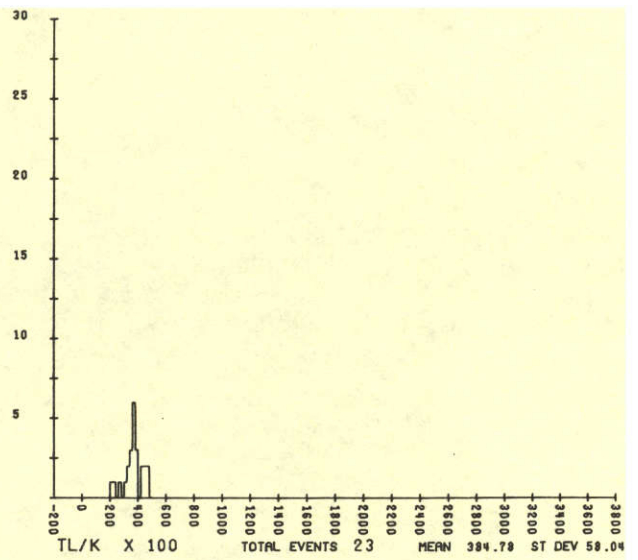
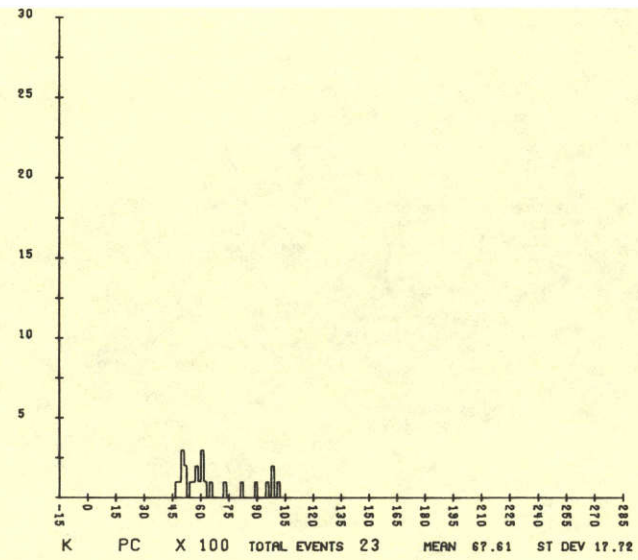
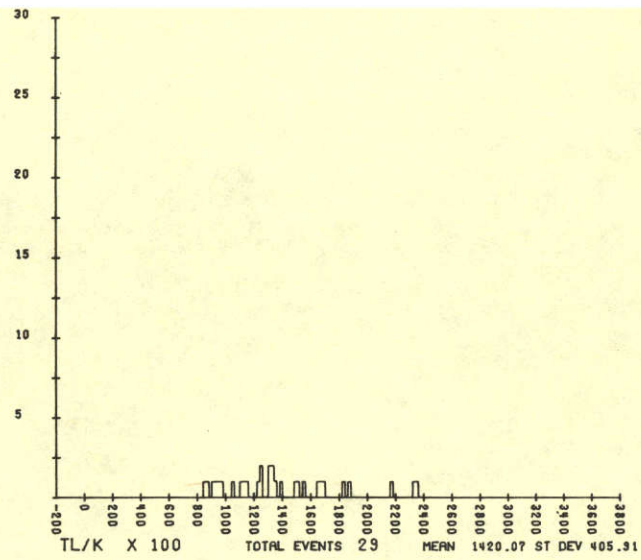
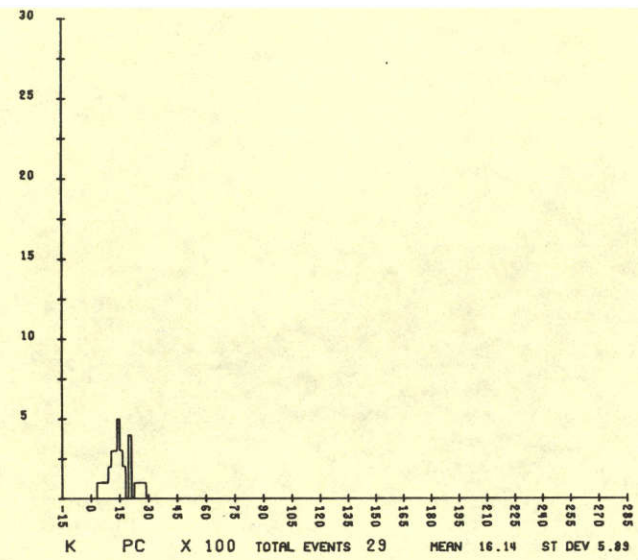
R2



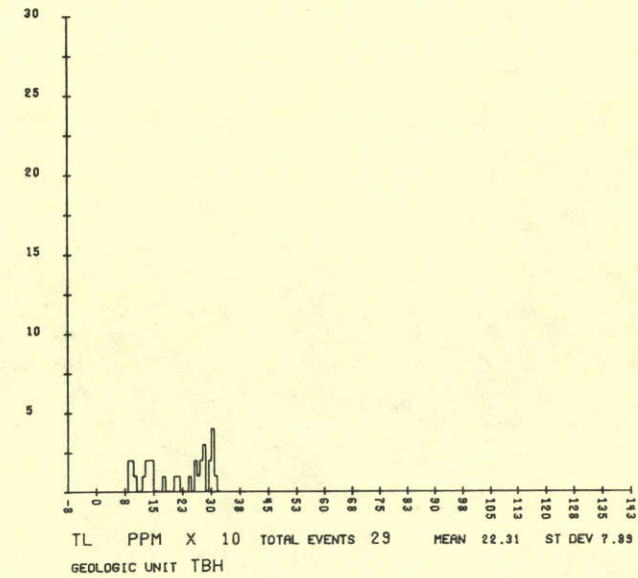
HILMINGTON

HILMINGTON

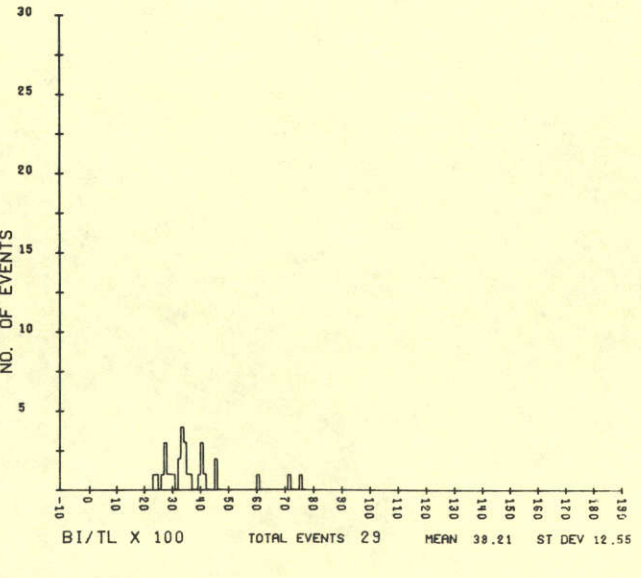




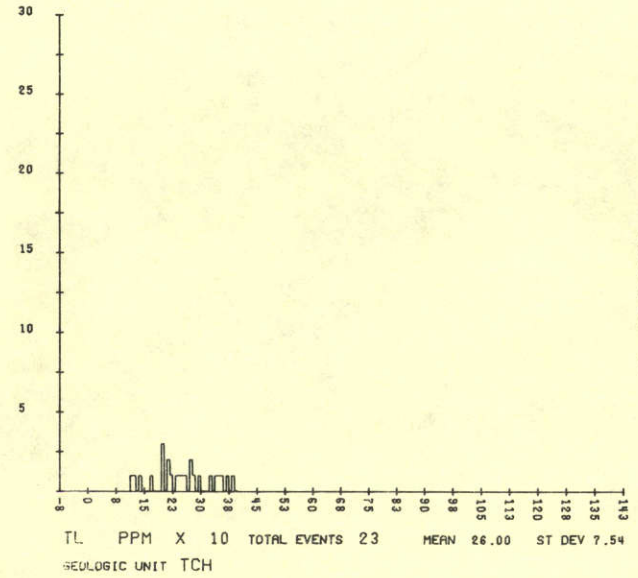
WILMINGTON



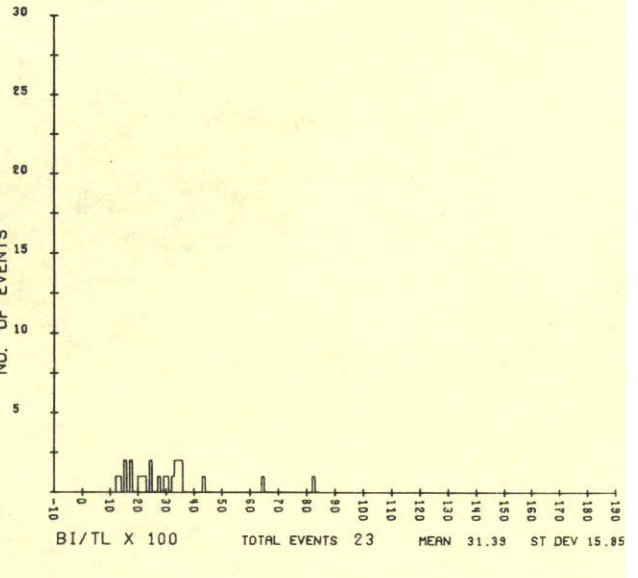
NO. OF EVENTS

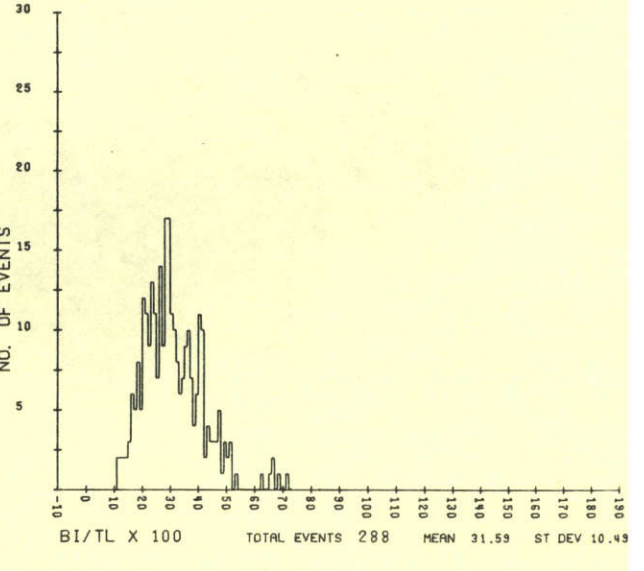
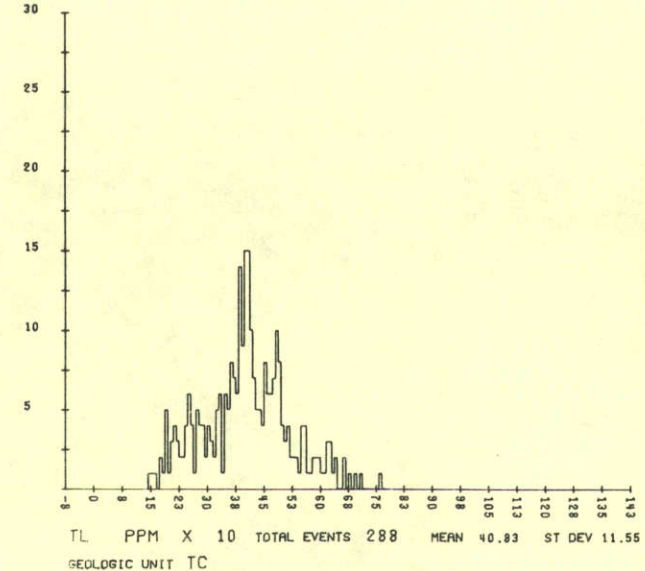
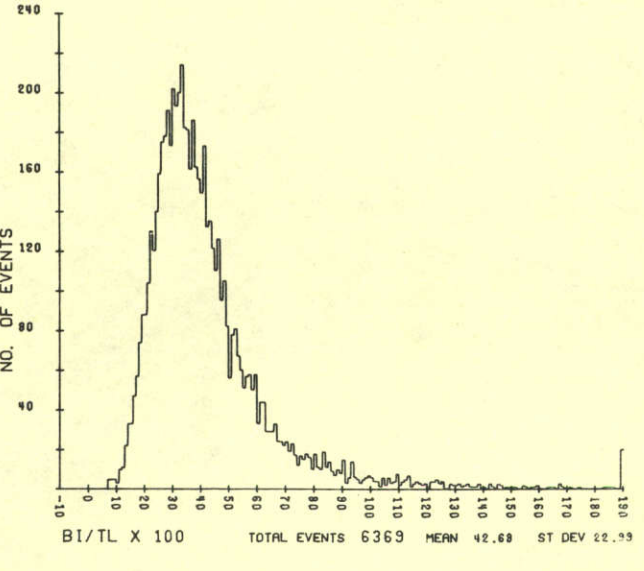
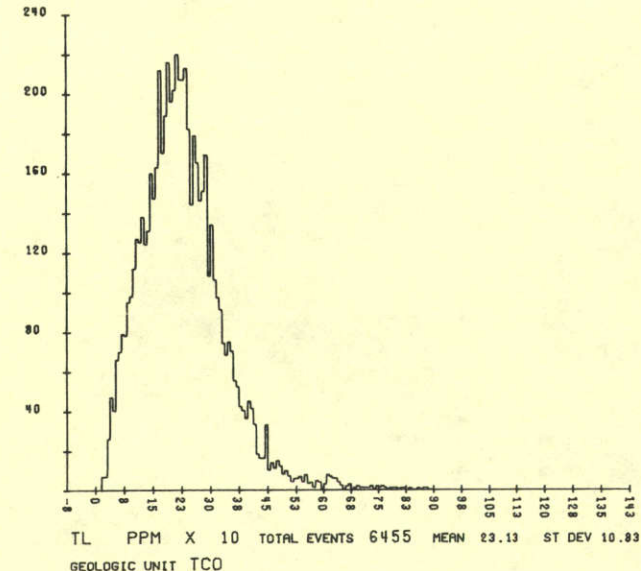
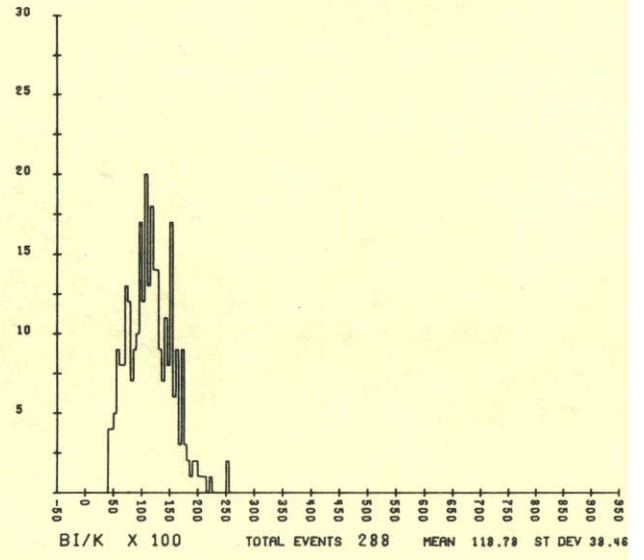
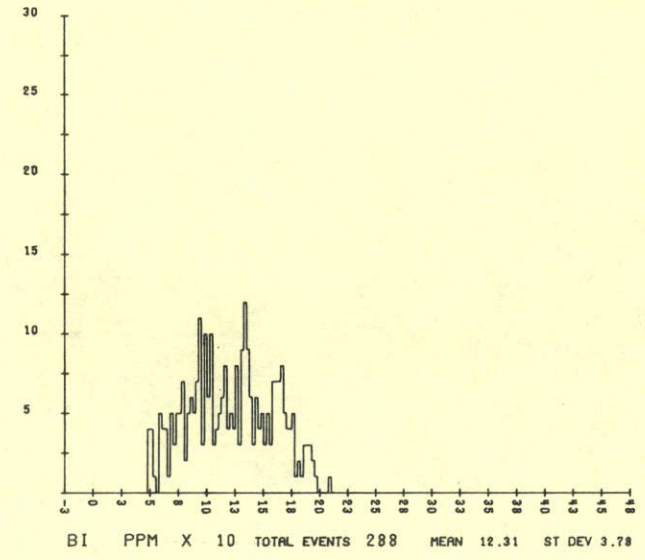
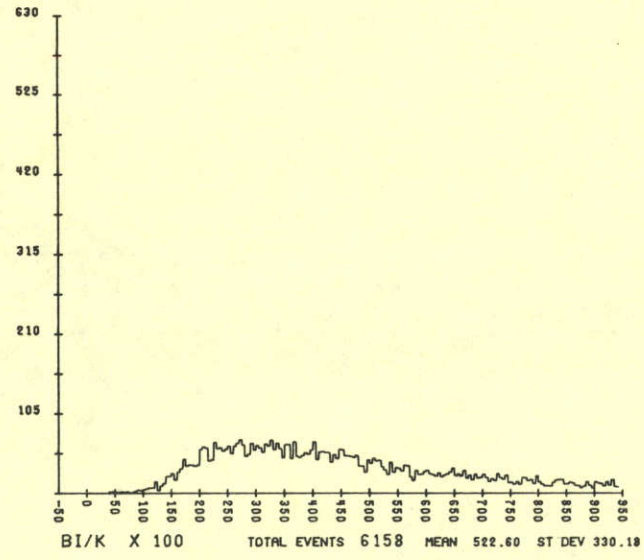
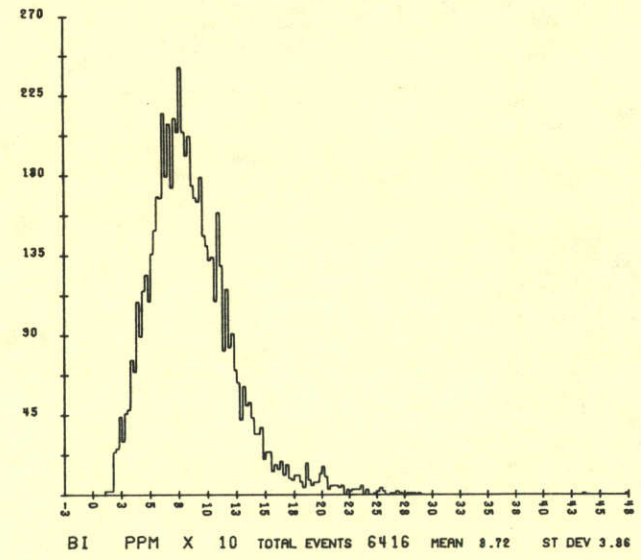
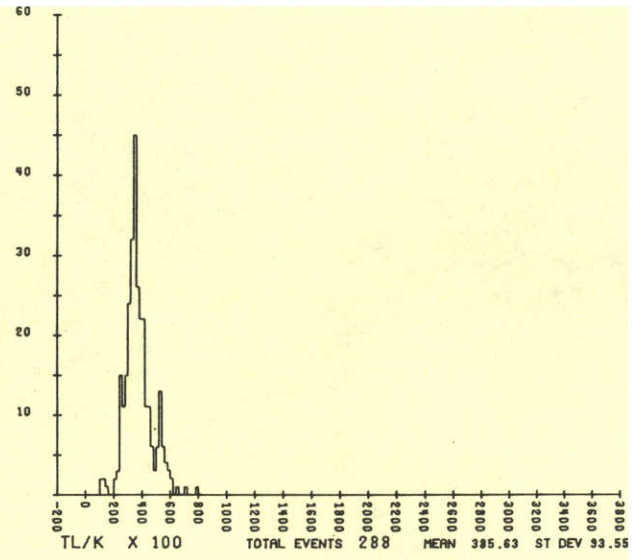
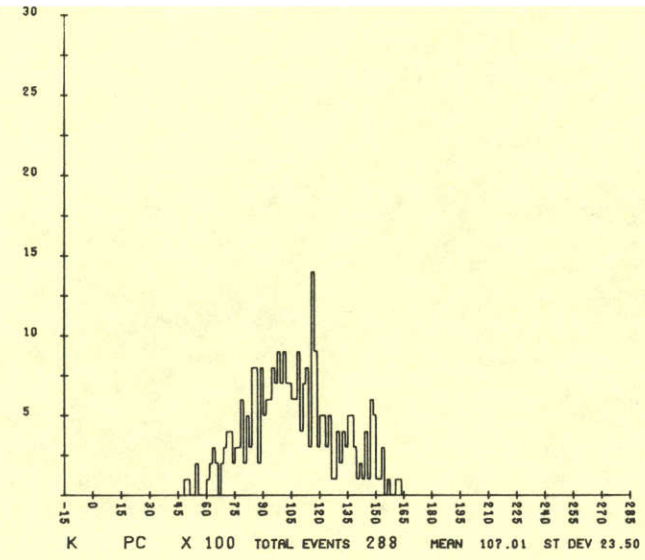
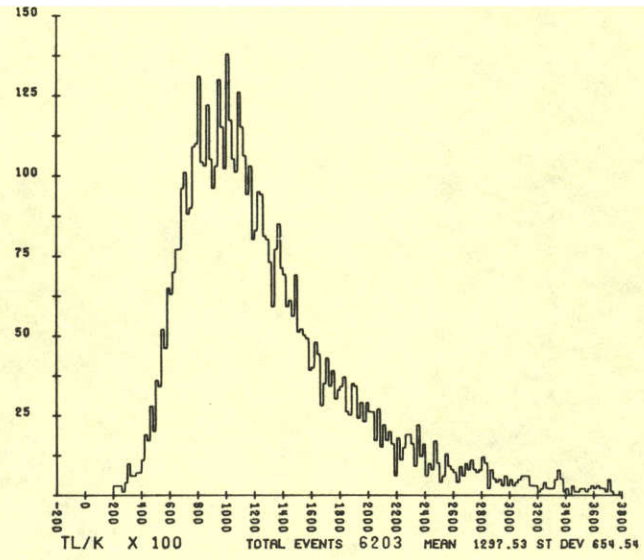
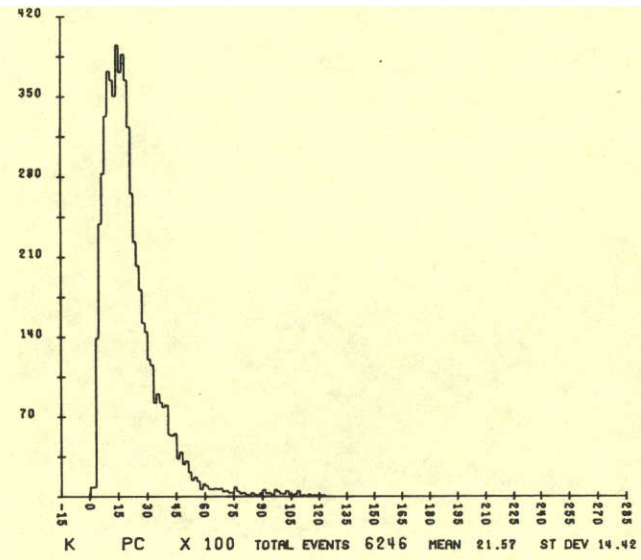


WILMINGTON



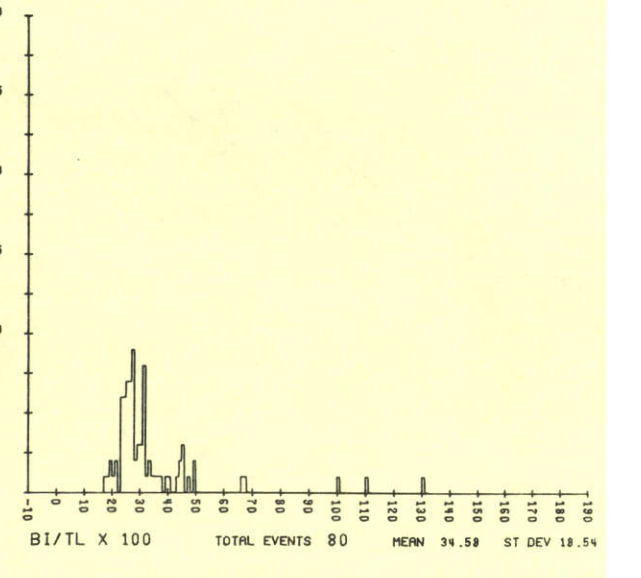
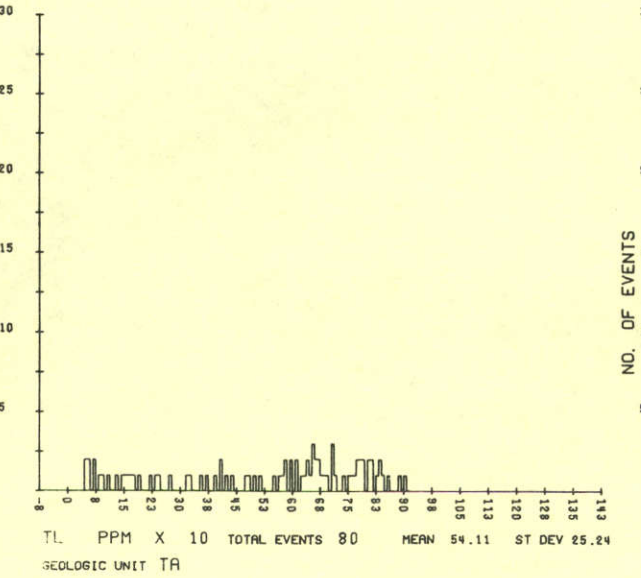
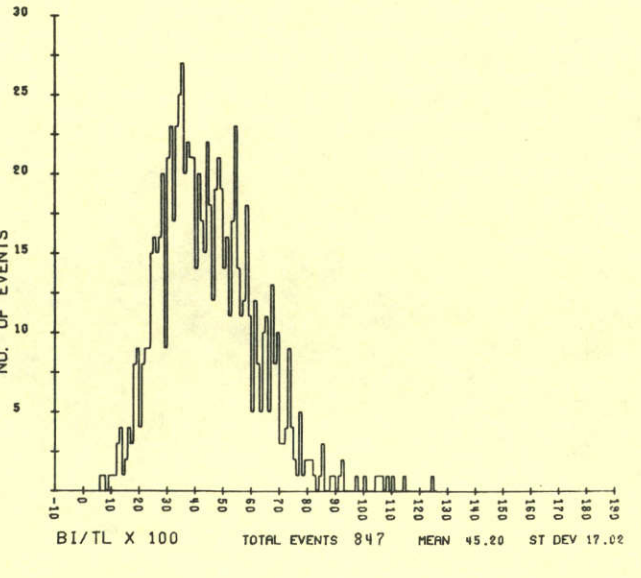
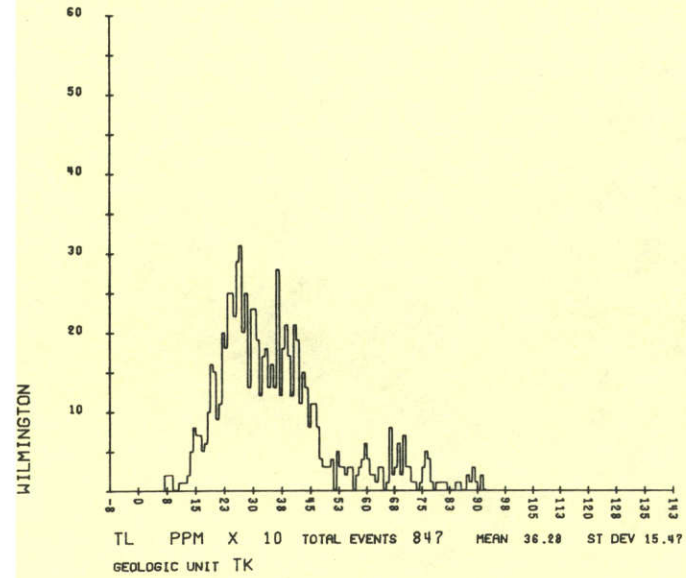
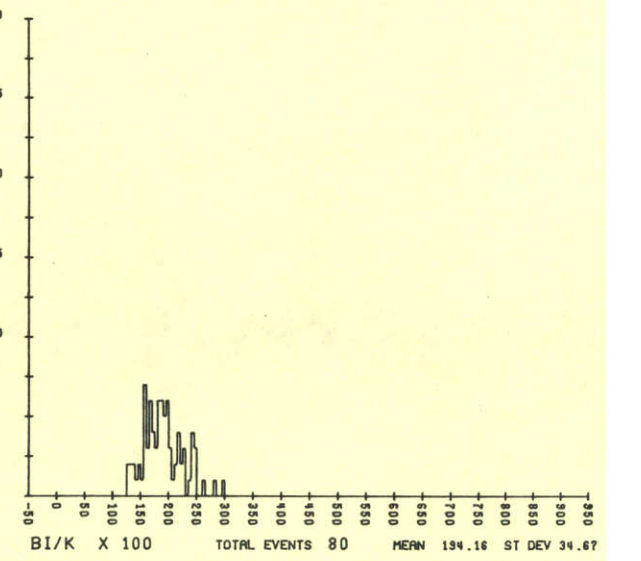
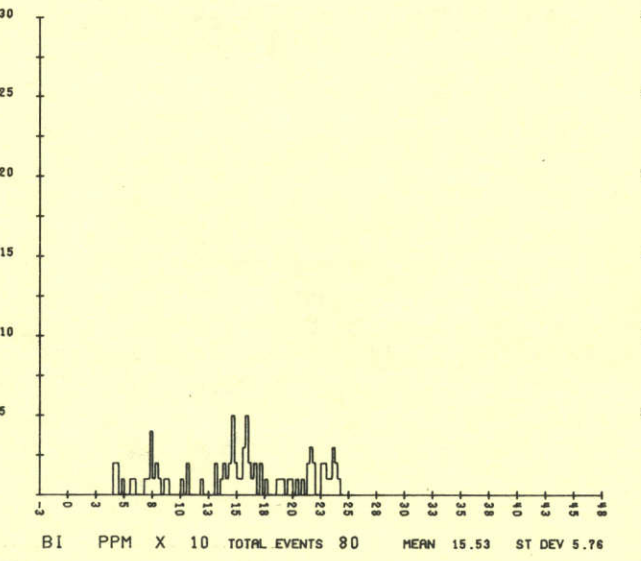
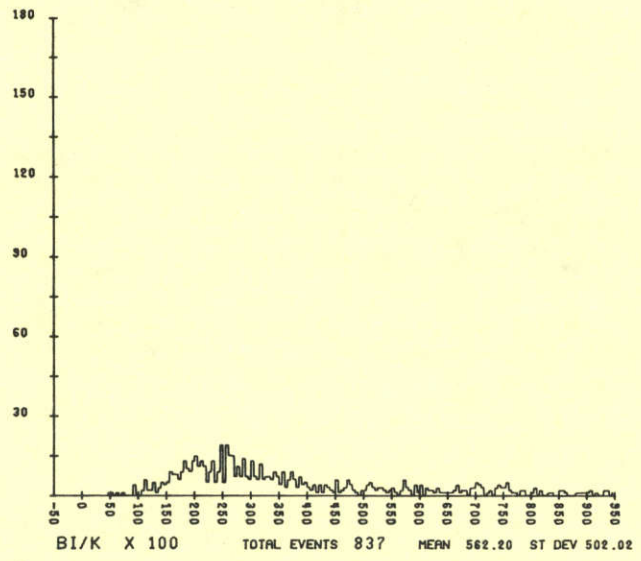
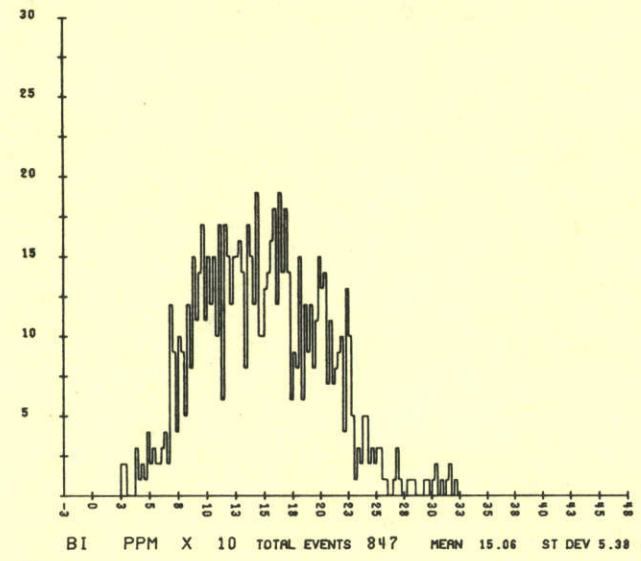
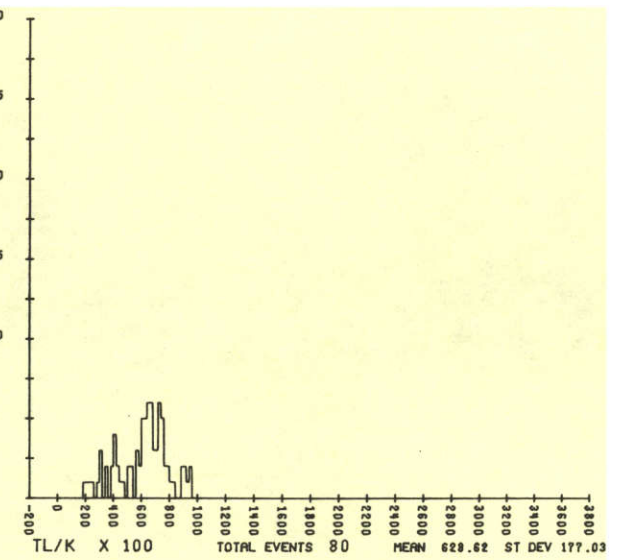
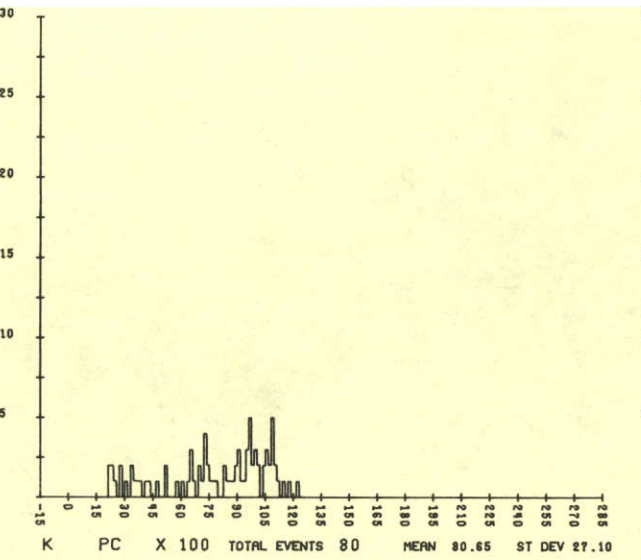
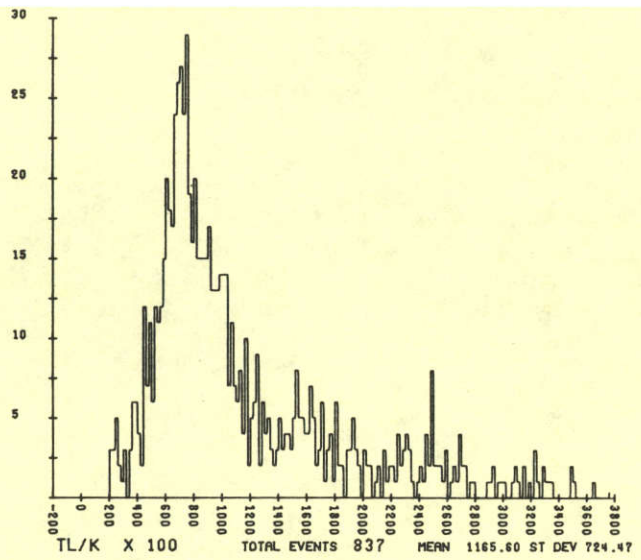
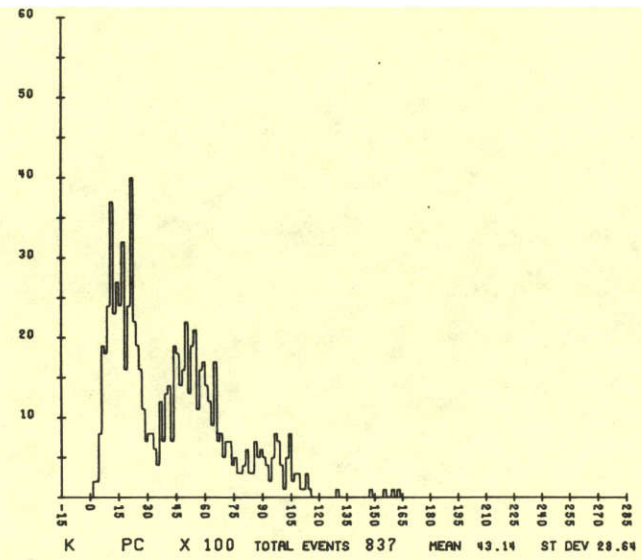
NO. OF EVENTS

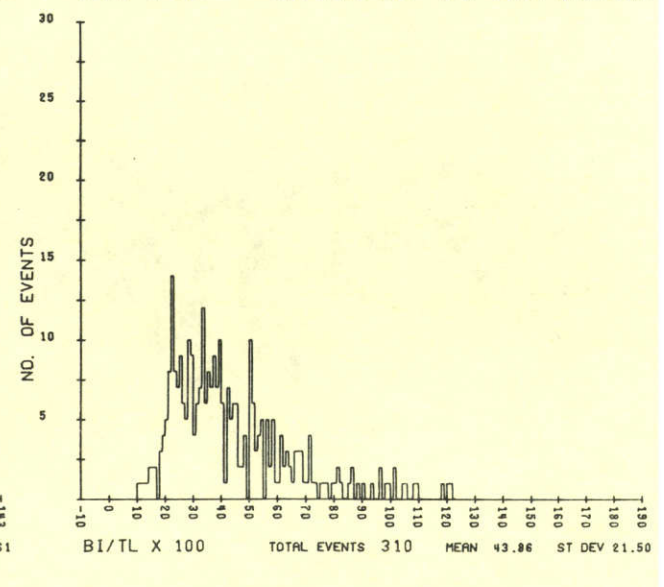
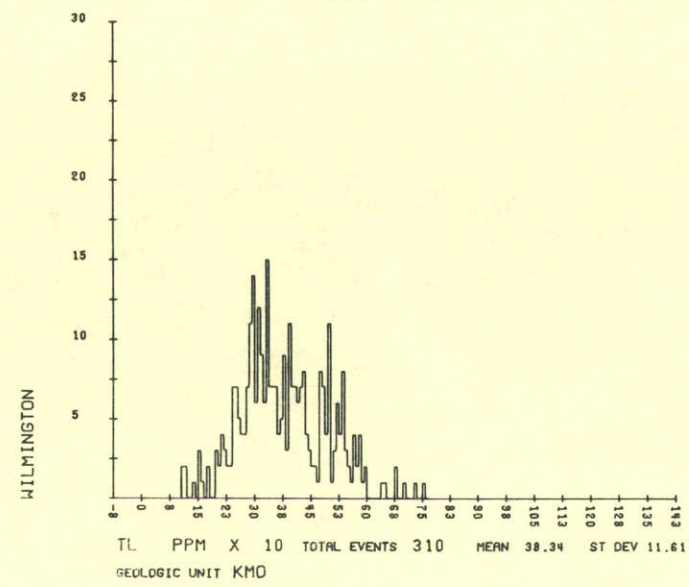
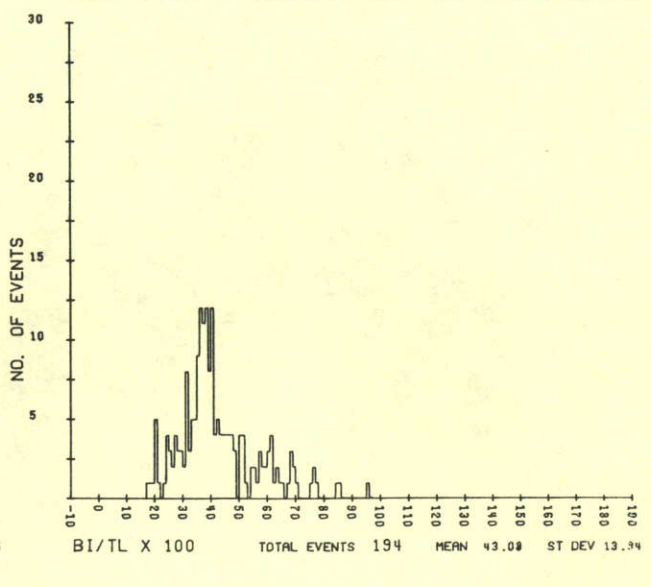
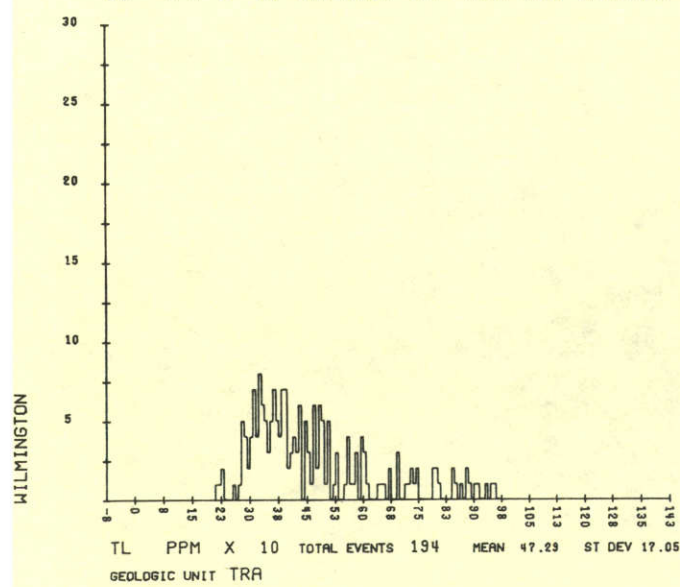
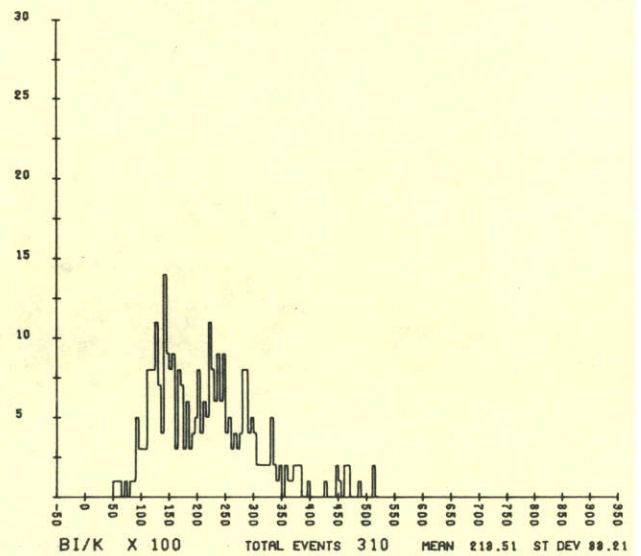
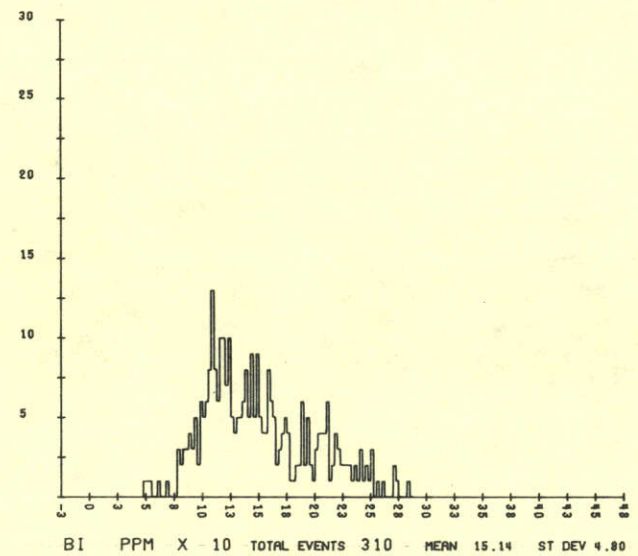
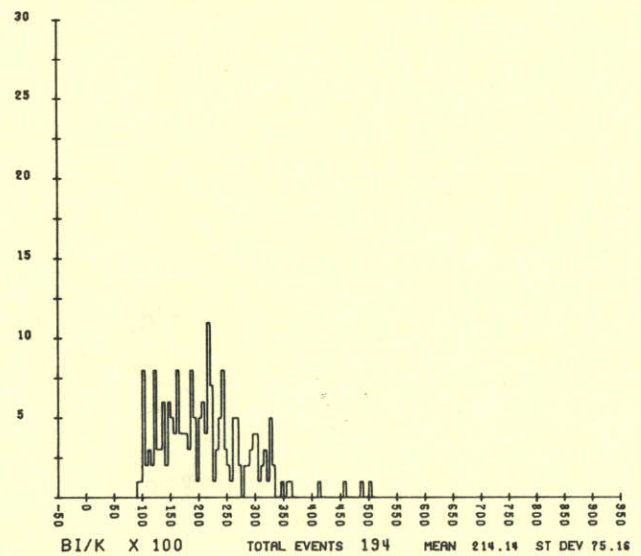
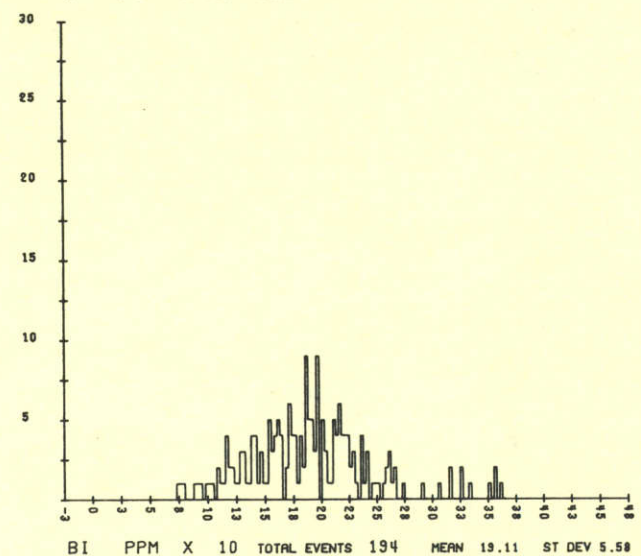
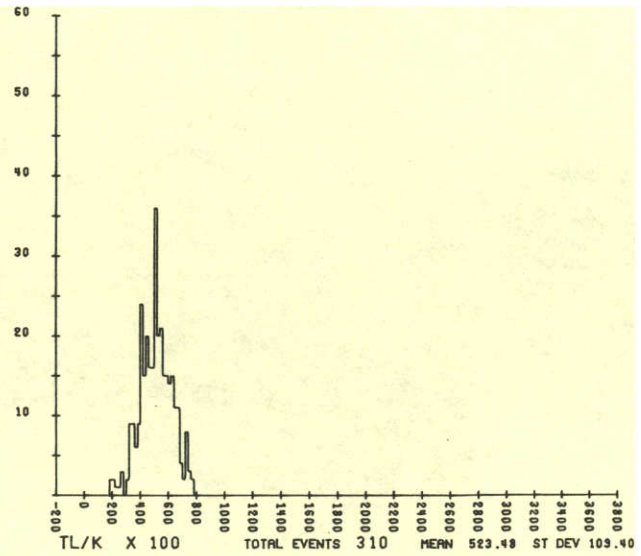
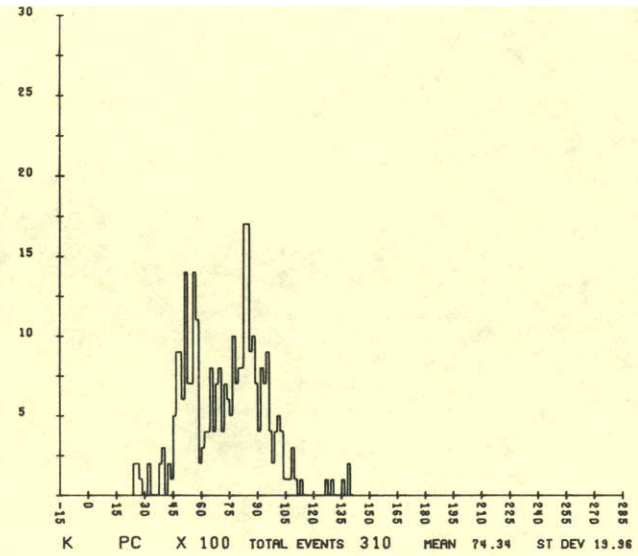
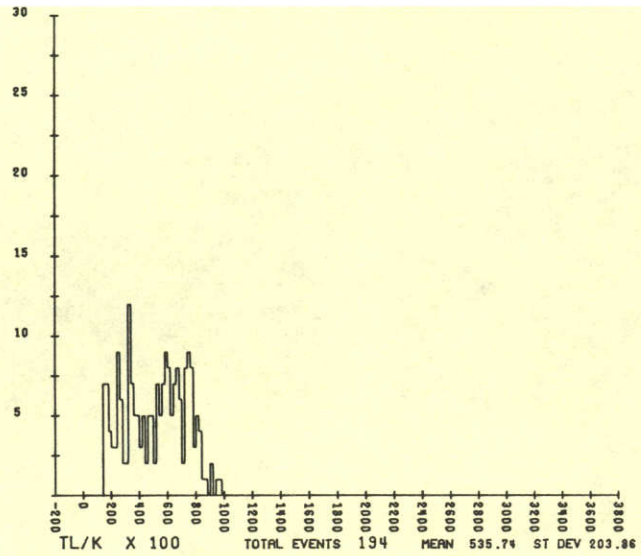
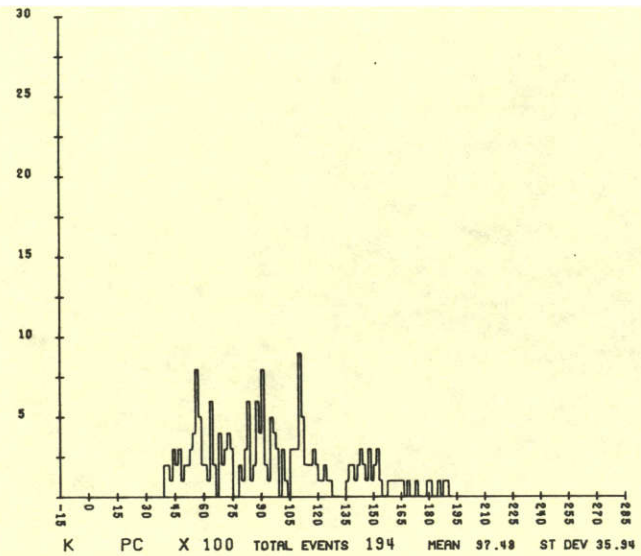


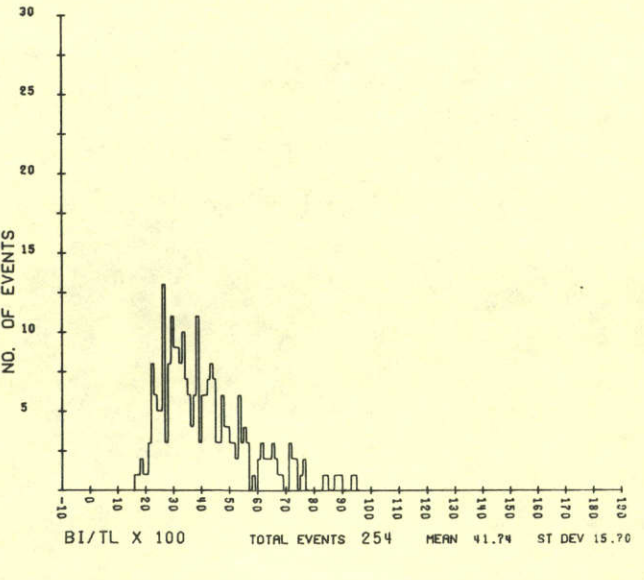
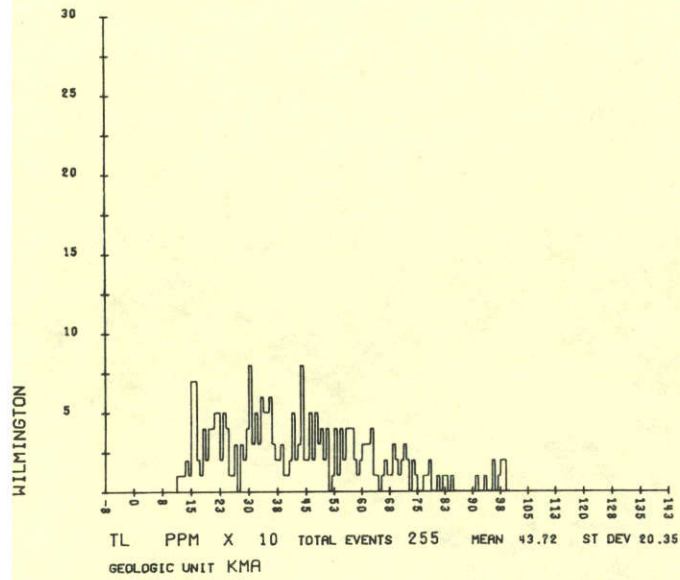
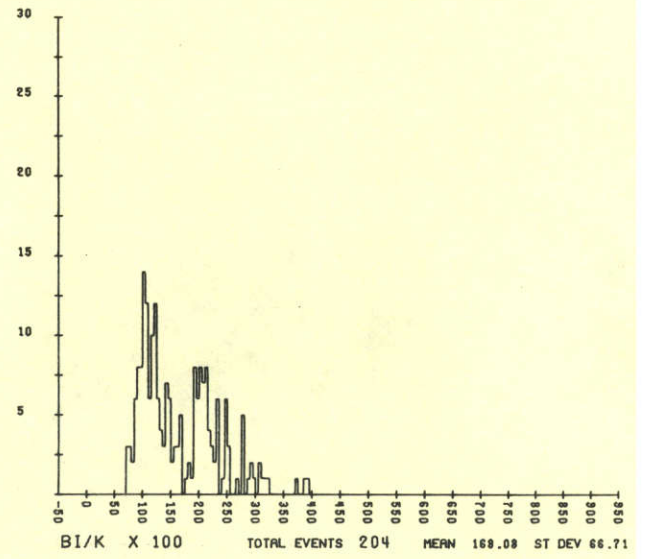
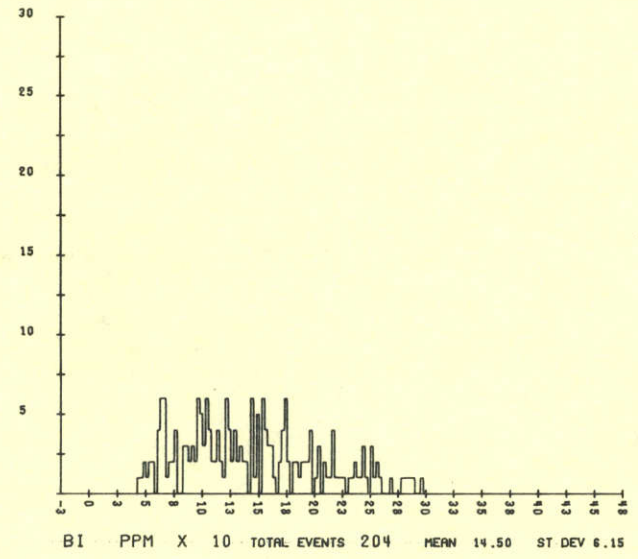
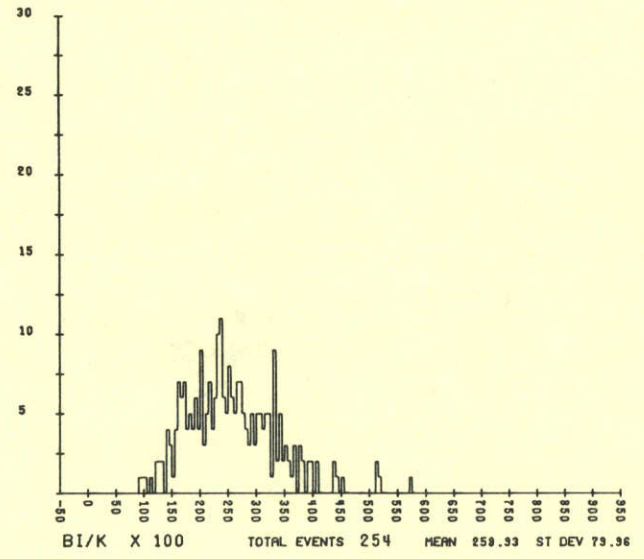
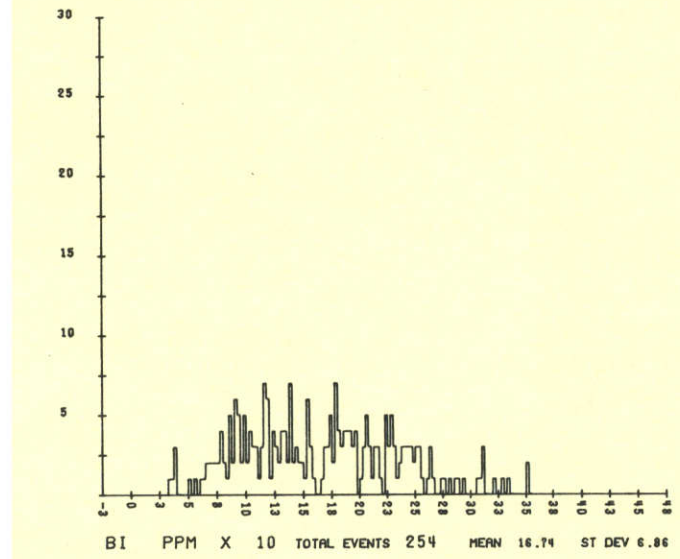
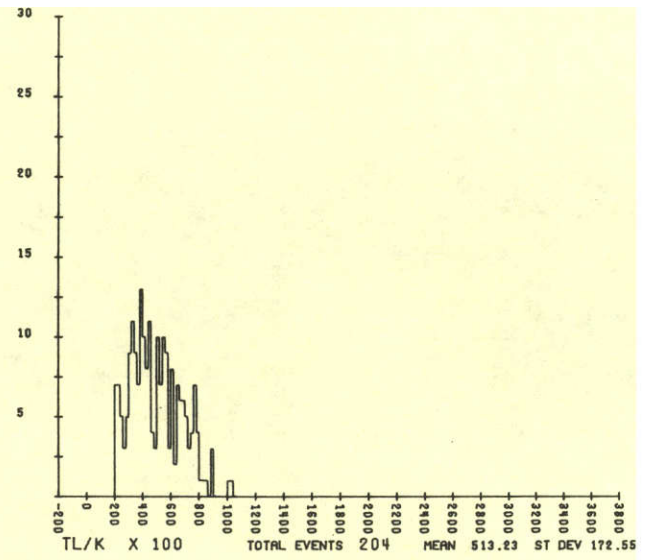
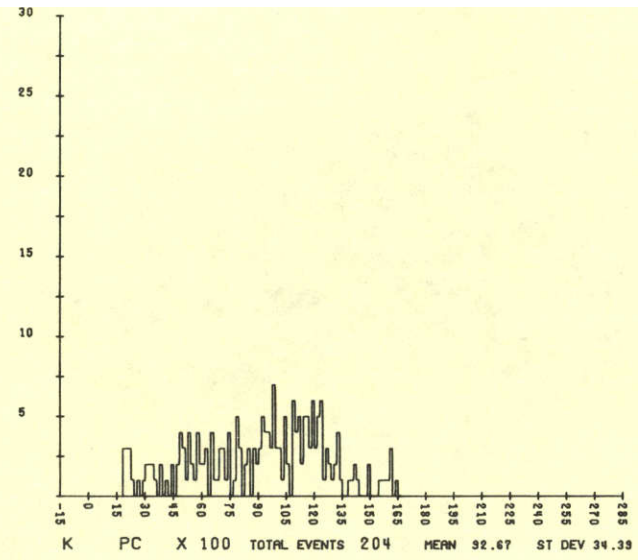
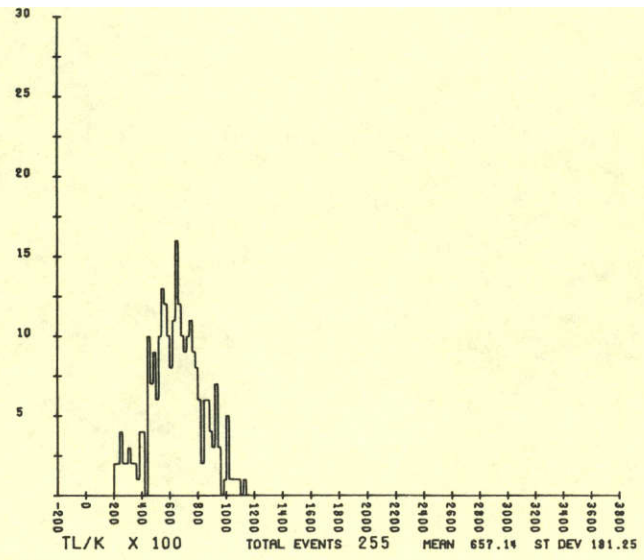
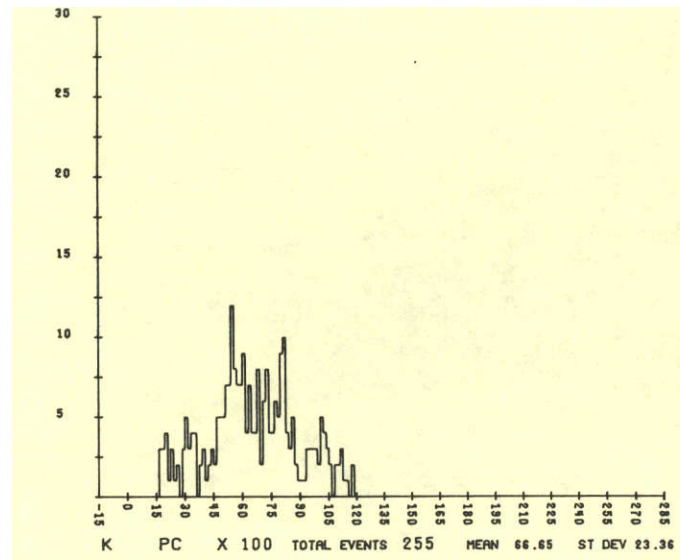


WILMINGTON

WILMINGTON

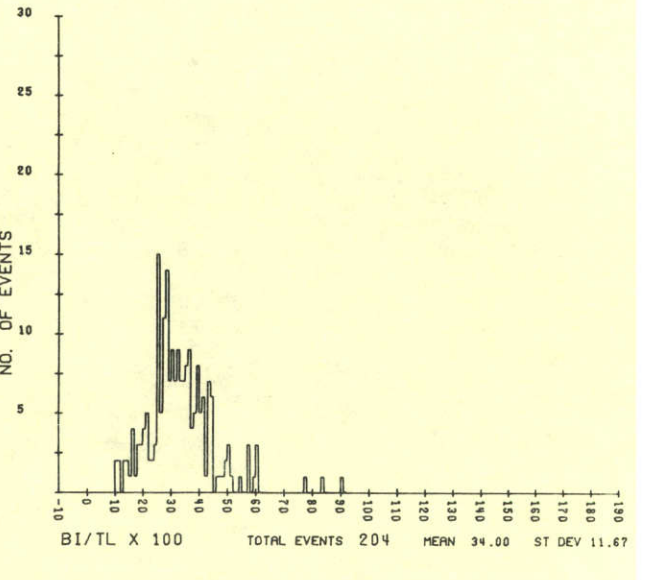
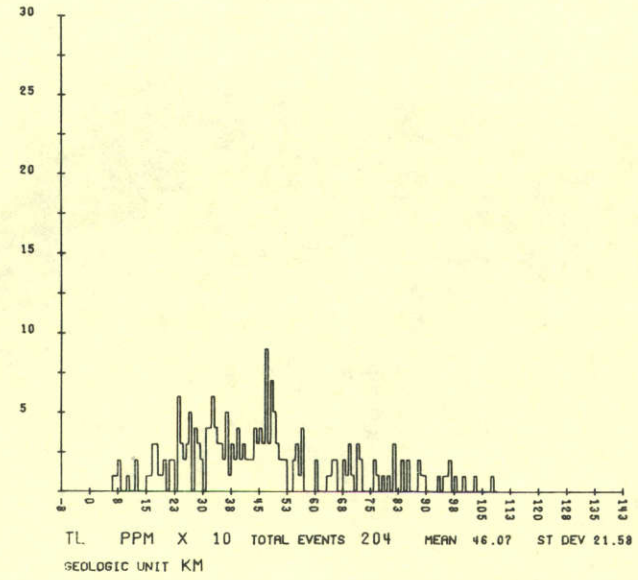




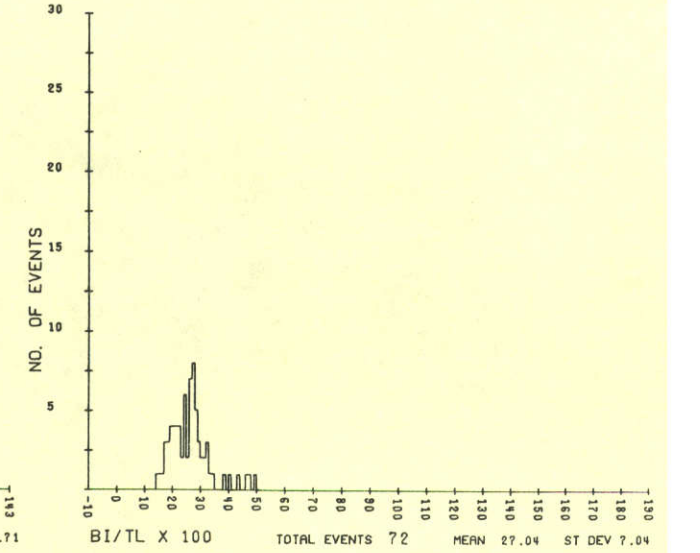
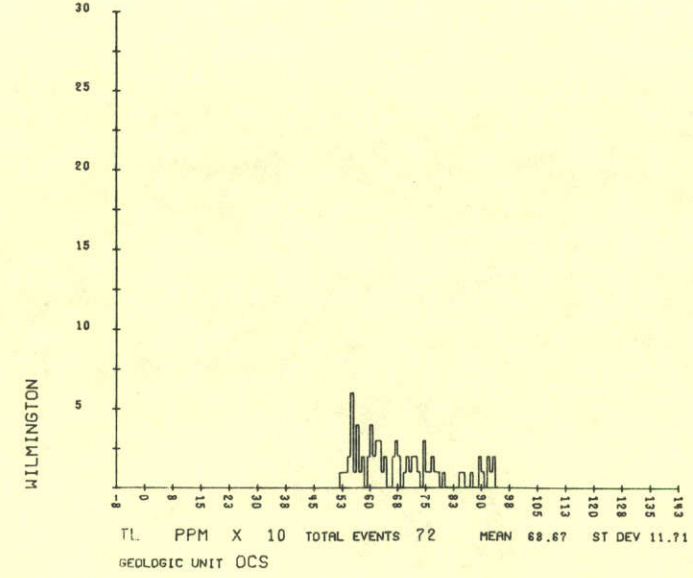
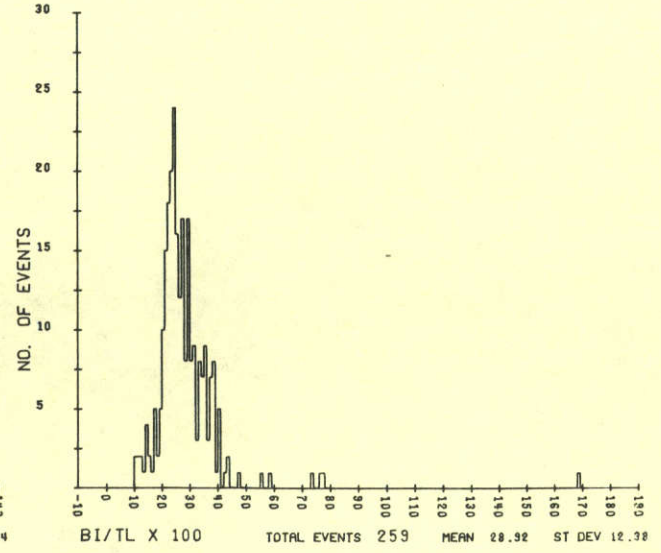
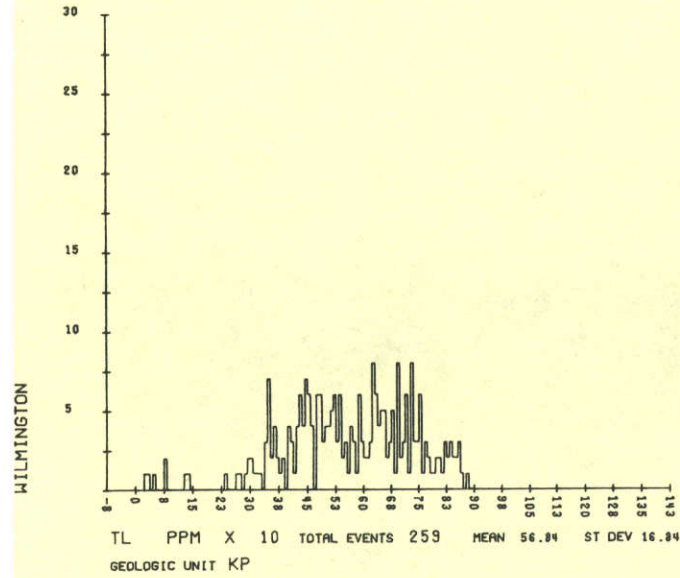
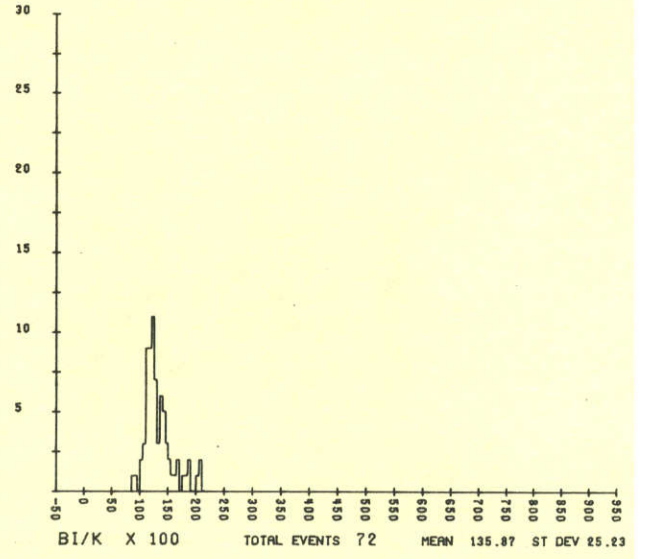
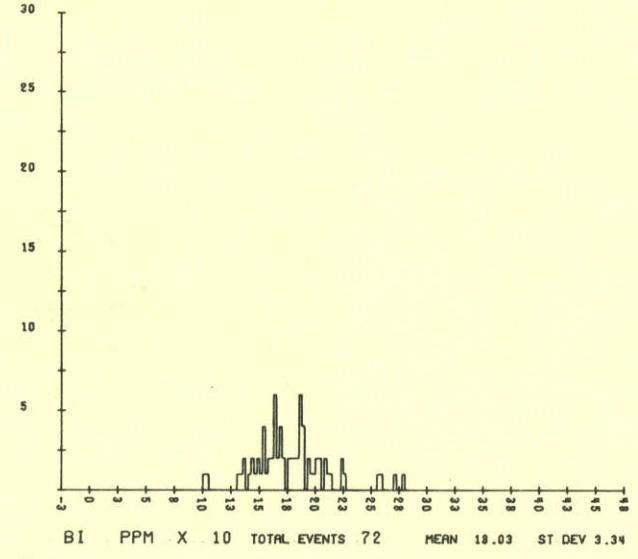
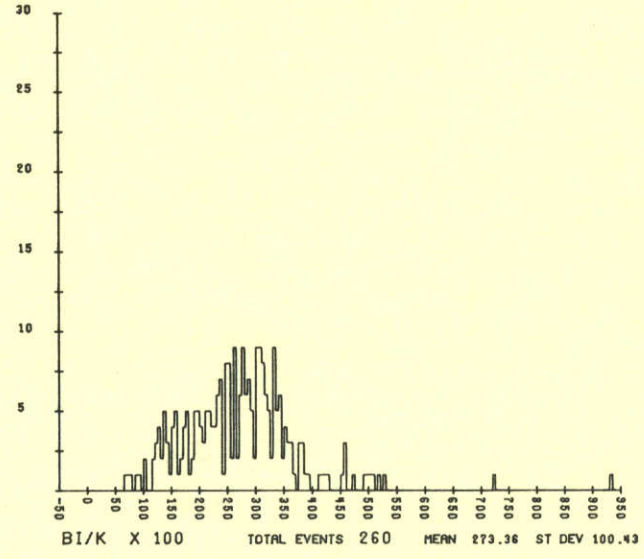
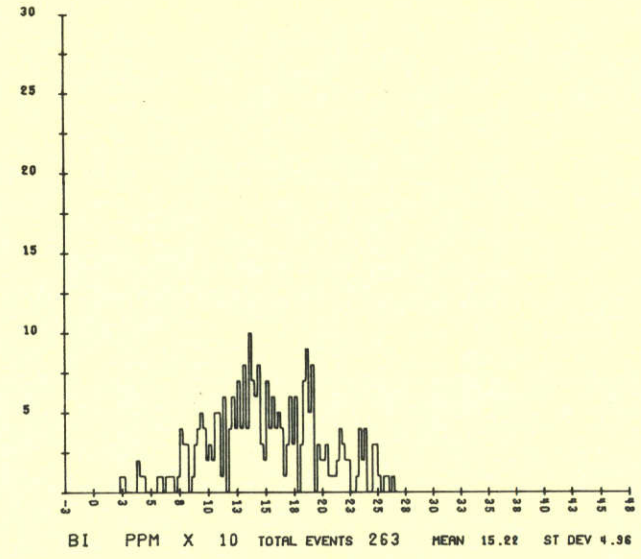
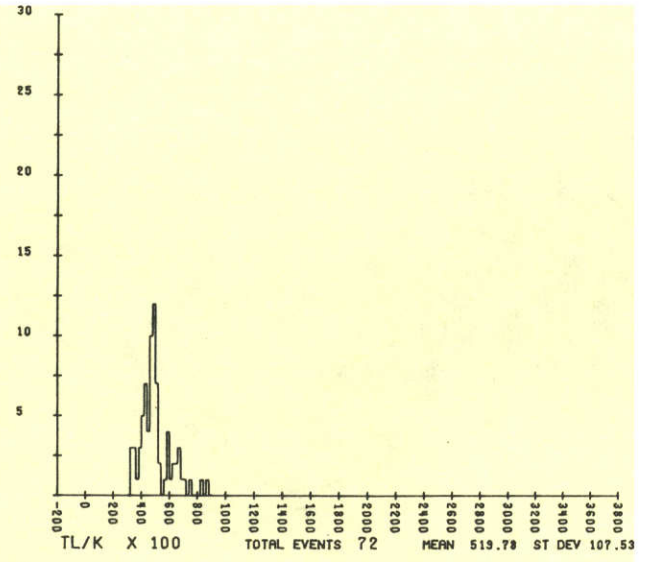
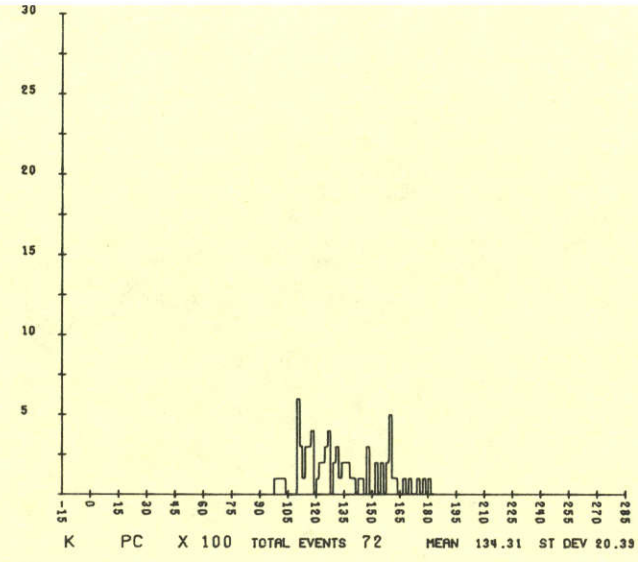
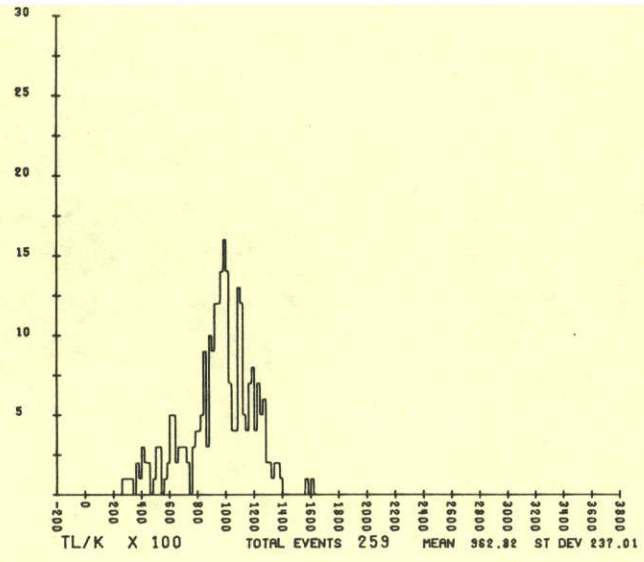
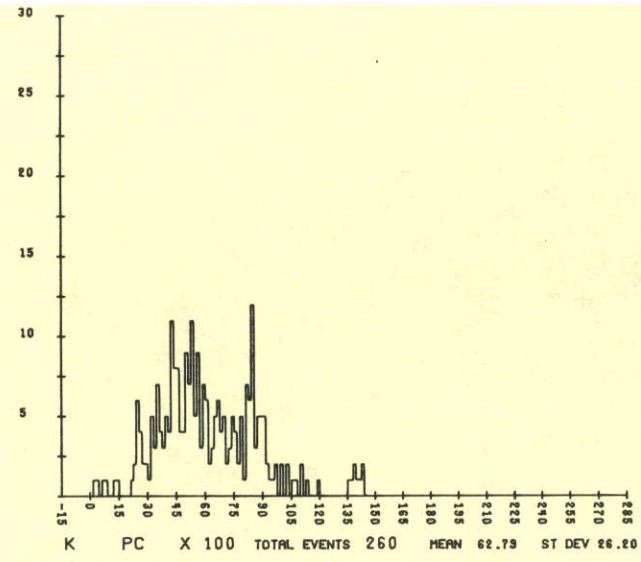


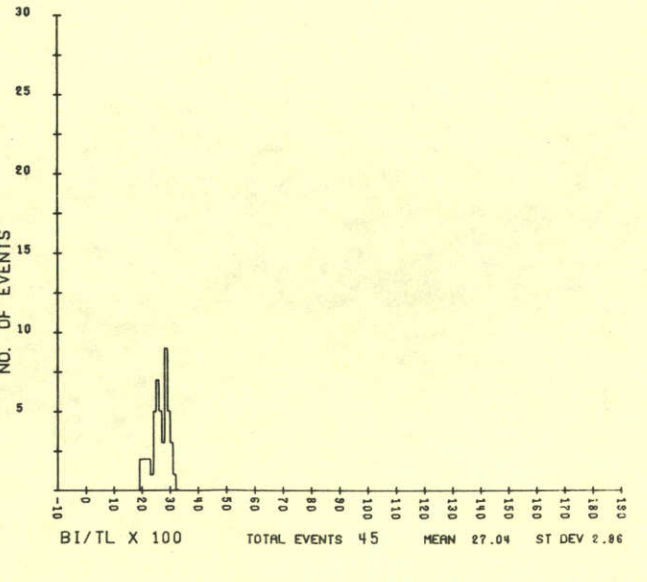
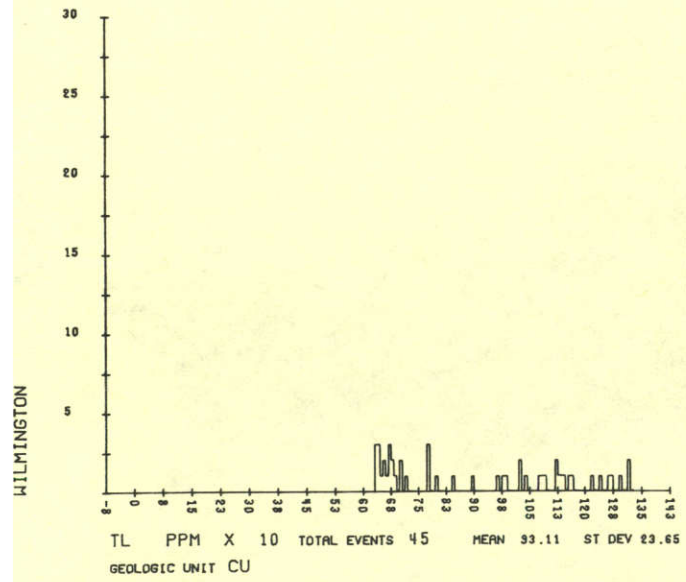
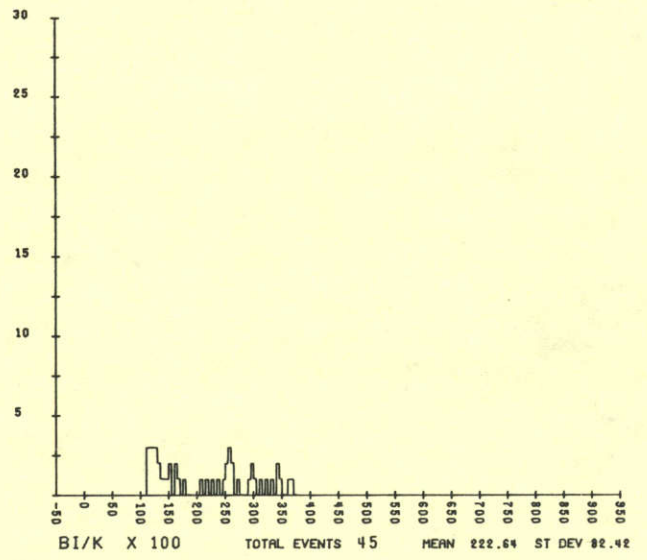
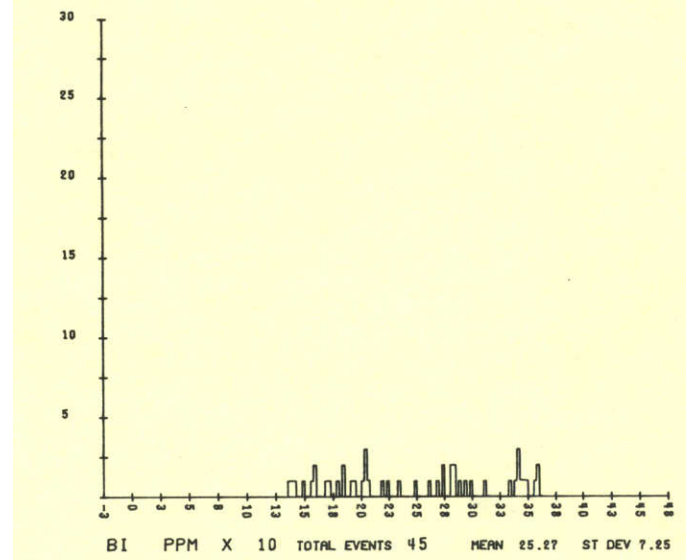
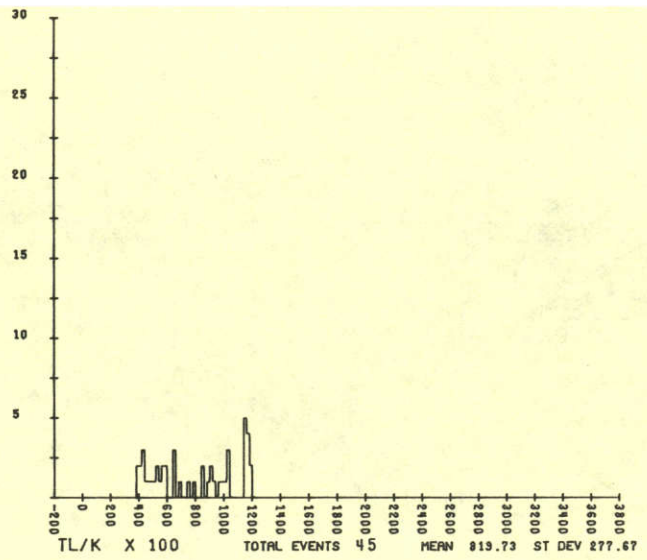
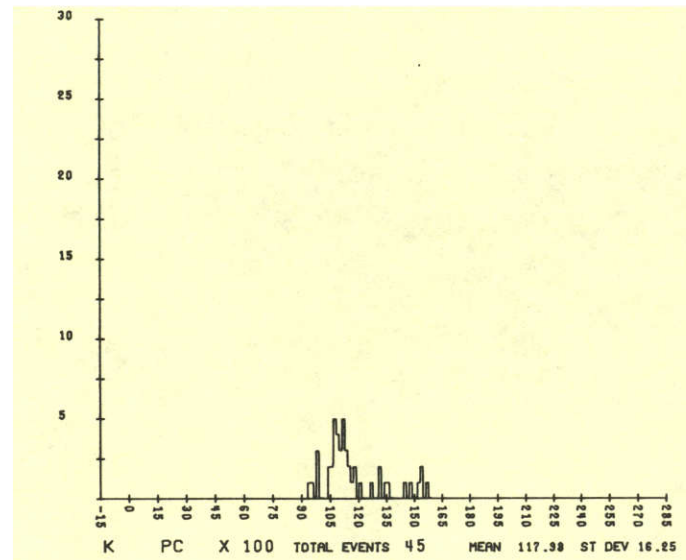
HILMINGTON

HILMINGTON

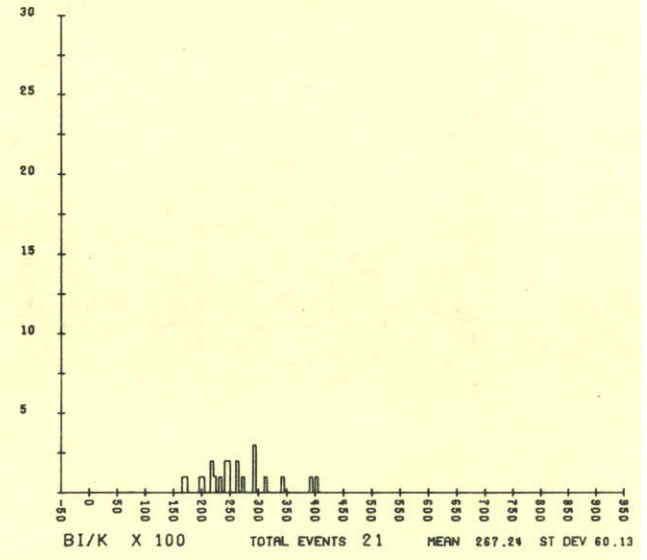
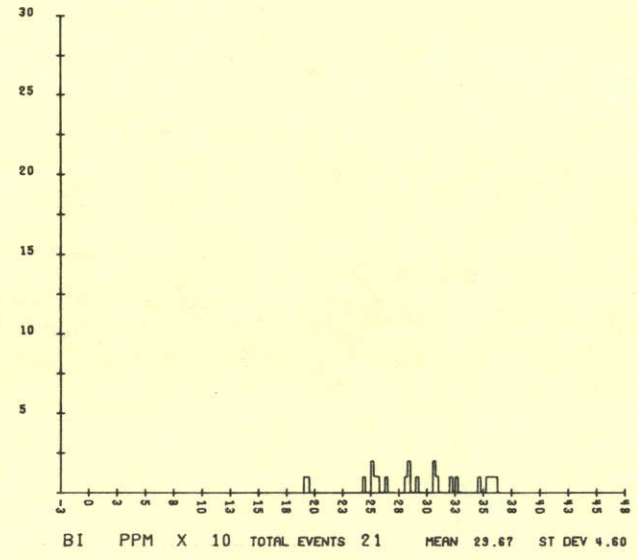
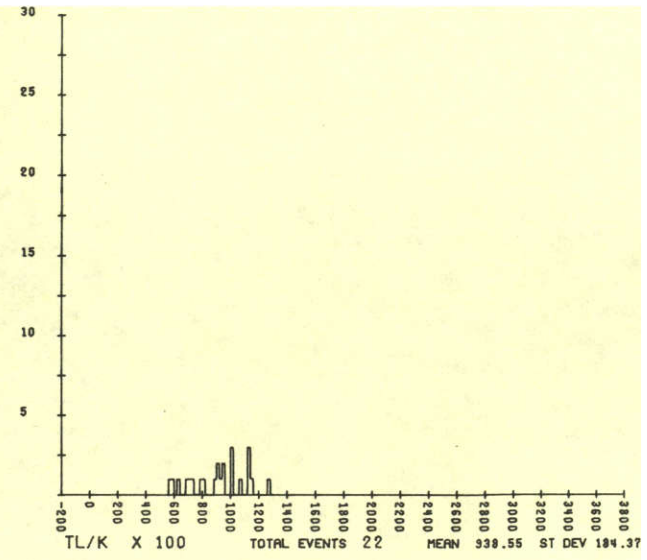
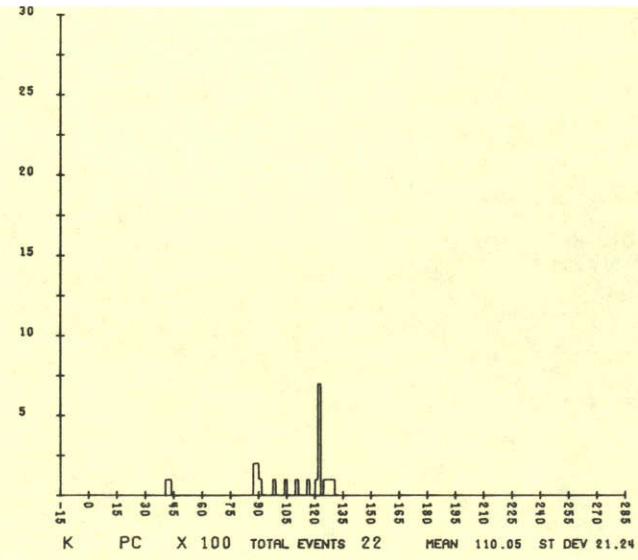


NO. OF EVENTS

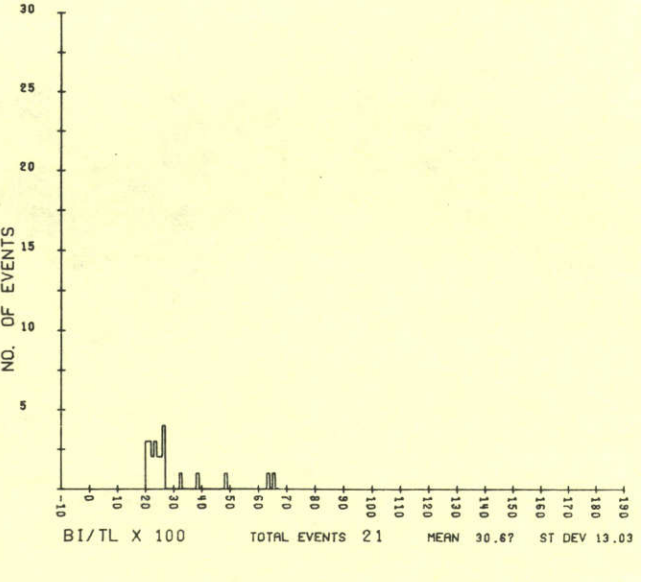
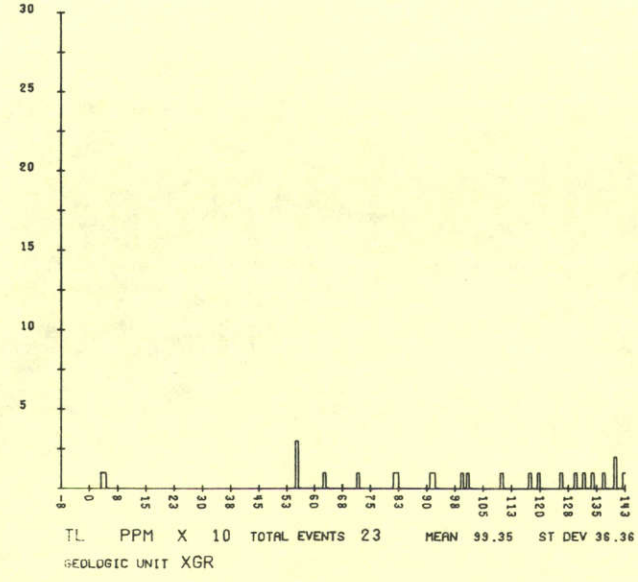




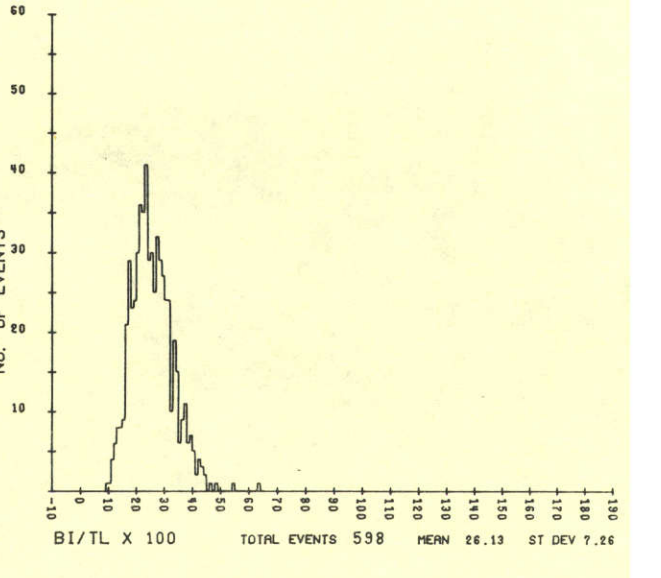
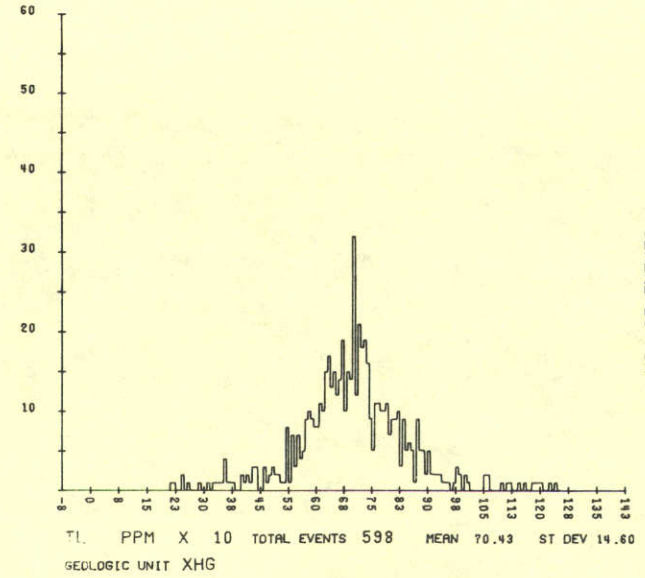
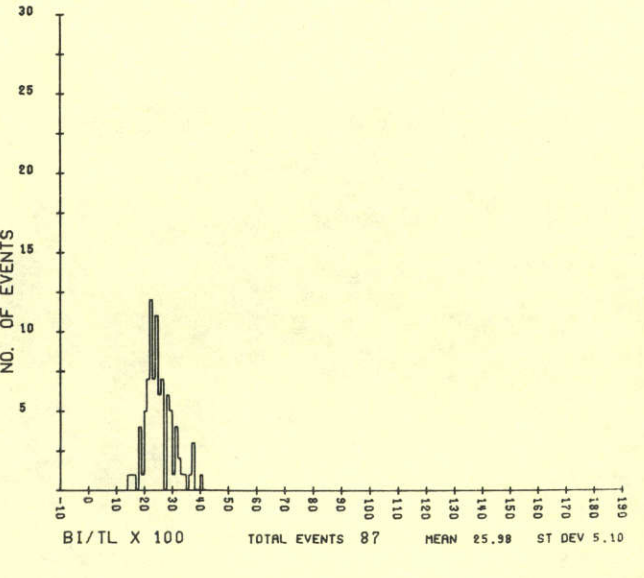
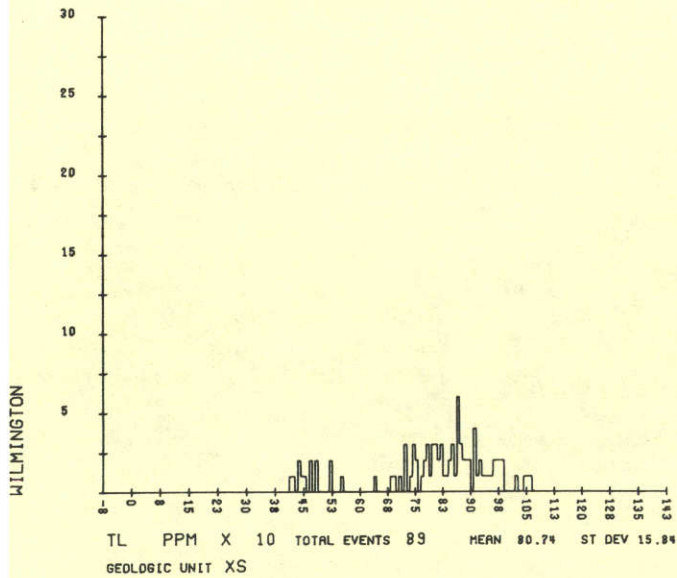
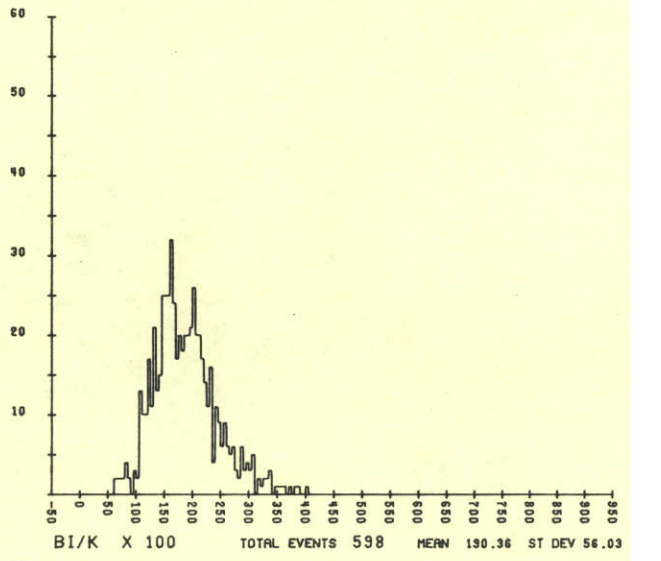
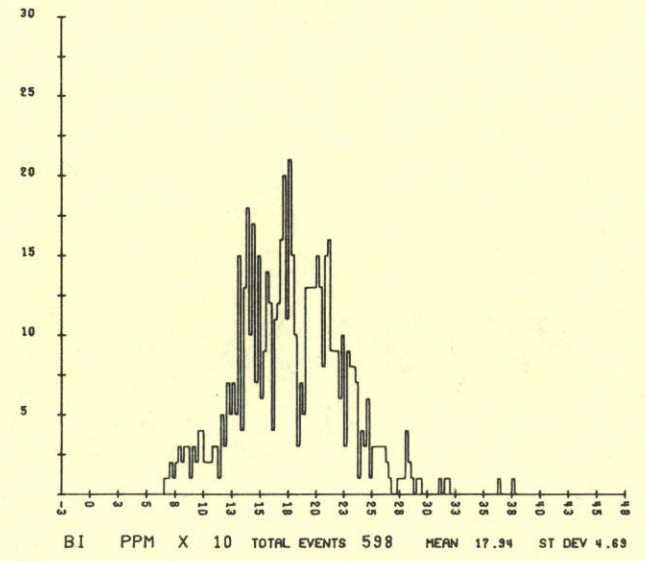
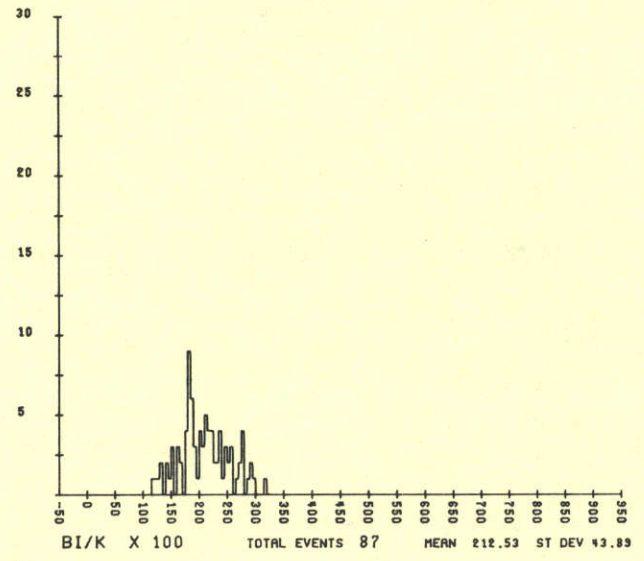
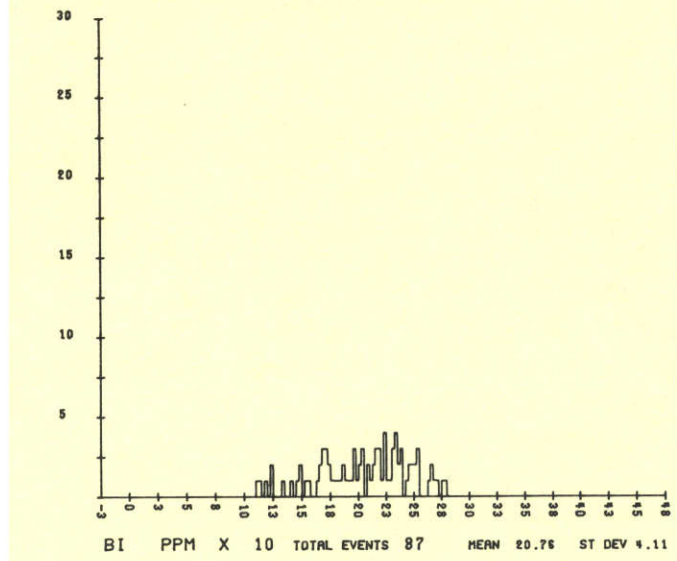
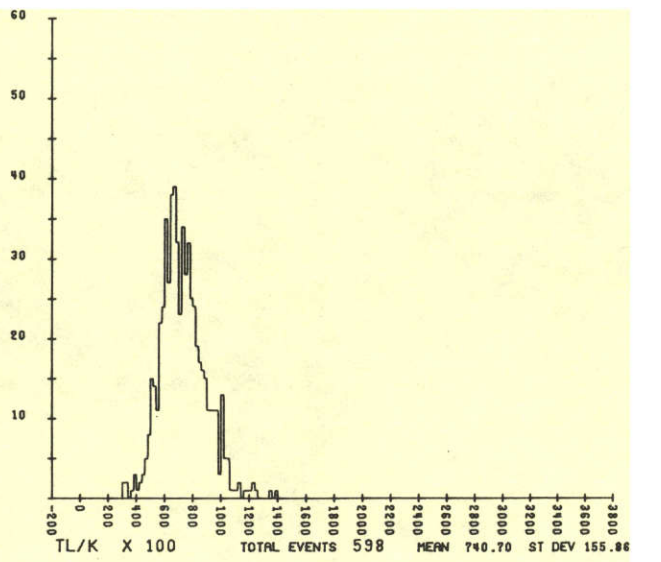
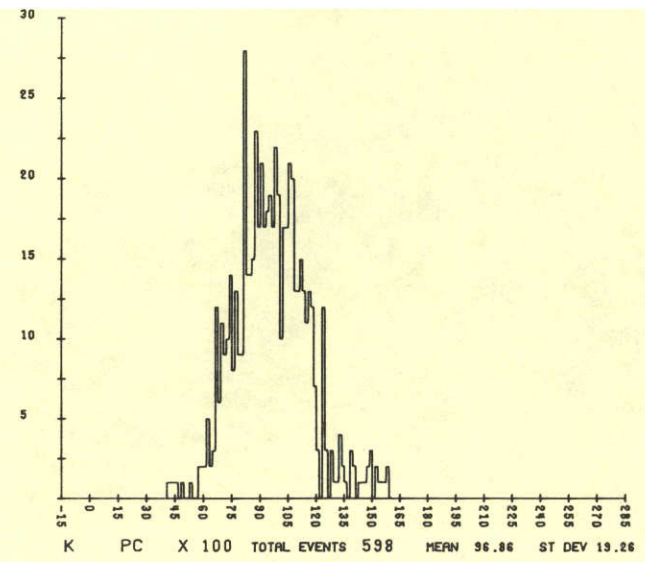
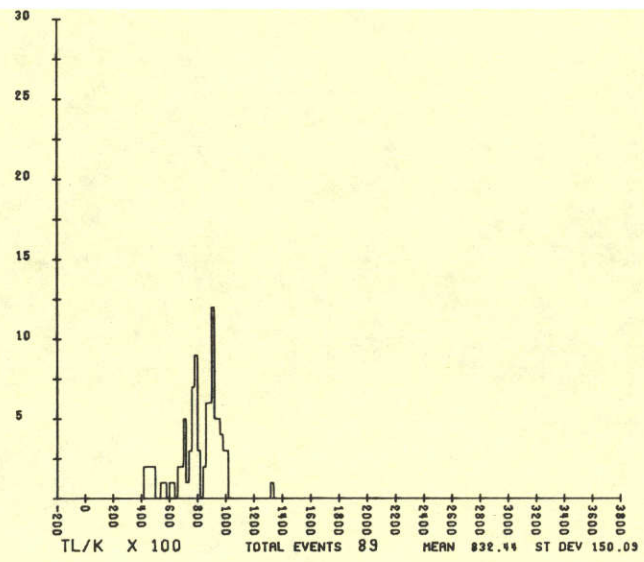
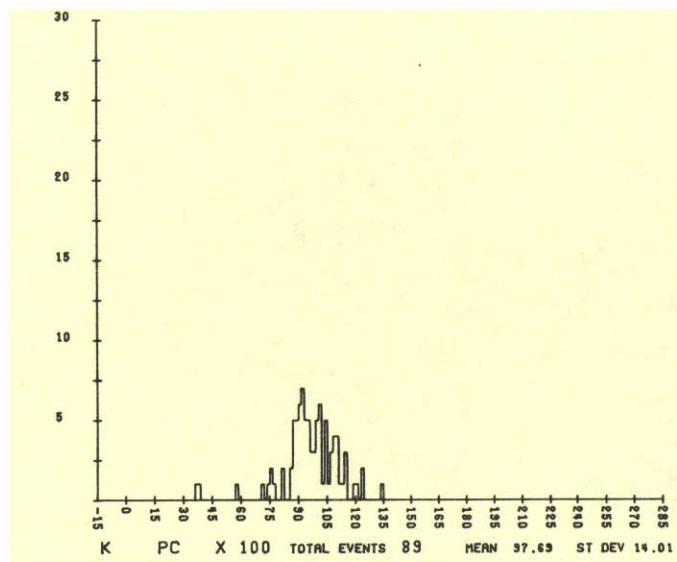
A19



WILMINGTON

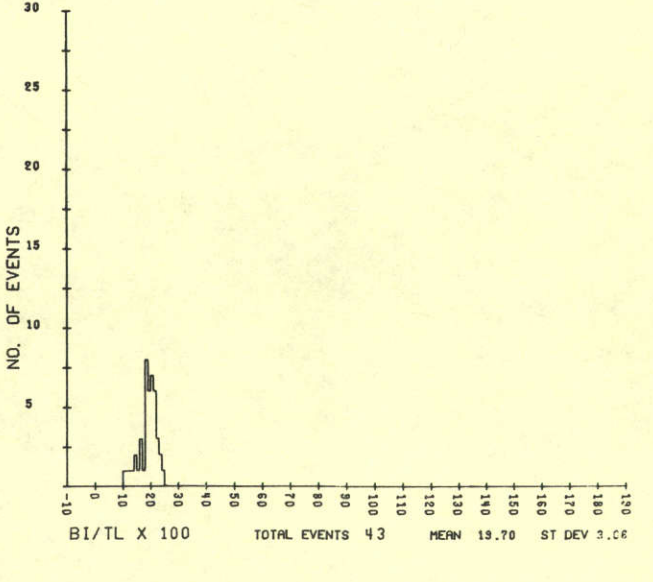
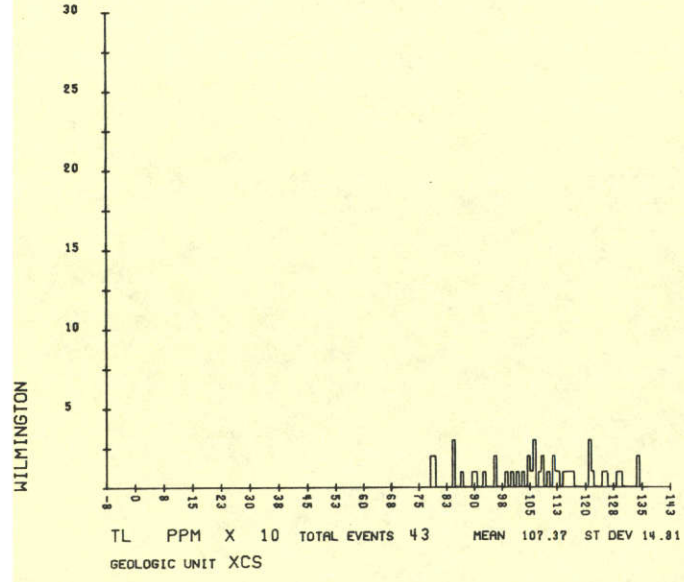
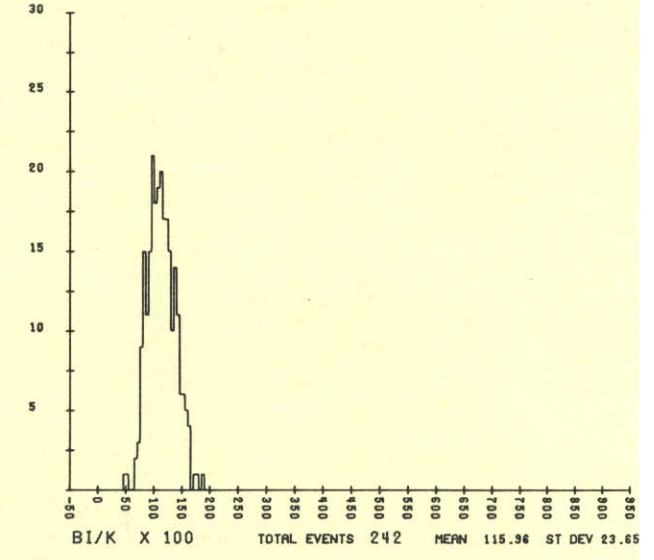
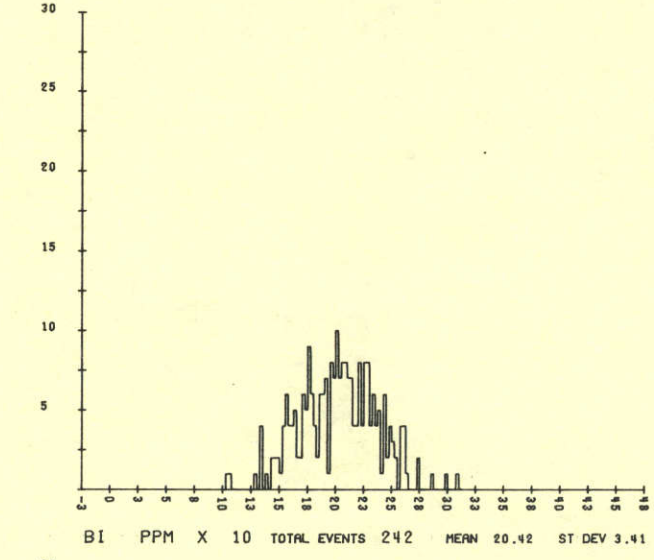
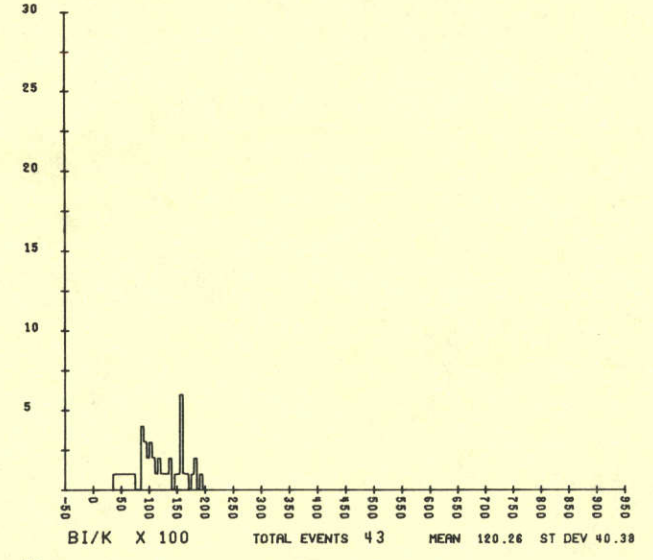
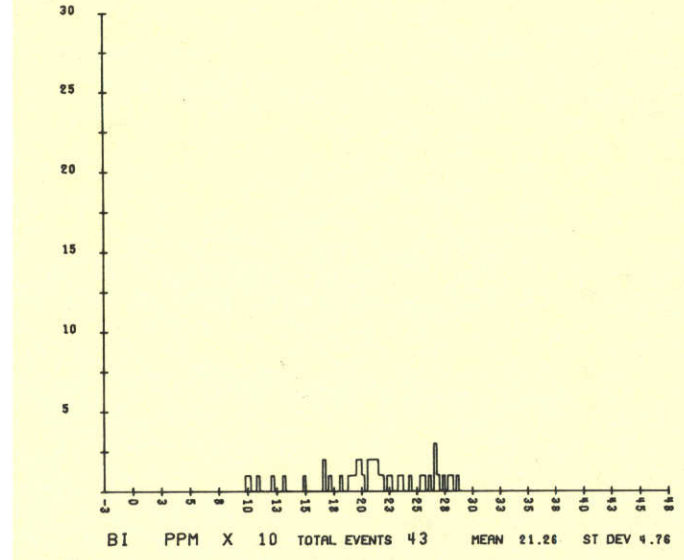
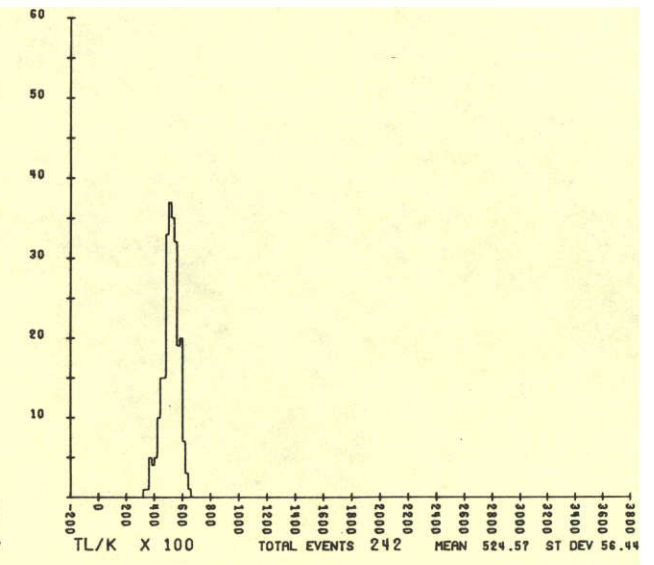
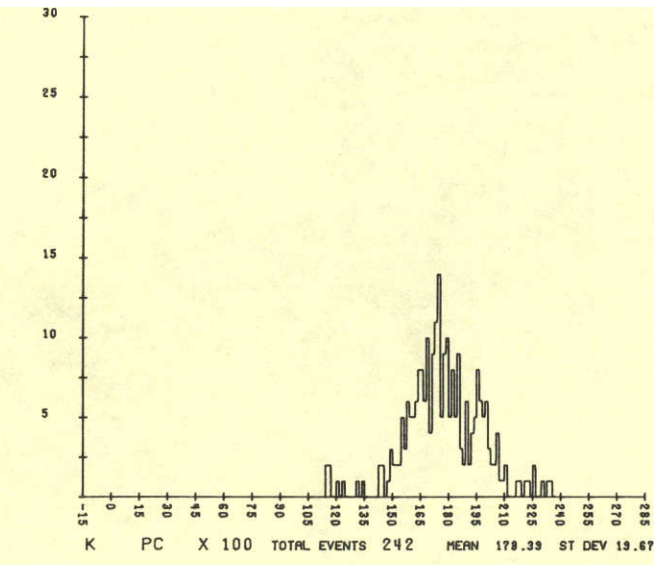
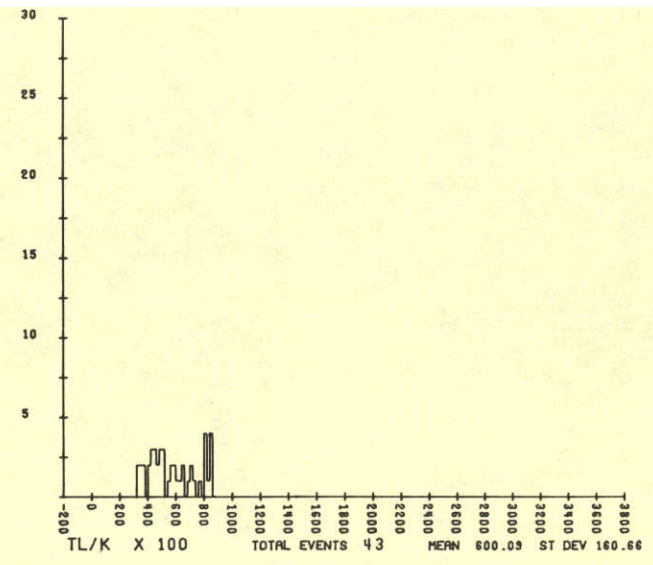
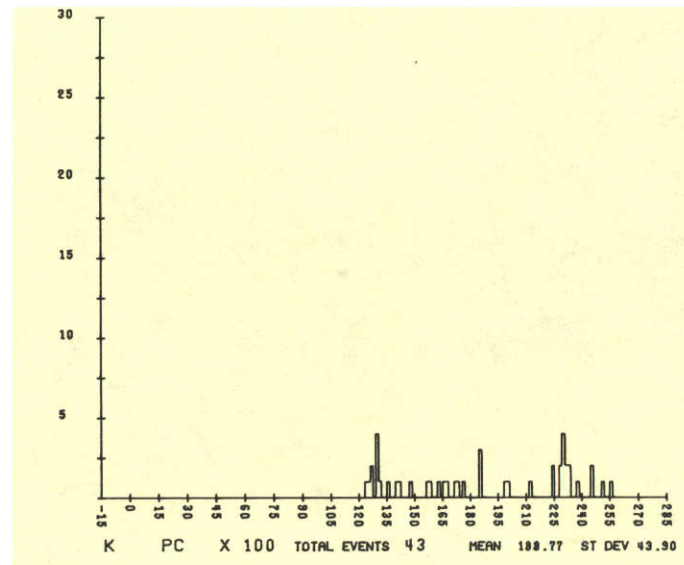


A20



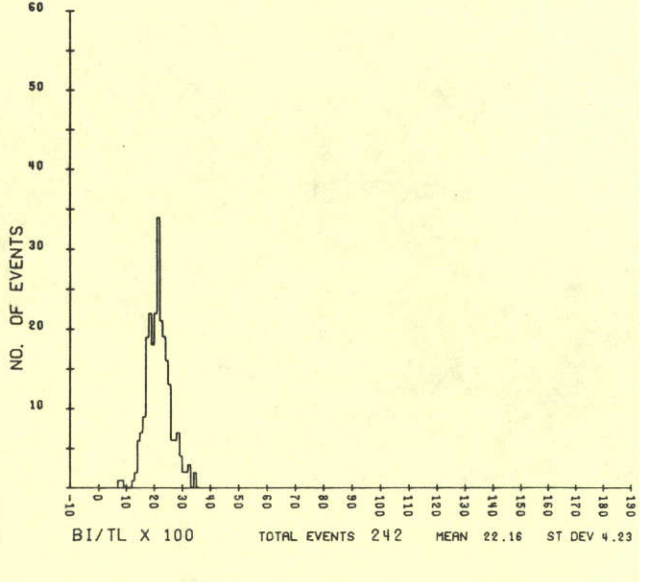
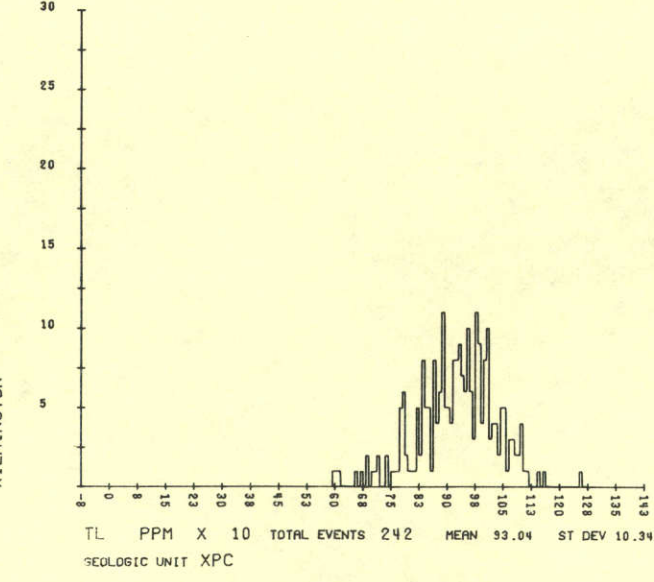
WILMINGTON

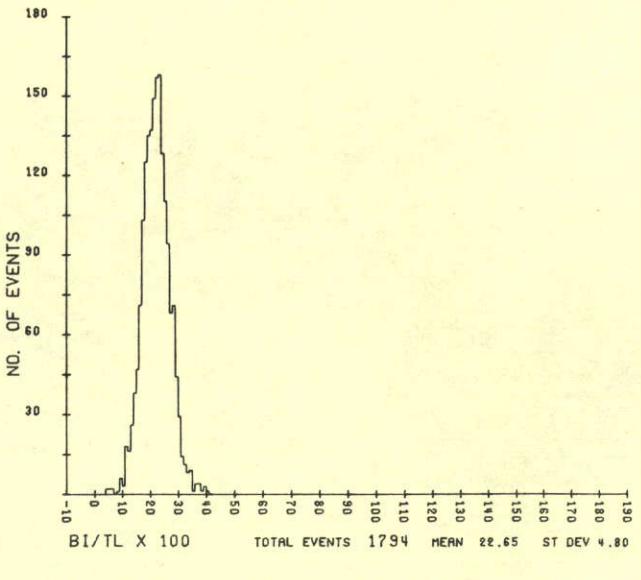
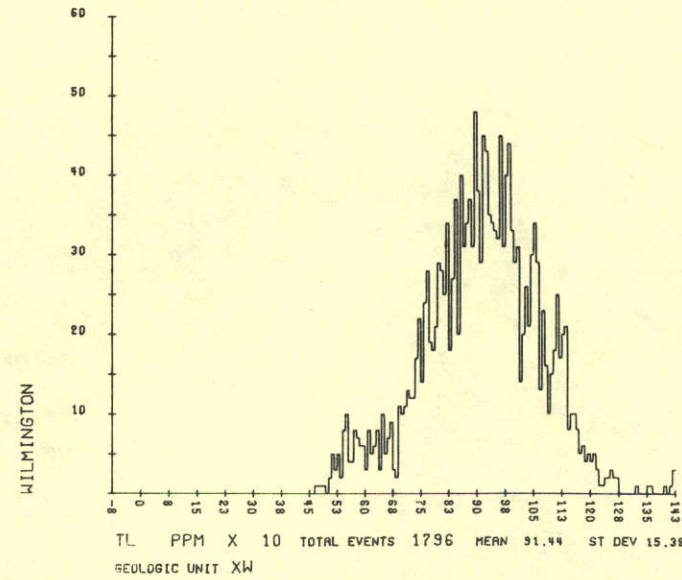
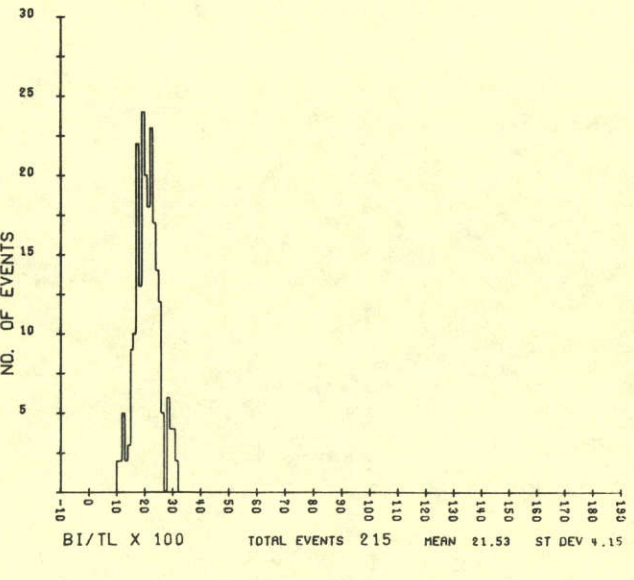
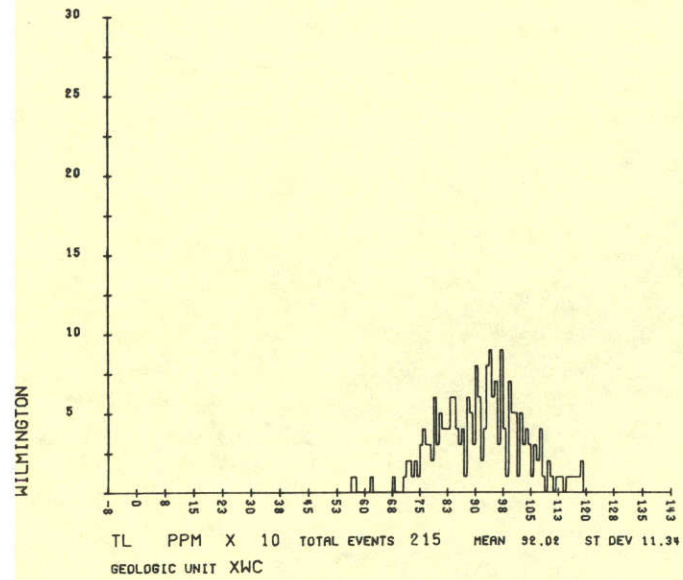
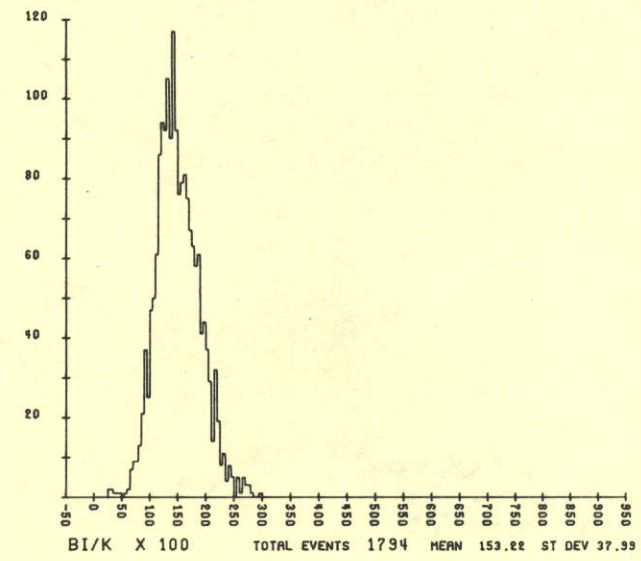
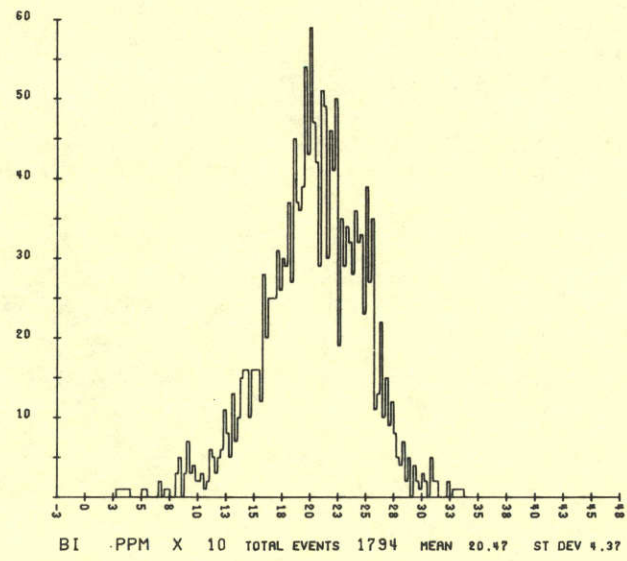
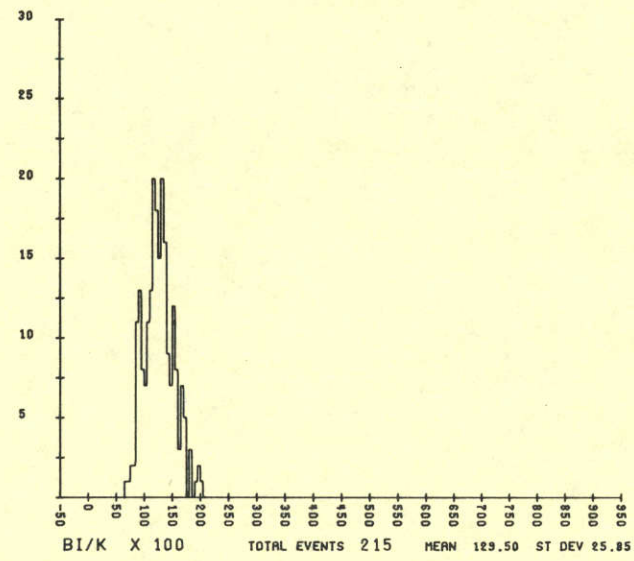
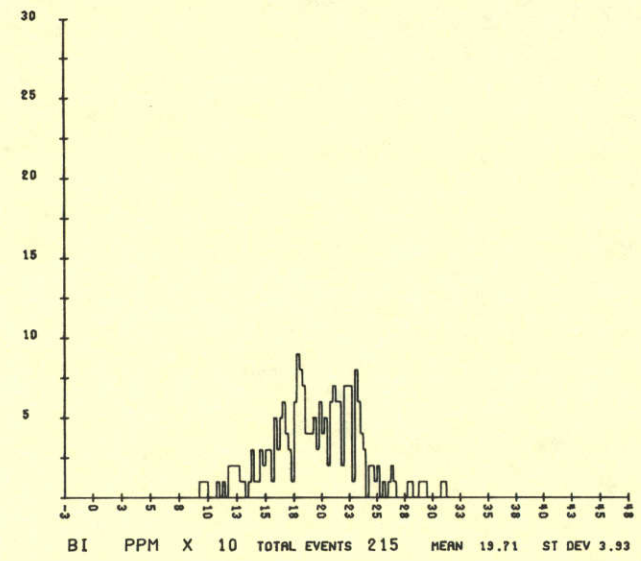
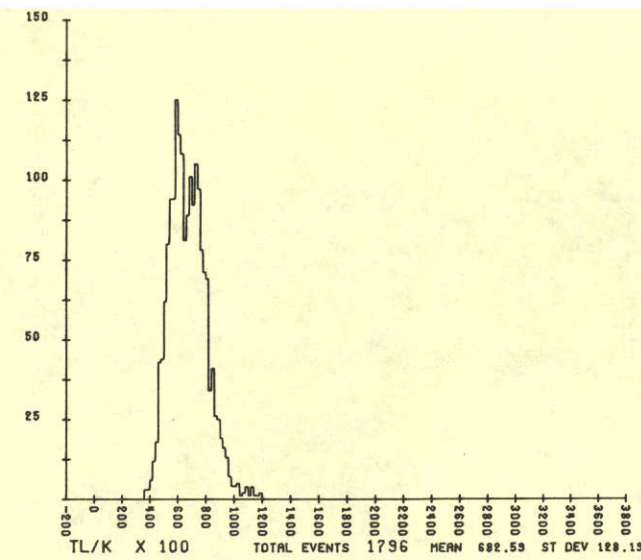
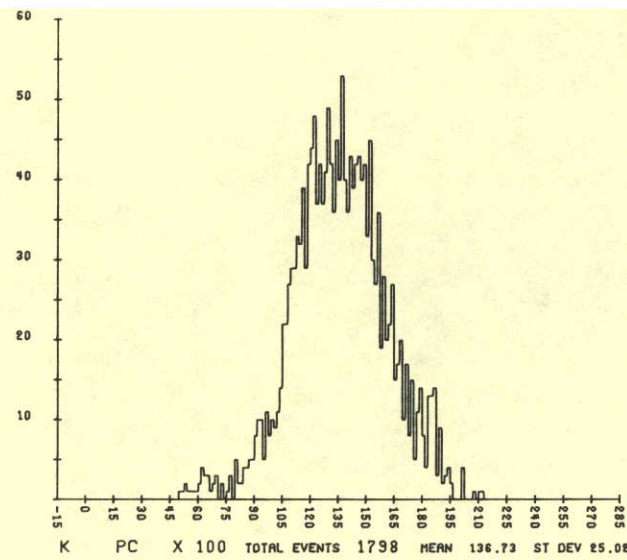
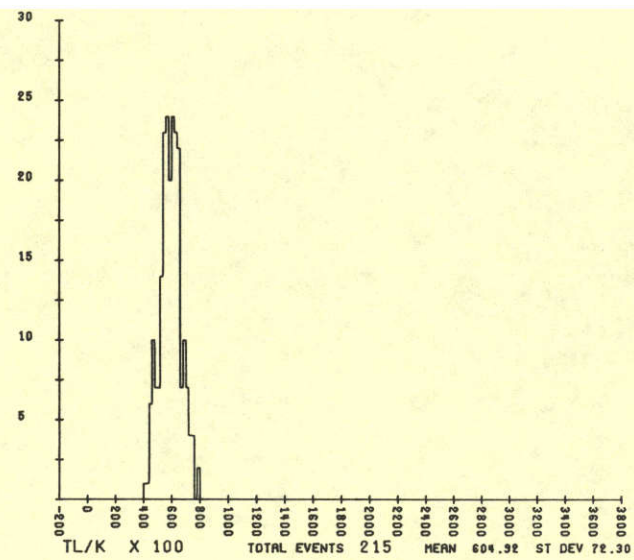
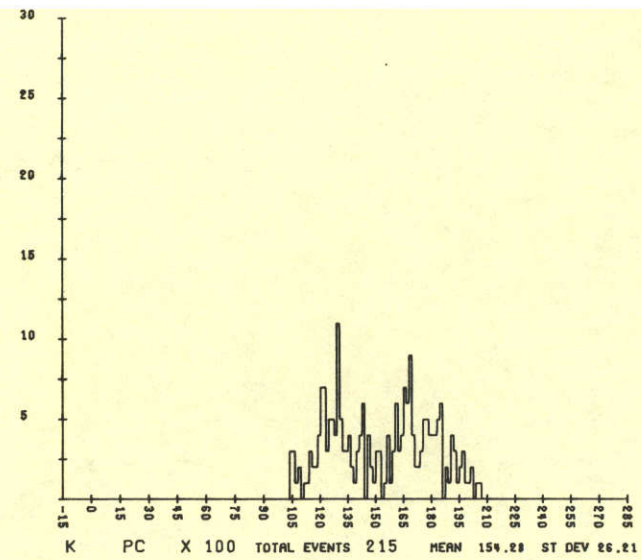
WILMINGTON

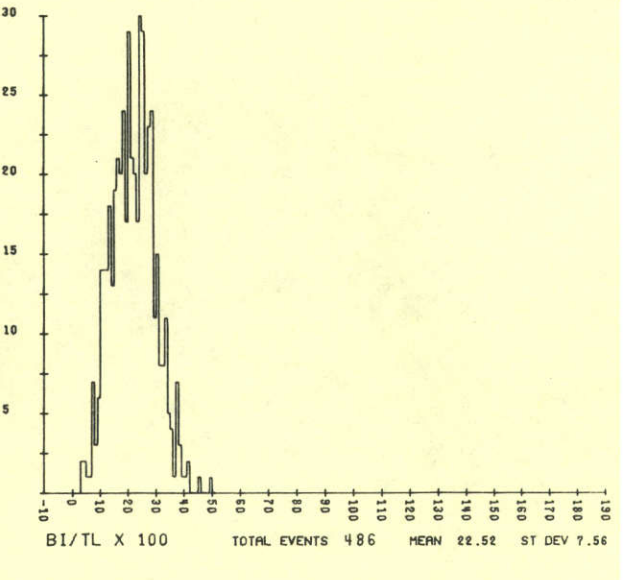
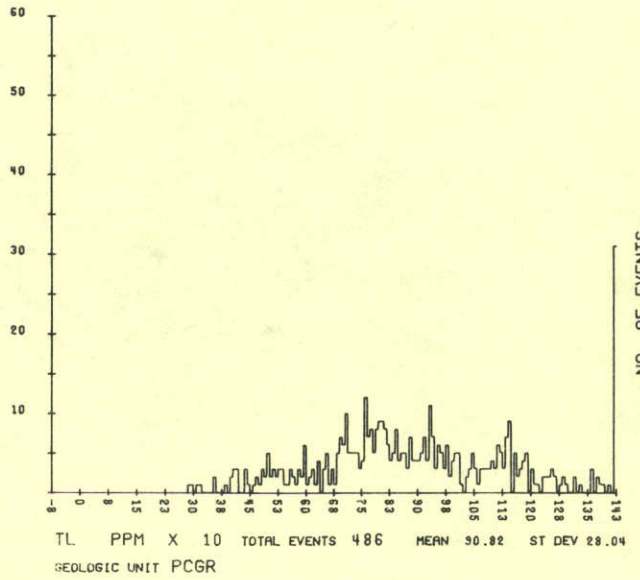
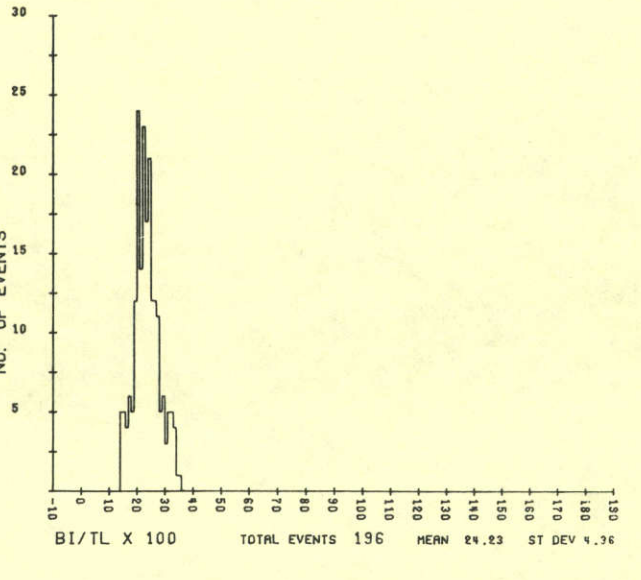
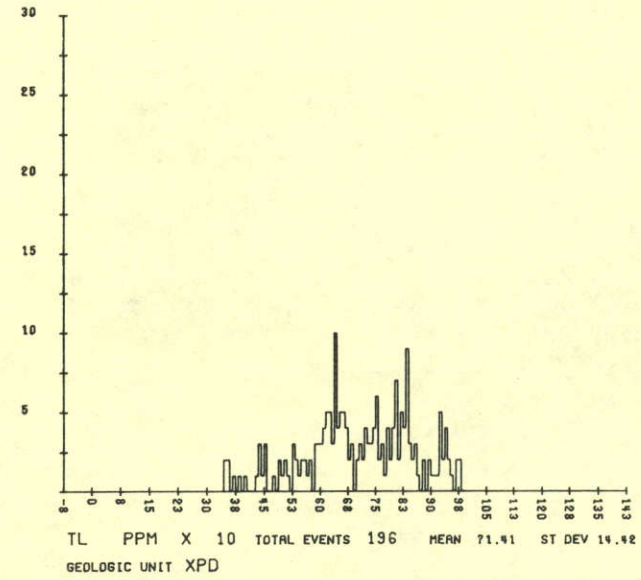
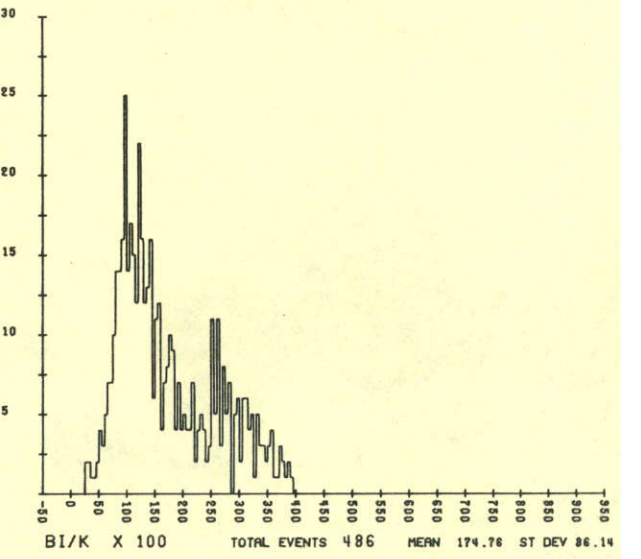
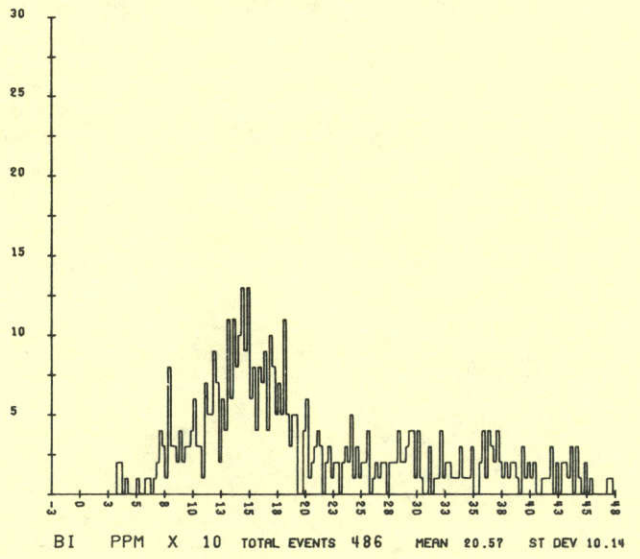
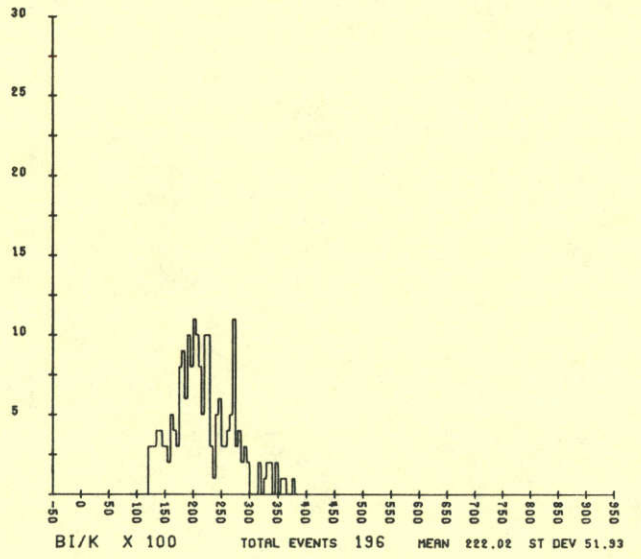
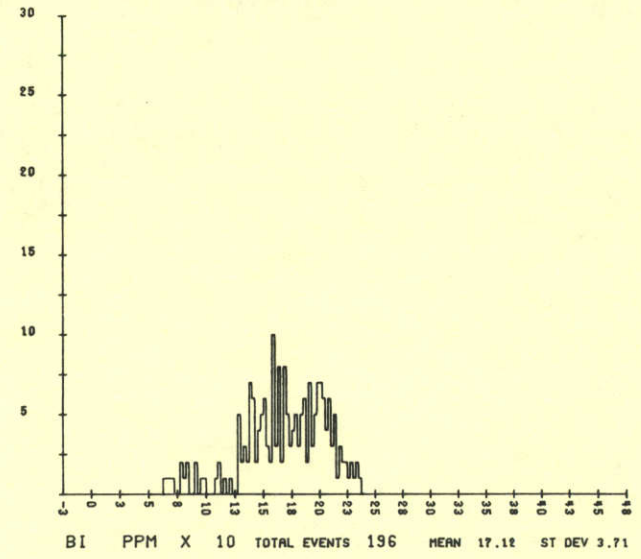
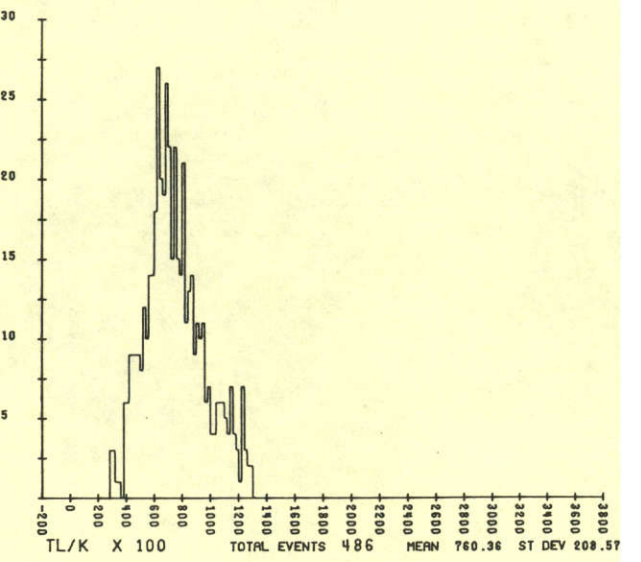
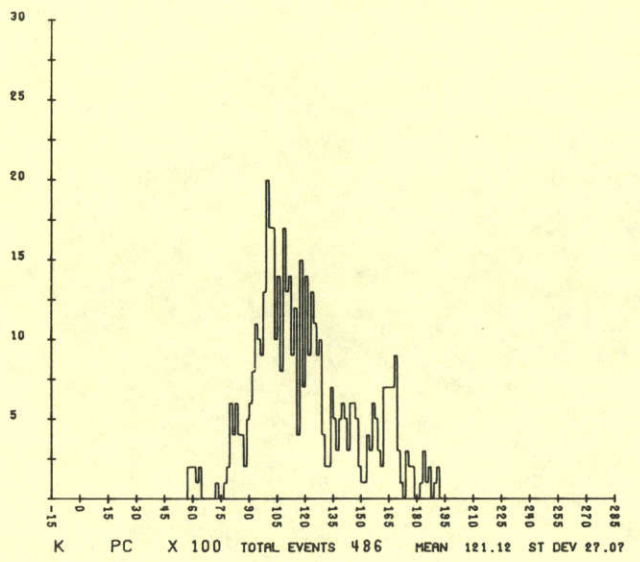
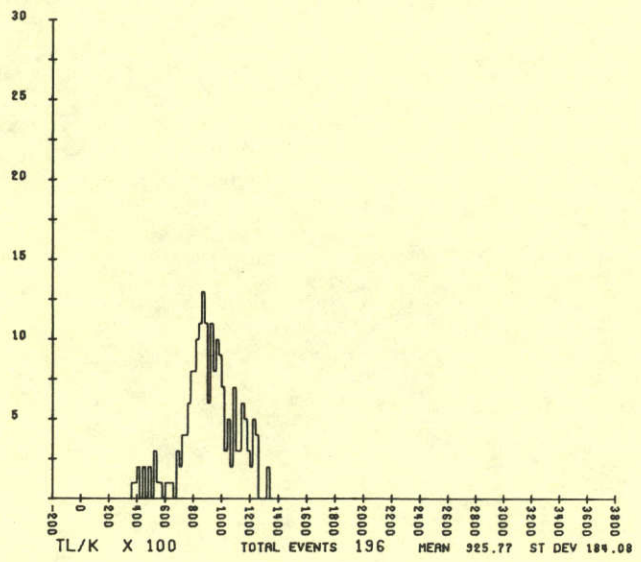
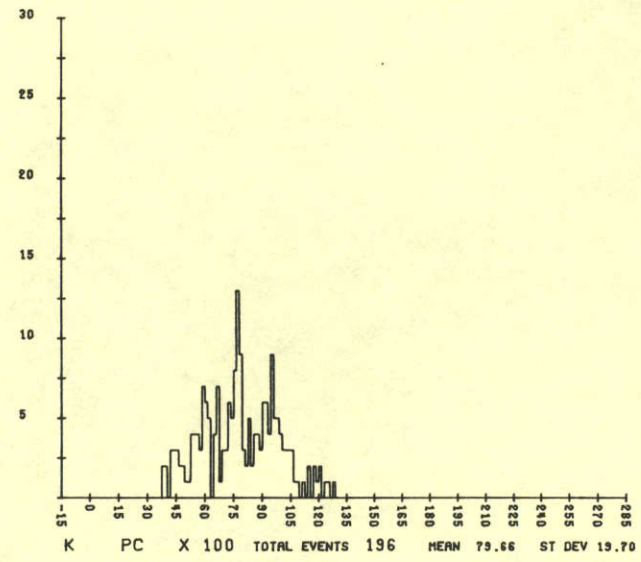


WILMINGTON

WILMINGTON

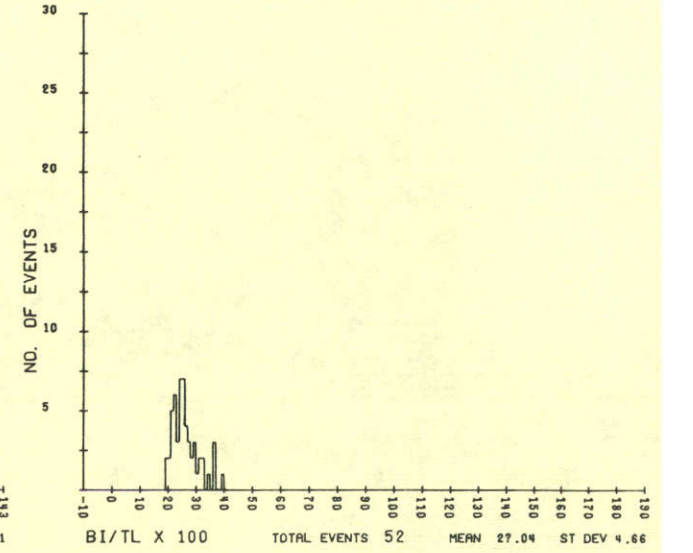
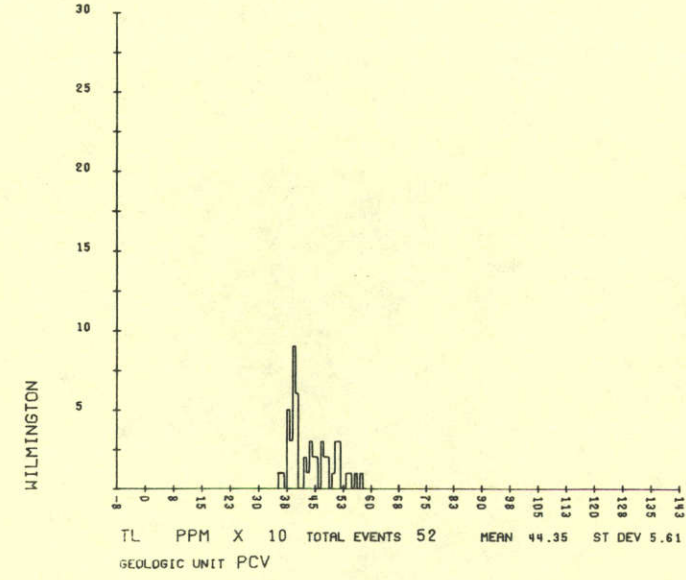
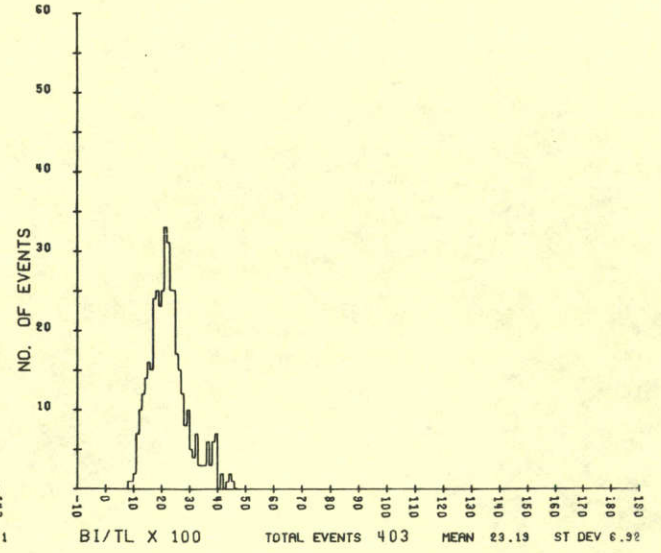
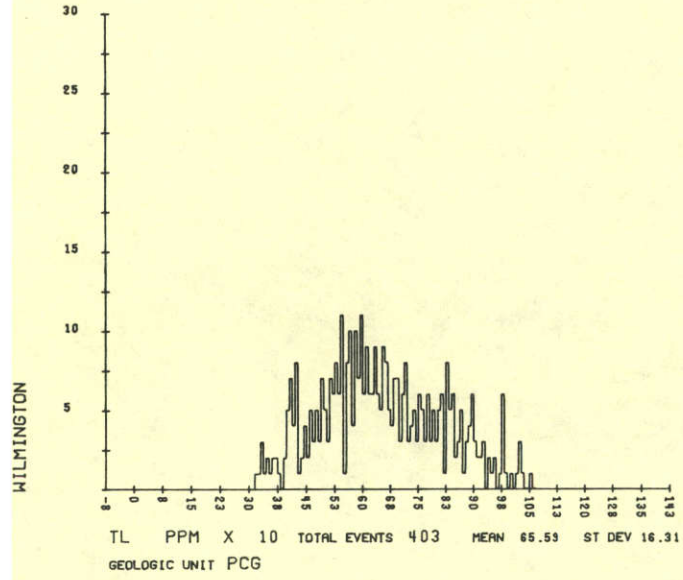
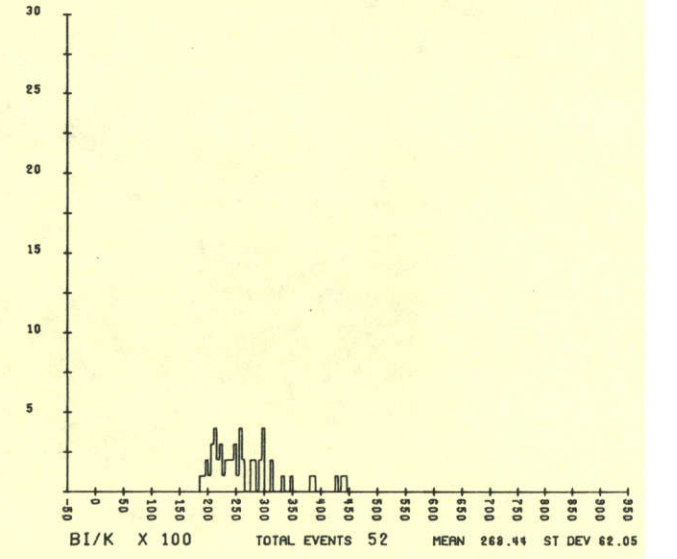
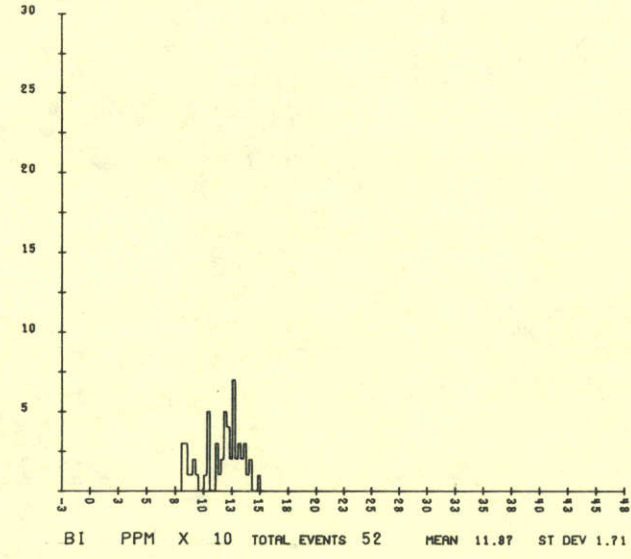
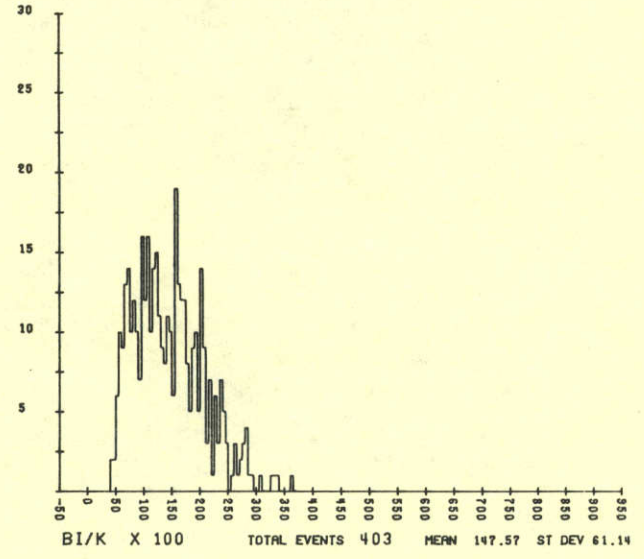
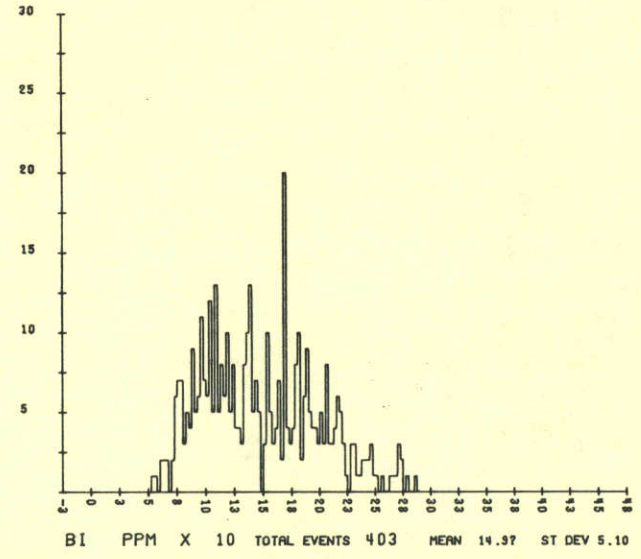
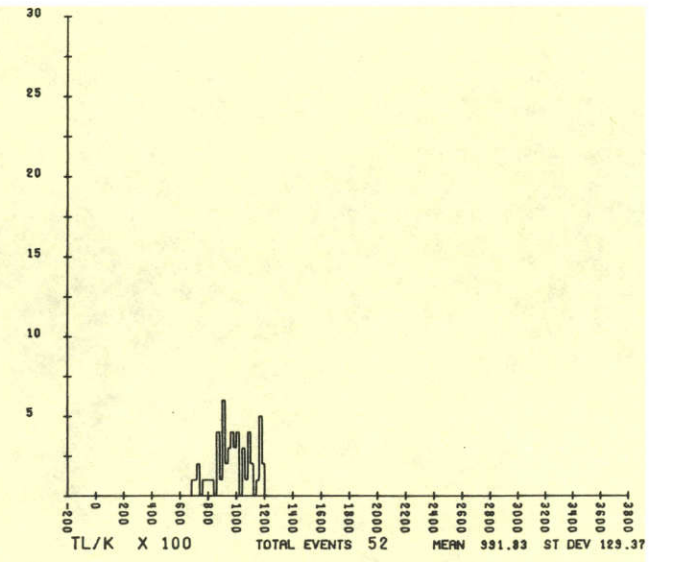
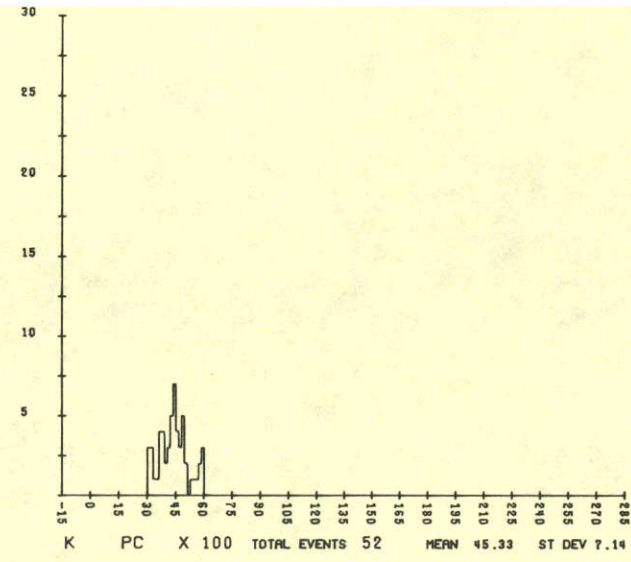
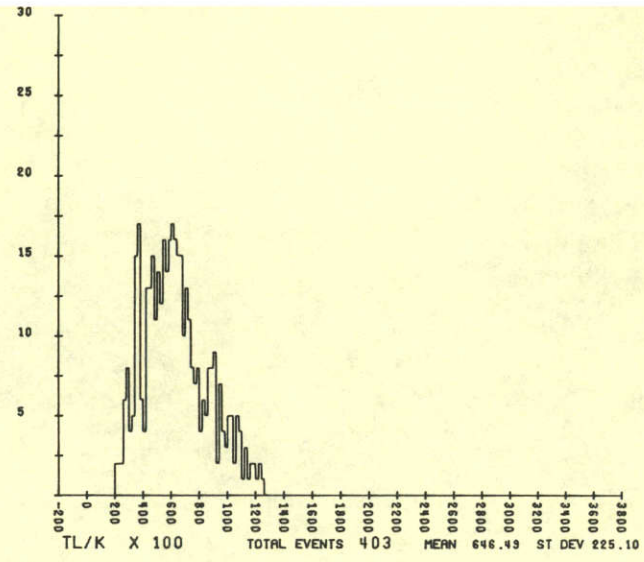
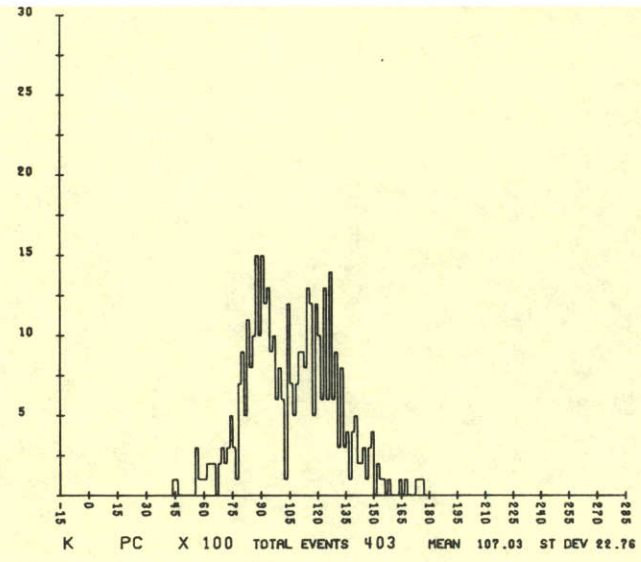


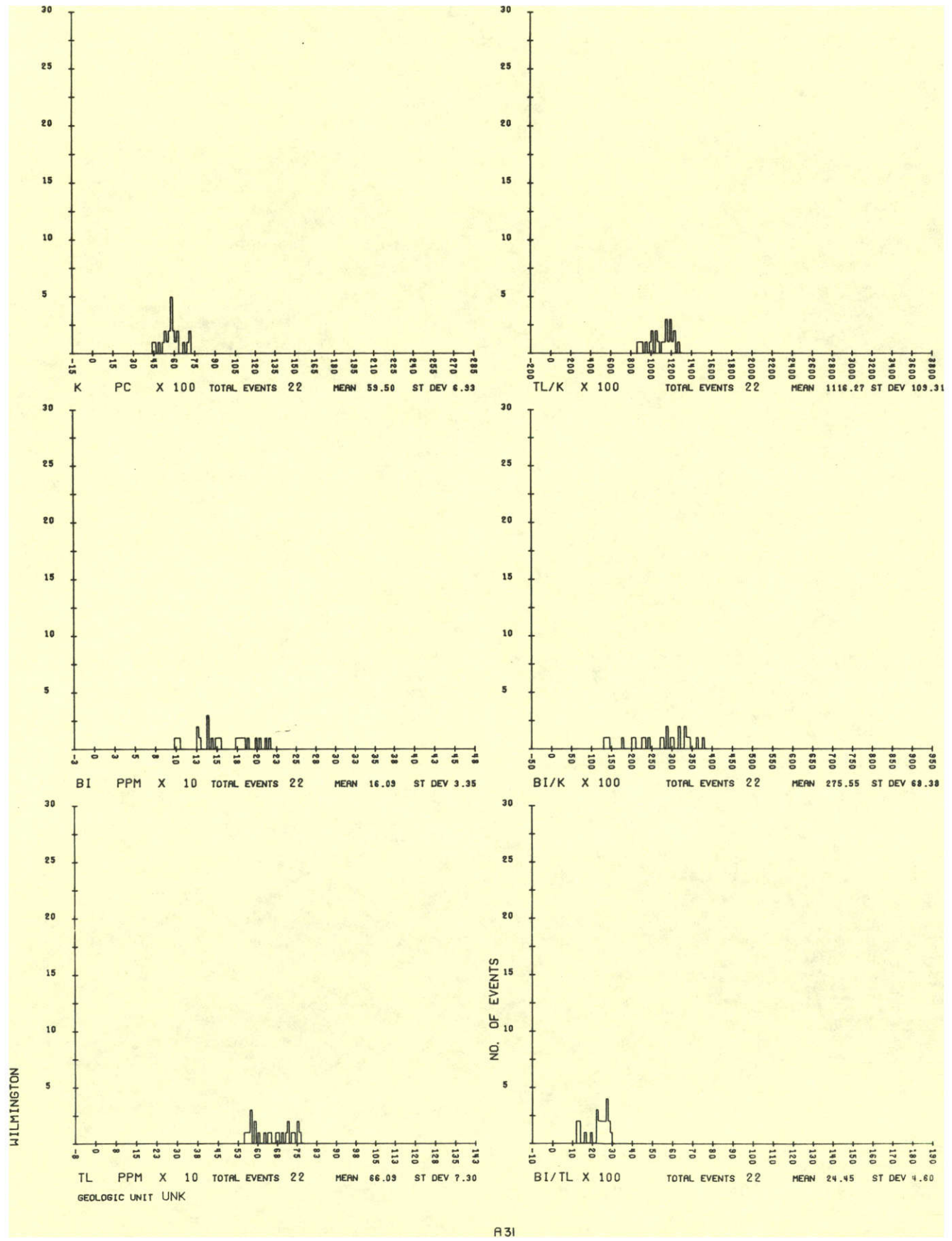




WILMINGTON

WILMINGTON





SECTION V

GEODATA DATA AQUISITION AND PROCESSING

SECTION V.

GEODATA DATA ACQUISITION AND PROCESSING

A. DATA ACQUISITION SYSTEM

A brief description of the computer-linked Geodata Data Acquisition System (GDAS), used in the present survey, is presented here. The five primary components of the GDAS, which are mounted aboard a Douglas Super DC-3 aircraft, Figure V.1, are:

- 1) An array of nine (9) 11½" dia. by 4" thick NaI(Tl) detectors;
- 2) a NOVA mini-computer system
- 3) a Collins ALT-50 radar altimeter system;
- 4) a proton precession magnetometer; and
- 5) a Bendix DRA-12C doppler navigation system.

The nine-crystal detector array has been calibrated to measure the gamma radiation spectrum between 0-6 MeV. The contents of the 3 to 6 MeV interval is monitored in order to reduce the contributions of the cosmic events in the 0-3 MeV interval, which is of primary interest in this survey. Eight of the nine detectors are mounted to measure the 4π solid angle gamma radiation spectrum emanating from the earth's surface. The ninth detector, which is partially shielded underneath by a 3.5-inch lead plate, is situated to measure the ²¹⁴Pb radiation incoming from the upper 2π solid angle.

Each crystal detector has an estimated volume of 415.5 cubic inches, resulting in a total volume for the entire 4π system of 3324 cubic inches. The estimated volume to velocity ratio for this system is 23.7, where the average speed for the DC3-S is approximately 140 mph.

The energy resolution of the GDAS as calculated from the ¹³⁷Cs 662 keV photopeak was 10.7%, where each individual crystal was 9.0% or better. Automatic digital gain calibration for the eight detector array and the single detector system was accomplished by stabilizing on the ⁴⁰K photopeak data.

The NOVA computer, shown in the system block diagram of Figure V.2, is the control center of the GDAS. The data is gathered by the computer for every one-second period in a manner giving no dead time when readout to the magnetic tapes for storage. Two magnetic tape recorders are used; one to record the total spectral data and the computer tabulated results (LDT), and the other to record only the computer tabulated results (CDT).

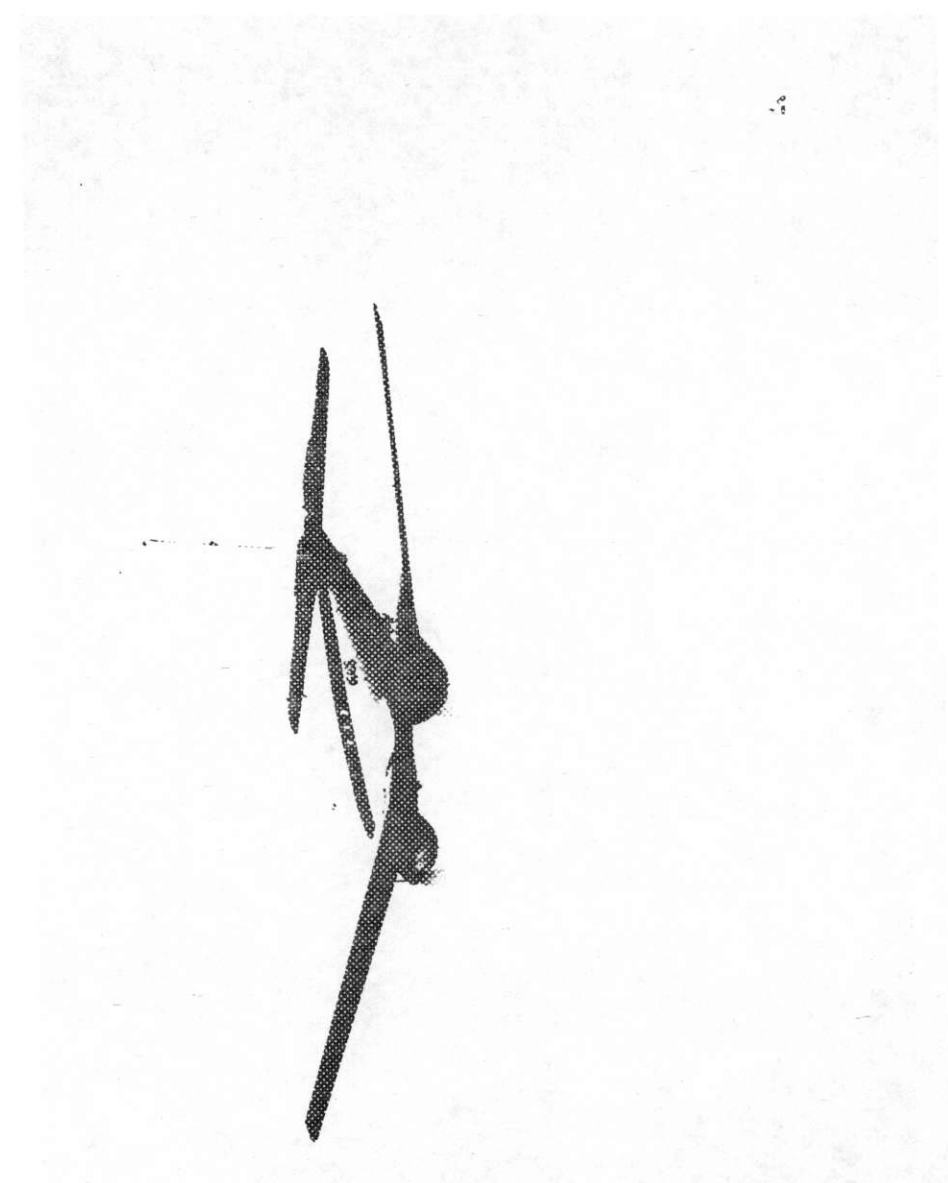


Figure V.1 Survey Aircraft

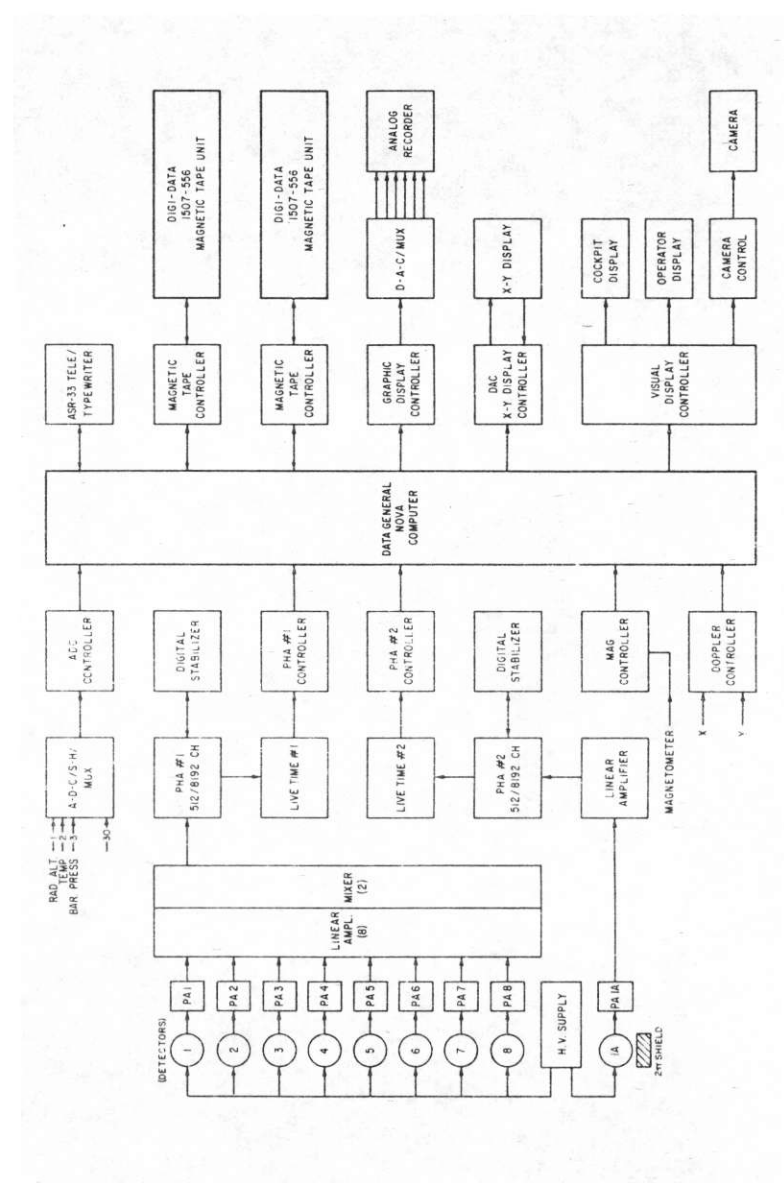


Figure V.2 System Block Diagram

Digital-to-analog conversion of the resultant intensities, their ratios and the magnetic field data are plotted on multi-track paper, allowing immediate examination for anomalous data.

The spectral data from the single detector system gathers and records the 2π spectral data every nine seconds. This 2π data is necessary to determine the amount of atmospheric ^{214}Bi radiation in the 4π spectral data. A third segment of the computer's core gathers and sums the total 2π and 4π gamma radiation spectra for each flight line, which can then be plotted as shown in Figure V.3 (EOFL spectrum).

Due to the dependence of the gamma ray data on altitude, a highly accurate radar altimeter is used. The Collins ALT-50 system is designed to make a series of 8 measurements per second, where the resulting altitude is the average.

Since the gathered data are dependent on the current ambient temperature and pressure readings, a Senso-Tek barometric pressure sensor and a Hy-Col thermocouple sensor were used to monitor conditions outside the aircraft.

A proton precession magnetometer sensor, having a 0.25 gamma readout resolution and less than a 1.0 gamma noise envelope, is sampled every second to yield a measurement of the total intensity of the earth's magnetic field below the aircraft. The sensor is carried as a "bird" on a 100-foot cable in order to minimize the magnetic effects of the aircraft.

A Bendix DRA-12C navigation system with a ± 100 th/nautical mile accuracy provides a doppler navigation cross-track and along-track analog signal to be recorded each second onto magnetic tape. Two other methods are used to properly locate the aircraft's track: visual sightings and photography. The first method is employed by the navigator who marks flight map location reference points with computer-displayed record numbers. The second method is a 35mm film that records a continuous, recoverable track which has a 20% overlap/frame at an elevation of 400 feet.

There are three basic operating modes of the GDAS that the operator can manipulate:

- 1) CALIBRATE, which allows proper gain calibration for the detectors;
- 2) OPERATE, which allows data to be collected, summed and recorded; and
- 3) PLAYBACK, which allows the operator to examine the newly acquired data.

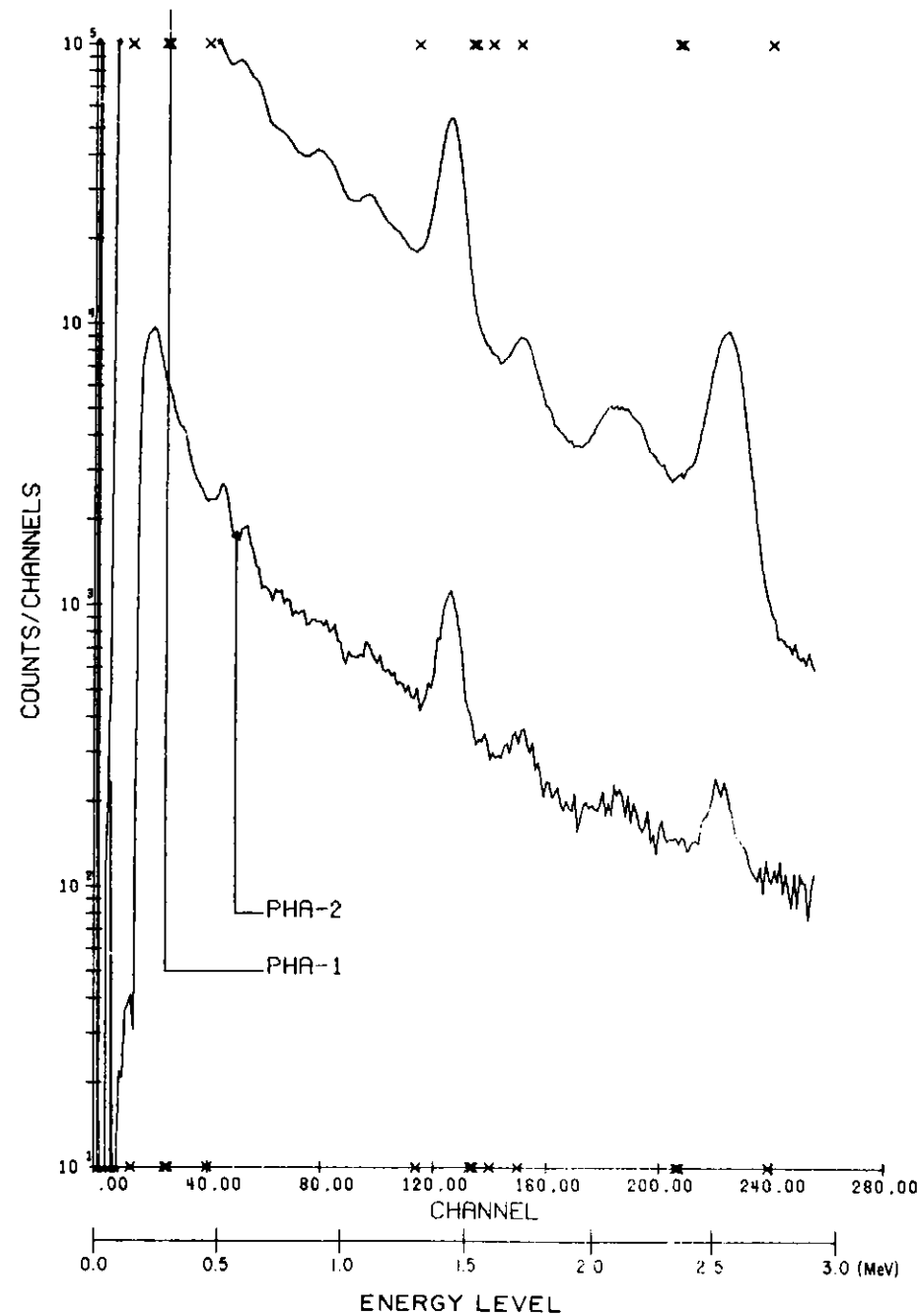


Figure V.3 Typical End-of-Flight-Line Spectral Plot

B. DATA PROCESSING

1. Data Reduction

The field data tapes produced by the data acquisition system (Section V.A) contain the 4π and 2π gamma radiation spectra, measured between 0 to 6 MeV. The resulting gamma ray spectra are composite spectra of the several different isotopes that emit gamma rays within the detectors' energy range. The method used in this work to determine the concentrations of the different isotopes monitored is discussed in this section.

In this work, there are four different isotopes which contributed to the resultant composite spectra under consideration. In order of the highest to lowest energy emitter, they are: cosmic, eTh, eU and K counting rates.

Isotope	Energy Interval (MeV)
Cosmic	3.0 to 6.0
^{208}Tl	2.410 to 2.796
^{214}Bi	1.661 to 1.860
^{40}K	1.357 to 1.556

Due to the occurrence of Compton scatter at all gamma ray energy intervals, a 4×4 matrix method approach is used to "spectrally strip" the group summed counting rates into their individual counting rates attributed only to the isotope associated with that energy interval.

This matrix method approach is theoretically applicable to a spectrum containing any number of isotopic gamma rays. For convenience, the four isotopes will be denoted as: COS, TL, BI and K. The channel group sum for each energy interval can be considered to consist of fractional components of each of its constituents. For instance, one can write for the TL channel group sum:

$$a\text{COS} + 1.0\text{TL} + b\text{BI} + 0.0\text{K} = \text{MTL}$$

where MTL is the channel group sum count;

and the coefficients, which are known as Compton coefficients, for each variable represent the responses of the data gathering system to each isotope over the entire energy spectrum.

Similarly, equations can be written for the energy interval group sums for MCOS, MBI and MK, as shown below in matrix notation by

$$\begin{bmatrix} 1.0 & 0.0 & 0.0 & 0.0 \\ a & 1.0 & f & 0.0 \\ b & \alpha & 1.0 & g \\ c & \beta & \gamma & 1.0 \end{bmatrix} \begin{bmatrix} \text{COS} \\ \text{TL} \\ \text{BI} \\ \text{K} \end{bmatrix} = \begin{bmatrix} \text{MCOS} \\ \text{MTL} \\ \text{MBI} \\ \text{MK} \end{bmatrix}$$

where each element of the 4 x 4 matrix is a Compton coefficient. By inverting the 4 x 4 matrix and multiplying on the left by the channel group sum matrix, the resulting column matrix, whose elements are COS, TL, BI, and K, represents the counts in each energy interval attributed only to the indicated isotope source.

Table V.1 contains the data reduction parameters, coefficients and backgrounds used in this survey. The listed Compton coefficients were determined from data acquired during high altitude flights and from "known" test pad data concentrations in Grand Junction, Colorado.

The resulting reduced counting rates for COS, TL, BI and K must then be normalized with respect to the measured live time counting rate of the data acquisition system. This is necessary in order to restore the linear relationship between the photopeak counts and the source's intensity. This procedure is accomplished by dividing the reduced counts by the live time, LTC1:

thus,

$$\begin{aligned} \text{COS1} &= \text{COS/LTC1} \\ \text{TL1} &= \text{TL/LTC1} \\ \text{BI1} &= \text{BI/LTC1} \\ \text{K1} &= \text{K/LTC1} \end{aligned}$$

The next step in the data processing involves the subtraction of the background counts present onboard the aircraft. The background counts, which exist in the aircraft and its equipment, are determined from high altitude data where the data acquisition is free from all ground sources and atmospheric ^{214}Bi contamination. The background counts, denoted as B_{TL} , B_{BI} and B_K , used in this work are listed in Table V.1. During the processing, the backgrounds are checked by observing the resulting counting rates over large bodies of water, where the rates would have near zero intensities. The gross count's background counting rate, B_{GC} , over channels 35-239, is also given in Table V.1.

After the backgrounds have been subtracted from the live time corrected photopeak counts, thus

$$\begin{aligned} \overline{\text{TLI}} &= \text{TL1} - B_{TL} \\ \overline{\text{BII}} &= \text{BI1} - B_{BI} \\ \overline{\text{KI}} &= \text{K1} - B_K \end{aligned}$$

The resulting counting rates for $\overline{\text{TLI}}$ and $\overline{\text{KI}}$ represent the counts contributed only by the sources below the aircraft on the earth's surface. In the case of $\overline{\text{BII}}$, an additional source of ^{214}Bi radiation, which is caused by atmospheric ^{214}Bi , BIAIR, is still eminent.

The 2π detector system data is used to determine the magnitude of the BIAIR to be subtracted. Since the predominate variable source affecting the 2π detector is the atmospheric ^{214}Bi , it is possible to utilize most of the 2π spectrum in the BIAIR determination, and thereby produce some improvement in the statistical error. The energy interval used for the 2π crystal is between 1.05 to 2.79 MeV. Within this interval, the aircraft's background, $B_{2\pi}$, and its Compton coefficient, $C_{2\pi}$, have been determined from the high altitude data. (See Table V.1).

The BIAIR associated with the unshielded detector array is determined, using the shielded detector by the relation:

$$\text{BIAIR} = \frac{G(x)}{[1 - k_2 G(x)]} [VC - C_{2\pi} \cdot \text{COS1} - b_{2\pi} \cdot \text{RVALM}]$$

where

$G(x)$ is the relationship between the 4π and 2π solid angles, the channel group sums and the number of detectors in the detector arrays;

VC is the 2π total count group sum of channels 91-239, c/s;

COS1 is the 4π cosmic count, greater than 3.0 MeV, c/s;

and,

$$\text{RVALM} = k_1 \overline{\text{TLI}} + k_2 \overline{\text{BII}} + k_3 \overline{\text{KI}}$$

where k_1 , k_2 , k_3 are constant factors that correct for the penetration/spill of the emanated surface radiation. These penetration/spill constants are dependent on the amount of lead shielding used on the 2π crystal. The values used in this work are listed in Table V.1.

$\overline{\text{TLI}}$, $\overline{\text{BII}}$ and $\overline{\text{KI}}$ have already been defined as the 4π reduced data counting rates, c/s.

Finally, the ^{214}Bi counting rate caused only by the surface sources is given by

$$\text{BISUR} = \overline{\text{BII}} - \text{BIAIR}$$

Briefly summarizing, $\overline{\text{TLI}}$, BISUR and $\overline{\text{KI}}$ are the counting rates as measured at the height of the aircraft. All interfering counts from cosmic, backgrounds and atmospheric ^{214}Bi have been removed.

Since the various counting rates are dependent upon the height of the aircraft above the surface terrain, it is necessary to correct the associated isotope's counting rate to an altitude of 400 feet above the surface terrain. This is accomplished through the equations indicated below:

$$\text{TLS} = \overline{\text{TLI}} \cdot e^{-\mu_1(400 - \frac{\rho}{\rho_0} x)}$$

$$\text{BIS} = \text{BISUR} \cdot e^{-\mu_2(400 - \frac{\rho}{\rho_0} x)}$$

$$\text{KS} = \overline{\text{KI}} \cdot e^{-\mu_3(400 - \frac{\rho}{\rho_0} x)}$$

and

$$\text{GC(gross count)} = (\overline{\text{GC}} - B_{GC} - S \cdot \text{BIAIR}) \cdot e^{-\mu_4(400 - \frac{\rho}{\rho_0} x)}$$

where

$\overline{\text{GC}}$ is the live time corrected gross count, channels 35-239,

S is the ratio of the BI data, channels 35-239 to channels 143-159,

B_{GC} is the gross count background,

TLS, BIS, KS are the respective photopeak's counting rates at 400 feet;

ρ_0 is the air density at standard temperature and pressure; 0.001293 gm/cc

ρ is the air density at the time the survey data was flown;

$\mu_1, \mu_2, \mu_3, \mu_4$ are the respective linear attenuation coefficients;

x is the aircraft's height above the surface terrain in feet.

The attenuation coefficients and other constants used in the altitude normalization are listed in Table V.1.

After each flight line of data has undergone the above data reduction, the average values for each radiation variable and variable ratios for each of the flight lines were plotted to demonstrate the consistency of the average values and that a smooth flow continues from day to day, and from the start to the finish of each day.

Diurnal variations of the magnetic field base station intensity were measured and applied to the field data. (See Section II.D and Appendix I.C). The magnetic heading corrections for the aircraft and its equipment used in this survey were determined by flying a predetermined path at a survey altitude in first an east to west direction, then in a west to east direction. The same procedure is used on a north to south path. Based on the data obtained in this fashion, see Table V.1, the heading corrections were removed from all the data. The magnetic field data were then IGRF corrected to give the residual magnetic field. The International Geomagnetic Reference Field subtracted was provided by the U.S. Geological Survey with reference to the IAGA Bulletin #38, "Grid Values and Charts by the IGRF 1975.0", National Technical Information Service Report #PB265483.

The system sensitivities at 400 feet used in this survey are shown in Table V.1.

2. Description of the Data Processing

The processing flow chart representative of the work performed in this survey is shown in Figure V.4.

As stated in Section V.A., the original field data tapes were recorded to contain the various tag words, 4 π and 2 π spectral

TABLE V.1: DATA REDUCTION PARAMETERS AND CONSTANTS - N540S 1979

AIRCRAFT BACKGROUNDS				COSMIC CORRECTION RATIOS	
Detector	Parameter	Window	Value (CPS)	Parameter	Value
Terrestrial (4 π)	B _K	Potassium	25.82	c	0.2028
	B _{Bi}	Uranium	9.42	b	0.1546
	B _{Th}	Thorium	7.60	a	0.1897
	B _{GC}	Gross	337.0	-	-
Atmospheric (2 π)	B _{2π}	Uranium	8.19	C _{2π}	0.2169

DERIVED STRIPPING COEFFICIENTS AND RATIOS			
Coefficient	Value	Coefficient	Value
α	0.2889	k ₁	0.053
β	0.3896	k ₂	0.0
γ	0.8669	k ₃	0.0
f	0.0	S	17.5
g	0.0		

LINEAR ABSORPTION COEFFICIENTS			MAGNETIC HEADING CORRECTION	
Radio Element	Parameter	Value (x10 ⁻³ per ft.)	Flight Direction	Correction (gammas)
Potassium	μ_1	2.795	West to East	+3.56
Uranium	μ_2	2.212	East to West	-3.56
Thorium	μ_3	2.129	North to South	-1.0
Gross	μ_4	2.160	South to North	+1.0

RADIOELEMENT	SYSTEM SENSITIVITIES AT 400 FEET
Potassium (cps/%K)	105.00
Uranium (cps/ppm eU)	13.85
Thorium (cps/ppm eTh)	7.24

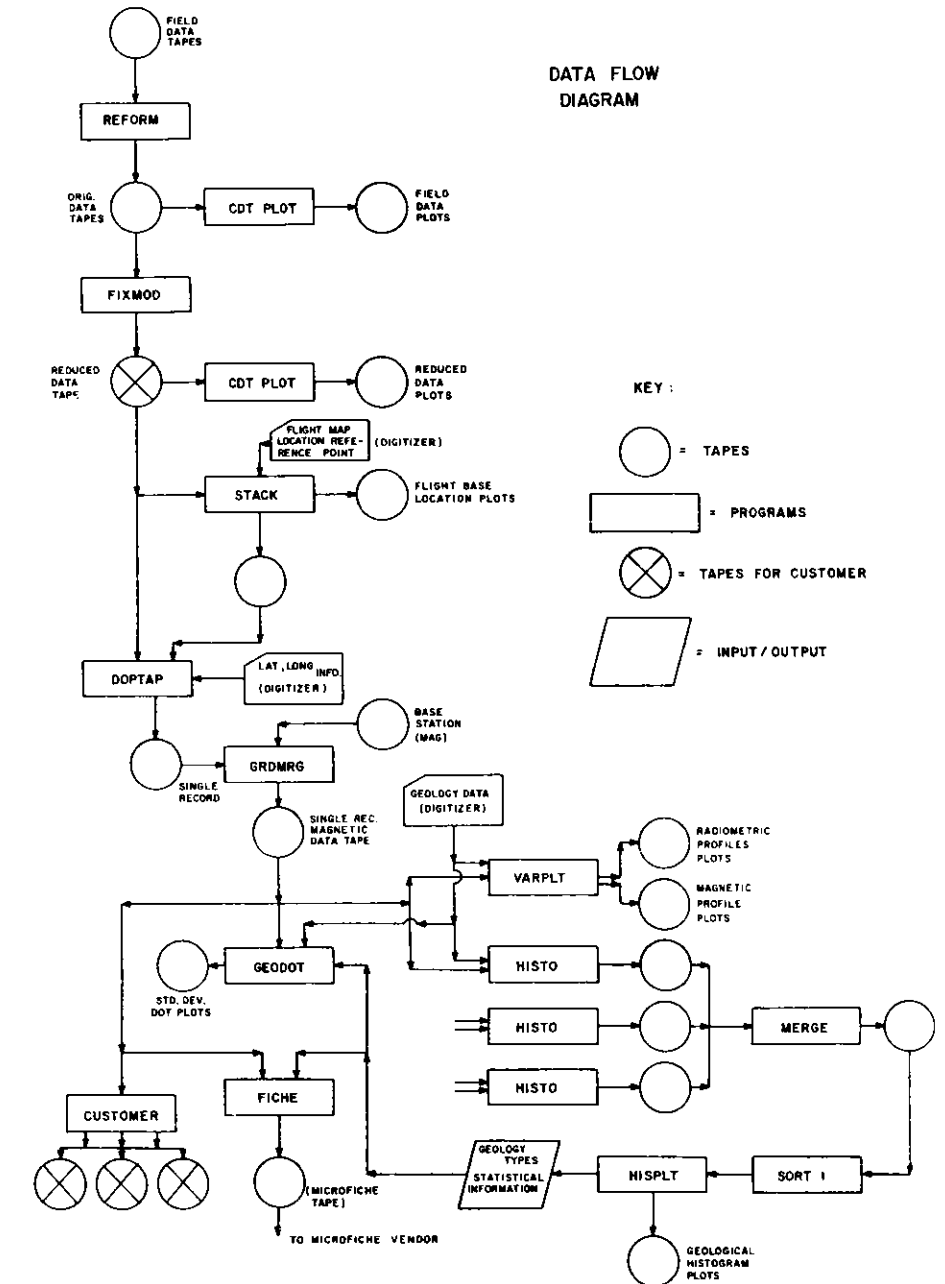


Figure V.4 Data Reduction Flow Chart

data and the trailer record sums for each flight line. The purpose of the REFORM program is to sum the raw spectral data (LDT) into the proper group sum energy intervals for each second for each line. The CDTPLT program is a data certification program that produces the EOFL spectral plots, Figure V.3, and profiles of each of the channel group sums, which are plotted as a function of each line's record numbers.

A brief summary of each program and its uses is given below:

PROGRAM	FUNCTION
REFORM	Produces energy group sums and EOFL spectra.
FIXMOD	Primary processing for "spectral stripping" matrix reduction, live time normalization, background and BIAIR subtraction, and altitude corrections.
STACK	Flight path recovery to produce record location map at a scale of 1:250,000.
DOPTAP	Single record processing with latitude/longitude positioning, IGRF and single point statistical adequacy computations, and magnetic heading corrections.
GNDMRG	Merges aircraft magnetometer and ground magnetometer in proper time sequence and applies diurnal corrections to the field data.
VARPLT	Produces radiometric and magnetic stacked profile plot tapes.
HISTO, MERGE, and SORT1	Preliminary programs to prepare/sort data as a function of geologic type for the entire area.
HISPLT	Produces geological histograms, mean and standard deviation tables, and plot tape for the entire area.
GEODOT	Produces plot tape for standard deviation "dot plots" related to geologic type.
FICHE	Produces average record and single record reduced data listings and microfiche tapes, which are sent to microfiche vendor.
CUSTOMER	Produces all customer required tapes.

3. Data Presentation

The surveyed area was positioned geographically to completely cover the specific National Topographic Map. Each topographic map has been used as the flight base and sufficient geographical and 15' location information has been shown. The flight line pattern has been superpositioned onto these created base maps, where the standard deviation levels for each independent variable and each ratio of these variables have been plotted (NGRMS), based on the data contained within the total map area. Every fifth data point along each map line has its standard deviation value shown at the location of that value. Therefore, there are six NGRMS sheets which indicate the location and magnitude of anomalous data.

The multivariable map line profile, which represents 10 variables as a function of their latitude and longitude location for each line, is presented at a scale of 1:500,000. Each profile presents:

1. Aircraft altitude above the surface
2. eTh (^{208}Tl from ^{232}Th decay series)
3. eU (^{214}Bi from ^{238}U decay series)
4. K (^{40}K from natural potassium)
5. BIAIR (atmospheric ^{214}Bi)
6. Residual magnetic field
7. Gross count (greater than 400 keV)
8. eU/eTh ($^{214}\text{Bi}/^{208}\text{Tl}$) ratio
9. eU/K ($^{214}\text{Bi}/^{40}\text{K}$) ratio
10. eTh/K ($^{208}\text{Tl}/^{40}\text{K}$) ratio
11. Geologic data, including aircraft flight path

The residual magnetic field map line profile, which represents five variables as a function of their latitude and longitude location for each line, plus geologic data at a scale of 1:500,000 is presented as:

1. Aircraft altitude
2. Atmospheric temperature
3. Atmospheric pressure
4. Residual magnetic field data
5. Magnetic field base line station data
6. Geological data, including aircraft flight path

The output of these various computations supplies, beyond two profile sets, the following data:

- * Histograms of the radiation data distribution within each geologic unit.

- * Histograms of the average velocity distribution for each one-second record for each map and tie line.
- * Histograms of the average altitude distribution for each one-second record for each map and tie line.
- * Tables giving the average radiation concentration of each geologic unit for each flight line.
- * Average radiation concentration for each variable as a function of flight line, including the atmospheric ^{214}Bi .
- * Set of maps showing the standard deviation data as a function of location and radiation variable.
- * Printer plot contour maps of eTh, eU, K, eU/K, eU/eTh, eTh/K and the magnetics at a scale of 1:500,000.

4. Statistical Analysis Procedures

It is necessary to exclude from the statistical analysis all variables which have too low a counting rate to be statistically valid, and data which were obtained at altitudes above 1,000 feet. To this end, a statistical adequacy test was run on all data for each data record. If a given value of T_w, Bi or K failed the test, that variable value, and any ratio value associated with it, were not used in the statistical determinations of mean and standard deviation values. In addition, such values are indicated on the radiometric profiles by a vertical (tick) mark along the base line for the variable, and are flagged in the single record and averaged record listings (microfiche). The ratio values are set to zero in the Radiometric Profile Plots. The flags in the listings appear under the heading AKUT for altitude, ^{40}K , ^{214}Bi and ^{208}Tl , respectively. The flags are zero for statistically valid data, and one for rejected data in the case of K, U and T. For altitude (A), a zero indicates altitudes to 700 feet, a one (1) indicates altitudes between 700 and 1,000 feet, and a two (2) indicates altitudes above 1,000 feet.

The tests used to reject data were as follows:

$$\begin{aligned}
 (1) \quad T\bar{L}I < 1.5 & \quad \sqrt{\frac{T\bar{L}W - T\bar{L}I}{T\bar{L}I}} = 1.5\sigma T \\
 (2) \quad B\bar{I}S\bar{U}R < 1.5 & \quad \sqrt{\frac{B\bar{I}W - B\bar{I}S\bar{U}R}{B\bar{I}S\bar{U}R}} = 1.5\sigma B \\
 (3) \quad K\bar{I} < 1.5 & \quad \sqrt{\frac{K\bar{W} - K\bar{I}}{K\bar{I}}} = 1.5\sigma K
 \end{aligned}$$

where the "w" subscript refers to the respective window counting rates from the raw data and \overline{KI} , BISUR and \overline{KI} have previously been defined. If any of the above inequalities were true, the associated variable was flagged, and that value was rejected in all statistical determinations.

The values of the radicals in the above equations, which are indicated as σT , σB , σK and the barred values, were calculated on the basis of a single record value for determining flags in the single record listings and the 7-point weighted values for determining flags in the averaged records listings.

The mean value and standard deviations were calculated assuming the data to have a normal distribution within a geologic type. The equation used in determining the variance is:

$$\sigma^2 = \frac{1}{N-1} \left\{ \sum_{i=1}^N x_i^2 - N\overline{x}^2 \right\}$$

where N is the number of statistically valid samples for a given geologic type, x_i is the value of the variable for sample number i, and \overline{x} is the mean value of the variable for the geologic type. Values from the entire survey of the area are used in these computations.

APPENDICES

I PRODUCTION SUMMARY

II TAPE FORMAT STATEMENTS

III COMPUTER LISTINGS

IV LINE PRINTER CONTOURS

AI.A PRODUCTION SUMMARY - SURVEY TIME PERIOD

ML/TL	DATE FLOWN	SURVEY LINE MILES	AVERAGE SPEED/DAY	AVERAGE ALTITUDE/DAY
TL 1-6,	7-22-79	315.6	135	394
ML (1-2,4) E/W, 3, 5-6	7-29-79	403.0	136	443
ML 7-10, (11-12) E/W	7-30-79	535.6	135	502
Total Mileage		1254.2		

*Note: The survey over the center of maplines 11 (23.5 miles) and 12 (23.5 miles) was prohibited due to the presence of the Terminal Control Area surrounding the Philadelphia International Airport.

Also, ML-12E detoured south around restricted area designated: R5001. ML-9 detoured north around Greater Wilmington Airport. ML-10 detoured south around Philadelphia International TCA. TL-5 detoured west around Dove Air Force Base.

AI-1

AI.B TEST LINE RESULTS

		July 1979	
UNIT		29	30*
PRE COS		29.9	30.1
POS COS		**	***
TL		21.2	20.8
TL		--	--
B1		12.5	11.8
B1		--	--
K		75.5	73.8
K		--	--
GC		971	943
GC		--	--
B1Air		2.7	4.3
B1Air		--	--
ALT		382	402
ALT		--	--

Wilmington

AI-2

AI.C DIURNAL CORRECTIONS TO LINE DATA

LINE	DIURNAL CORRECTIONS IN GAMMAS	LINE	DIURNAL CORRECTIONS IN GAMMAS	LINE	DIURNAL CORRECTIONS IN GAMMAS
ML 1F	7	ML 6	-4	ML 12W	-17
ML 1W	20	ML 7	-25	TL 1	-9
ML 2F	5	ML 8	-21	TL 2	-6
ML 2W	22	ML 9	-17	TL 3	8
ML 3	14	ML 10	-7	TL 4	14
ML 4F	-4	ML 11E	7	TL 5	15
ML 4W	1	ML 11W	-18	TL 6	15
ML 5	-4	ML 12F	12		

AI-3

* New Test Line Base Flown - Elwood
 ** No Test Line due to Equipment Failure (Goldsboro Test)
 *** Rainshowers at Test Line (Goldsboro Test)

AI.D EXPLANATORY NOTES

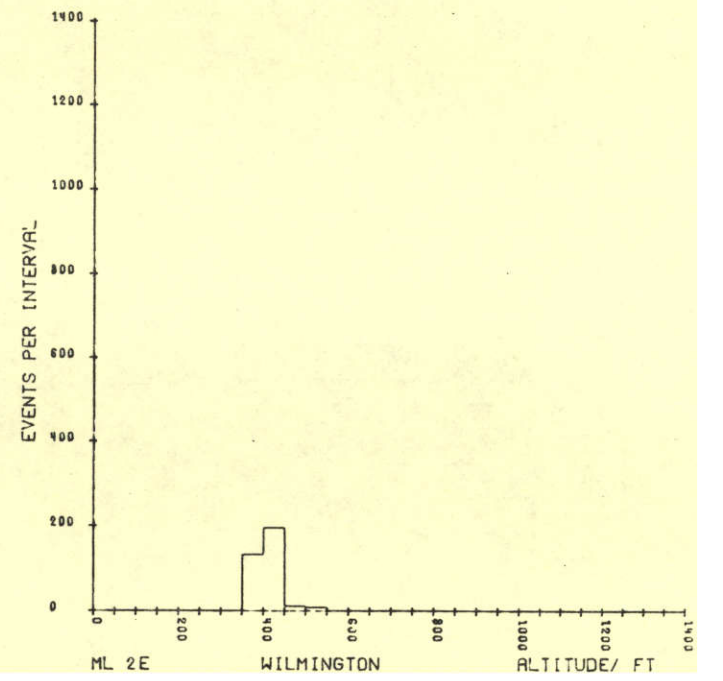
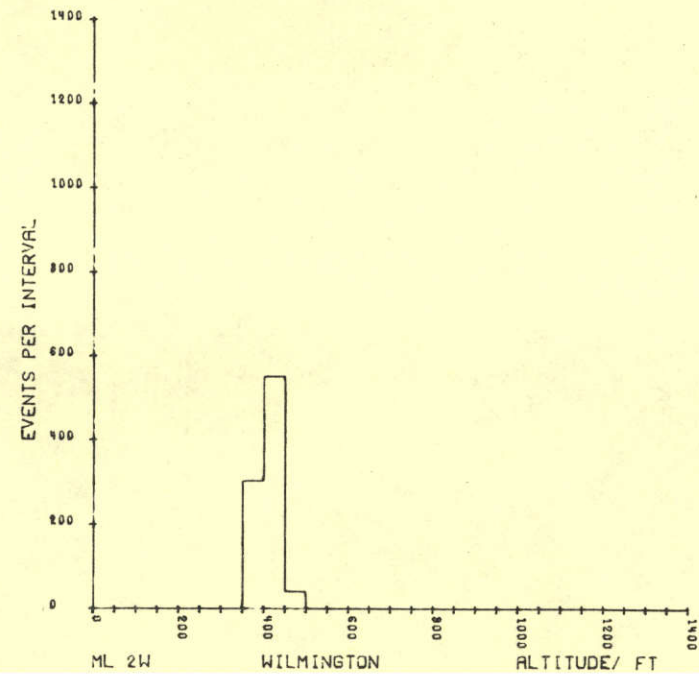
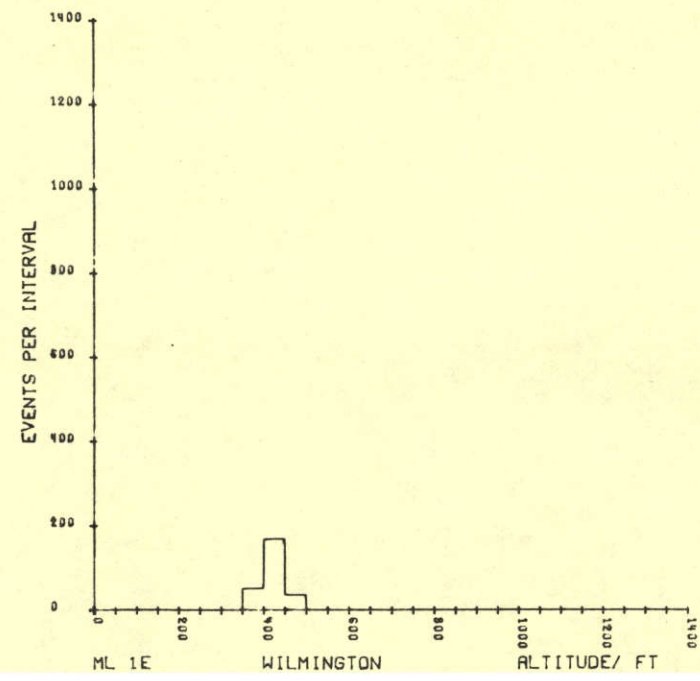
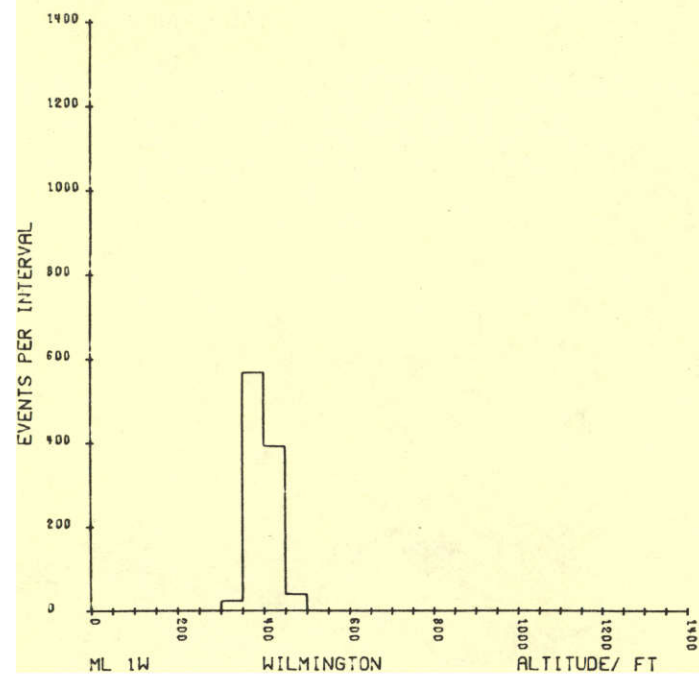
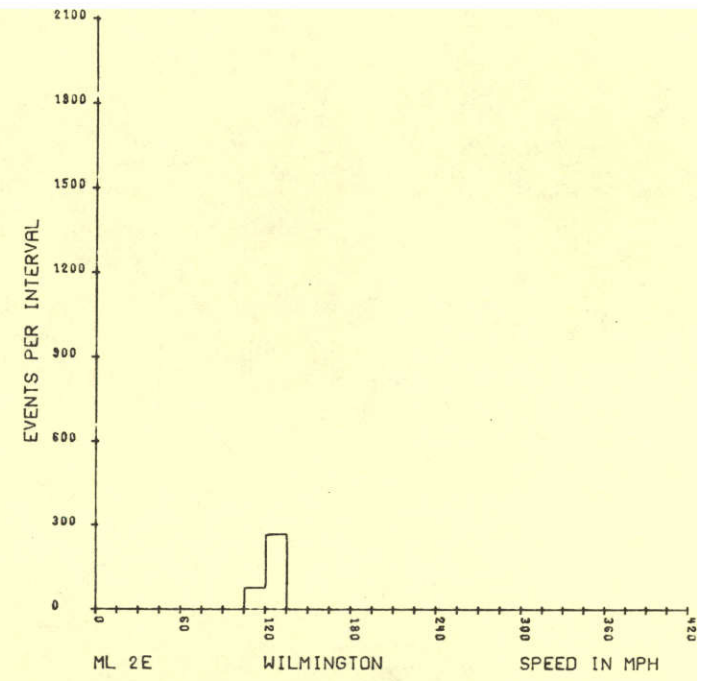
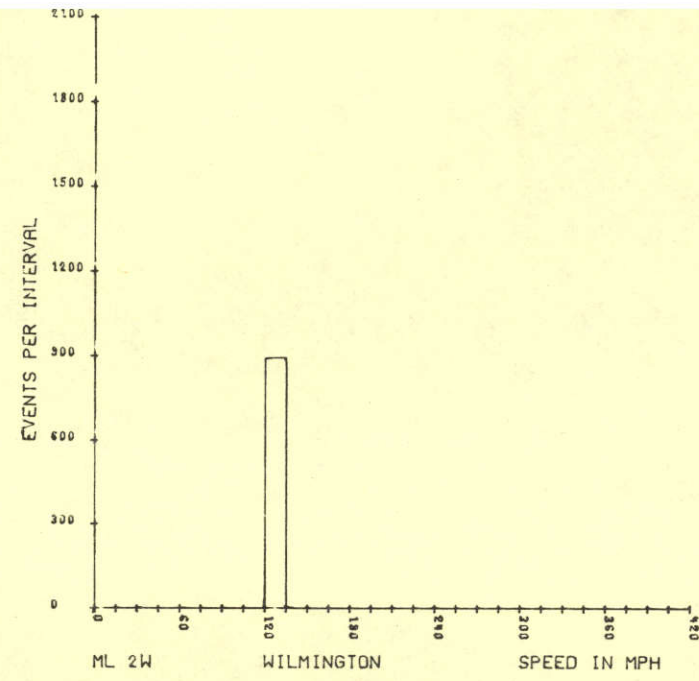
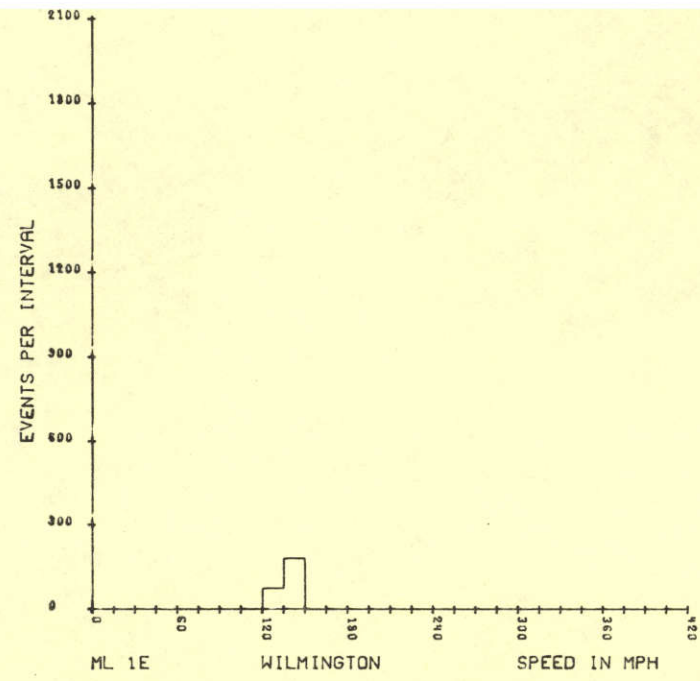
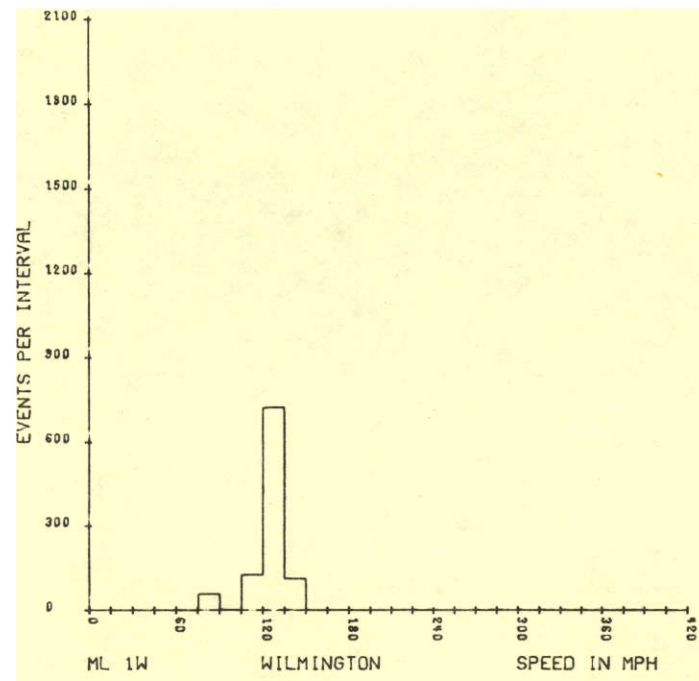
The correspondence between the map/tie line numbering systems of the base maps and profiles of this report to those listed on the customer magnetic tapes is given below:

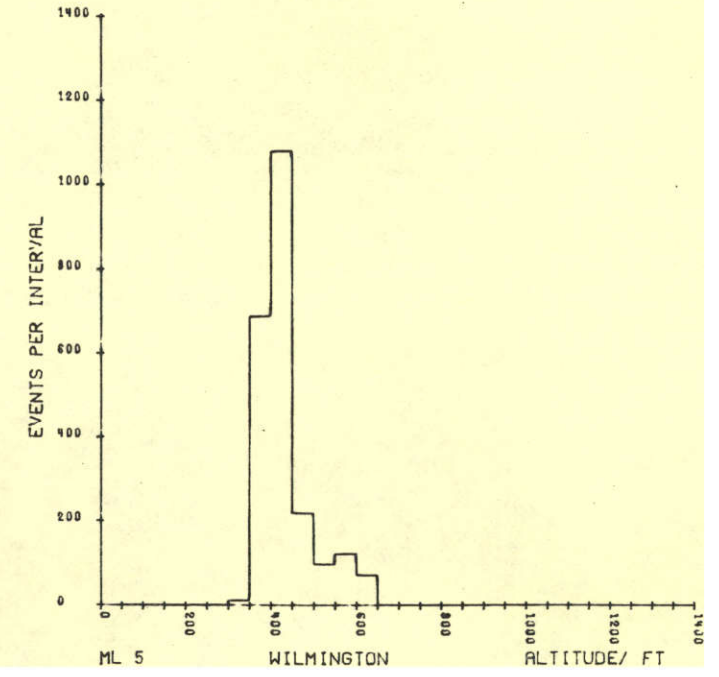
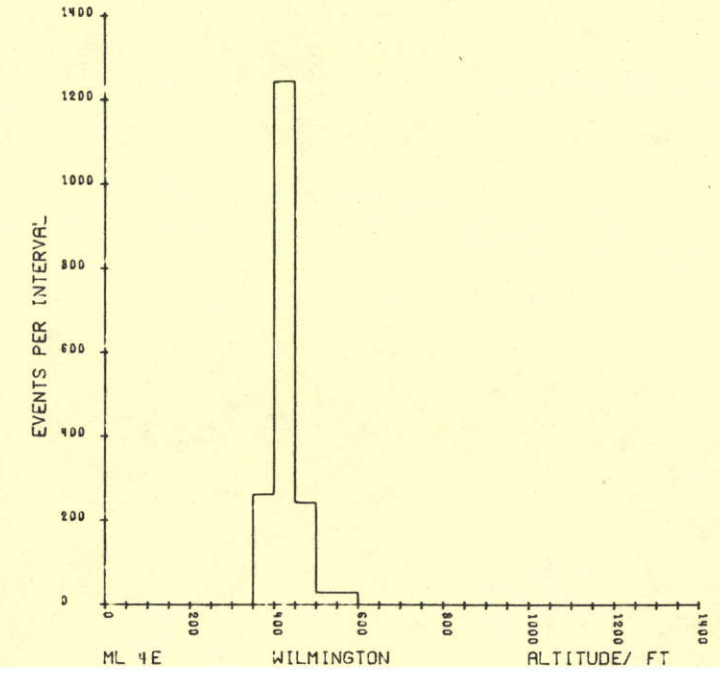
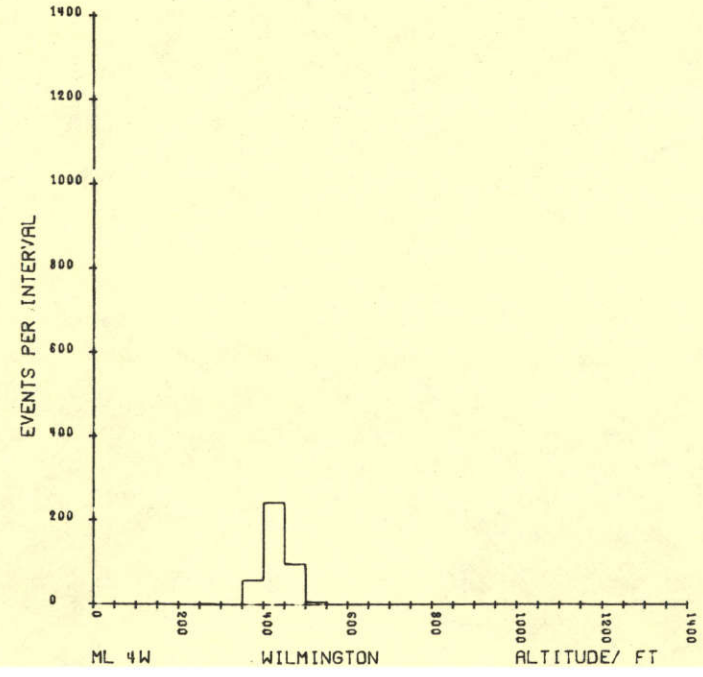
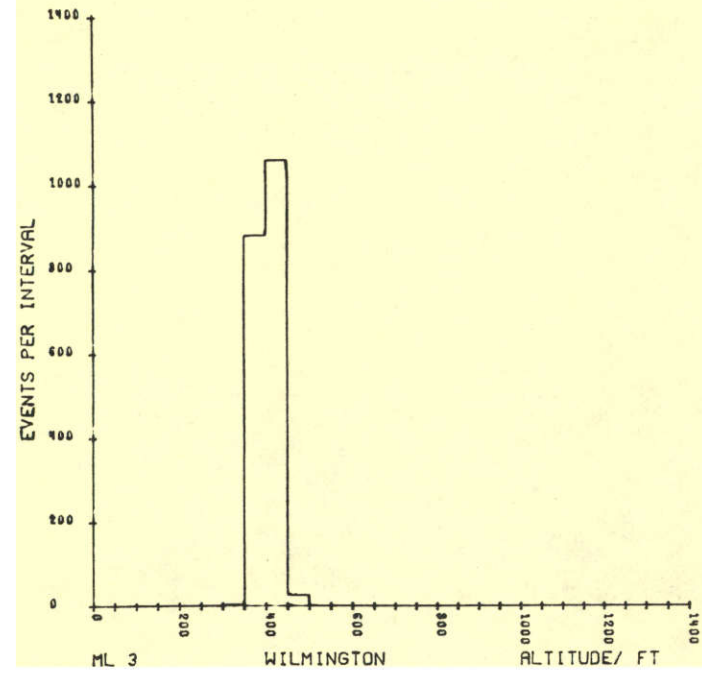
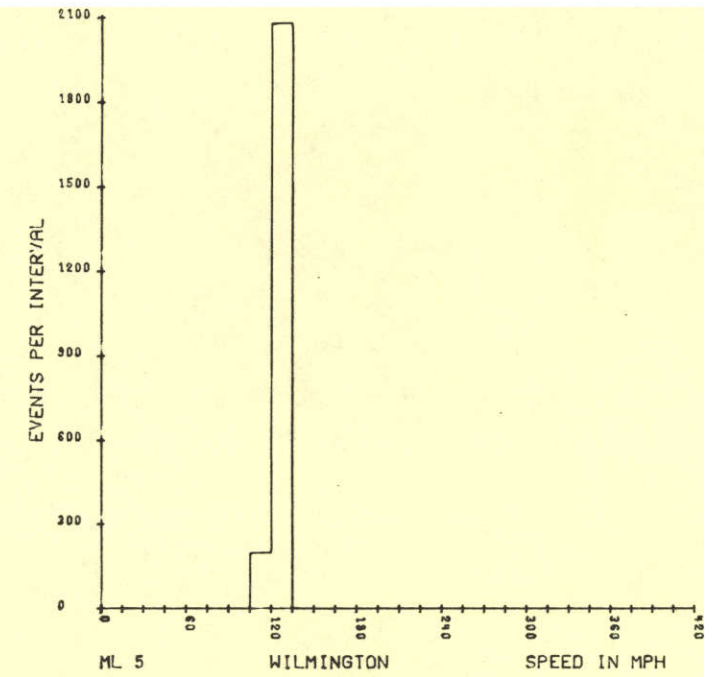
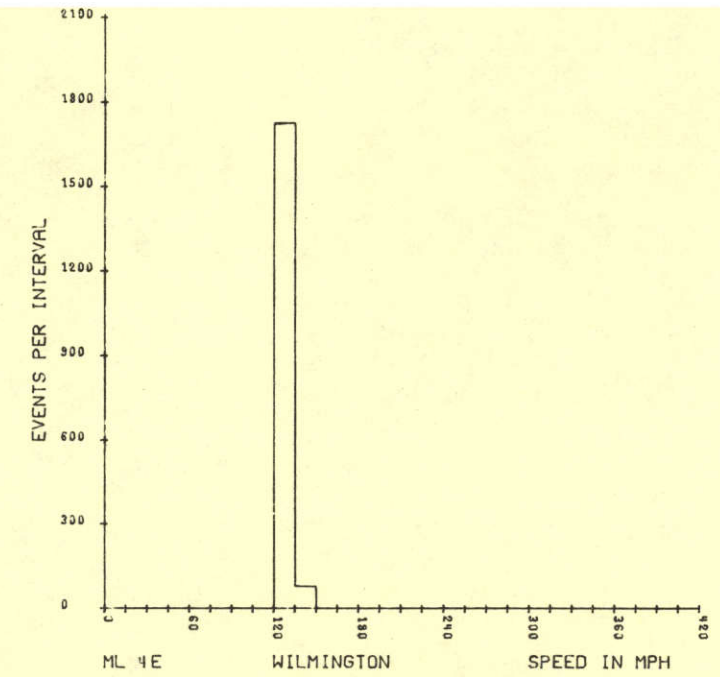
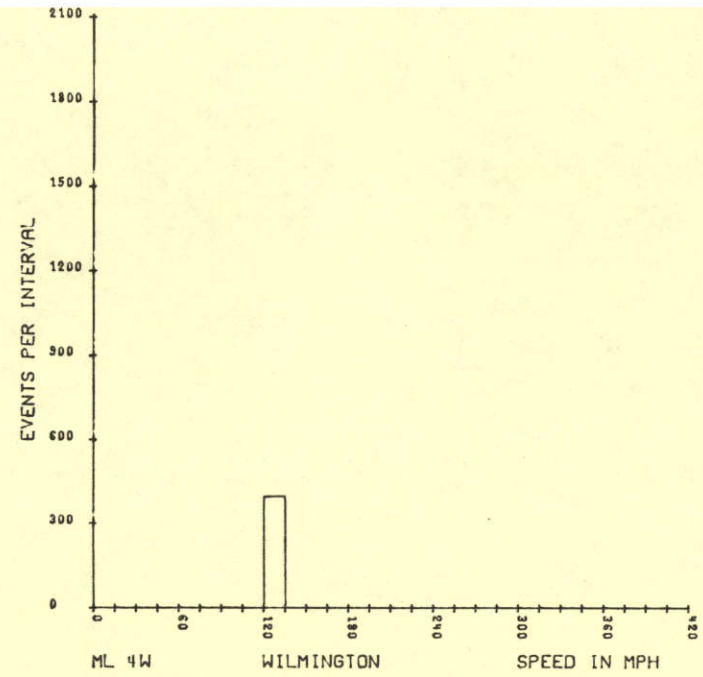
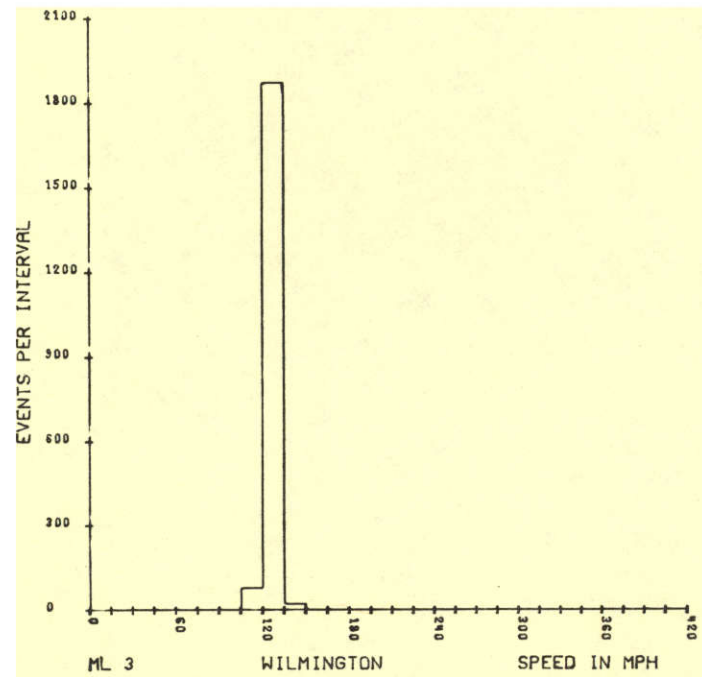
Report	Customer Tapes	Report	Customer Tapes
ML 1W	20	TL 1	5020
1E	21	2	5040
2W	40	3	5060
2E	41	4	5080
3	60	5	5100
4W	80	6	5120
4E	81		
5	100		
6	120		
7	140		
8	160		
9	180		
10	200		
11W	220		
11E	221		
12W	240		
12E	241		

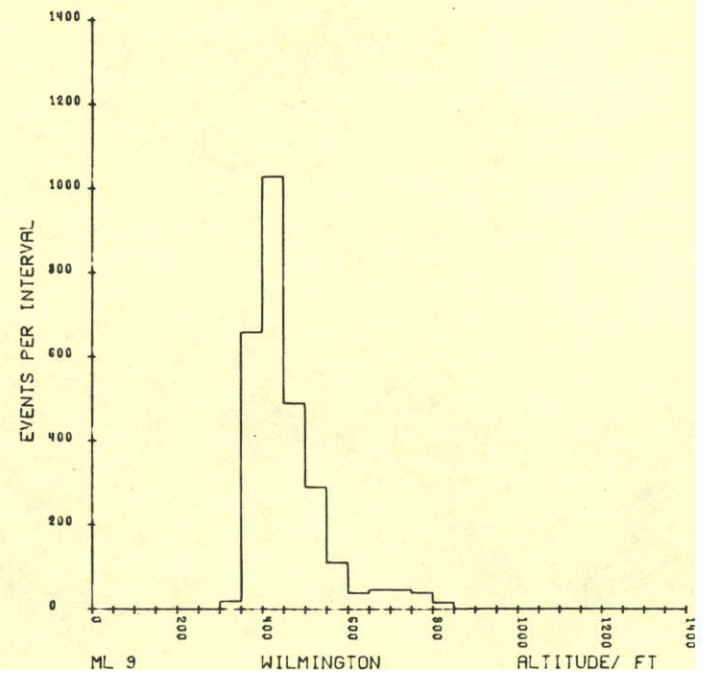
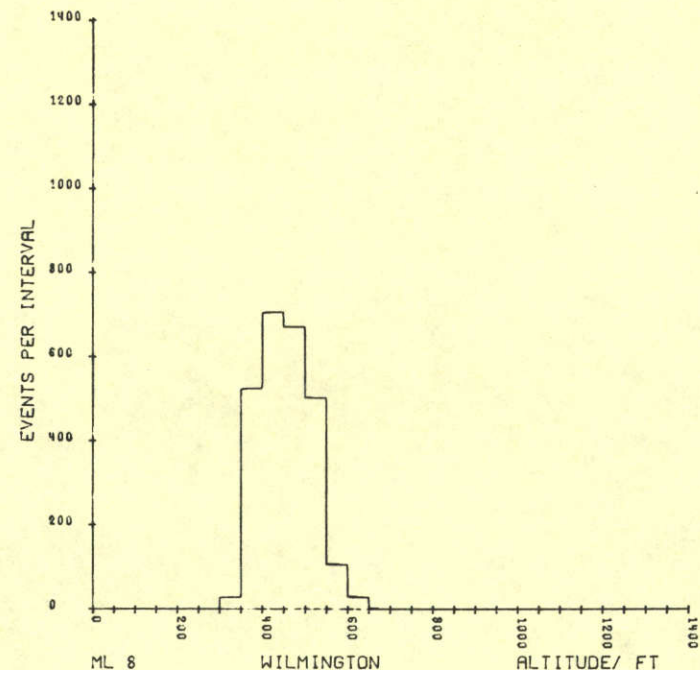
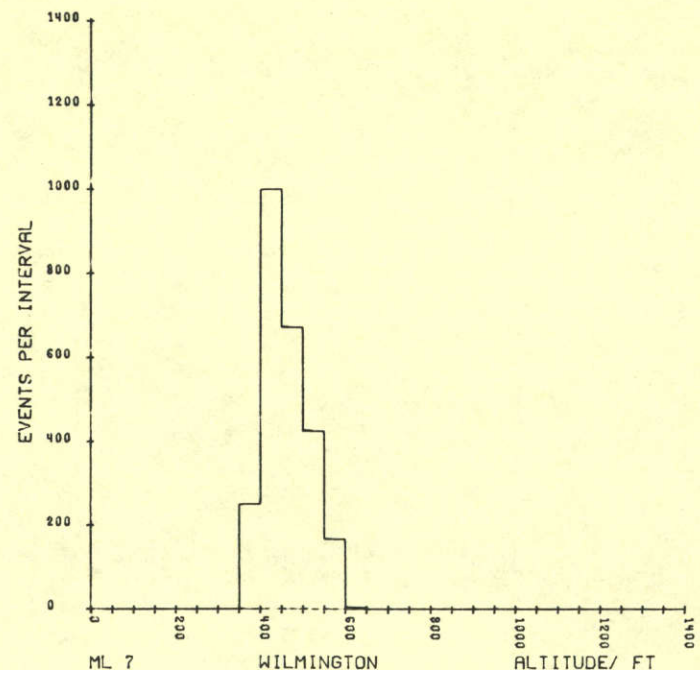
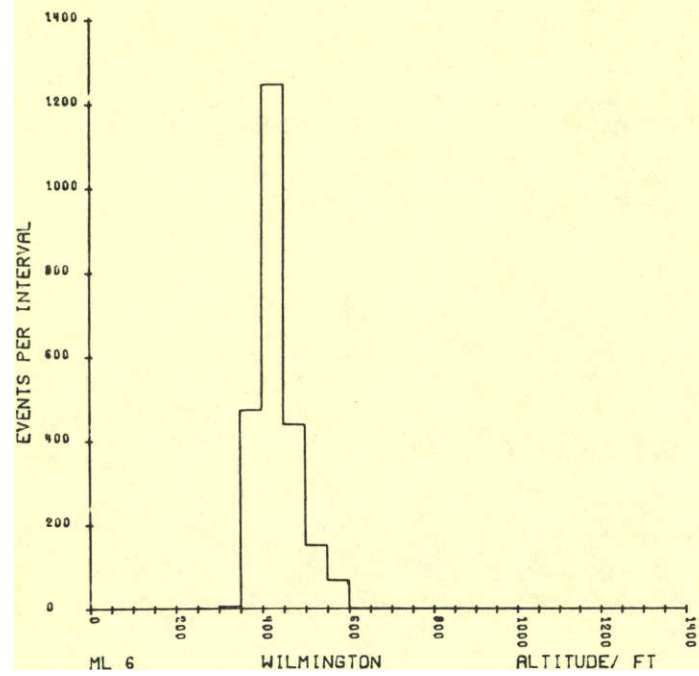
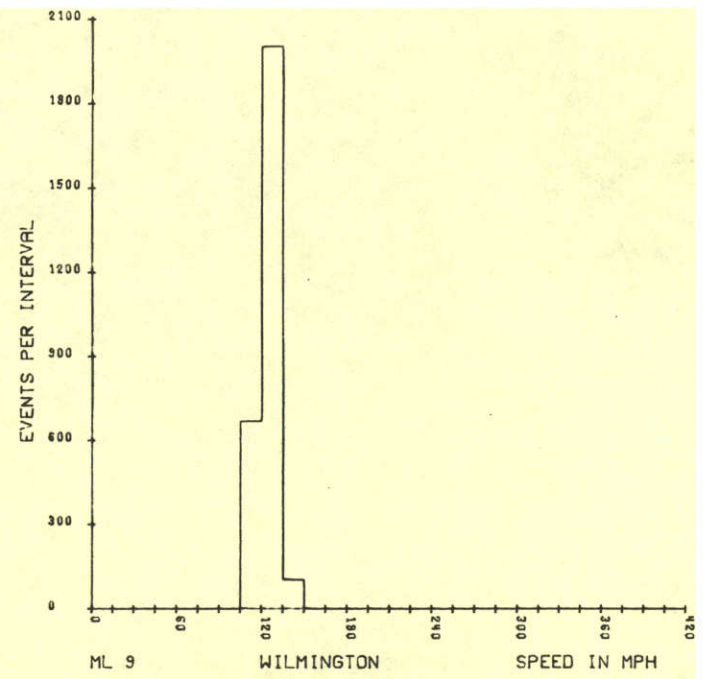
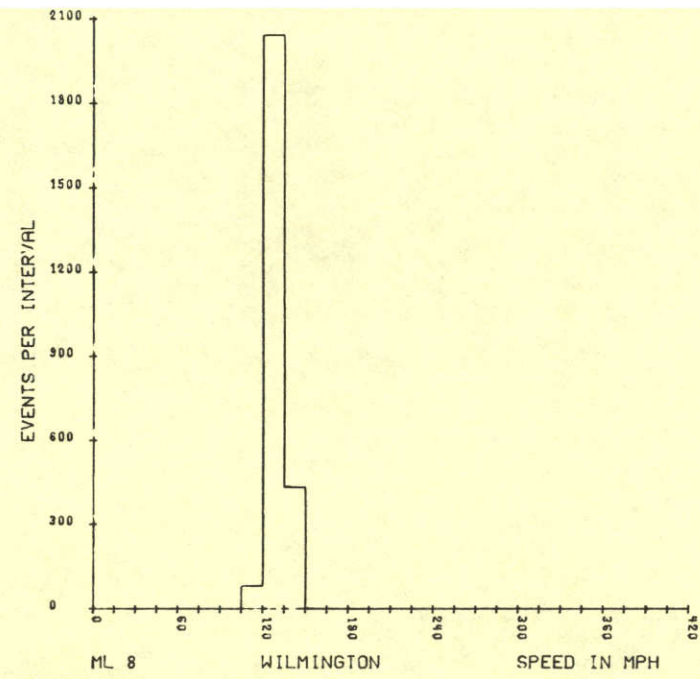
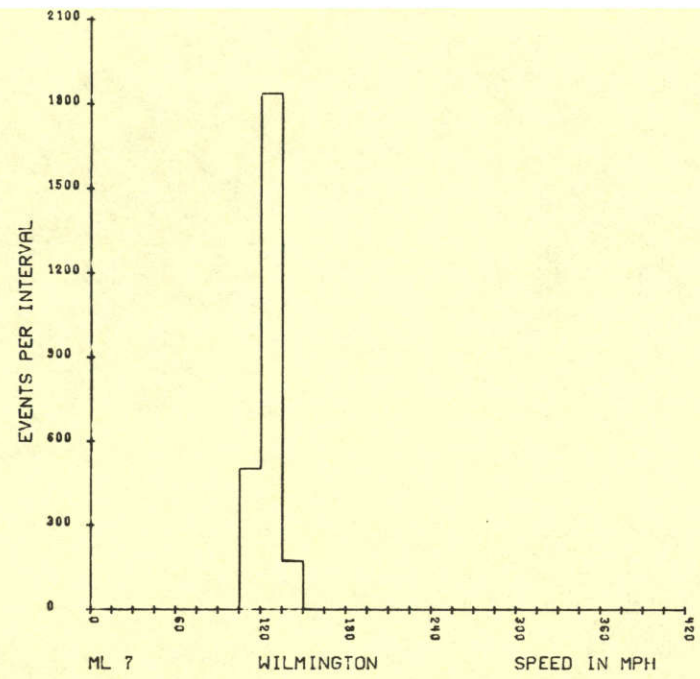
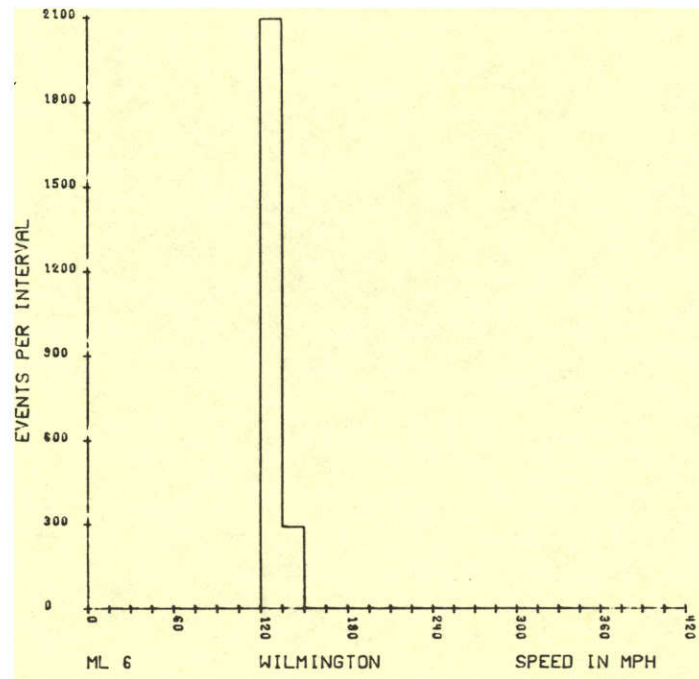
Due to the existence of several restricted areas within the Wilmington survey area, the survey aircraft had to deviate from their proposed flight paths for ML 12E (R5001), ML 10 (Philadelphia International TCA) and TL 5 (Dove Air Force Base). Also, survey over the center of ML 11 (23.5 miles) and ML 12 (23.5 miles) was prohibited due to the presence of the Philadelphia International Airport Terminal Control Area.

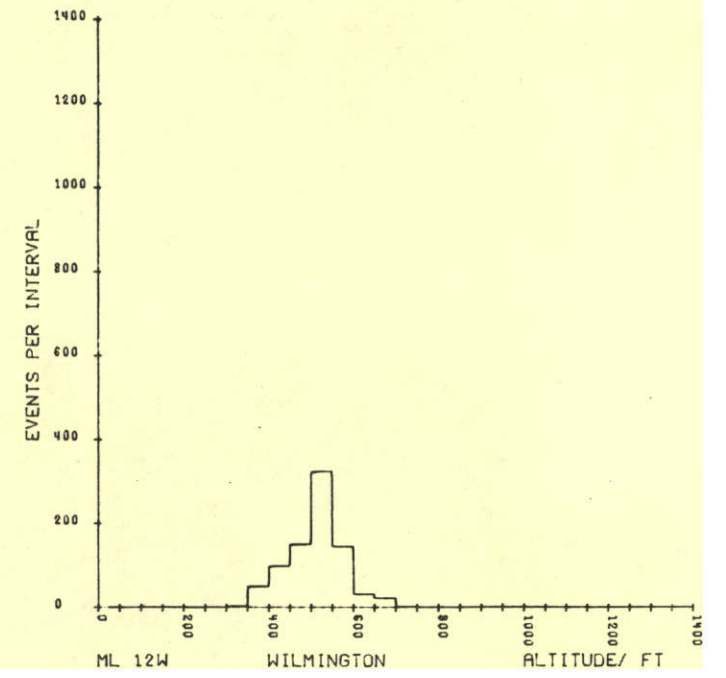
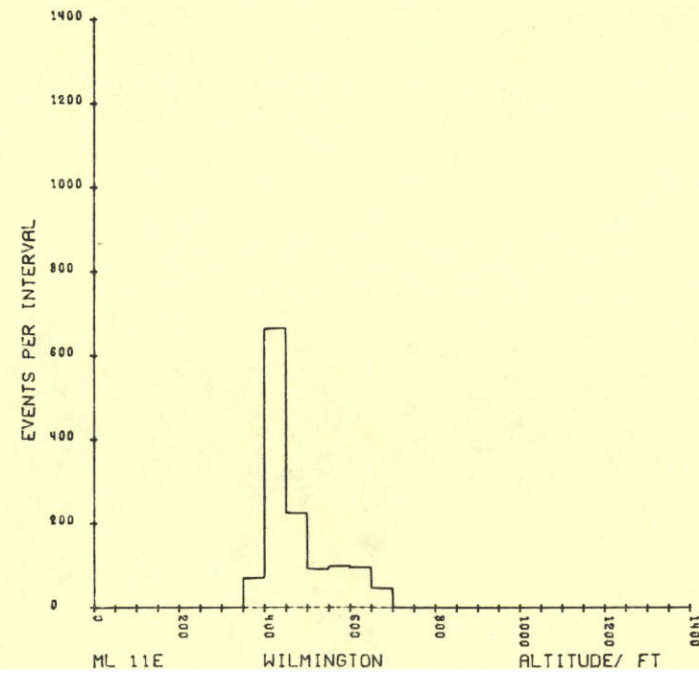
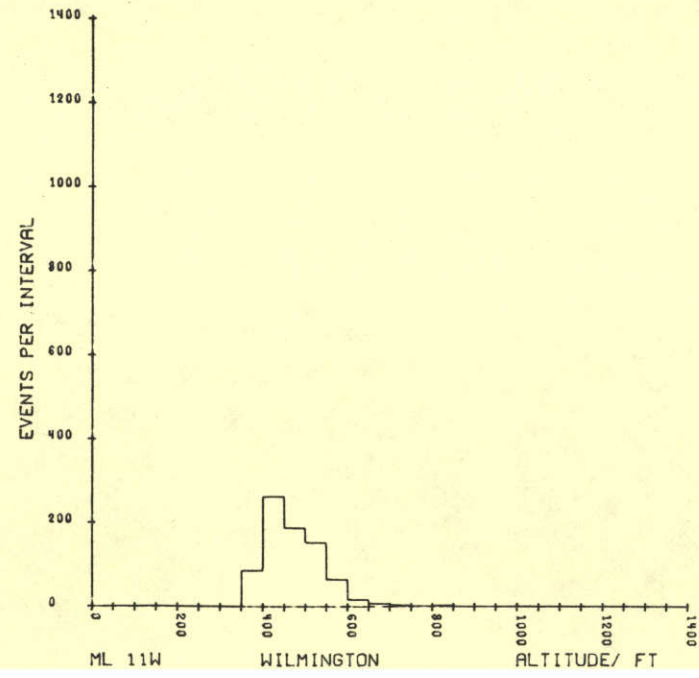
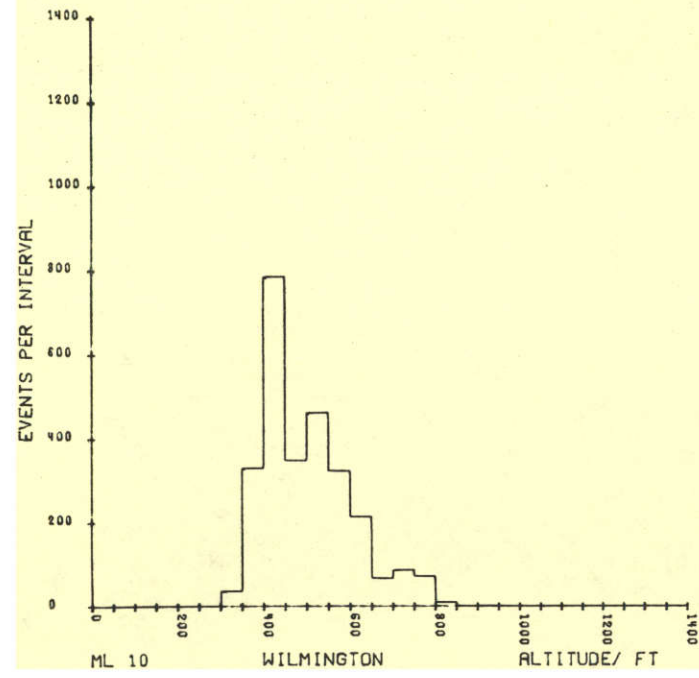
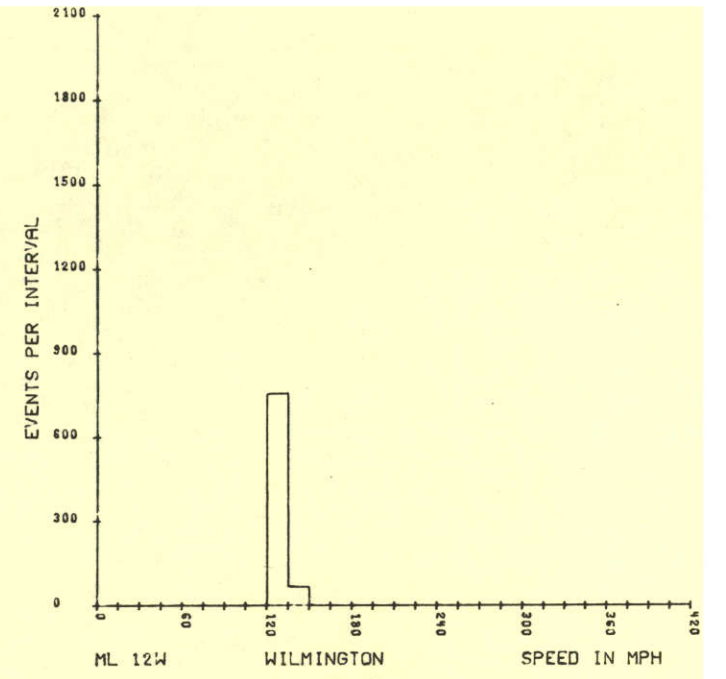
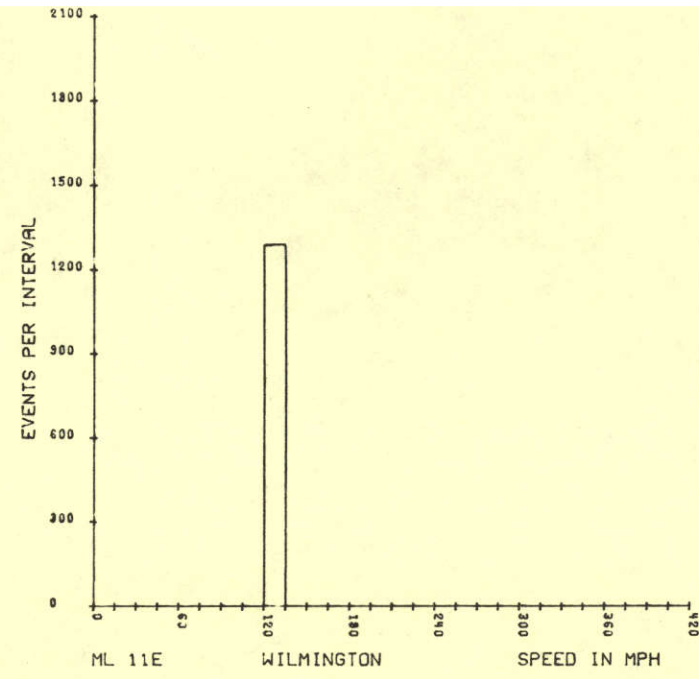
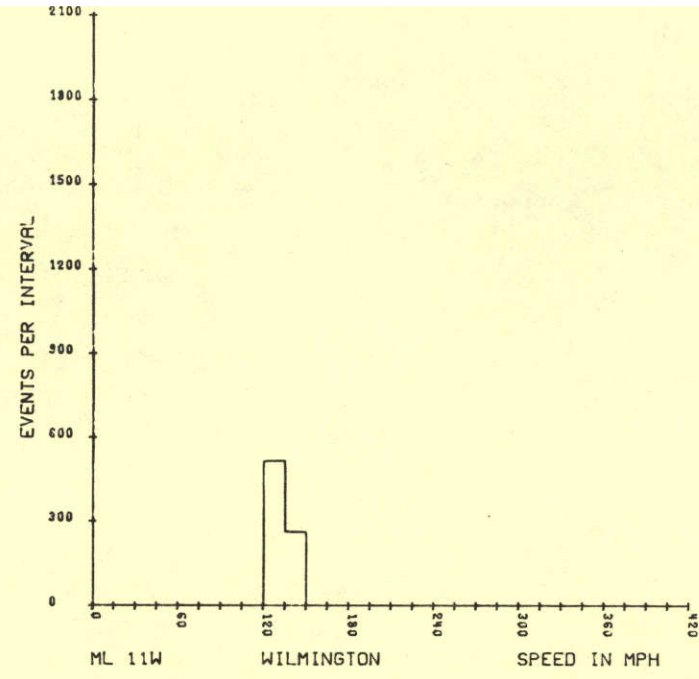
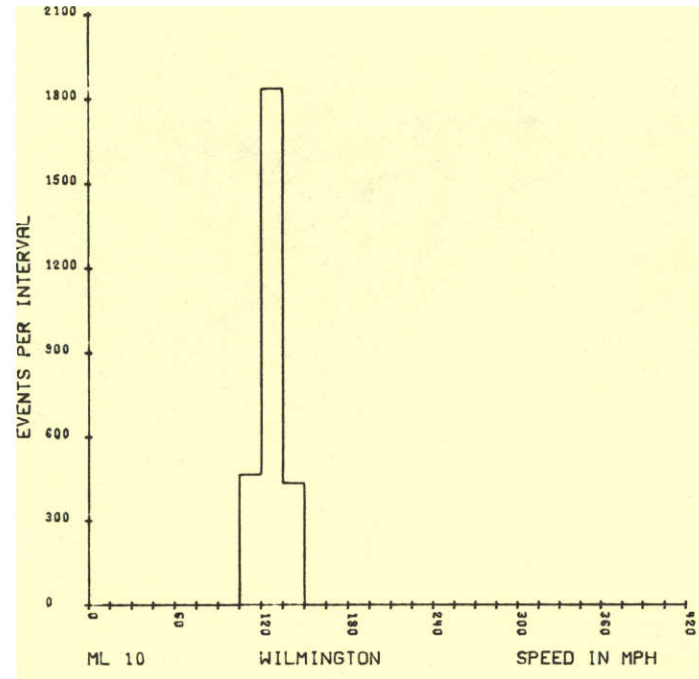
AI.E AVERAGE SPEED AND ALTITUDE DATA SUMMARY

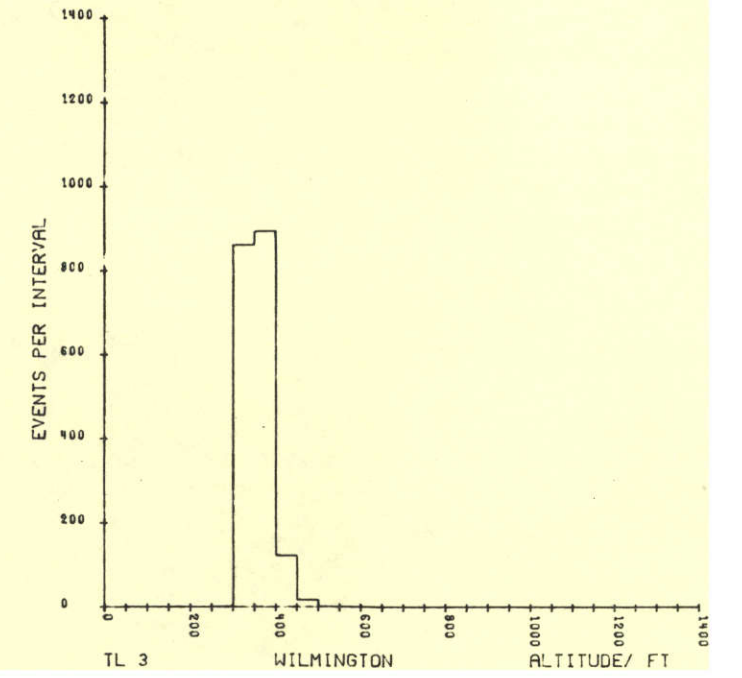
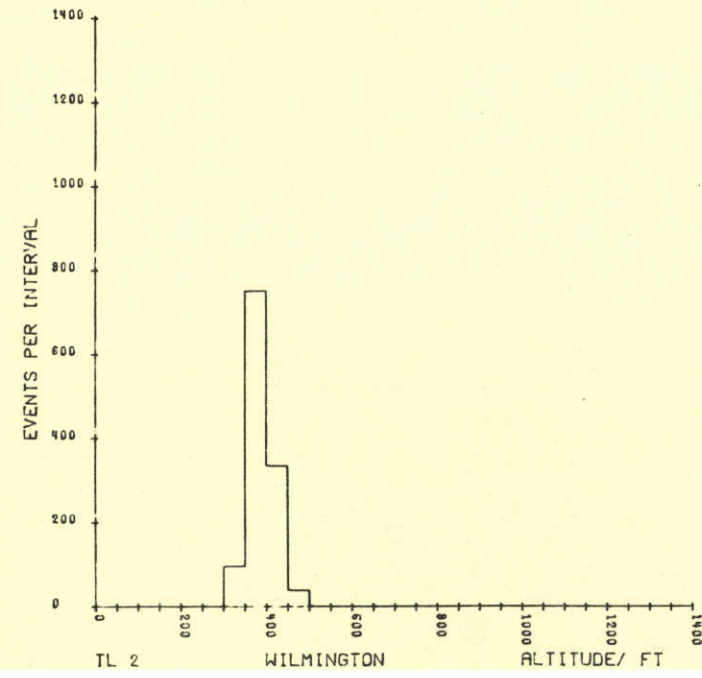
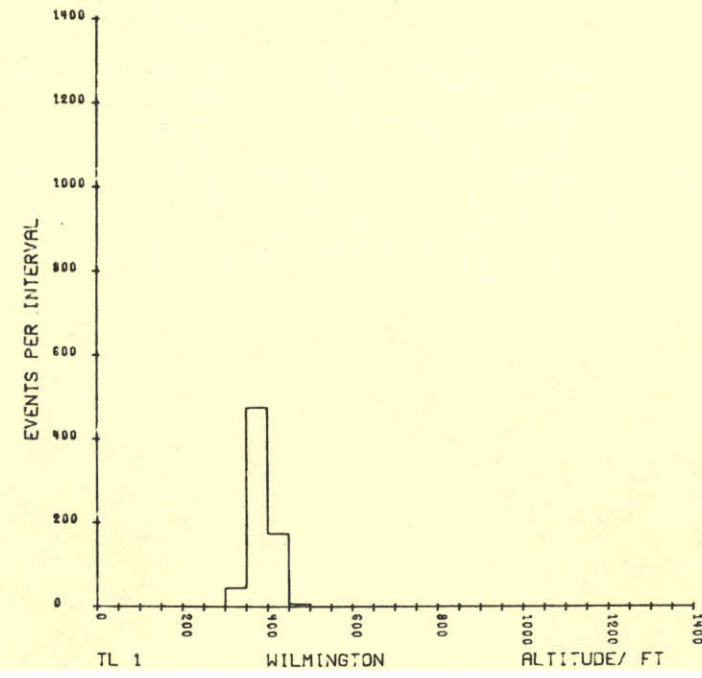
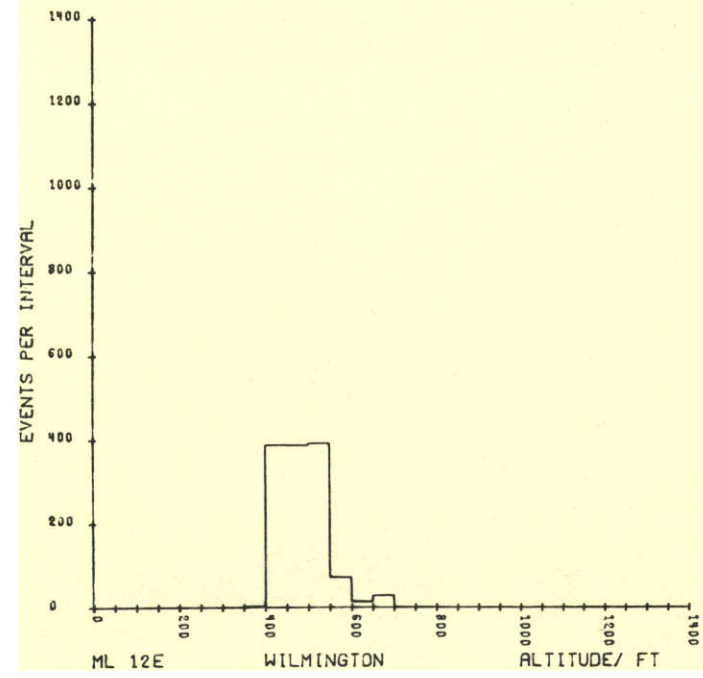
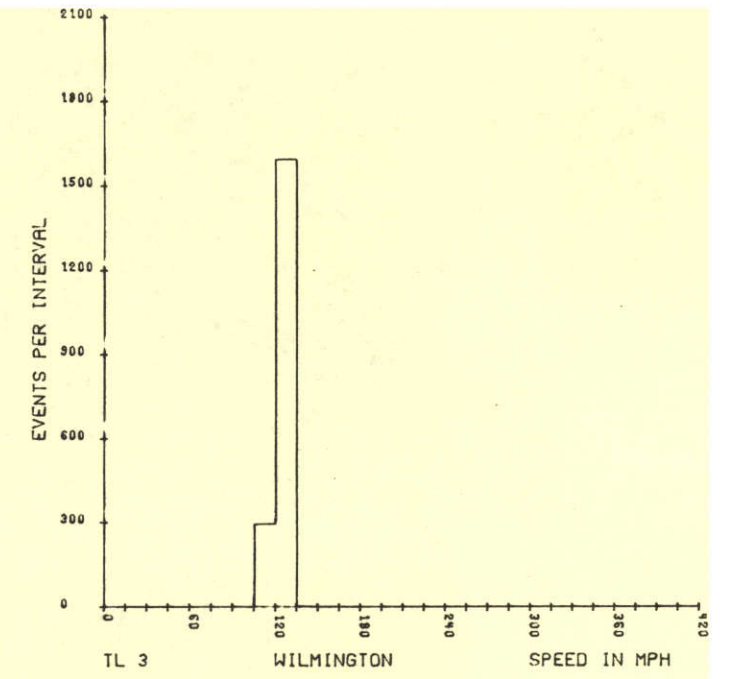
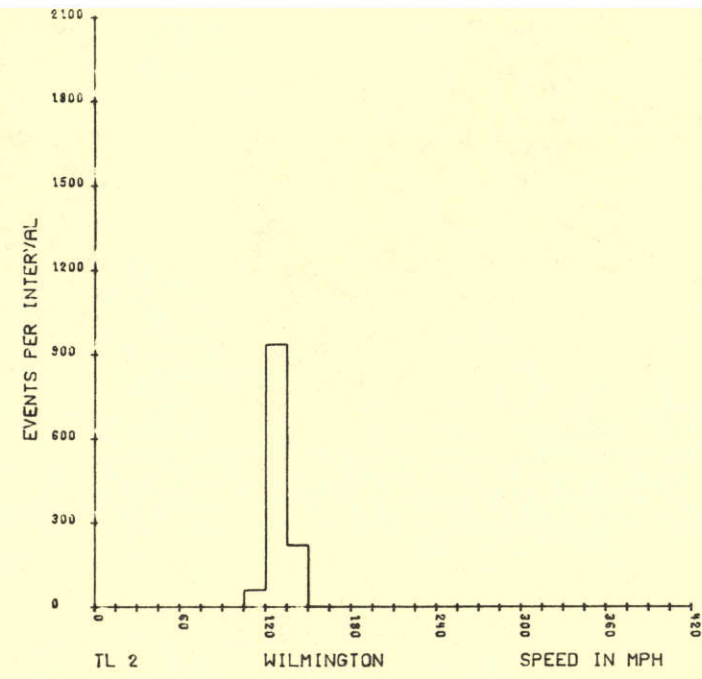
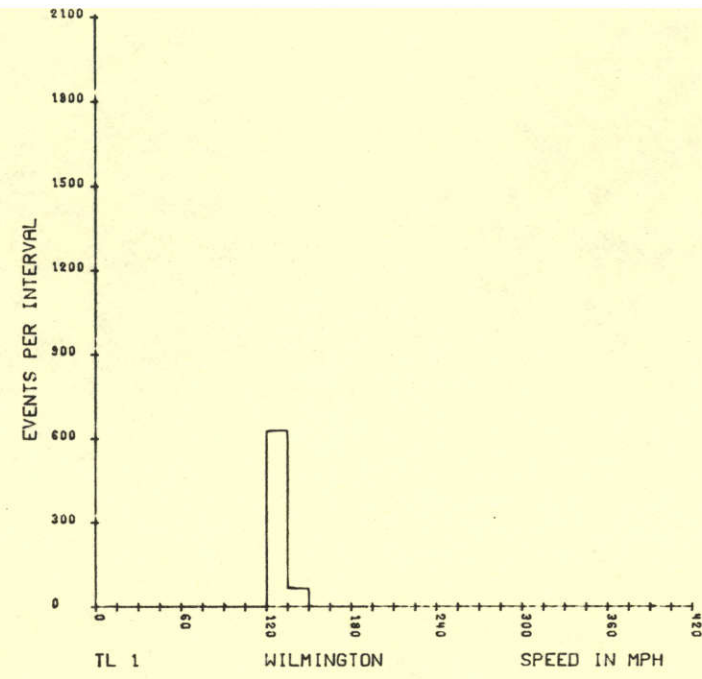
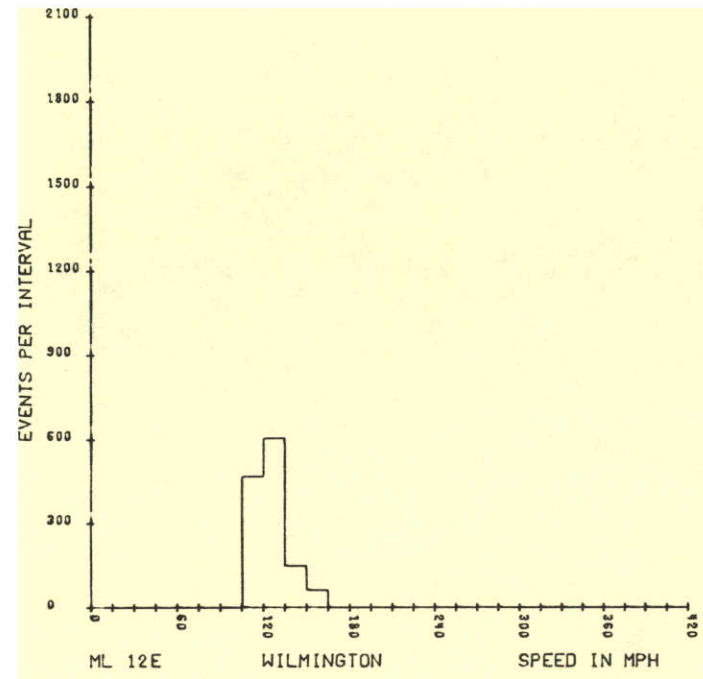
LINE	AVERAGE SPEED, MPH	AVERAGE ALTITUDE, FT
ML 1F	146	447
ML 1W	132	422
ML 2E	132	434
ML 2W	135	435
ML 3	135	428
ML 4E	136	453
ML 4W	135	456
ML 5	134	457
ML 6	137	460
ML 7	133	485
ML 8	137	480
ML 9	132	482
ML 10	135	526
ML 11E	135	499
ML 11W	140	498
ML 12E	133	512
ML 12W	136	536
TL 1	136	410
TL 2	137	413
TL 3	133	381
TL 4	132	373
TL 5	135	403
TL 6	135	385

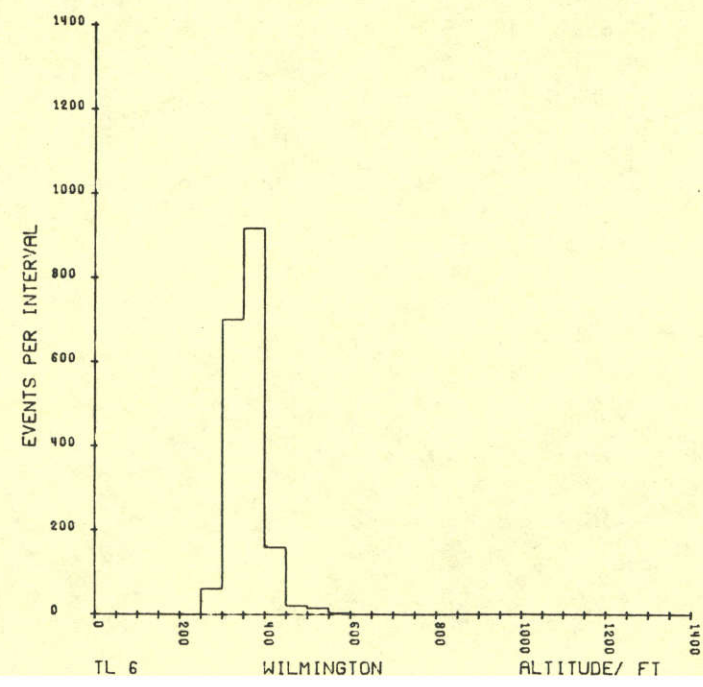
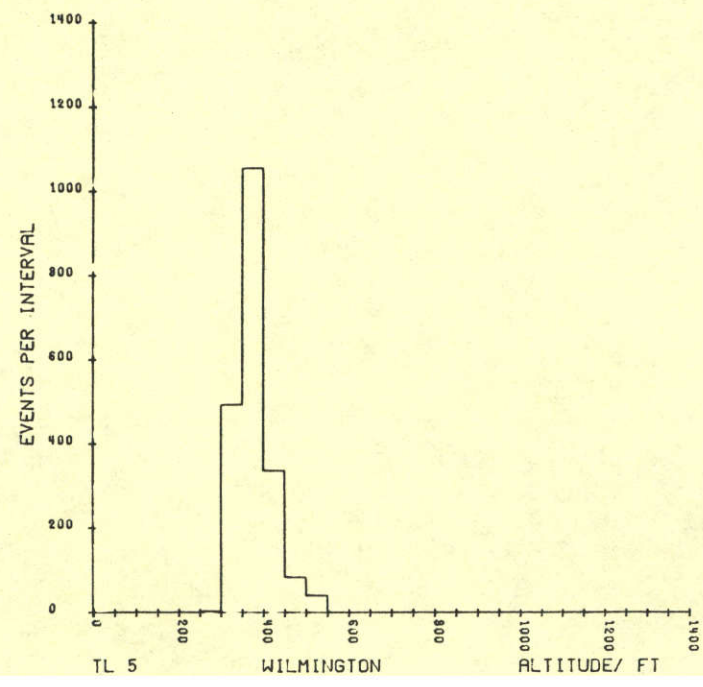
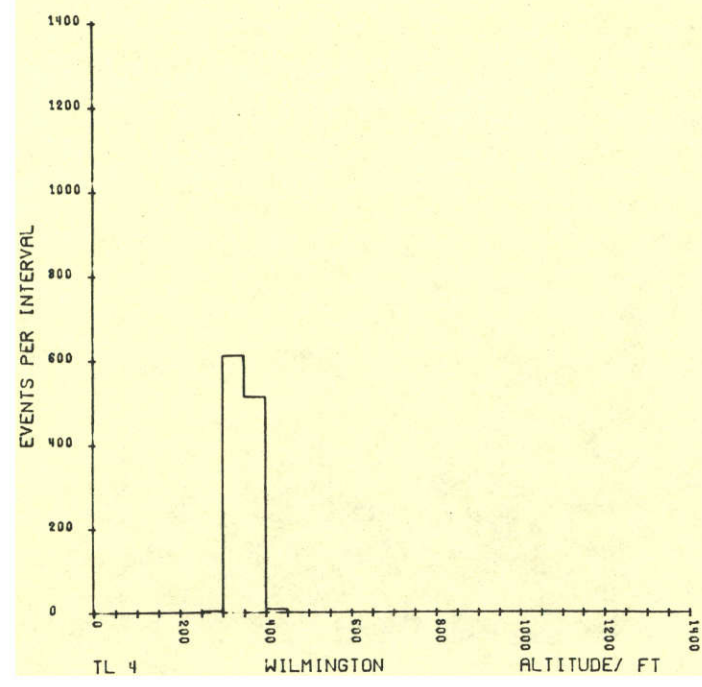
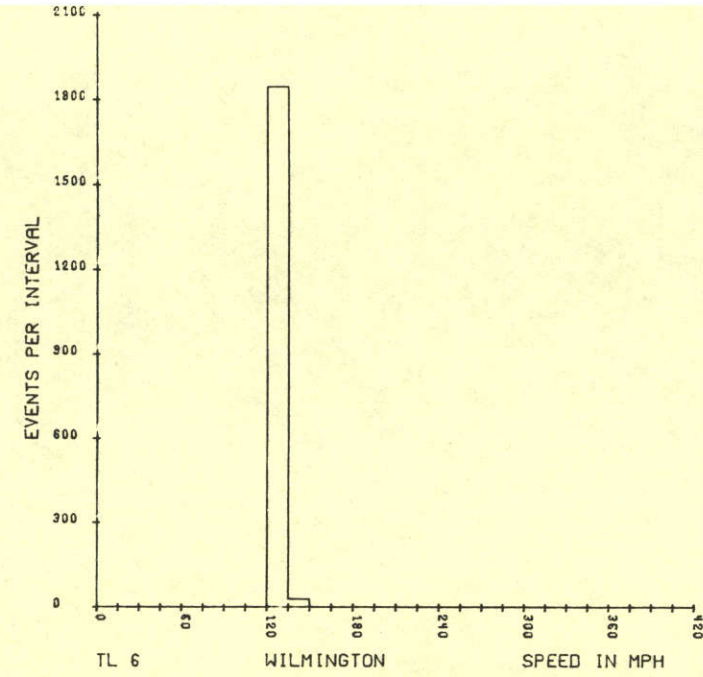
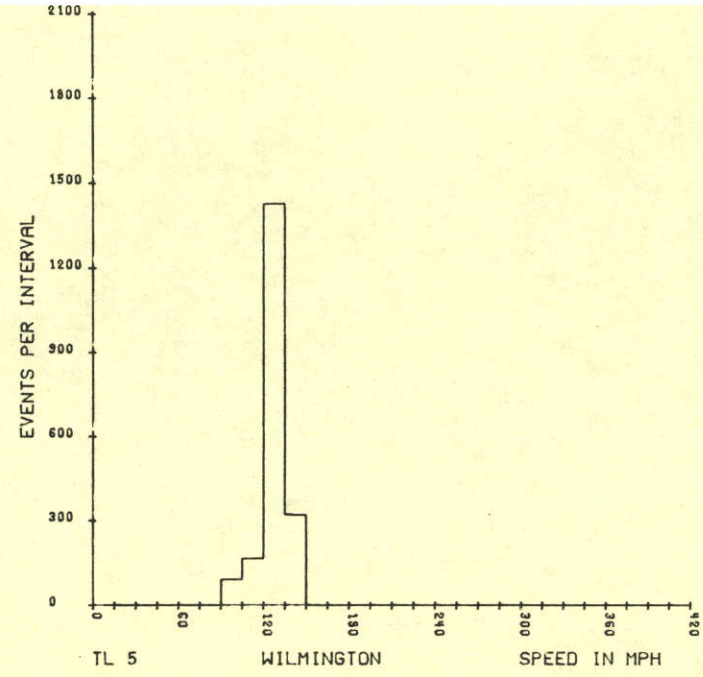
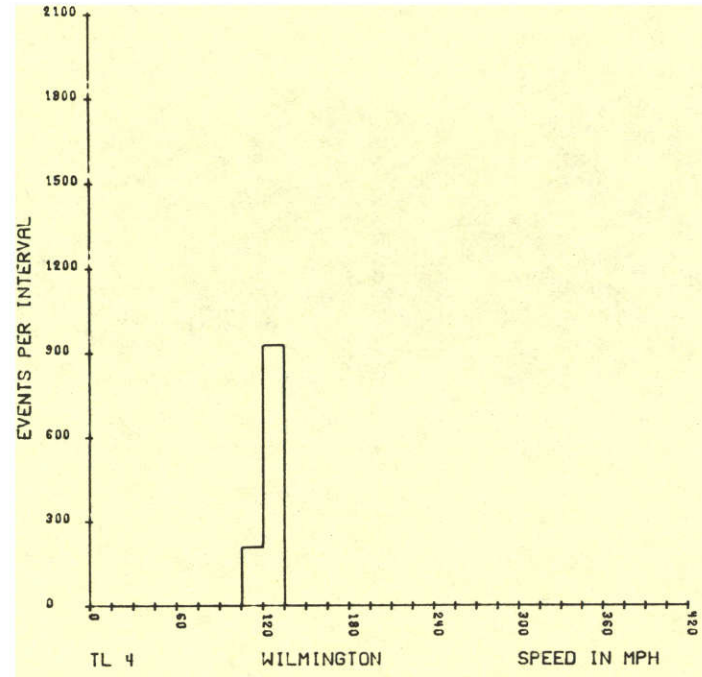












APPENDIX II
TAPE FORMAT STATEMENTS

A. DESCRIPTION OF DATA TAPES

A1. General

All data tapes are 9-track, 800 BPI (NRZI), odd parity, EBCDIC code. Each tape contains a gum label giving the survey project name, month and year of survey, tape type, subcontractor name, date tape created, tape reel count, tape recording characteristics, block size in Bytes and location of tape format information.

The general description for each of the tape types is as follows:

Block Number	Description
1	Format Description
2	Tape Identification
3	First Data Block
4	Second Data Block
.	.
.	.
.	.
EOF	Last Data Block

A2. Raw Spectral Data Tapes

Block Size (Physical Record): 6600 characters
Logical Record, Data : 1100 characters

1. Format Description Block (Block 1)

The Format Description utilizes 4248 characters. The remaining 2352 characters of this block are blanks.

Line Number	Character Number
12345678901234567890123456789012345678901234567890123456789012	12345678901234567890123456789012345678901234567890123456789012
1	01 0978 (DATA TAPE TYPE AND FORMAT SPECIFICATION DATE CODES)
2	
3	RAW SPECTRAL DATA TAPE
4	
5	FORMAT FOR TAPE IDENTIFICATION BLOCK (SECOND BLOCK ON TAPE)
6	
7	ITEM FORMAT DESCRIPTION
8	1 A40 QUADRANGLE NAME AS PROJECT IDENTIFICATION
9	2 A20 NAME OF SUBCONTRACTOR
10	3 I4 APPROXIMATE DATE OF SURVEY (MONTH, YEAR)

Line Number	Character Number
12345678901234567890123456789012345678901234567890123456789012	12345678901234567890123456789012345678901234567890123456789012
11	4 I1 AERIAL SYSTEM IDENTIFICATION CODE
12	5 A20 AIRCRAFT IDENTIFICATION BY TYPE AND FAA NUMBER
13	6 I3 BFEC CALIBRATION REPORT NUMBER
14	7 F6.3 4PI SYSTEM DATA COLLECTION INTERVAL TO THREE DECIMAL PLACES IN SECONDS
15	
16	8 F6.3 2PI SYSTEM DATA COLLECTION INTERVAL TO THREE DECIMAL PLACES IN SECONDS
17	
18	9 I3 NUMBER OF CHANNELS (0-3 MEV) FOR 4PI SYSTEM
19	10 I3 NUMBER OF CHANNELS (0-3 MEV) FOR 2PI SYSTEM
20	11 I3 NUMBER OF FLIGHT LINES ON THIS TAPE
21	12 I4 FIRST FLIGHT LINE NUMBER ON THIS TAPE
22	13 I6 FIRST RECORD NUMBER OF FIRST FLIGHT LINE
23	14 I3 JULIAN DATE (DAY OF YEAR) FIRST FLIGHT LINE WAS COLLECTED
24	
25	15-17 I4,I6,I3 REPEAT OF ITEMS 12-14 FOR SECOND FLIGHT LINE ON THIS TAPE
26	
27	* * *
28	* * *
29	* * *
30	306-308 I4,I6,I3 REPEAT OF ITEMS 12-14 FOR 99TH FLIGHT LINE ON THIS TAPE
31	
32	
33	FORMAT FOR RAW SPECTRAL DATA RECORD (THIRD THRU LAST BLOCK ON TAPE)
34	
35	ITEM FORMAT DESCRIPTION
36	1 I1 AERIAL SYSTEM IDENTIFICATION CODE
37	2 I4 FLIGHT LINE NUMBER
38	3 I6 RECORD IDENTIFICATION NUMBER
39	4 I6 GMT TIME OF DAY (HHMMSS)
40	5 F8.4 LATITUDE TO FOUR DECIMAL PLACES IN DEGREES
41	6 F8.4 LONGITUDE TO FOUR DECIMAL PLACES IN DEGREES
42	7 F6.1 TERRAIN CLEARANCE TO ONE DECIMAL PLACE IN METERS
43	8 F7.1 TOTAL MAGNETIC FIELD INTENSITY TO ONE DECIMAL PLACE IN GAMMAS
44	
45	9 A8 SURFACE GEOLOGIC MAP UNIT CODE
46	10 I4 QUALITY FLAG CODES
47	11 F4.1 OUTSIDE AIR TEMPERATURE TO ONE DECIMAL PLACE IN DEGREES CELSIUS
48	
49	12 F5.1 OUTSIDE AIR PRESSURE TO ONE DECIMAL PLACE IN MMHG
50	13 F5.3 LIVE TIME COUNTING PERIOD TO THREE DECIMAL PLACES IN SECONDS
51	
52	14 I4 SUMMED RAW OUTPUT FROM COSMIC CHANNELS (3-6 MEV) IN COUNTS
53	
54	15 I4 RAW OUTPUT FROM CHANNEL 1 IN COUNTS
55	16 I4 RAW OUTPUT FROM CHANNEL 2 IN COUNTS
56	* * *
57	* * *
58	* * *
59	270 I4 RAW OUTPUT FROM CHANNEL 256 IN COUNTS
-	- - 2352 BLANK CHARACTERS

2. Tape Identification Block (Block 2)

The information and format for this block are indicated in lines 8 through 30 of the Format Description Block A2.1, and 1396 characters are produced. The remaining 5204 characters in this block are blanks.

If fewer than 99 flight lines exist, the unused flight line information, 13 characters per flight line, is filled with 9's through the 99th flight line.

3. Raw Spectral Data Blocks

The information and format for the logical records in these blocks are indicated in lines 36 through 59 of the Format Description Block A2.1. One logical record contains 1100 characters. There are six such logical records per 6600 character physical record or block.

The 2 π data logical record is recorded after the corresponding 4 π data collection intervals at a frequency dependent on the 2 π system data collection interval. For example, if the 4 π data collection interval is 1 second and the 2 π data collection interval is 10 seconds, then 10 records of 4 π data are recorded followed by 1 record of the 2 π data which was collected during the preceding 10 seconds. The format for the 2 π data is identical to that of the 4 π data, except for lines 40 through 49 of the Format Description Block given above. These variables are expressed in the 2 π record as all nines in the format specified for I and F fields, and all zeros for A fields.

A3. Single Record Reduced Data Tapes

Block Size (Physical Record): 6900 characters
Logical Record, Data : 138 characters

1. Format Description Block (Block 1)

The Format Description utilizes 6768 characters. The remaining 132 characters of this block are blanks.

Line Number	Character Number
1	02 0978 (DATA TAPE TYPE AND FORMAT SPECIFICATION DATE CODES)
2	
3	SINGLE RECORD REDUCED DATA TAPE
4	
5	FORMAT FOR TAPE IDENTIFICATION BLOCK (SECOND BLOCK)
6	

Line Number	Character Number
7	ITEM FORMAT DESCRIPTION
8	1 A40 QUADRANGLE NAME AS PROJECT IDENTIFICATION
9	2 A20 NAME OF SUBCONTRACTOR
10	3 I4 APPROXIMATE DATE OF SURVEY (MONTH, YEAR)
11	4 I1 NUMBER OF AERIAL SYSTEMS USED TO COLLECT DATA FOR THIS QUADRANGLE
12	
13	5 I1 AERIAL SYSTEM IDENTIFICATION CODE FOR FIRST SYSTEM
14	6 A20 AIRCRAFT IDENTIFICATION BY TYPE AND FAA NUMBER FOR FIRST SYSTEM
15	
16	7 F6.1 NOMINAL ALTITUDE SYSTEM SENSITIVITY RELATIVE TO TERRESTRIAL POTASSIUM (K-40) TO ONE DECIMAL PLACE IN CPS PER PERCENT K FOR FIRST SYSTEM
17	
18	8 F6.1 NOMINAL ALTITUDE SYSTEM SENSITIVITY RELATIVE TO TERRESTRIAL URANIUM (BI-214) TO ONE DECIMAL PLACE IN CPS PER PPM EQUIVALENT U
19	
20	9 F6.1 NOMINAL ALTITUDE SYSTEM SENSITIVITY RELATIVE TO TERRESTRIAL THORIUM (TL-208) TO ONE DECIMAL PLACE IN CPS PER PPM EQUIVALENT TH
21	
22	10 I6 BLANK FIELD (999999)
23	11 F6.3 4PI-SYSTEM DATA COLLECTION INTERVAL TO THREE DECIMAL PLACES IN SECONDS FOR FIRST SYSTEM
24	
25	12 F6.3 2PI-SYSTEM DATA COLLECTION INTERVAL TO THREE DECIMAL PLACES IN SECONDS FOR FIRST SYSTEM
26	
27	13 I3 NUMBER OF CHANNELS (0-3 MEV) IN 4PI SYSTEM FOR FIRST AERIAL SYSTEM
28	
29	14 I3 NUMBER OF CHANNELS (0-3 MEV) IN 2PI SYSTEM FOR FIRST AERIAL SYSTEM
30	
31	15-24 (SAME) REPEAT OF ITEMS 5-14 FOR SECOND AERIAL SYSTEM
32	* * * * *
33	
34	85-94 (SAME) REPEAT OF ITEMS 5-14 FOR NINTH AERIAL SYSTEM
35	
36	95 I3 NUMBER OF FLIGHT LINES ON THIS TAPE
37	
38	96 I4 FIRST FLIGHT LINE NUMBER ON THIS TAPE
39	
40	97 I6 FIRST RECORD NUMBER OF FIRST FLIGHT LINE
41	
42	98 I3 JULIAN DATE (DAY OF YEAR) FIRST FLIGHT-LINE DATA WAS COLLECTED
43	
44	99-101 I4,I6,I3 REPEAT OF ITEMS 96-98 FOR SECOND FLIGHT LINE ON THIS TAPE
45	* * * * *
46	
47	
48	
49	390-392 I4,I6,I3 REPEAT OF ITEMS 96-98 FOR 99TH FLIGHT LINE ON THIS TAPE
50	
51	
52	FORMAT FOR SINGLE RECORD REDUCED DATA RECORD (THIRD THRU LAST BLOCK)
53	
54	ITEM FORMAT DESCRIPTION
55	1 I1 AERIAL SYSTEM IDENTIFICATION CODE
56	2 I4 FLIGHT LINE NUMBER
57	3 I6 RECORD IDENTIFICATION NUMBER
58	4 I6 GMT TIME OF DAY (HHMMSS)
59	5 F8.4 LATITUDE TO FOUR DECIMAL PLACES IN DEGREES

Line Number	Character Number
60	6 F8.4 LONGITUDE TO FOUR DECIMAL PLACES IN DEGREES
61	7 F6.1 TERRAIN CLEARANCE TO ONE DECIMAL PLACE IN METERS
62	8 F7.1 RESIDUAL (IGRF REMOVED) MAGNETIC FIELD INTENSITY TO ONE DECIMAL PLACE IN GAMMAS
63	
64	9 A8 SURFACE GEOLOGIC MAP UNIT CODE
65	10 I4 QUALITY FLAG CODES
66	11 F6.1 APPARENT CONCENTRATION OF TERRESTRIAL POTASSIUM (K-40) TO ONE DECIMAL PLACE IN PERCENT K
67	
68	12 F4.1 UNCERTAINTY IN TERRESTRIAL POTASSIUM TO ONE DECIMAL PLACE IN PERCENT K
69	
70	13 F6.1 APPARENT CONCENTRATION OF TERRESTRIAL URANIUM (BI-214) TO ONE DECIMAL PLACE IN PPM EQUIVALENT U
71	
72	14 F4.1 UNCERTAINTY IN TERRESTRIAL URANIUM TO ONE DECIMAL PLACE IN PPM EQUIVALENT U
73	
74	15 F6.1 APPARENT CONCENTRATION OF TERRESTRIAL THORIUM (TL-208) TO ONE DECIMAL PLACE IN PPM EQUIVALENT TH
75	
76	16 F4.1 UNCERTAINTY IN TERRESTRIAL THORIUM TO ONE DECIMAL PLACE IN PPM EQUIVALENT TH
77	
78	17 F6.1 URANIUM-TO-THORIUM RATIO TO ONE DECIMAL PLACE IN PPM EQUIVALENT U PER PPM EQUIVALENT TH
79	
80	18 F6.1 URANIUM-TO-POTASSIUM RATIO TO ONE DECIMAL PLACE IN PPM EQUIVALENT U PER PERCENT K
81	
82	19 F6.1 THORIUM-TO-POTASSIUM RATIO TO ONE DECIMAL PLACE IN PPM EQUIVALENT TH PER PERCENT K
83	
84	20 F8.1 GROSS GAMMA (0.4-3.0 MEV) COUNT RATE TO ONE DECIMAL PLACE IN COUNTS PER SECOND
85	
86	21 F6.1 UNCERTAINTY IN GROSS GAMMA COUNT RATE TO ONE DECIMAL PLACE IN COUNTS PER SECOND
87	
88	22 F5.1 ATMOSPHERIC BI-214 4PI CORRECTION TO ONE DECIMAL PLACE IN PPM EQUIVALENT U
89	
90	23 F4.1 UNCERTAINTY IN ATMOSPHERIC BI-214 4PI CORRECTION TO ONE DECIMAL PLACE IN PPM EQUIVALENT U
91	
92	24 F4.1 OUTSIDE AIR TEMPERATURE TO ONE DECIMAL PLACE IN DEGREES CELSIUS
93	
94	25 F5.1 OUTSIDE AIR PRESSURE TO ONE DECIMAL PLACE IN MMHG

2. Tape Identification Block (Block 2)

The information and format for this block are indicated in lines 8 through 49 of the Format Description Block A3.1, and 1922 characters are produced. The remaining 4978 characters of this block are blanks.

If less than nine aerial systems are used, the space allocated for additional systems is filled with 9's in the format specified for each item using I and F fields, and with zeros for A fields.

Similarly, if fewer than 99 flight lines exist, the unused flight line information, 13 characters per flight line, is filled with 9's through the 99th flight line.

File 2: Statistical Analysis Summary

Block Size (Physical Record): 7000 characters
 Logical Record (Data) : 140 characters

1. Format Description Block (Block 1)

The Format Description utilizes 4320 characters. The remaining 2680 characters are blanks.

Line Number	Character Number	12345678901234567890123456789012345678901234567890123456789012
1	05	0978 (DATA TAPE TYPE AND FORMAT SPECIFICATION DATE CODE)
2		
3		STATISTICAL ANALYSIS SUMMARY TAPE (OR FILE)
4		
5		FORMAT FOR TAPE IDENTIFICATION BLOCK (SECOND BLOCK)
6		
7	ITEM	FORMAT DESCRIPTION
8	1	A40 QUADRANGLE NAME AS PROJECT IDENTIFICATION
9	2	A20 NAME OF SUBCONTRACTOR
10	3	I4 APPROXIMATE DATE OF SURVEY (MONTH, YEAR)
11	4	I6 NUMBER OF GEOLOGIC MAP UNITS USED FOR THIS QUADRANGLE
12		
13		
14		FORMAT FOR STATISTICAL ANALYSIS SUMMARY DATA RECORD (THIRD THRU LAST BLOCK)
15		
16		
17	ITEM	FORMAT DESCRIPTION
18	1	A8 SURFACE GEOLOGIC MAP UNIT IDENTIFYING CODE
19	2	I6 TOTAL RECORDS FOR GEOLOGIC MAP UNIT
20	3	I6 NUMBER OF POTASSIUM RECORDS COMPUTED FOR GEOLOGIC UNIT
21		
22	4	F6.1 POTASSIUM CONCENTRATION MEAN TO ONE DECIMAL PLACE IN PERCENT K
23		
24	5	F6.1 POTASSIUM CONCENTRATION STANDARD DEVIATION TO ONE DECIMAL PLACE IN PERCENT K
25		
26	6	A3 POTASSIUM CONCENTRATION DISTRIBUTION CODE
27	7	I6 NUMBER OF URANIUM RECORDS COMPUTED FOR GEOLOGIC UNIT
28	8	F6.1 URANIUM CONCENTRATION MEAN TO ONE DECIMAL PLACE IN PPM EQUIVALENT U
29		
30	9	F6.1 URANIUM CONCENTRATION STANDARD DEVIATION TO ONE DECIMAL PLACE IN PPM EQUIVALENT U
31		
32	10	A3 URANIUM CONCENTRATION DISTRIBUTION CODE
33	11	I6 NUMBER OF THORIUM RECORDS COMPUTED FOR GEOLOGIC UNIT
34	12	F6.1 THORIUM CONCENTRATION MEAN TO ONE DECIMAL PLACE IN PPM EQUIVALENT TH
35		
36	13	F6.1 THORIUM CONCENTRATION STANDARD DEVIATION TO ONE DECIMAL PLACE IN PPM EQUIVALENT TH
37		

Line Character Number
 Number 12345678901234567890123456789012345678901234567890123456789012

38	14	A3	THORIUM CONCENTRATION DISTRIBUTION CODE
39	15	I6	NUMBER OF URANIUM-TO-THORIUM RATIO RECORDS COMPUTED FOR GEOLOGIC UNIT
40			
41	16	F6.1	URANIUM-TO-THORIUM RATIO MEAN TO ONE DECIMAL PLACE IN PPM EQUIVALENT U PER PPM EQUIVALENT TH
42			
43	17	F6.1	URANIUM-TO-THORIUM RATIO STANDARD DEVIATION TO ONE DECIMAL PLACE IN PPM EQUIVALENT U PER PPM EQUIVALENT TH
44			
45			
46	18	A3	URANIUM-TO-THORIUM RATIO DISTRIBUTION CODE
47	19	I6	NUMBER OF URANIUM-TO-POTASSIUM RATIO RECORDS COMPUTED FOR GEOLOGIC UNIT
48			
49	20	F6.1	URANIUM-TO-POTASSIUM RATIO MEAN TO ONE DECIMAL PLACE IN PPM EQUIVALENT U PER PERCENT K
50			
51	21	F6.1	URANIUM-TO-POTASSIUM RATIO STANDARD DEVIATION TO ONE DECIMAL PLACE IN PPM EQUIVALENT U PER PERCENT K
52			
53	22	A3	URANIUM-TO-POTASSIUM RATIO DISTRIBUTION CODE
54	23	I6	NUMBER OF THORIUM-TO-POTASSIUM RATIO RECORDS COMPUTED FOR GEOLOGIC UNIT
55			
56	24	F6.1	THORIUM-TO-POTASSIUM RATIO MEAN TO ONE DECIMAL PLACE IN PPM EQUIVALENT TH PER PERCENT K
57			
58	25	F6.1	THORIUM-TO-POTASSIUM RATIO STANDARD DEVIATION TO ONE DECIMAL PLACE IN PPM EQUIVALENT TH PER PERCENT K
59			
60	26	A3	THORIUM-TO-POTASSIUM RATIO DISTRIBUTION CODE

2. Tape Identification Block (Block 2)

The information and format for this block are indicated in lines 8 through 11 of the Format Description Block A6.1, and 70 characters are produced. The remaining 6930 characters of this block are blanks.

3. Statistical Analysis Summary Data Blocks

The information and format for the logical records in these blocks are indicated in lines 18 through 60 of the Format Description Block A6.1. One logical record contains 140 characters. There are 50 such logical records per 7000 character physical record or block.

A5. Magnetic Data Tapes

Block Size (Physical Record): 8000 characters
 Logical Record (Data) : 80 characters

1. Format Description Block (Block 1)

The Format Description utilizes 3384 characters. The remaining 4616 characters are blanks.

Line Character Number
 Number 12345678901234567890123456789012345678901234567890123456789012

1	04	0978	(DATA TAPE TYPE AND FORMAT SPECIFICATION DATE CODES)
2			
3			MAGNETIC DATA TAPE
4			
5			FORMAT FOR TAPE IDENTIFICATION BLOCK (SECOND BLOCK)
6			
7	ITEM	FORMAT	DESCRIPTION
8	1	A40	QUADRANGLE NAME AS PROJECT IDENTIFICATION
9	2	A20	NAME OF SUBCONTRACTOR
10	3	I4	APPROXIMATE DATE OF SURVEY (MONTH, YEAR)
11	4	I3	NUMBER OF FLIGHT LINES ON THIS TAPE
12	5	I4	FIRST FLIGHT LINE ON THIS TAPE
13	6	I6	FIRST RECORD NUMBER OF FIRST FLIGHT LINE
14	7	I3	JULIAN DATE (DAY OF YEAR) FIRST FLIGHT LINE DATA WAS COLLECTED
15			
16	8	F8.4	LATITUDE OF GROUND BASE STATION TO FOUR DECIMAL PLACES IN DEGREES FOR FIRST FLIGHT LINE
17			
18	9	F8.4	LONGITUDE OF GROUND BASE STATION TO FOUR DECIMAL PLACES IN DEGREES FOR FIRST FLIGHT LINE
19			
20	10-14	(SAME)	REPEAT OF ITEMS 5-9 FOR SECOND FLIGHT LINE ON THIS TAPE
21			
22	*	*	*
23	*	*	*
24	*	*	*
25	495-499	(SAME)	REPEAT OF ITEMS 5-9 FOR 99TH FLIGHT LINE ON THIS TAPE
26			
27			
28			FORMAT FOR MAGNETIC DATA RECORD (THIRD THRU LAST BLOCK)
29			
30	ITEM	FORMAT	DESCRIPTION
31	1	I1	AERIAL SYSTEM IDENTIFICATION CODE
32	2	I4	FLIGHT LINE NUMBER
33	3	I6	RECORD IDENTIFICATION NUMBER
34	4	I6	GMT TIME OF DAY (HHMMSS)
35	5	F8.4	LATITUDE TO FOUR DECIMAL PLACES IN DEGREES
36	6	F8.4	LONGITUDE TO FOUR DECIMAL PLACES IN DEGREES
37	7	F6.1	TERRAIN CLEARANCE TO ONE DECIMAL PLACE IN METERS
38	8	F5.1	OUTSIDE AIR PRESSURE TO ONE DECIMAL PLACE IN MMHG
39	9	A8	SURFACE GEOLOGIC MAP UNIT CODE
40	10	F7.1	TOTAL MAGNETIC FIELD INTENSITY TO ONE DECIMAL PLACE IN GAMMAS
41			
42	11	F7.1	RESIDUAL (IGRF REMOVED) MAGNETIC FIELD INTENSITY TO ONE DECIMAL PLACE IN GAMMAS
43			
44	12	F7.1	DAILY MAGNETIC INTENSITY VARIATION TO ONE DECIMAL PLACE IN GAMMAS
45			
46	13	F7.1	MAGNETIC DEPTH-TO-BASEMENT TO ONE DECIMAL PLACE IN METERS (IF REQUIRED)
47			

2. Tape Identification Block (Block 2)

The information and format for this block are indicated in lines 8 through 25 of the Format Description Block A5.1, and 2938 characters are produced. The remaining 5062 characters of this block are blanks.

If fewer than 99 flight lines exist, the unused flight line information, 29 characters per flight line, is filled with 9's through the 99th flight line in the format indicated.

3. Magnetic Data Blocks

The information and format for the logical records in these blocks are indicated in lines 31 through 46 of the Format Description Block A5.1. One logical record contains 80 characters. There are 100 such logical records per 8000 character physical record or block.

If the magnetic depth-to-basement is not required, this item is expressed as 99999.9.

B. DESCRIPTION OF LISTINGS

B1. Single record reduced data listings: include the following information on Microfiche:

<u>ITEM</u>	<u>DESCRIPTION</u>
REC	Sequential record number
Lat	Location Y in latitude
Long	Location X in longitude
RMag	Residual magnetic field, gammas
Alt	Surface altitude
GEO UNIT	Geologic Type
AKUT	A=Altitude; K=Potassium; U=Uranium T=Thorium - Results of statistical adequacy test
COS	Cosmic c/s
BiAir	Airborne ²¹⁴ Bi, 4π data
GC	Gross count, .4 MeV - 2.8 MeV
T ₂	²⁰⁸ Tl c/s
Bi	²¹⁴ Bi c/s
K	⁴⁰ K c/s
BI:T ₂	Ratio
BI:k	Ratio
T ₂ :K	Ratio
TEMP	Outside Air Temperature (°C)
BP	Atmospheric Pressure (In. Hg)

B2. Averaged record data listings: include the following information on Microfiche:

<u>ITEM</u>	<u>DESCRIPTION</u>
REC	Sequential Record number
GEO UNIT	Geologic type
AKUT	A=Altitude; K=Potassium; U=Uranium; T=Thorium - Results of statistical adequacy test
Long	Longitude of X location of geologic type
Lat	latitude of Y location of geologic type
RMag	Residual magnetic field, gammas
COS	Cosmic, 4π
BiAir	Atmospheric Bi, 4π
GC	Gross count, c/s

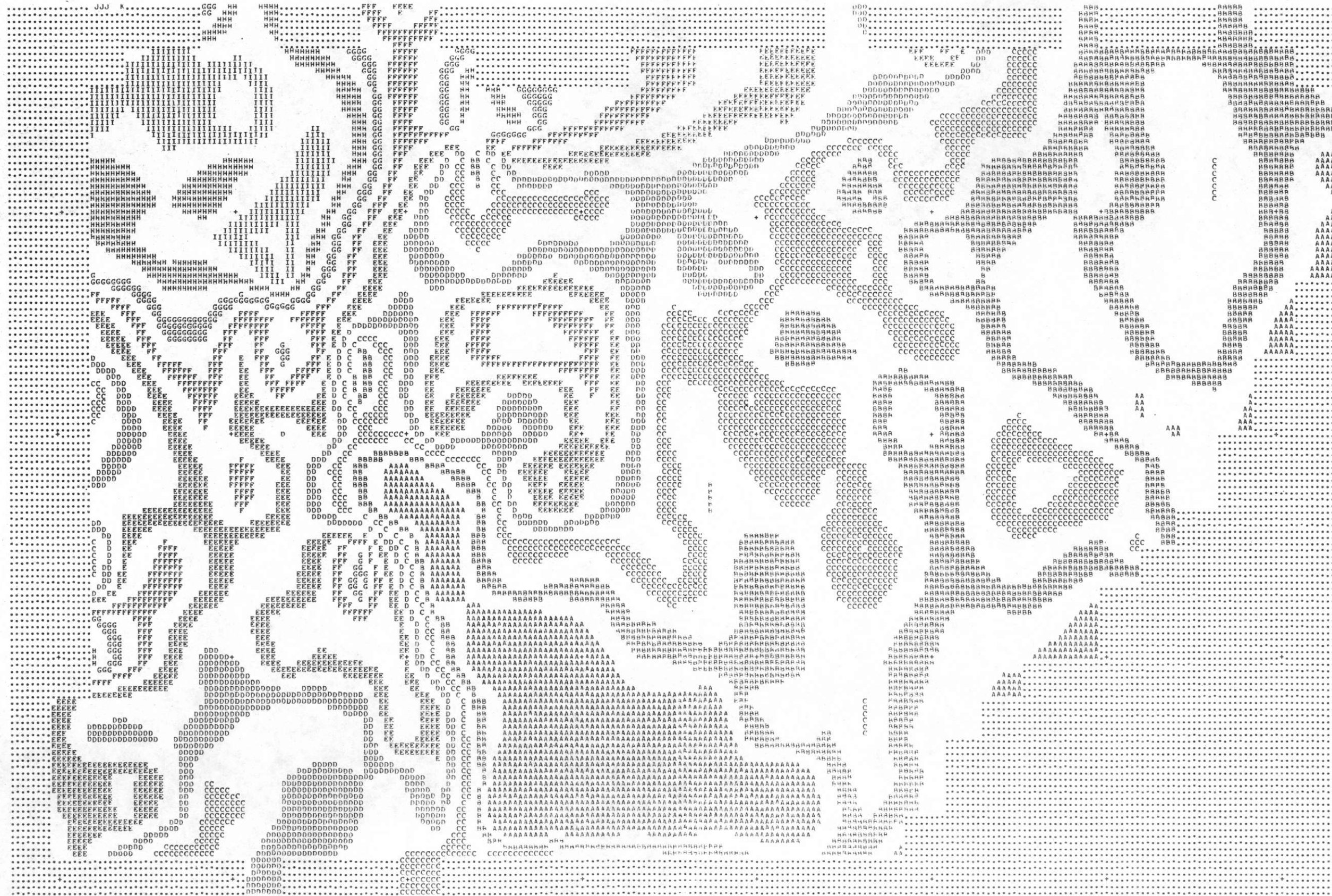
ITEM

DESCRIPTION

T ₂	T ₂ value, c/s
Rank	T ₂ standard deviation rank
Bi	Bi value, c/s
Rank	Bi standard deviation rank
K	K value, c/s
Rank	K standard deviation rank
Bi/T ₂	Ratio value
Rank	Bi/T ₂ standard deviation rank
Bi/K	Ratio value
Rank	Bi/K standard deviation rank
T ₂ /K	Ratio value
Rank	T ₂ /K standard deviation rank

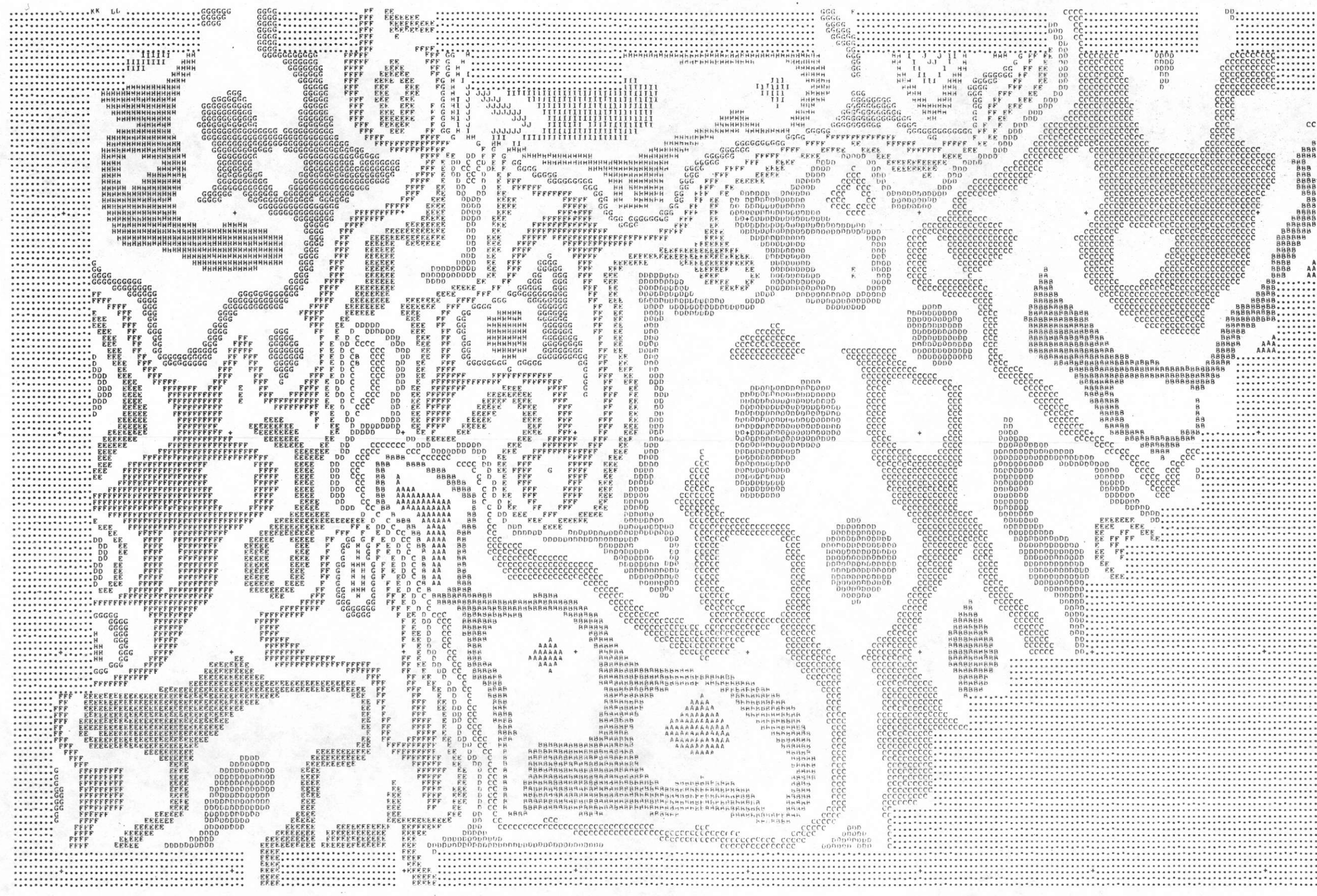
RCN	GFOUNT	AKUT	LAT	LONG	RMAG	COS	GC	MAPLINE	1W	AIT	TEMP	RP	TL	RT	K	RT/TL	RT/K	TL/K
28	ZNA	0000	39.0214	76.0368	-563.6	31	1975	3.8	441	24.4	740.9	8.0	2.4	1.3	0.30	1.79	6.01	
29	ZNA	0011	39.0214	76.0364	-579.5	5	107	3.8	0	24.5	742.4	0.3	0.1	0.1	0.36	1.75	4.84	
30	ZNA	0000	39.0214	76.0360	-576.0	32	1504	3.8	419	24.4	743.4	3.7	1.2	1.2	0.33	1.05	3.18	
31	ZNA	0000	39.0213	76.0355	-578.2	30	1602	3.8	417	24.5	742.4	3.9	1.7	1.2	0.43	1.36	3.17	
32	ZNA	0000	39.0213	76.0346	-576.5	39	1736	3.8	416	24.4	742.4	5.8	2.5	1.2	0.42	1.97	4.65	
33	ZNA	0000	39.0213	76.0342	-576.7	28	1586	3.8	414	24.5	742.4	4.1	2.7	1.1	0.64	2.48	3.85	
34	ZNA	0000	39.0213	76.0337	-577.7	29	1792	3.8	411	24.6	742.9	6.1	1.9	1.5	0.31	1.28	4.14	
35	ZNA	0000	39.0213	76.0333	-579.4	45	1830	3.8	408	24.5	742.9	6.2	2.0	1.3	0.33	1.58	4.87	
36	ZNA	0000	39.0212	76.0329	-580.1	44	1876	3.8	408	24.4	742.9	5.8	2.8	1.2	0.49	2.27	4.69	
37	ZNA	0000	39.0212	76.0324	-580.5	25	1663	3.8	407	24.5	743.4	3.3	3.1	1.2	0.94	2.65	2.83	
38	ZNA	0000	39.0212	76.0320	-581.7	35	1850	3.8	407	24.4	742.9	6.2	2.2	1.4	0.36	1.66	4.60	
39	ZNA	0000	39.0212	76.0316	-581.7	30	1879	3.8	400	24.5	743.4	6.1	2.4	1.5	0.39	1.60	4.09	
40	ZNA	0000	39.0212	76.0311	-582.2	42	1765	3.8	394	24.4	743.4	5.4	2.3	1.3	0.43	1.81	4.22	
41	ZNA	0000	39.0211	76.0307	-584.1	28	1699	3.8	393	24.5	743.4	6.4	1.7	1.2	0.27	1.50	5.51	
42	ZNA	0000	39.0211	76.0303	-584.8	33	1531	3.8	388	24.4	744.5	6.5	1.8	0.9	0.28	1.91	6.89	
43	ZNA	0000	39.0211	76.0298	-585.5	38	1413	3.8	394	24.3	743.4	4.4	1.6	1.0	0.36	1.59	4.42	
44	ZNA	0000	39.0211	76.0294	-586.2	31	1396	3.8	384	24.4	744.5	5.5	0.6	1.1	0.10	0.54	5.13	
45	ZNA	0000	39.0211	76.0290	-588.0	28	1636	3.8	374	24.5	744.0	6.2	1.5	0.9	0.24	1.62	6.66	
46	ZNA	0000	39.0211	76.0285	-588.5	30	1877	3.8	390	24.6	744.0	5.8	1.9	1.3	0.34	1.45	4.32	
47	ZNA	0000	39.0210	76.0281	-590.7	32	1861	3.8	395	24.5	743.4	4.4	3.2	1.2	0.74	2.62	3.57	
48	ZNA	0000	39.0210	76.0277	-589.3	31	1845	3.8	401	24.6	741.4	6.5	2.0	1.2	0.31	1.63	5.24	
49	ZNA	0000	39.0210	76.0272	-588.9	36	1855	3.8	408	24.5	742.9	6.8	2.4	1.2	0.35	2.05	5.82	
50	ZNA	0000	39.0210	76.0268	-591.1	25	1875	3.8	412	24.6	743.4	5.1	2.8	1.2	0.55	2.27	4.13	
51	ZNA	0000	39.0210	76.0264	-591.7	23	1796	3.8	414	24.7	742.4	6.5	2.4	1.1	0.37	2.08	5.68	
52	ZNA	0000	39.0210	76.0259	-592.9	39	1910	3.8	413	24.6	742.4	7.0	1.6	1.3	0.23	1.24	5.48	
53	ZNA	0000	39.0209	76.0255	-593.6	37	1840	3.8	413	24.5	740.9	7.6	1.7	1.3	0.22	1.24	5.66	
54	ZNA	0000	39.0209	76.0251	-593.3	35	1843	3.8	414	24.4	742.4	6.6	1.8	1.3	0.27	1.44	5.27	
55	ZNA	0000	39.0209	76.0246	-593.4	33	1768	7.5	418	24.3	740.9	5.7	2.5	1.1	0.45	2.23	5.00	
56	ZNA	0000	39.0209	76.0242	-594.8	40	1698	7.5	417	24.2	742.9	5.1	2.4	1.4	0.47	1.71	3.68	
57	ZNA	0000	39.0209	76.0238	-595.5	31	1781	7.5	417	24.3	742.4	6.6	1.5	1.6	0.23	0.93	4.05	
58	ZNA	0000	39.0209	76.0233	-595.5	43	1710	7.5	413	24.2	743.4	5.0	1.7	1.3	0.33	1.32	3.96	
59	ZNA	0000	39.0208	76.0229	-597.2	37	1604	7.5	412	24.1	742.4	5.1	2.5	1.1	0.48	2.32	4.83	
60	ZNA	0000	39.0208	76.0225	-597.4	34	1549	7.5	406	24.0	745.0	4.3	2.5	0.9	0.57	2.66	4.63	
61	ZNA	0000	39.0208	76.0220	-596.9	32	1546	7.5	401	24.1	744.5	5.5	2.6	1.1	0.47	2.44	5.18	
62	ZNA	0000	39.0208	76.0216	-597.3	36	1435	7.5	400	24.0	742.9	4.8	2.2	0.8	0.45	2.61	5.83	
63	ZNA	0000	39.0208	76.0212	-597.5	35	1215	7.5	402	23.9	744.5	3.2	0.9	0.9	0.27	0.93	3.40	
64	ZNA	0000	39.0207	76.0207	-597.2	30	1192	8.2	395	24.0	743.4	3.5	0.9	0.8	0.27	1.25	4.59	
65	ZNA	0010	39.0207	76.0203	-598.8	34	1233	8.2	382	23.9	743.4	4.4	0.5	0.9	0.11	0.58	5.10	
66	ZNA	0000	39.0207	76.0199	-599.7	28	1303	8.2	386	24.0	744.5	2.5	1.3	1.1	0.52	1.18	2.25	
67	ZNA	0000	39.0207	76.0194	-600.3	38	1449	8.2	389	23.9	742.9	5.8	0.9	0.9	0.16	1.00	6.15	
68	ZNA	0000	39.0207	76.0190	-600.2	29	1463	8.2	393	24.0	743.4	3.9	1.4	1.2	0.35	1.11	3.12	
69	ZNA	0000	39.0207	76.0186	-598.3	30	1407	8.2	401	24.1	744.0	3.9	1.2	1.1	0.30	1.06	3.56	
70	ZNA	0000	39.0206	76.0181	-598.5	32	1545	8.2	406	24.2	742.4	4.1	1.1	1.3	0.26	0.84	3.22	
71	ZNA	0000	39.0206	76.0177	-598.4	44	1453	8.2	409	24.1	742.4	3.6	1.2	1.2	0.34	1.04	3.04	
72	ZNA	0000	39.0206	76.0173	-600.0	43	1605	8.2	413	24.0	742.9	5.0	1.7	1.4	0.35	1.24	3.55	
73	ZNA	0000	39.0206	76.0168	-600.9	39	1516	9.2	413	23.9	742.4	4.3	2.6	0.9	0.61	2.84	4.68	
74	ZNA	0000	39.0206	76.0164	-601.6	30	1470	9.2	410	24.0	742.4	4.0	2.5	1.1	0.61	2.26	3.69	
75	ZNA	0000	39.0206	76.0160	-602.0	23	1480	9.2	413	24.0	742.4	5.1	0.6	1.2	0.13	0.55	4.29	
76	ZNA	0000	39.0205	76.0155	-602.0	21	1387	9.2	414	24.2	742.4	4.1	0.9	1.2	0.23	0.76	3.35	
77	ZNA	0000	39.0205	76.0151	-603.1	20	1515	9.2	416	24.3	742.4	7.2	1.2	1.3	0.16	0.47	5.43	
78	ZNA	0000	39.0205	76.0147	-602.6	40	1457	9.2	414	24.2	741.9	3.6	1.0	1.3	0.28	0.78	2.77	
79	ZNA	0000	39.0205	76.0142	-603.0	34	1538	9.2	416	24.1	742.9	5.0	2.3	1.1	0.46	2.02	4.35	
80	ZNA	0000	39.0205	76.0138	-604.4	30	1631	9.2	414	24.2	742.4	4.8	1.4	1.3	0.28	1.07	3.76	
81	ZNA	0000	39.0205	76.0134	-604.9	23	1569	9.2	416	24.3	742.9	3.7	3.6	1.0	0.97	3.79	3.92	
82	ZNA	0010	39.0204	76.0129	-605.6	41	1479	10.4	414	24.2	742.4	5.1	0.4	1.2	0.08	0.36	4.26	
83	ZNA	0000	39.0204	76.0125	-607.3	37	1637	10.4	411	24.1	743.4	4.4	1.5	1.4	0.34	1.11	3.22	
84	ZNA	0000	39.0204	76.0121	-608.5	32	1515	10.4	406	24.2	743.4	5.7	1.0	1.1	0.18	0.93	5.22	

RCN	GFOUNT	AKUT	LAT	LONG	RMAG	COS	GC	MAPLINE	1W	TI RANK	RI RANK	K RANK	RT/TL RANK	RT/K RANK	TL/K RANK
28	ZNA	0000	39.0214	76.0368	-563.6	31	1975	3.8	8.0+ 1	2.4+ 1	1.3+ 1	0.30- 0	1.79- 0	6.01- 0	
29	ZNA	0010	39.0214	76.0364	-579.5	5	107	3.8	0.3- 2	0.1- 2	0.1- 2	0.36+ 0	1.75- 0	4.84- 1	
30	ZNA	0000	39.0214	76.0360	-576.0	32	1504	3.8	3.7- 1	1.2- 1	1.2+ 1	0.33+ 0	1.05- 1	3.18- 1	
31	ZNA	0000	39.0213	76.0355	-578.2	30	1602	3.8	4.2- 1	1.7+ 0	1.1+ 1	0.41+ 1	1.60- 1	3.89- 1	
32	ZNA	0000	39.0213	76.0346	-576.5	39	1736	3.8	4.6- 0	1.9+ 0	1.2+ 1	0.42+ 1	1.68- 1	3.97- 1	
33	ZNA	0000	39.0213	76.0342	-576.7	28	1586	3.8	5.1- 0	2.2+ 1	1.2+ 1	0.43+ 1	1.77- 0	4.13- 1	
34	ZNA	0000	39.0213	76.0337	-577.7	29	1792	3.8	5.4- 0	2.3+ 1	1.3+ 1	0.43+ 1	1.82- 0	4.23- 1	
35	ZNA	0000	39.0213	76.0333	-579.4	45	1830	3.8	5.5+ 0	2.4+ 1	1.3+ 1	0.44+ 1	1.89- 0	4.30- 1	
36	ZNA	0000	39.0212	76.0329	-580.1	44	1876	3.8	5.4+ 0	2.5+ 1	1.3+ 1	0.46+ 1	1.95- 0	4.23- 1	
37	ZNA	0000	39.0212	76.0324	-580.5	25	1663	3.8	5.3- 0	2.5+ 1	1.3+ 1	0.48+ 2	1.96- 0	4.12- 1	
38	ZNA	0000	39.0212	76.0320	-581.7	35	1850	3.8	5.5+ 0	2.5+ 1	1.3+ 1	0.45+ 1	1.89- 0	4.22- 1	
39	ZNA	0000	39.0212	76.0316	-581.7	30	1879	3.8	5.7+ 0	2.3+ 1	1.3+ 1	0.41+ 1	1.81- 0	4.39- 1	
40	ZNA	0000	39.0212	76.0311	-582.2	42	1765	3.8	5.7+ 0	2.1+ 1	1.2+ 1	0.37+ 1	1.74- 0	4.65- 1	
41	ZNA	0000	39.0211	76.0307	-584.1	28	1699	3.8	5.9+ 0	1.9+ 0	1.2+ 1	0.32+ 0	1.61- 1	5.02- 1	
42	ZNA	0000	39.0211	76.0303	-584.8	33	1531	3.8	5.8+ 0	1.7- 0	1.1+ 1	0.29- 0	1.55- 1	5.33- 1	
43	ZNA	0000	39.0211	76.0298	-585.5	38	1413	3.8	5.6+ 0	1.5- 0	1.1+ 1	0.27- 0	1.44- 1	5.35- 1	
44	ZNA	0000	39.0211	76.0294	-58										

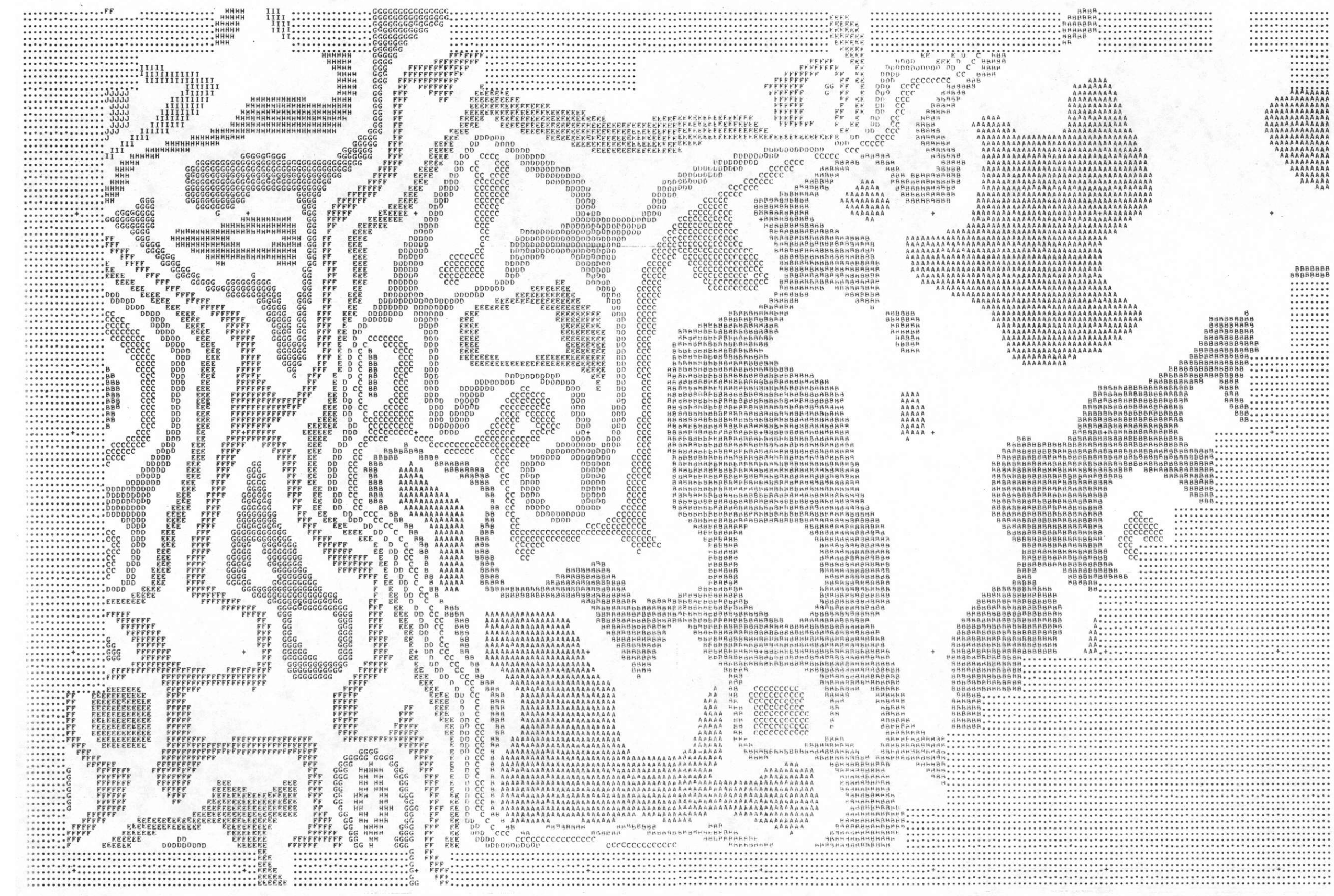


ATV-1 Line Printer Contour.

GPO DATA INTERNATIONAL, INC.
 DALLAS, TEXAS
 AC 0.50 3.20<K 1.80 2.40<K 3.00 3.60<K 4.20 4.80<K 5.40 6.00<K 6.60
 7.20<K 7.80 8.40<K 9.00 9.60<K 10.20 10.80<K 11.40 12.00<K 12.60



ATV-2 Line Printer Contour



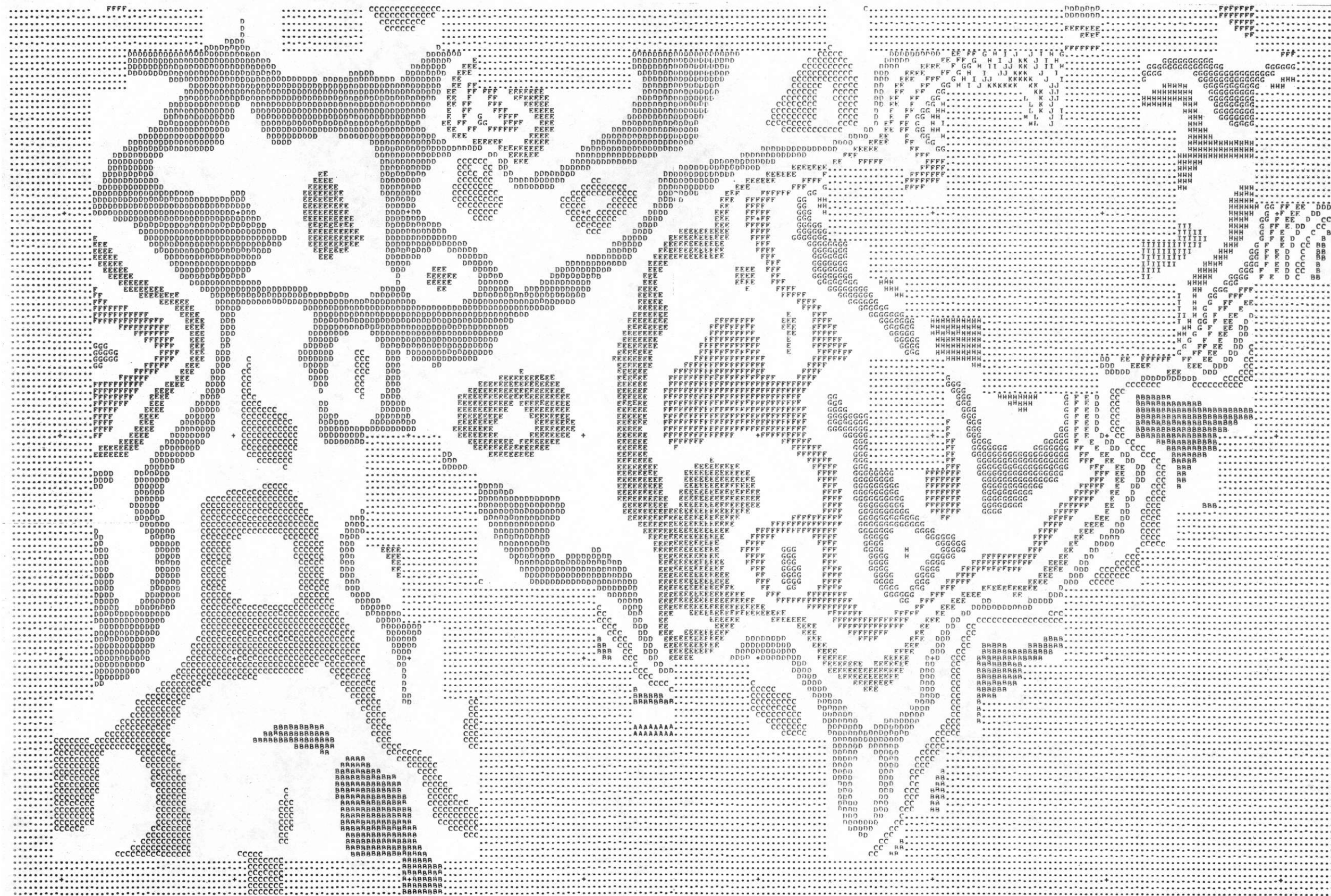
ATI-3 Line Printer Contour



ALV-4 Line Printer Contour

GEODATA INTERNATIONAL, INC.
DALLAS, TEXAS

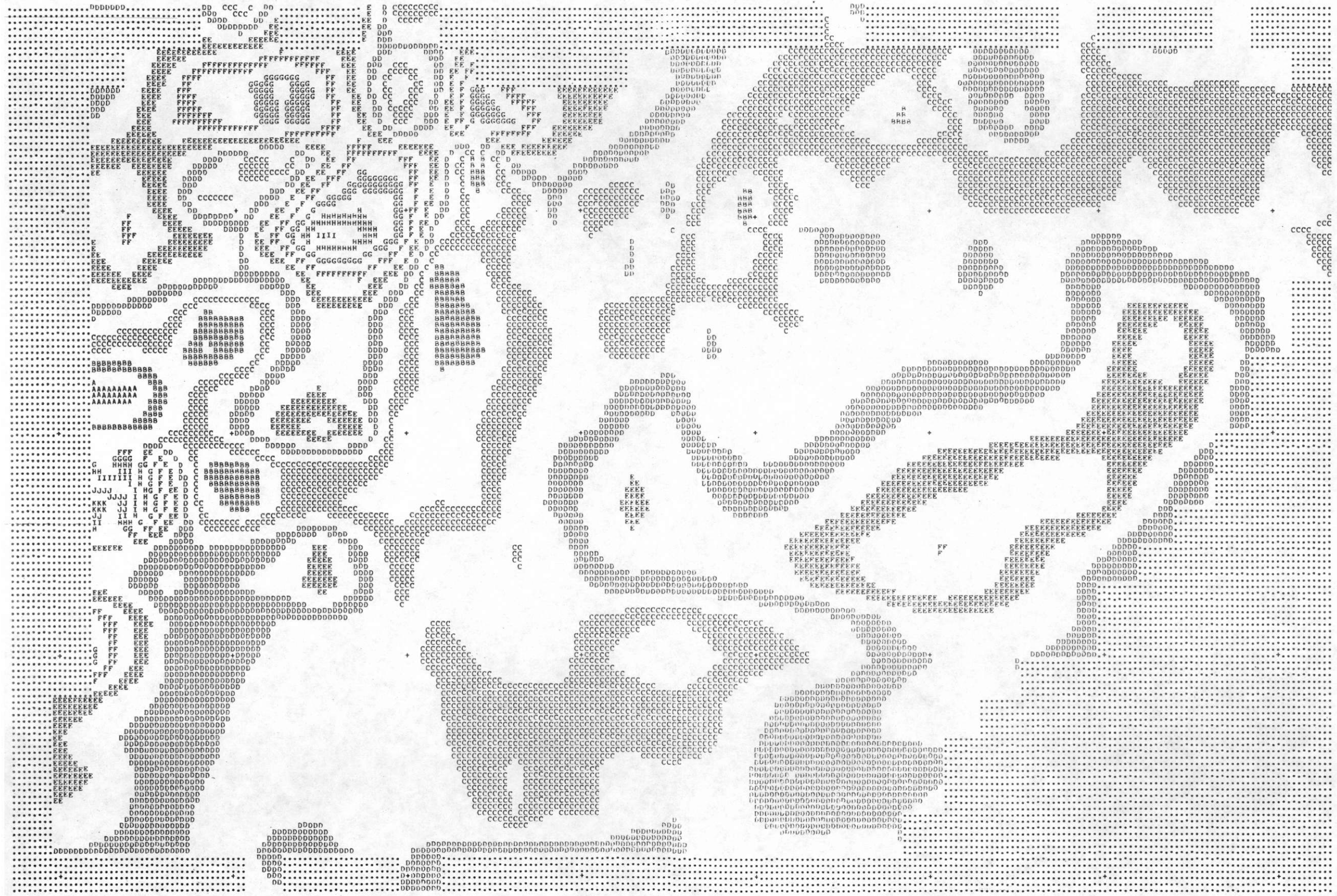
0.20<K< 0.30	0.40<K< 0.50	0.60<K< 0.70	0.80<K< 0.90	1.00<K< 1.10
1.20<K< 1.30	1.40<K< 1.50	1.60<K< 1.70	1.80<K< 1.90	2.00<K< 2.10
2.20<K< 2.30	2.40<K< 2.50	2.60<K< 2.70	2.80<K< 2.90	3.00<K< 3.10
3.20<K< 3.30	3.40<K< 3.50	3.60<K< 3.70	3.80<K< 3.90	4.00<K< 4.10
4.20<K< 4.30	4.40<K< 4.50	4.60<K< 4.70	4.80<K< 4.90	5.00<K< 5.10
5.20<K< 5.30				



Line Printer Contour

GEODATA INTERNATIONAL, INC.
DALLAS, TEXAS

1.0	2.0	3.0	4.0	5.0	6.0	7.0	8.0	9.0	10.0	11.0
12.0	13.0	14.0	15.0	16.0	17.0	18.0	19.0	20.0	21.0	
22.0	23.0	24.0	25.0	26.0	27.0					



ATI-7 Line Printer Contour

BIBLIOGRAPHY

- Bascom, F., and Stose, G.W., 1932, Description of the Coatsville and West Chester Quadrangles, U.S. Geological Survey Atlas, Folio N. 233.
- Buckwalter, T.V., 1955, The Lithology, Stratigraphic Relations and Structure of Precambrian Rocks in Eastern Pennsylvania; in Field Guidebook of Appalachian Geology Pittsburgh to New York, Pittsburgh Geological Society in conjunction with the Annual Meeting of the American Association of Petroleum Geologists, New York, 1952, pp. 93-97.
- Cooper, M., 1958, Bibliography and Index of Literature on Uranium and Thorium and Radioactive Occurrences in the United States; Part 5: Connecticut, Delaware, Illinois, Indiana, Maine, Maryland, Massachusetts, Michigan, New Hampshire, New Jersey, New York, Ohio, Pennsylvania, Rhode Island, Vermont, and Wisconsin; Geological Society of America, Special Paper 67, 472 pp.
- Fenneman, N.M., 1938, Physiography of Eastern United States; New York, McGraw-Hill Book Co., Inc., 1938, 714 pp.
- Fisher, G.W., 1970, Introduction; Section IV: The Piedmont; in Fisher, G.W., et alia, eds., 1970, Studies of Appalachian Geology, Central and Southern; New York, John Wiley and Sons, pp. 295-298.
- Fisher, G.W., 1970b, The Metamorphosed Sedimentary Rocks along the Potomac River near Washington, D.C.; in Fisher, G.W., et alia, eds., 1970, Studies of Appalachian Geology, Central and Southern; New York, John Wiley and Sons, pp. 299-316.
- Fisher, G.W., Pettijohn, F.J., Reed, J.C., and Weaver, K.N., eds., 1970, Studies of Appalachian Geology, Central and Southern; New York, John Wiley and Sons, 460 pp.
- Jordan, R.R., 1976, The Columbia Group (Pleistocene) of Delaware; in Thompson, A.M., ed., Guidebook to the Stratigraphy of the Atlantic Coastal Plain in Delaware; Petroleum Exploration Society of New York, Third Annual Field Trip, 1976, pp. 103-110.
- Kummel, H.B., 1940, The Geology of New Jersey; Department of Conservation and Development, State of New Jersey; Bulletin 50, Geologic Series.
- McGee, W.J., 1888, Three Formations of the Middle Atlantic Slope; American Journal of Science, 3rd Series, v. 35, pp. 120-143, 328-330, 365-388, 448-466.

(Bibliography Cont'd.)

- McKinstry, H., 1941, Structure of the Glenarm Series in Chester County, Pennsylvania, Geological Society of America, Bulletin v. 72, pp. 557-578.
- Mineral Resources Development, Inc., 1979, Geology of the Wilmington Quadrangle; Map, scale 1:250,000, by Mineral Resources Development, Inc. for U.S. Department of Energy.
- N.T.B.M.S., 1972, National Topographic-Bathymetric Map Series, Wilmington Sheet, Delaware, New Jersey, Pennsylvania, Maryland; U.S. Geological Survey and National Ocean Survey, Eastern U.S., map, scale 1:250,000, NJ18-2 series, 1972.
- Pickett, T., 1976, Synopsis of Atlantic Coastal Plain Stratigraphy in Delaware; in Thompson, A.M., 1976, Guidebook to the Stratigraphy of the Atlantic Coastal Plain in Delaware; Third Annual Field Trip, Petroleum Exploration Society of New York, 1976, pp. 2-11.
- Southern Interstate Nuclear Board, 1969, Uranium in the Southern United States; report prepared for the Atomic Energy Commission, Division of Raw Materials, by the Southern Interstate Nuclear Board, updated November, 1970.
- Sundstrom, R.W., Pickett, T., and Varrin, R.D., 1975, Hydrology, Geology and Mineral Resources of the Coastal Zone of Delaware: Water Resources Center, University of Delaware, 268 pp.
- Vokes, H.E., 1957, Geography and Geology of Maryland; Department of Geology Mines and Water Resources, Bulletin 19, 243 pp.
- Ward, R.F., and Groot, J.J., 1957, Engineering Materials of Northern New Castle County; State of Delaware, Delaware Geological Survey, Bulletin No. 7, 103 pp.
- Wise, D.U., 1970b, Multiple Deformation, Geosynclinal Transitions, and the Martic Problem in Pennsylvania; in Fisher, G.W., et alia, eds., 1970, Studies of Appalachian Geology, Central and Southern; New York, John Wiley and Sons, pp. 317-334.

